Bioactive phytochemicals from Libyan medicinal plants: *Cynara cyrenaica* Maire &Weill and *Cyclamen rohlfsianum* Aschers

A thesis submitted by

Tahani M Mohamed El-Tomi

Strathclyde Institute of Pharmacy and Biomedical Sciences

University of Strathclyde

Glasgow, UK

Presented in fulfilment of the requirements for the degree of

Doctor of Philosophy

2018

Copyright

Signed:

Date:

بسم الله الرحمن الرحيم

By the name of Allah

****

Acknowledgments

First and foremost, I would like to express my gratitude and thankfulness to Allah for blessing me and giving me strength to complete this research study.

I would like to express my sincere gratitude and appreciation to my supervisors: Dr. Valerie Ferro and Prof. Alexander Gray for their excellent guidance, invaluable insights, encouragement, constructive criticism and patience during the entire period of this research. Their help and guidance made my PhD study the best experience I have ever had. It was a great honour to be their student.

I would like to express my sincere thanks to Prof. John Igoli for his valuable time, knowledge and support. I am grateful to Mr. Craig Irving for helping me out with NMR experiments. I also thank Dr. Tong Zhang (Alex) for his assistance in MS experiments, and Mr. Gavin Bain for his help in Optical Rotation measurements. I also would like to thank Dr. Abedawn Khalaf for carrying out the infra-red measurements.

I would like to express my deepest gratitude to my mother for her prayers and strong encouragement in my academic endeavours over the years. Thanks to my sisters and brothers for supporting me at all times.

My sincere appreciation respect and love to my husband for ongoing support and standing beside me throughout my PhD. I could not finish my PhD without his support and help. He has been my inspiration and motivation for continuing to improve my career for a brighter future for our family. Special thanks also go to my lovely kids for their unending love.

My appreciation also goes to all my lab mates in RW 321 in SIPBS for their friendship. My acknowledgements also go to the Ministry of Higher Education in Libya for awarding me the scholarship and funding this PhD study.

Abstract

Medicinal plants have a long history in the treatment of diseases. Studies on phytochemicals from medicinal plants have continued to increase due to their importance in the search for new drugs. The El-Jabal El-Akhdar region (Green Mountain) of Libya has a high diversity of medicinal plants which are presently poorly studied. This dissertation describes studies on *Cynara cyrenaica* and *Cyclamen rohlfsianum*, collected from the region, for phytochemical, anticancer and antidiabetic evaluation. The phytochemical evaluation revealed one saponin 3-*O*-{β-D-xylopyranosyl-(1→2)-β-D-glucopyranosyl-(1→4)-[β-D-glucopyranosyl-(1→2)]-α-L-arabinopyranosyl}-cyclamiretin A (CY1) isolated from *C. rohlfsianum*. Thirteen compounds were isolated from *C. cyrenaica*, including two identified as novel sesquiterpene lactones named 3β-hydroxy-8α-[(S)-4-hydroxy-3- methylbutanyloxy]-guaian-4(15), 10(14), 11(13)-trien-1α, 5α, 7α, 6βH-12, 6-olide (CC12) and 11, 13 epoxy-guaian-4(15), 10(14)-dien-1α, 5α, 7α, 6βH-12, 6-olide-3-yl acetate (CC13). The other compounds were taraxasterol, pseudotaraxasterol, ll,13-epoxysolstitialin (CC5), apigenin, luteolin-7-*O*-β-D-glucopyranoside, luteolin, catechin 7-*O*-gallate, ferulic acid, 1,3-dicaffeoylquinic acid, daucosterol and 1-monoacetyl glycerol.

A preliminary *in vitro* antidiabetic assessment of all crude solvent extracts and most of the isolated compounds was carried out using α-glucosidase, protein tyrosine phosphatase 1B (PTP1B) and α-amylase inhibition tests. For α-glucosidase, only catechin 7-*O*-gallate from *C. cyrenaica* was found to be active with significant ($p < 0.001$) inhibition and produced concentration-dependent inhibition with an IC_{50} value of 3.94 ± 1.1µM. For the *C. rohlfsianum* tuber, the crude methanol extract and CY1 isolated from this extract produced marked inhibitory activity on α-glucosidase with IC_{50} values of 3.46 ± 1.13µg/ml and 5.53 ± 1.1µM, respectively. For PTP1B assay only luteolin from *C. cyrenaica* was found to be significantly ($p < 0.001$) active and showed dose-dependent inhibition activity with an IC_{50} value of 15.94 ± 1.12µM. In an α-amylase assay, no inhibition of the enzyme was produced by both plants. These findings provide some scientific support for the traditional use of this plant as an anti-diabetic.

The crude solvent extracts and some of the isolated compounds were also screened *in vitro* for cytotoxicity against human cancer cell lines: A375 (malignant melanoma),

PANC-1 (pancreatic carcinoma), and HeLa (cervical cancer) in comparison with a non-cancer PNT2 cell line (prostate cell line) using an AlamarBlue® assay. Among the crude solvent extracts tested, the n-hexane and ethyl acetate extract of *C. cyrenaica* flower heads showed inhibition of metabolic activity on all the cell lines, including the PNT2 cells, but those of the ethyl acetate extract of the root, leaf and stem were the most potent against PANC-1 cells with IC_{50} values of 2.73 ± 1.18, 0.004 ± 1.02 and 1.40 ± 1.87µg/ml, respectively and showed inhibition effect on PNT2 cells with different ranges of IC_{50}. For the ethyl acetate extracts of *C. cyrenaica* root and stem this effect could be linked in part to the presence of sesquiterpene lactones (CC5, CC12 and C13). Furthermore, the n-hexane extract of *C. cyrenaica* leaf also showed inhibitory metabolic activity in HeLa and PANC-1 cells at 25µg/ml and showed inhibition effect on PNT2 cells with IC_{50} value of 10.71 ± 1.30µg/ml. For the *C. rohlfsianum* tuber, the only inhibition was observed with the methanol extract on all the cell lines, including the PNT2 cells with an IC_{50} value of 3.16 ± 1.08µg/ml for PNT2 and 6.35 ± 1.09, 42.37 ± 1.13 and 4.19 ± 1.11µg/ml for A375, HeLa and PANC-1, respectively.

Among the screened compounds, taraxasterol showed selective activity against HeLa cells with no toxic effect on normal cells. While luteolin, ll, 13-epoxysolstitialin, CY1 and CC12 were active against all the cancer cell lines. However, ll, 13-epoxysolstitialin was potent against PANC-1 cells with an IC_{50} value of 4.70 ± 1.06µM, while CC12 showed marked inhibitory effect on PANC-1 cells with an IC_{50} value of 24.43 ± 1.32µM. Both compounds were then tested for their ability to prevent metastatic dissemination of PANC-1 cells using the following kits: Cytoselect™ 48-well Adhesion Assays (collagen IV and fibronectin), Poly-L-lysine Adhesion Assay, InnoCyte™ Cell Migration Assay and InnoCyte™ Cell Invasion Assay. The results revealed that both compounds inhibited adhesion, migration and invasion of PANC-1 cancer cells. These findings, although preliminary, propose a new potential therapeutic use of *C. cyrenaica* and *C. rohlfsianum* which could lead to the discovery of potent agents for the treatment of pancreatic carcinoma and diabetes.

Table of Contents

List of Figures

List of Tables

List of Abbreviations

Acetone-d_6	Deuterated acetone
Brs	Broad singlet
BSA	Bovine serum albumin
CC	Column chromatography
$CDCl_3$	Deuterated Chloroform
COSY	Correlation Spectroscopy
D	Doublet
Dd	Doublet of a doublet
DEPT	Distortionless Enhancement by Polarisation Transfer
DMEM	Dulbecco's Modified Eagle Medium
DMSO	Dimethyl sulfoxide
DMSO- d_6	Deuterated dimethyl sulfoxide
DPPH	2,2-diphenylpicrylhydrazyl
ECM	Extra cellular matrix
EtOAc	Ethyl acetate
FBS	Fatal Bovine solution
HBSS	Hank's balanced salt solution
HEPES	(4-(2-hydroxyethyl)-1-piperazineethanesulfonic acid)
HMBC	Heteronuclear Multiple Bond Coherence
HRESI-MS	High-resolution Electrospray Ionisation Mass Spectroscopy
HSQC	^{1}H-detected Heteronuclear Single Quantum Coherence
IC_{50}	50% Inhibitory concentration
IR	InfraRed spectroscopy
M	Multiplet
MMPs	Matrix metalloproteinases
MeOH	Methanol
Methanol-d_5	Deuterated methanol
NMR	Nuclear Magnetic Resonance
NOESY	Nuclear Overhauser Enhancement Spectroscopy
OR	Optical rotation
PBS	Phosphate-buffered saline

PTLC	Preparative Thin Layer Chromatography
PTP1B	Protein tyrosine phosphatase 1B
Pyridine-d_5	Deuterated pyridine
R_f	Retardation factor
ROS	Reactive oxygen species
RPMI	Roswell Park Memorial Institute
S	Singlet
T2D	Type 2 diabetes
TLC	Thin Layer Chromatography
UV	Ultraviolet light
VLC	Vacuum Liquid Chromatography
WHO	World Health Organization

CHAPTER I
1. INTRODUCTION

1.1 Importance of medicinal plants in drug discovery

The demand for natural products for medicine and health has been enormous because of the increasing problem of drug resistance (Obeid *et al*., 2017) and due to the side effects associated with synthetic medicines, which could be avoided using metabolites discovered from medicinal plants (Lahlou, 2013). The importance of medicinal plants due to the presence of bioactive phytochemical constituents that could be considered the basis of modern drugs, can be discovered through phytochemical screening (Sheikh *et al.*, 2013), and they provide a worldwide valuable source of new drugs as they play a very significant role in the field of drug discovery and development (Newman and Cragg, 2016; Chen *et al.*, 2016). In the early1900s, 80% of all medicines were estimated to have been obtained from different plant parts and in more recent times, natural products have continued to be significant sources of drugs and lead compounds (McChesney *et al.*, 2007).

Phytochemicals from medicinal plants possess therapeutic activity for numerous diseases including chronic diseases like diabetic and cancer and reduces risks of cancer and diabetes with lower mortality rates of many other human diseases (Ozkan *et al.*, 2016). Diabetes mellitus is a chronic metabolic disorder, characterised by high levels of blood glucose, altered metabolism of lipids, carbohydrates and proteins. Along with cancer, diabetes is considered the third "killer" of mankind (Patel *et al.*, 2012). It has been reported that the oxidative stress induced by the production of free radicals may be related to the complications associated with diabetes. Pancreatic β-cells are particularly affected by the detrimental effects of reactive oxygen species (ROS) as they show low expression of antioxidant enzymes compared with the other tissues, and this makes them susceptible to ROS. Therefore, the increase of ROS causes damage to β-cells by the induction of apoptosis and suppression of insulin biosynthesis. Thus, antioxidants may provide protection against the development of diabetes, as they have been shown to prevent the destruction of β-cells by inhibiting the peroxidation chain reaction (Ozkan *et al*., 2016).

Although the pharmacological treatment of diabetes mellitus is based on insulin injections and oral hypoglycaemic agents, in many countries, numerous antioxidant plants are traditionally used for the treatment of diabetes as an alternative strategy (Ozkan *et al*., 2016). Medicines from plant resources play an important role in the treatment of diabetes mellitus, particularly in the developing countries due to their cost

effectiveness. Type 2 diabetes (T2D) is a chronic disease of interest because of its increasing incidence and economic burden, also due to the potential role of natural products in its management (Gobert and Duncan, 2008). The current options available in modern medicine for diabetic treatment have adverse effects such as hypoglycaemia, nausea, vomiting, weight gain, dyspepsia, dizziness and joint pain (Kumari *et al.*, 2016). For this reason, there is a need to develop effective and safe drugs for diabetes. It has been reported that plants have an essential role to provide the best option for safe and effective drugs and many plants have been found to have significant anti-diabetic effects following preclinical and clinical evaluation (Patel *et al*., 2012).

Plant materials contain many kinds of phytoconstituents of different chemical classes, for example: alkaloids such as pyrrolidine, quinolizidine and isoquinoline alkaloid show inhibitory activity on α-glucosidase and decrease glucose transport through the intestinal epithelium; flavonoids have the ability to suppress glucose levels, significantly reduce plasma cholesterol and triglycerides and increase hepatic glucokinase activity by enhancing insulin release from pancreatic islets; imidazoline compounds stimulate insulin secretion in a glucose-dependent manner; polysaccharides can increase serum insulin levels, reduce blood glucose levels and enhance tolerance to glucose; saponins also play a role in diabetic treatment by stimulating release of insulin and blocking formation of glucose in the bloodstream and ferulic acid also stimulates insulin secretion. In addition, dietary fibres have showed an effective role to adsorbs glucose and retard glucose diffusion and have also showed inhibitory activity on α-amylase and may be responsible for decreasing the rate of glucose absorption and concentration of postprandial serum glucose (Patel *et al*., 2012).

In addition, plants have a long history of use in cancer treatment and are considered a source of potential anticancer agents. Approximately 60% of currently used anti-cancer agents are derived from natural sources (Cragg and Newman, 2005; Alonso-Castro *et al.*, 2011). Cancer treatments such as radiotherapy and chemotherapy are expensive and have many side effects, including vomiting, alopecia, diarrhoea, constipation, myelosuppression, neurological, pulmonary, cardiac, and renal toxicity. Hence, there a need for more new, alternative anticancer drugs which are more selective and less toxic than those currently in use (Alonso-Castro *et al*., 2011). The

search for anticancer drugs from plant resources started in earnest in the 1950s with isolation of the cytotoxic podophyllotoxins and discovery and development of the vinca alkaloids, vincristine and vinblastine which isolated from the Madagascar periwinkle, *Catharanthus roseus* G. Don. (Apocynaceae). As a result, an extensive plant collection programme was initiated in 1960 from the United States National Cancer Institute (NCI), which led to the discovery of several novel chemotherapies including the taxanes, paclitaxel (taxol®) initially was isolated from the bark the Pacific Yew, *Taxus brevifolia* Nutt. (Taxaceae), and camptothecins isolated from the Chinese ornamental tree, *Camptotheca acuminata* Decne (Nyssaceae) (Cragg and Newman, 2005).

Natural product research continues to discover a variety of lead structures, which may be used by pharmaceutical industry as templates for the development of new drugs and these approved substances are representative of a wide range of chemical diversity and continue to demonstrate the important role of compounds from natural resources in modern drug discovery efforts (Lahlou, 2013).

1.2 The genus *Cynara* L.

Cynara is a relatively small genus, originating from the Mediterranean area (Christaki *et al.*, 2012). *Cynara* spp. belong to the Asteraceae family and can be divided into two groups. The first encompasses seven species: *C. baetica* (Spreng.), *C. algarbiensis* Coss. ex Mariz, *C. humilis* L which are spread widely in the West Mediterranean regions, and *C. cornigera* Lind., *C. syriaca* Boiss, *C. cyrenaica* Maire and Weill which are located in the Centre-East of the Mediterranean basin and *C. aurantica* Pos which is more equally distributed than the other species. The second group includes *C. cardunculus* (L.) subsp. *scolymus* (L) Hegi, the globe artichoke; *C. cardunculus* (L.) subsp. *altilis* DC, the cultivated cardoon and *C. cardunculus* (L.) subsp. *sylvestris* Lam., the wild artichoke (de Falco *et al.*, 2015; Pinelli *et al.*, 2007; Pagnotta and Noorani, 2014).

1.2.1 Cynara cyrenaica Maire &Weill

C. cyrenaica is a Libyan endemic species found in the El-Jabal El-Akhdar region (El-Darier and El-Mogaspi, 2009) and collected from the Wadi Alkuf region, locally known as Qahmoul (El-Mokasabi, 2014).

Figure 1. 1: *C. cyrenaica* (http://es.treknature.com/gallery/photo279766.htm)

Table 1. 1: Botanical characters of *C. cyrenaica* (Hand and Hadjikyriakou, 2009)

Characters	*C. Cyrenaica*
Leaf rachis width (mm)*	1.5-4
Leaf segments rachis width(mm)*	1.5-5
Leaf segments	14-33, apically caudate
Petiole of basal leaves	The base with marginal fringes of small spines
Involucre	Broadly ovoid
Corolla length(mm)	29.3-38.6
Anther length(mm)	6.7-7.7
Style length(mm)	37.7-40.9, incl. branches 6.6-8.2

1.2.1.1 Traditional use

On searching the literature, no phytochemical and pharmacological studies have been carried out on *C. cyrenaica*. However, an ethnopharmacologyical survey was carried out in the el-Jabal el-Akhdar region to identify endemic plant species among the diverse flora of this ecosystem that are used therapeutically and economically (El-Darier and El-Mogaspi, 2009). *C. cyrenaica* was one of the plants that was included

in this survey. The field work involved interviews with local inhabitants, practitioners and herbalists. It concluded that *C. cyrenaica* is used for food and in traditional medicines. *C. cyrenaica* root and heads (immature flowers) are used by the inhabitants of the region to treat gallstones, anaemia, liver disorders and rheumatic pains either as a decoction or eaten fresh (El-Darier and El-Mogaspi, 2009). *C. cyrenaica* is also used in honey production and used traditionally to treat ulcers, gastritis, colic, arteriosclerosis, burns, metritis and ovulation (El-Mokasabi, 2014). In general, the genus *Cynara* L. is used for medical treatments, including diabetes, liver disease, rheumatism, reducing blood glucose and cholesterol, and digestive, urinary, abdominal and intestinal disorders (Pedro *et al.*, 2013).

1.2.1.2 Previous phytochemical studies

This section reviews the phytochemicals isolated previously from *Cynara* species, which are a rich source of polyphenolic compounds, mainly flavonoids and caffeoylquinic acids (isolated from polar extracts of the plant), together with the polysaccharide inulin. In addition, fatty acids, triterpenes and sesquiterpenes are major metabolites found in the lipophilic fraction. These compounds occur in variable amounts in the plants due to several factors, such as environment, genetic factors, stress, harvest time, agronomical processes, parts of the plant analysed as well as use of different drying methods (De Falco *et al*., 2015; Lombardo *et al.*, 2010; Garbetta *et al.*, 2014). The bitter taste of artichoke plants is a result of its high content of sesquiterpene lactones (Elsebai *et al.*, 2016). In addition, anthocyanin pigments are present only in the flower heads in the form of glucosides and sophorosides (Salem *et al.*, 2015), and they are responsible for the colour of the artichoke capitula that ranges from green to violet (Christaki *et al.*, 2012). Anthocyanins also play an important role for the plant and give it the appearance of fresh globe artichokes and act as visual signals for pollinating insects (Pandino *et al.*, 2012). See Tables 1.2 to 1.3 and Figures 1.2 to 1.9 for the compounds isolated from *Cynara* species.

Table 1. 2: Phenolic compounds isolated from *Cynara* species

Compounds isolated	Plant species (*)	Reference
Caffeoylquinic acids		
1-*O*-caffeoylquinic acid (**1**)	*C. scolymus* L.(l) (h)	(Lattanzio *et al.*, 2009)
1,3-*O*-dicaffeoylquinicacid (**2**)	*C. scolymus* L.(l)(h)	(de Assis Carneiro *et al.*, 2017)/(Mutalib A.G Nasser, 2017)
1,4-*O*-dicaffeoylquinic acid (**3**)	*C. scolymus* L.(l)(h)	(Lattanzio *et al*., 2009)
1,5-*O*-dicaffeoylquinic acid (**4**)	*C. scolymus* L.(s)(l)	(Romani *et al*., 2006)/ (Fritsche *et al*., 2002)
3,5-*O*-dicaffeoylquinic acid (**5**)	*C. scolymus* L.(l)(h)	(Lattanzio *et al*., 2009)
4,5-di-*O*-caffeoylquinic acid (**6**)	*C. scolymus* L.(l)	(Zhu *et al.*, 2004)
3-*O*-caffeoylquinic acid (**7**)	*C. scolymus* L.(l)(h) *C. scolymus* L.(h)	(Azzini *et al*., 2007)/ (Jacociunas *et al*., 2014)/ (Fritsche *et al*., 2002)
4-*O*-caffeoylquinic acid (**8**)	*C. scolymus* L.(l)(h)	Lattanzio *et al*., 2009)
5-*O*-caffeoylquinic acid (**9**)	*C. scolymus* L.(l)(h)	(Garbetta *et al*., 2014)
Flavonoids		
Luteolin (**10**)	*C. scolymus* L.(l)(h)	(Nassar *et al*., 2013)
Luteolin 4-*O*-glucoside (**11**)	*C.* scolymus L.(l)	(Rangboo *et al.*, 2016)
Luteolin 7-*O*-glucoside (**12**)	*C.* scolymus L.(l) *C. cornigera*. (l)	(Shimoda *et al.*, 2003)/ (Elsayed *et al*., 2012)
Luteolin 7-*O*-glucoronide (**13**)	*C.cardunculus* L. var. *altilis* (l)(h)(s)	(Ramos *et al.*, 2014)
Luteolin-7-*O*-rutinoside (**14**)	*C.* scolymus L.(l) *C. cardunculus* L. var. *sylvestris*	(Pinelli *et al.*, 2007)
Luteolin 7-*O*-malonylglucoside (**15**)	*C. cardunculus* L. var. *sylvestris*. (l)	(Pinelli *et al*., 2007)

* Studied plant parts; (l): leaves, (s): stem, (h): head. Bold numbers show structure of compounds.

Table 1.2 (cont.): Phenolic compounds isolated from *Cynara* species

Compounds isolated	Plant species (*)	Reference
Apigenin (**16**)	*C. scolymus* L.(l)(h)	(Lattanzio *et al*., 2009)
Apigenin 7-*O*-glucoside (**17**)	*C. cornigera*. (l) *C. scolymus* L. (l)	(Elsayed *et al*., 2012)/ (Ben Salem *et al*., 2017)
Apigenin 7-*O*-glucoronide (**18**)	*C. scolymus* L.(h)	(Schutz *et al*., 2004)
Apigenin 7-*O*-rutinoside (**19**)	*C. scolymus* L.(l)	Pinelli *et al*., 2007)/ (Zhu *et al*., 2004)/
Apigenin-7-*O*-acetyl-glucoside (**20**)	*C. scolymus* L.(l)	(Farag *et al*., 2013)
Naringenin (**21**)	*C. cardunculus* L. var. *altilis* (h)	(Ramos *et al*., 2014)
Naringenin 7-*O*-glucoside (**22**) Naringenin 7-*O*-rutinoside (**23**)	*C. scolymus* L.(l)(h)	(Lattanzio *et al*., 2009)
Scopoletin (**24**)	*C. cardunculus* L. var. *altilis* (h)	(Ramos *et al*., 2014)
Anthocyanidins and anthocyanins		
Cyanidin (**25**) Peonidin (**26**) Delphinidin (**27**)	*C. scolymus* L.(h)	(Schütz *et al*., 2006)
Cyanidin 3,5-diglucoside (**28**)	*C. scolymus* L.(h)	(Lattanzio *et al*., 2009)/ (Schütz *et al*., 2006)
Cyanidin3,5-(3”-malonyl) diglucoside (**29**)	*C. scolymus* L.(h)	(Lattanzio *et al*., 2009)
Cyanidin 3-sophoroside (**30**) Cyanidin malonylsophoroside (**31**) Cyanidin 3-*O*-β-glucoside (**32**) Cyanidin3-(3”-malonyl) glucoside (**33**) peonidin 3-*O*-β-glucoside (**34**) Cyanidin 3-(6”-malonyl) glucoside (**35**) Peonidin 3-(6”-malonyl) glycoside (**36**)	*C. scolymus* L.(h)	(Schütz *et al*., 2006)

* Studied plant parts; (l): leaf, (h): head. Bold numbers show structure of compounds.

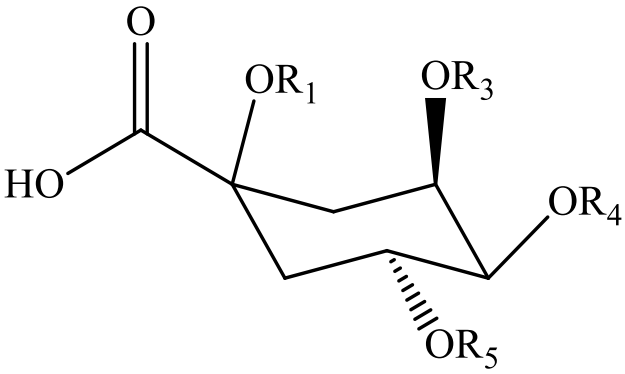

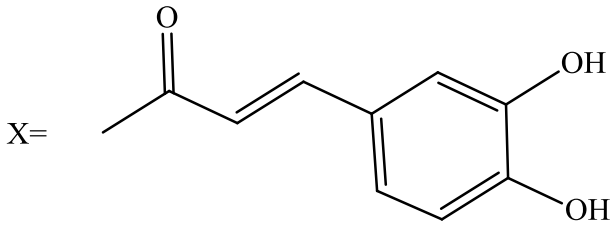

Compound	R1	R3	R4	R5
1	X	H	H	H
2	X	X	H	H
3	X	H	X	H
4	X	H	H	X
5	H	X	H	X
6	H	H	X	X
7	H	X	H	H
8	H	H	X	H
9	H	H	H	X

Figure 1. 2: Structures of caffeoylquinic acids

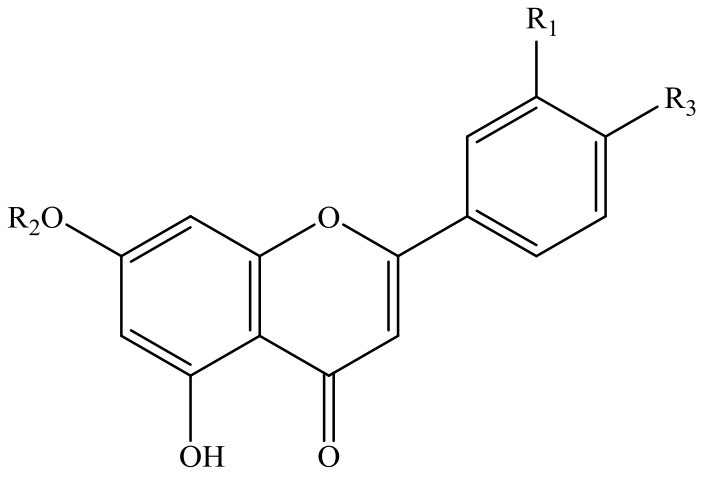

Compound	R_1	R_2	R_3
10	OH	H	OH
11	OH	H	X_1
12	OH	X_1	OH
13	OH	X_2	OH
14	OH	X_3	OH
15	OH	X_4	OH
16	H	H	OH
17	H	X_1	OH
18	H	X_2	OH
19	H	X_3	OH
20	H	X_5	OH

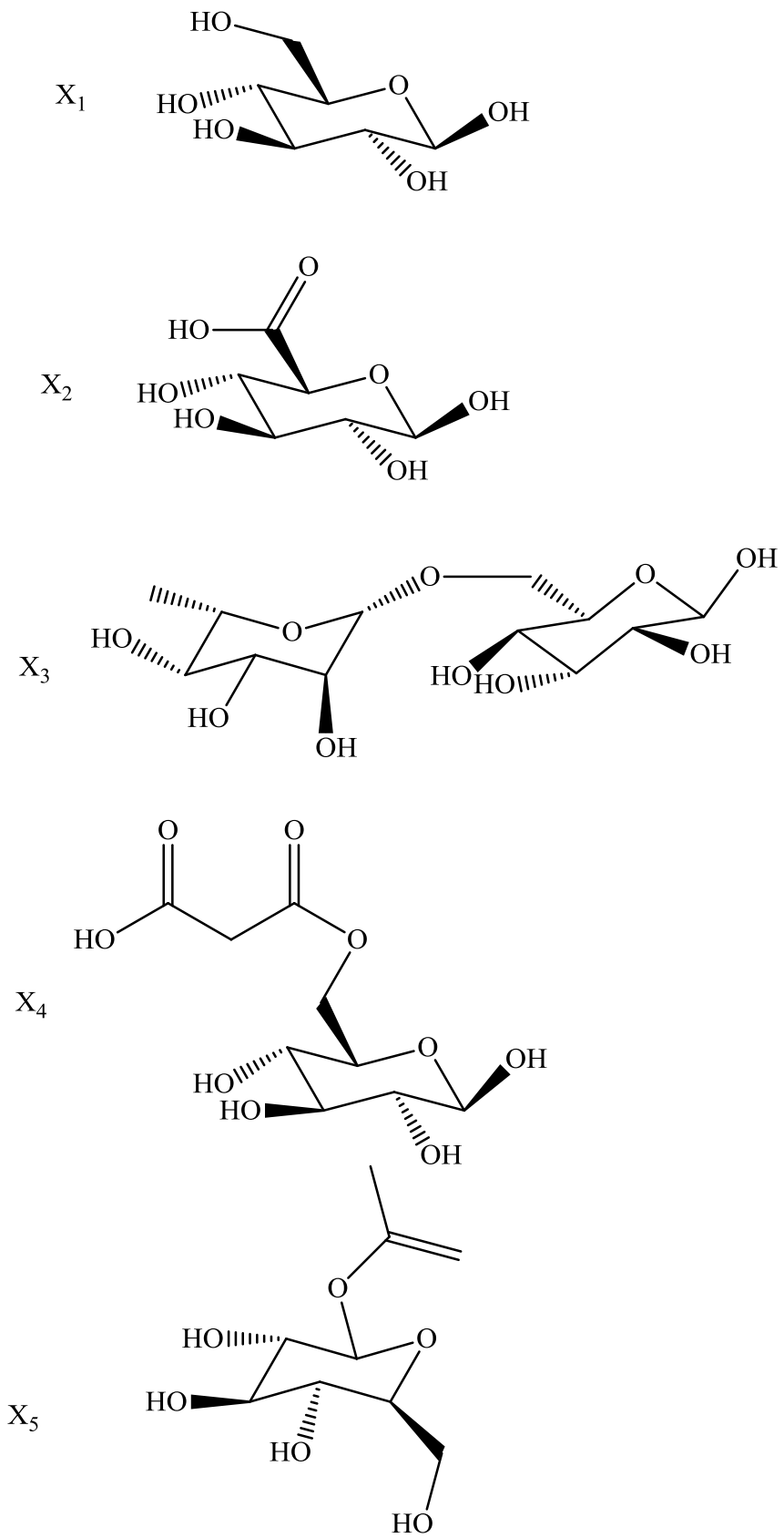

Figure 1. 3: Structures of flavonoids and flavonoid glycosides

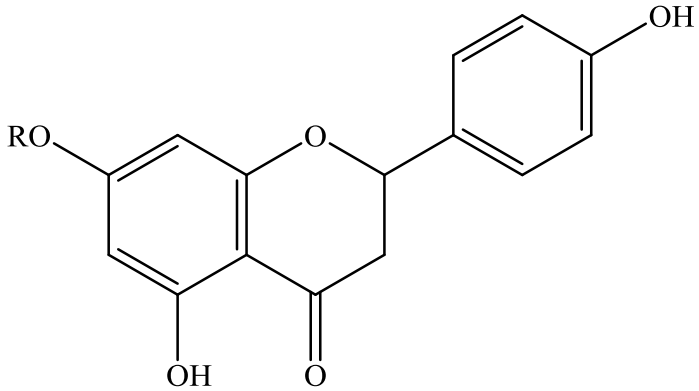

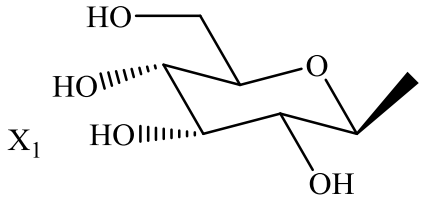

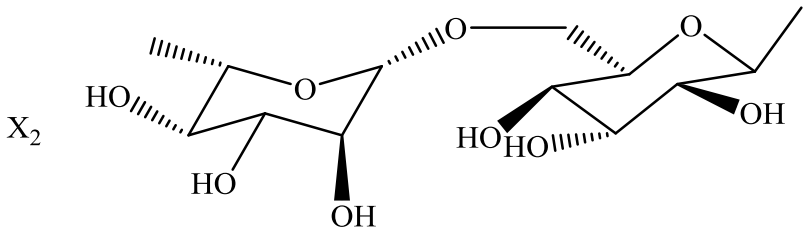

Compound	R
21	H
22	X_1
23	X_2

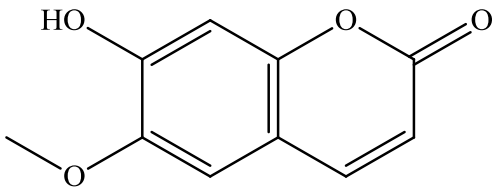

24

Figure 1.3 (cont.): Structures of flavonoids and flavonoid glycosides

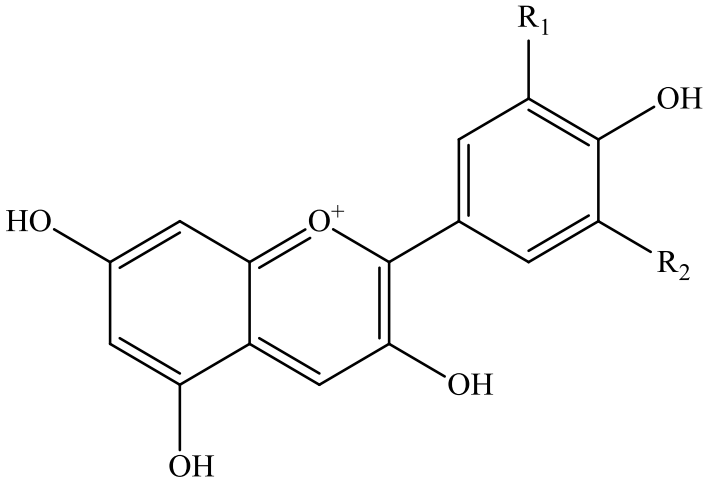

25 R_1 = OH R_2 = H
26 R_1 = OCH_3 R_2 = H
27 R_1 = OH R_2 = OH

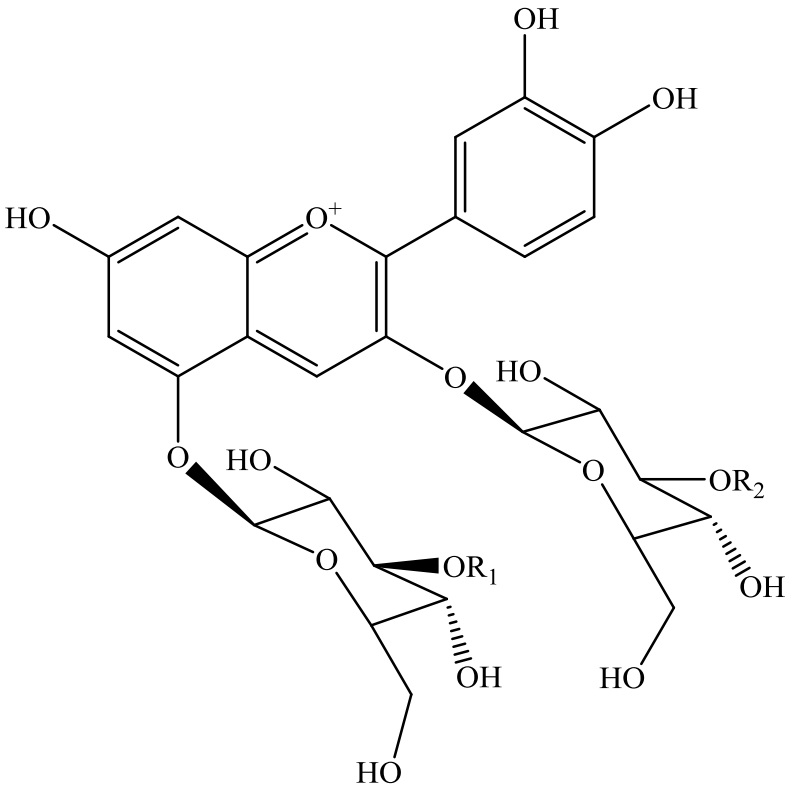

Compound	R_1	R_2
28	H	H
29	$COCH_2COOH$	$COCH_2COOH$

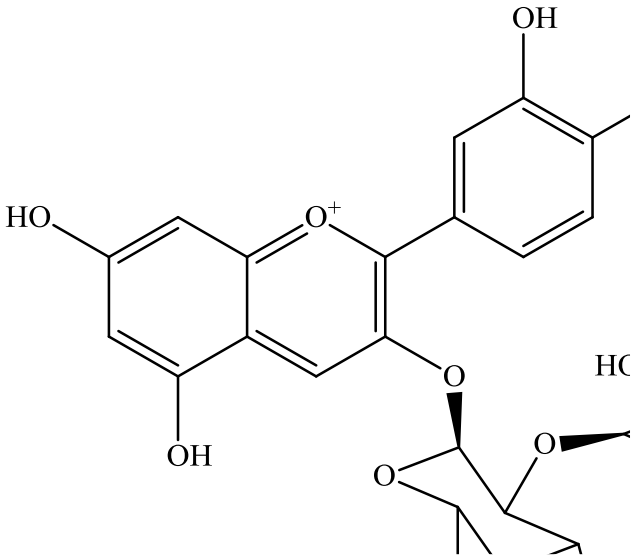

30 R = H
31 R = $COCH_2COOH$

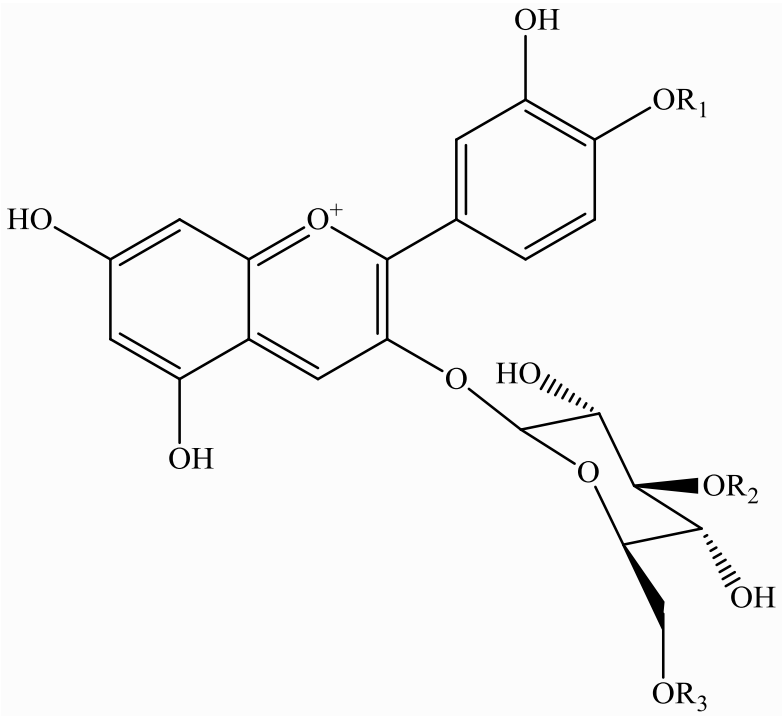

Compound	R_1	R_2	R_3
32	H	H	H
33	H	$COCH_2COOH$	H
34	CH_3	H	H
35	H	H	$COCH_2COOH$
36	CH_3	H	$COCH_2COOH$

Figure 1.4: Structure of anthocyanidins and anthocyanins

Table 1. 3: Terpenoid compounds isolated from *Cynara* species

Compounds isolated	Plant species (*)	Reference
Sesquiterpenes		
Aguerin B (**37**)	*C. scolymus* L.(l)	(Shimoda *et al*., 2003)
Cynaropicrin (**38**)	*C. cornigera*. (l)	(Hegazy *et al*., 2016)
Deacylcynaropicrin (**39**)	*C. cardunculus* L. var. *altilis* (l)	(Ramos *et al*., 2013)
Grosheimin (**40**)	*C. cardunculus* L. var. *altilis* (l)	(Ramos *et al*., 2013)
Cynarascoloside A (**41**) Cynarascoloside B (**42**) Cynarascoloside C (**43**)	*C. scolymus* L.(l)	(Shimoda *et al*., 2003)
β-Cubebene (**44**)	*C. scolymus* L.(h)(s)(r))	(Hădărugă *et al.*, 2009)
Guaianolides (sesquiterpenes lactones)		
8-deoxy-11-hydroxy-13-chlorogrosheimin (**45**)	*C. scolymus* L.(l)	(Fritsche *et al*., 2002)
8-deoxy-11,13-dihydroxygrosheimin (**46**)		(Fritsche *et al*., 2002)
Solstitialin (**47**)	*C. humilis* L.(ap)	(Reis *et al.*, 1992)
13-chlorosolstitialin (**48**)	*C. cornigera*. (l)	(Hegazy *et al*., 2016)
3-acetyl-13-chlorosolstitialin (**49**) ll,13-epoxysolstitialin (**50**)	*C. humilis* L.(ap)	(Reis *et al*., 1992)
Triterpenes		
Cynarasaponin A (**51**) Cynarasaponin B (**52**) Cynarasaponin C (**53**) Cynarasaponin D (**54**) Cynarasaponin E (**55**) Cynarasaponin F (**56**) Cynarasaponin G (**57**) Cynarasaponin H (**58**) Cynarasaponin I (**59**) Cynarasaponin J (**60**)	*C. scolymus* (l)	(de Falco *et al.*, 2015)

* Studied plant parts; (l): leaf, (s): stem, (h): head, (ap): aerial parts, (r): root. Bold numbers show structure of compounds.

Table 1.3 (cont.): Terpenoid compounds isolated from *Cynara* species

Compounds isolated	Plant species (*)	Reference
α amyrin (**61**) α amyrin acetate (**62**) β amyrin (**63**) β amyrin acetate (**64**) Lupeol (**65**) Lupenyl acetate (**66**) ψ-Taraxasterol (**67**) ψ -Taraxasteryl acetate (**68**)	*C. cardunculus* L. var. *altilis* (l)(s)(h)	(Ramos *et al*., 2013)
Taraxasterol (**69**)	*C. cardunculus* L. var. *altilis* (l)(s)(h) *C. scolymus* L.(r)	(Shakeri and Ahmadian, 2014)/ (Shakeri and Ahmadian, 2014)
Taraxasteryl acetate (**70**)	*C. cardunculus* L. var. altilis (l)(s)(h)	(Ramos *et al*., 2016)(Ramos *et al*., 2017)
Inulin (**71**)	*C. scolymus* L.(l)(h)	(Lattanzio *et al*., 2009)

* Studied plant parts; (l): leaf, (s): stem, (h): head, (r): root. Bold numbers show structure of compounds.

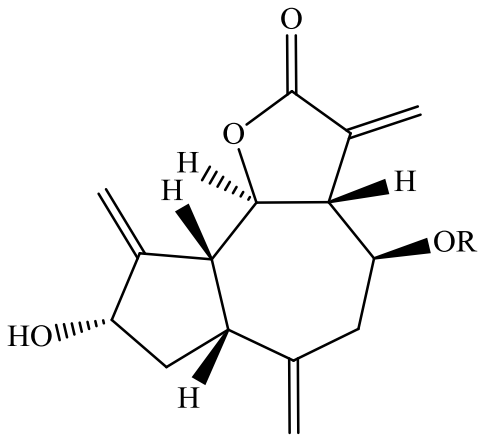

Compound	R
37	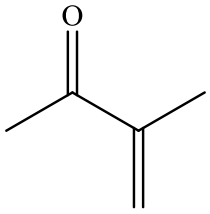
38	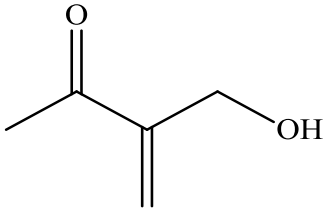
39	OH

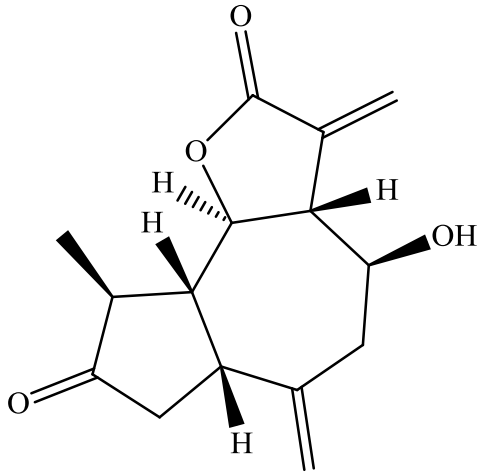

40

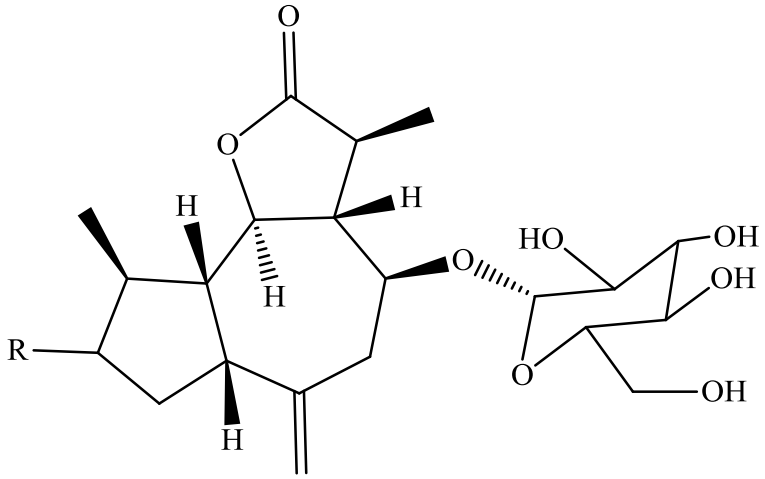

41 OH

42 OH

R = **43** O

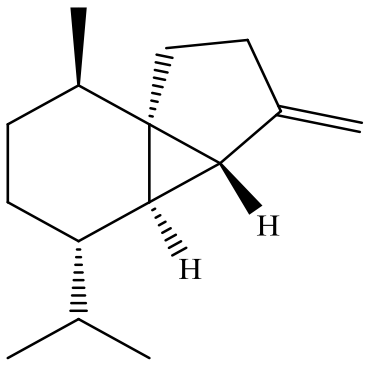

44

Figure 1. 4: Structures of sesquiterpene and sesquiterpene glycosides

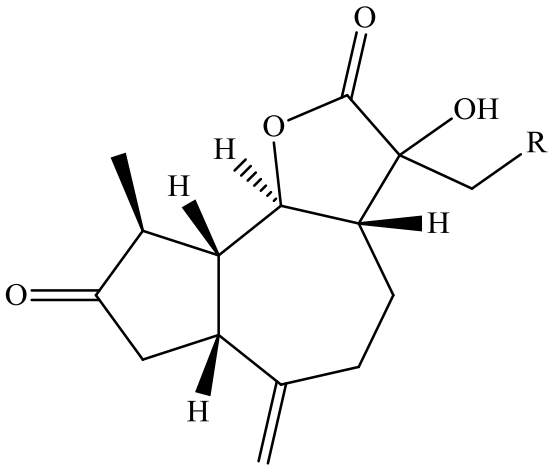

45 R = Cl
46 R = OH

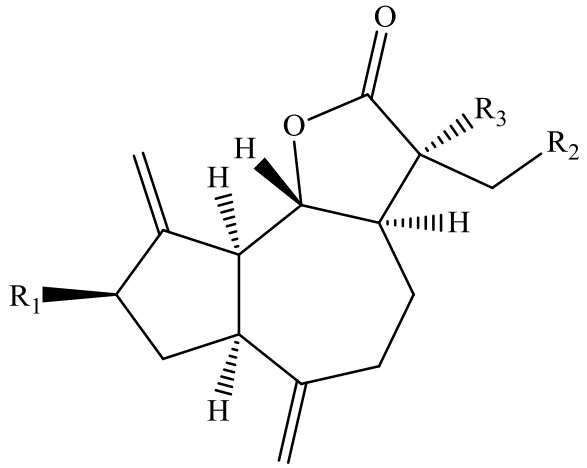

Compound	R_1	R_2	R_3
47	OH	OH	OH
48	OH	Cl	OH
49	OAc	Cl	OH

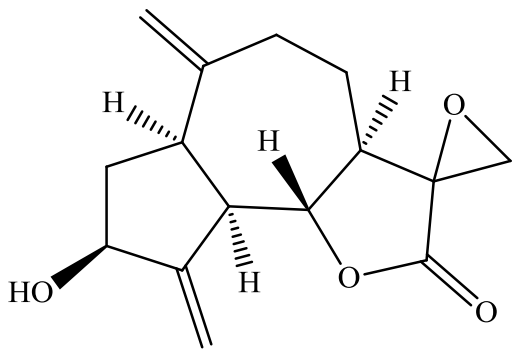

50

Figure 1. 5: Structure of sesquiterpenes lactones

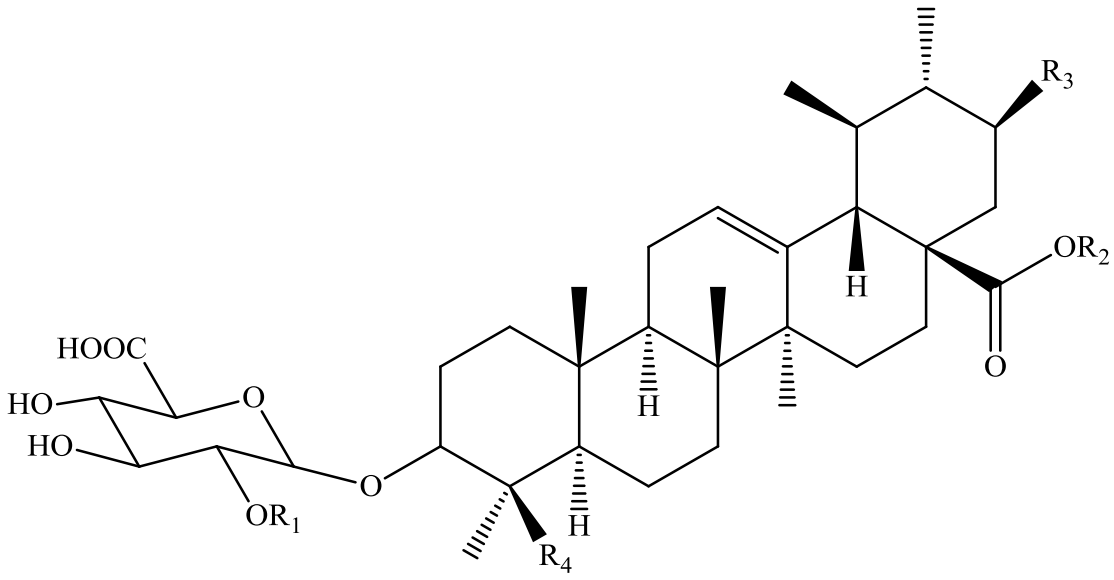

Compound	R_1	R_2	R_3	R_4
51	Arabinose	Glucose	H	CH_3
52	Arabinose	H	H	H
53	H	Glucose	H	CH_3
54	Arabinose	Glucose	H	CH_2OH
55	H	CH_3	H	CH_2OH
56	Arabinose	H	OH	H
57	Arabinose	Glucose	OH	H

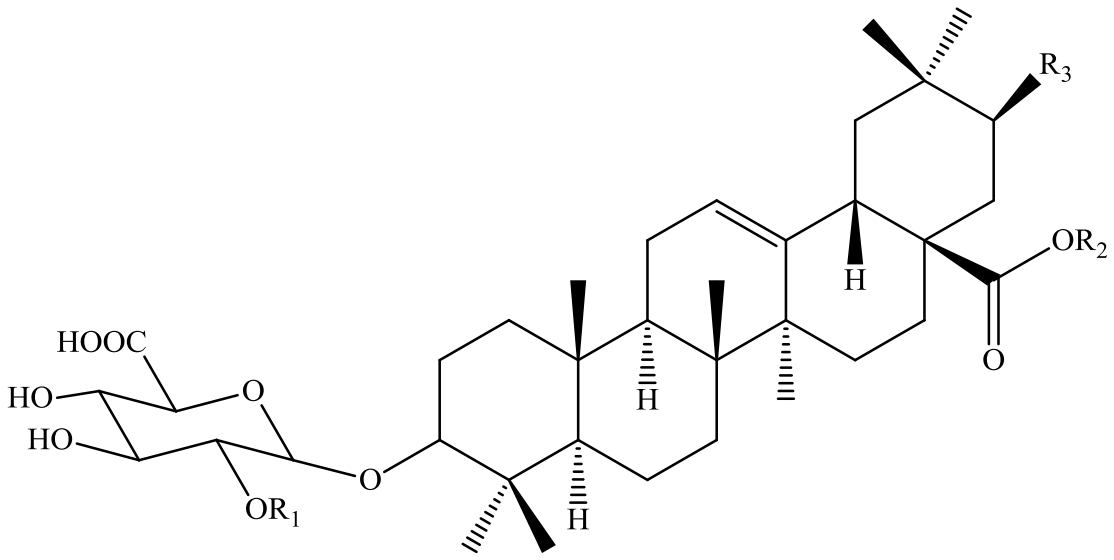

Compound	R_1	R_2	R_3
58	Arabinose	Glucose	H
59	Arabinose	H	OH
60	Arabinose	Glucose	OH

Figure 1. 6: Structure of cynarasaponins

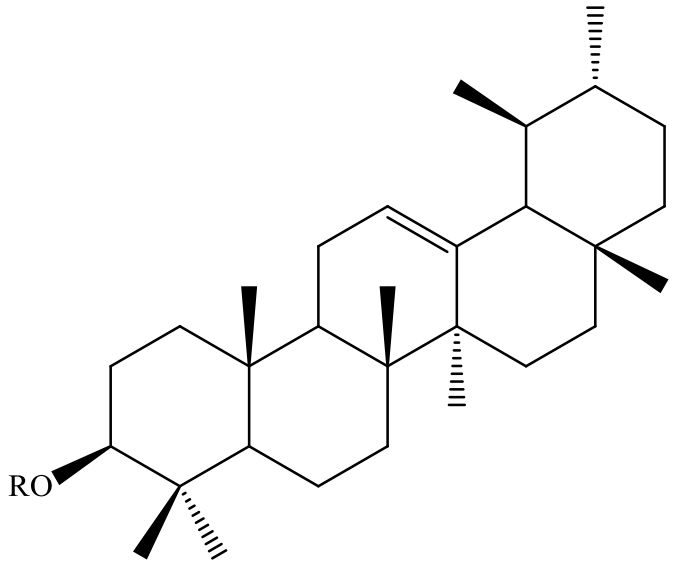

61 R = H
62 R = $COCH_3$

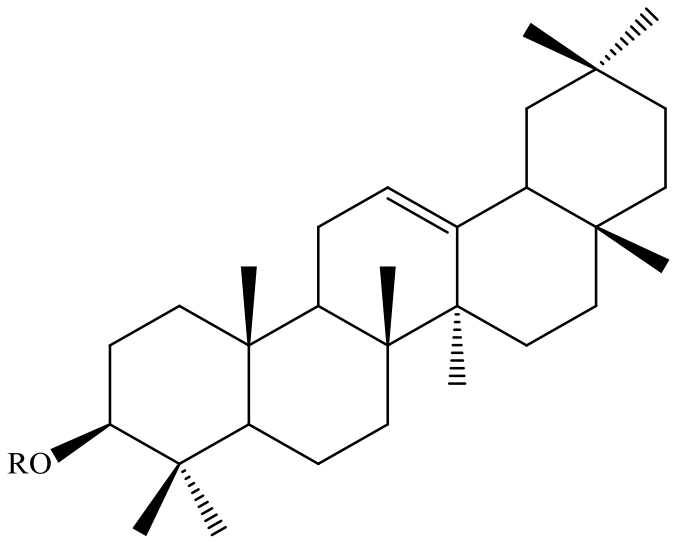

63 R = H
64 R = $COCH_3$

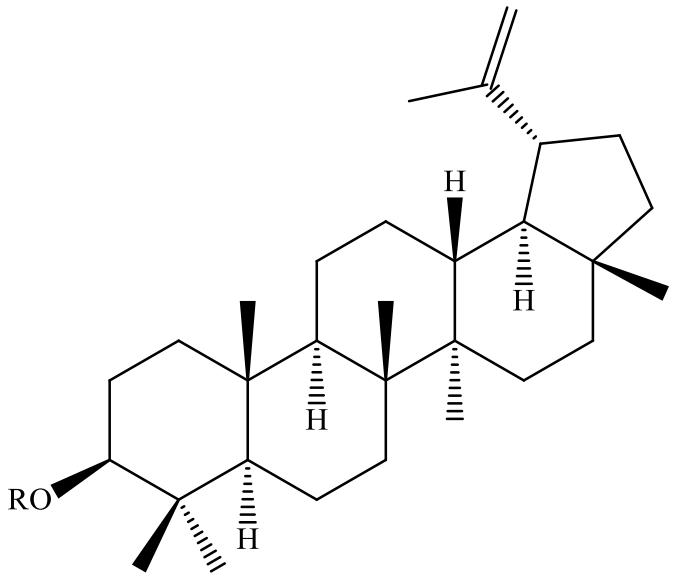

65 R = H
66 R = $COCH_3$

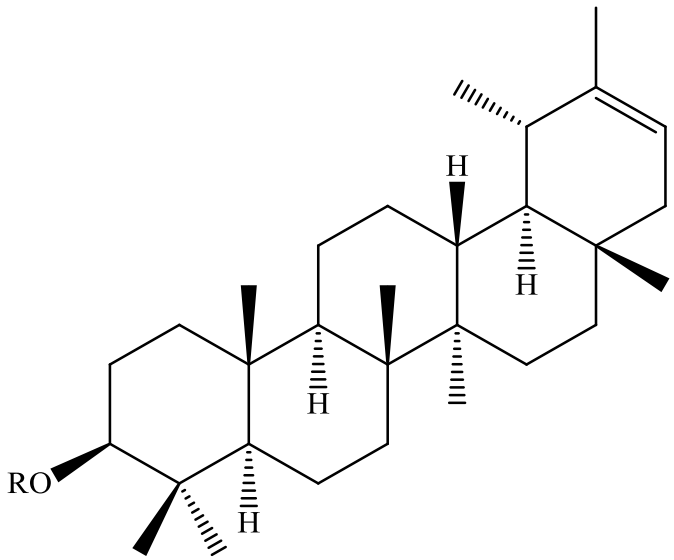

67 R = H
68 R = $COCH_3$

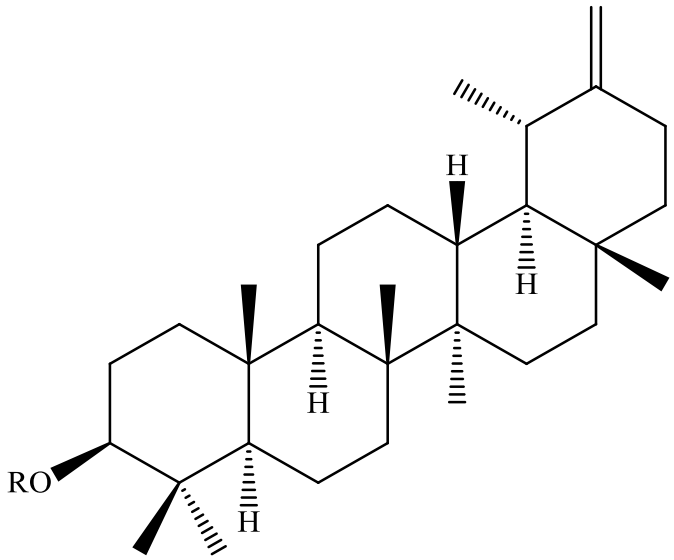

69 R = H
70 R = $COCH_3$

Figure 1. 7: Structures of triterpenes

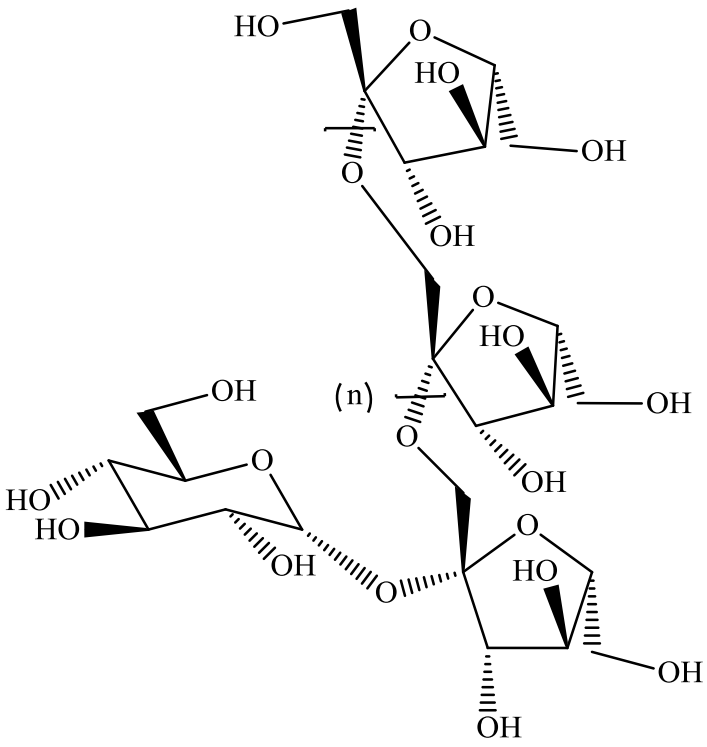

71

Figure 1. 8: Structure of inulin

1.2.1.3 Previous pharmacological reports on Cynara L.

Most of the aforementioned compounds and/or crude extracts were tested for their activities in various biological studies. This section includes these studies by addressing them according to each plant species. There are no published studies reporting any medicinal activities for *C. cyrenaica*, however, some other *Cynara* species especially *C. cardunculus* (L.) subsp. *scolymus* (L) Hegi, which is the globe artichoke have been studied widely for bioactive phytochemicals.

C. cardunculus (L.) subsp. *scolymus* (L) Hegi (*C. scolymus.* L*)* have been used in traditional medicine for their recognised therapeutic effects such as anticholesterol, hepatoprotective, antioxidative, anticarcinogenic, urinative, antibacterial, glycaemia reduction which are linked principally to the high content of polyphenolic compounds, including flavonoids and mono- and di-caffeoylquinic acids. All these compounds have strong antioxidant properties and protect low-density lipoproteins from oxidative damage (Ciancolini *et al.*, 2013; Fratianni *et al.*, 2007; Garbetta *et al.*, 2014). It has been reported that the ethanol extract of *C. scolymus* leaves and rhizomes showed antioxidant and antimicrobial activities (Vamanu *et al.*, 2011; Alghazeer *et al.*, 2012). Soofiniya (2011) reported the antidiabetic and hypolipidemic effects of *C. scolymus* leaf aqueous extract on streptozotocin-induced diabetic rats, since the oral administration of the extract for 21 days exhibited significant reduction in total cholesterol, triglyceride, low-density lipoprotein cholesterol, very low-density lipoprotein cholesterol and hyperglycemia in treated diabetic rats, compared with a diabetic control group.

Salem *et al.* (2015) reported that caffeoylquinic acid **2** stimulated the production of bile, which enabled fats to be digested and absorption of vitamins from food to occur. This was further confirmed by studies which showed that *C. scolymus* leaf aqueous extract could be very helpful for people suffering from irritable bowel syndrome (IBS) and dyspepsia. In a study carried out at the University of Reading, UK, 208 adults suffering from IBS and dyspepsia were subjected to intervention with the extract and were monitored over two months. At the end of the trial, the results showed a 26.4 % reduction in IBS incidence among the participants and the dyspepsia symptoms had decreased by 41 % after treatment. Also, a methanol extract of *C. scolymus* heads showed gastroprotective activity (Nassar *et al.*, 2013). El Sohafy *et al.* (2016) reported that the ethanol extract of *C. cornigera* aerial parts exhibited hepatoprotective activity.

Compound **64** was found to have an anti-inflammatory effect by decreasing the secretion of tumour necrosis factor (TNF-a) at low concentrations (Ding *et al.*, 2009), and triterpenes (**61**, **63**,**65**, **67**and **69**) have been reported to have an anti-inflammatory effect against 12-*O*-tetradecanoylphorbol-13-acetate (TPA) induced inflammation (1 µg per ear) in mice. The results showed that the sample completely inhibited TPA-induced inflammation in a dose-dependent manner (Akihisa *et al.*, 1996). Krimkova *et al*. (2004) reported that triterpenes (**51**, **52** and **58**) exhibited a reduction of chemically induced mutagenesis *in vitro*. The isolated caffeoylquinic acids (**2** and **7)** and flavonoids (**10** and **11)** from *C. scolymus* L. leaf liquid extract exhibited antioxidative effects (Fritsche *et al.*, 2002). Sesquiterpenes (**37**, **38** and **40**) from the methanolic extract of *C. scolymus* L. leaves were found to possess potent anti-hyperlipidemic activity by suppressing serum triglyceride elevation (Shimoda *et al*., 2003). Cynaroside (**11)** was isolated from the ethyl acetate extract of *C. cornigera* leaf and showed antioxidant and hepatoprotective activity (Elsayed *et al*., 2012). The flavonoids (**13**, **12**, **17** and **19**) and caffeoylquinic acids (**2**,**5**,**6** and **7**) isolated from *C. scolymus* L. leaf were found to exhibit antimicrobial activity against *Bacillus subtilis, Staphylococcus aureus, Agrobacterium tumefaciens, Micrococcus luteus, Escherichia coli, Salmonella typhimurium, Pseudomonas aeruginosa, Candida albicans, Candida lusitaniae, Saccharomyces cerevisiae, Saccharomyces carlsbergensis, Aspergillus niger, Penicillium oxalicum, Mucor mucedo and Cladosporium cucumerinum* (Zhu *et al*., 2004). Cynaropicrin **38** which was first isolated in 1960 from artichoke *C. scolymus* L and was found to exhibit potential activity against all genotypes of hepatitis C virus and showed a wide range of other pharmacologic properties such as anti-hyperlipidemic, anti-trypanosomal, anti-malarial, antifeedant, antispasmodic, anti-photoaging, anti-tumour action, and anti-inflammatory properties (Elsebai *et al*., 2016). For anticarcinogenic activity, green leaf of cultivated C. *cardunculus* (var. *altilis*) methanolic extract exhibited inhibition of angiogenesis, tumour cell viability and migration capacity in a breast tumour cell line (MDA-MB-231) and exhibited antioxidant effects as it showed a high capacity to scavenge 2,2-diphenylpicrylhydrazyl (DPPH) free radicals (Velez *et al.*, 2012).

1.3 The genus *Cyclamen* L.

The genus *cyclamen* L. (Primulaceae) is represented by around 20 wild and cultivated species (Speroni *et al.*, 2007). The major commercial plant is *C. persicum* Mill (Ishizaka *et al.*, 2002). The genus *cyclamen* L. (Primulaceae) is rich in saponins which are known to have interesting biological activities (El Hosry *et al.*, 2014). It has been reported that *cyclamen* tubers have been used in folk medicine for a wide range of activity such as cytotoxicity, analgesic, antimicrobial, spermicidal, and anti-inflammatory properties (El Hosry *et al*., 2014).

Table 1. 4: Geographical distribution of *Cyclamen* species (Mazouz and Djeddi, 2013)

Species	Geographical distribution
C. africanum Boiss & Reut	Algeria (N) and Tunisia (NW)
C. balearicum Willk	France (S), Spain (Balearic island)
C.cilicium Boiss & Heldr	Turkey (S)
C. colchicum	Georgia
C. coum Mill	Armenia, Azerbaijan, Bulgaria (E), Georgia, Iran, Lebanon, Russia, Syria (W), Turkey
C. certicum	Greece (Crete, Karpathos)
C. cyprium Kotschy	Cyprus
C. graecum Link	Cyprus, Greece, Turkey
C. hederifolium Aiton	Albania, France (Corsica), Greece (Crete), Italy (Sardinia, Sicily), Switzerland, Turkey (W), Yugoslavia (Former)
C. intaminatum	Turkey (W and SW)
C. libanoticum Hildebr	Lebanon
C. mirabile Hildebr	Turkey
C. parviflorum Poped	Turkey (NE)
C. persicum Mill	Algeria, Cyprus, Greece (E of Crete, Karpathos, E of Aegean IS, Rhodes), Jordan, Lebanon, Syria (W), Tunisia (N), Turkey (S)
C. pseudibericum Hildebr	Turkey (S)
C. purpurascens Mill	Austria, Czech Republic, France (E), Germany (S), Hungary, Italy (N), Poland (S), Slovakia, Switzerland,Yugoslavia (Former).
C. repandum	France (SE of Corsica), Greece, Italy (Sardinia), Switzerland (S), Yugoslavia (Former).
C. rohfsianum Asch	Libya (N)
C. somalense Thulin & Warfa	Somalia (N)
C. trochopteranthum	Turkey

N: North; E: East; W: west; S: South; IS: Island

1.3.1 Cyclamen rohlfsianum Aschers

C. rohlfsianum is one of the *Cyclamen* species that belongs to the Primulaceae family and is an endemic plant growing in Libya in the wilds of al-Jabal al-Akdar, collected from Wadi Alkuf region, locally known as Rakaf (El-Mokasabi, 2014).

Figure 1. 9: *Cyclamen rohlfsianum*
(http://www.flickr.com/photos/tiggrx/10570158013/)

It grows in scrubby and rocky habitats (Phillipson, 2001; Oliver-Bever, 1983). *C. rohlfsianum* is a very distinct species with roots appearing all over the lower surface and leaves that have growing points distributed over the upper surface in the summer, with kidney-shaped and broad triangular dentate lobes. The upper surface appears shiny bright green, with an irregular silver-grey marbling in an uneven band and the lower surface of the leaves is either purplish or red (Figure 1.10) (Phillipson, 2001).

1.3.2 Traditional use

It is used in folk medicine to treat diabetes and the tuber is used by local Bedouin in a fermentation process of milk for cheese production (Elabbar *et al*., 2014). In addition, it is reported that *C. rohlfsianum* is used traditionally to treat anaemia and abscess (El-Mokasabi, 2014).

1.3.3 Previous phytochemical studies

The only chemical study on the plant was carried out by Elabbar *et al*. (2014) that revealed the presence of triterpenoids, phenolics, saponins and steroidal compounds. See Tables 1.5 and 1.6 and Figures 1.11 to 1.15 for the compounds isolated from *Cyclamen* species.

Table 1. 5: Terpenoid compounds isolated from *Cyclamen* species

Compounds isolated	Plant species (*)	Reference
triterpenoid		
Oleanolic acid (**1**)	*C. rohlfsianum* (ap)	(Elabbar *et al*., 2014)
Triterpene saponins		
Hederifolioside A (**2**) Hederifolioside B (**3**) Hederifolioside C (**4**) Hederifolioside D (**5**) Hederifolioside E (**6**)	*C. hederifolium* (t)	(Altunkeyik *et al*., 2012)
Cyclaminorin (**7**)	*C. mirabile* (t)	(Calis *et al*., 1997)
Deglucocyclamin (**8**)	*C. persicum* (t) *C. libanoticum* (t)	(El Hosry *et al*., 2014)
Cyclacoumin (**9**)	C. mirabile (t)	(Calis *et al*., 1997)
Cyclamin (**10**)	*C.purpurascens* (t)	(Winder *et al*., 1995)
Isocyclamin (**11**)	*C. mirabile* (t)	(Calis *et al*., 1997)
Mirabilin (**12**)	*C. repandum* (t)	(Calis *et al*., 1997)
Lysikokianoside (**13**) Anagalloside B (**14**) Deglucoanagalloside B (**15**)	*C. repandum* (t)	(Speroni *et al*., 2007)/
Coumoside A (**16**)	*C. repandum* (t)	(Yayli *et al*., 1998)
Coumoside B (**17**)	*C. repandum* (t)	(Speroni *et al*., 2007)/ (Dall'Acqua *et al*., 2010)
Repandoside (**18**)	*C. repandum* (t)	(Dall'Acqua *et al*., 2010)
Sterols		
Stigmasterol (**19**) Poriferasterol (**20**) Stigma-or poriferosta-Δ3,5,22-triene [(22E)-24-ethylcholesta- Δ3,5,22-triene] (**21**) Stigma-or poriferosta-Δ3,5,7,22-tetrane [(22E)-24-ethylcholesta- Δ3, 5,7,22-tetrane] (**22**)	*C. coum*	(Yayli and Baltaci, 1996)

* Studied plant parts; (t): tuber, (ap): ariel parts. Bold numbers show structure of compounds.

Table 1. 6: Phenolic compounds isolated from *Cyclamen* species

Compounds isolated	Plant species (*)	Reference
Flavonoids		
7, 8, 4`-trihydroxyflavone (**23**) Genistein (**24**) Hesperetin (**25**) Kaempferol (**26**)	*C. rohlfsianum* (t)	(Elabbar *et al*., 2014)
Anthocyanidins and anthocyanins		
Cyanidin (**27**) Peonidin (**28**) Delphinidin (**29**) Malvidin (**30**) peonidin 3-*O*-neohesperidoside (**31**) Cyanidin neohesperidoside (**32**) Pelargonidin 3-*O*-neohesperidosides (**33**) **Flavonoid glycoside** Quercetin 3-*O*-2^{G}rhamnosylrutinoside (**34**)	*C. persicum* (p)	(Webby and Boase, 1999)

* Studied plant parts; (t): tuber, (p): petals. Bold numbers show structure of compounds.

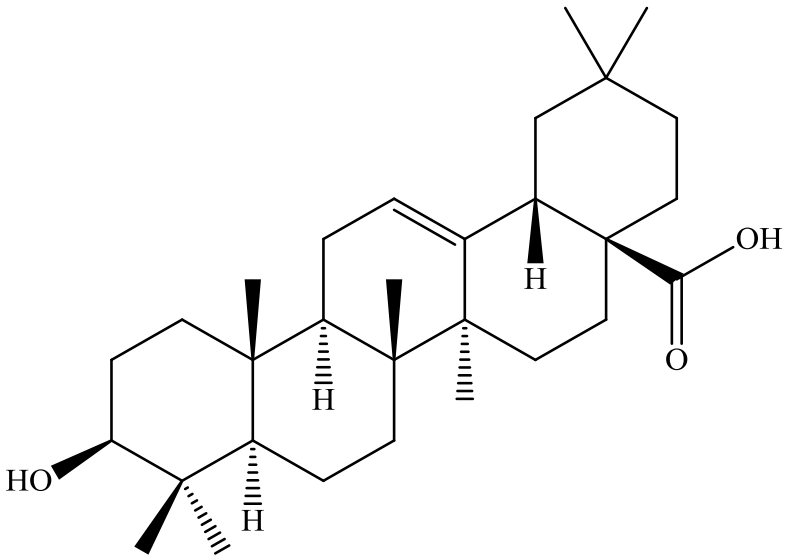

1

Figure 1. 10: Structure of oleanolic acid

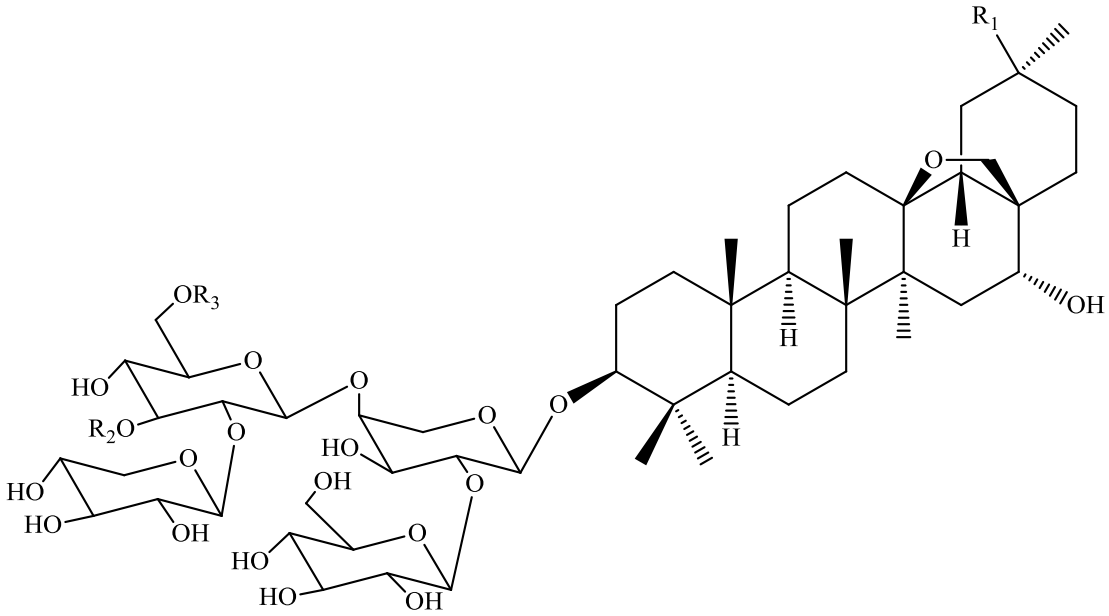

Compound	R_1	R_2	R_3
2	COOH	H	H
3	COOH	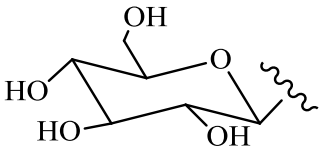	H
4	CHO	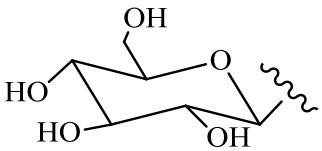	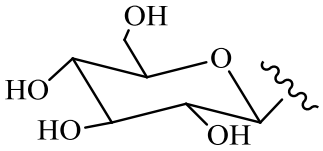

Figure 1. 11: Structure of triterpene saponins

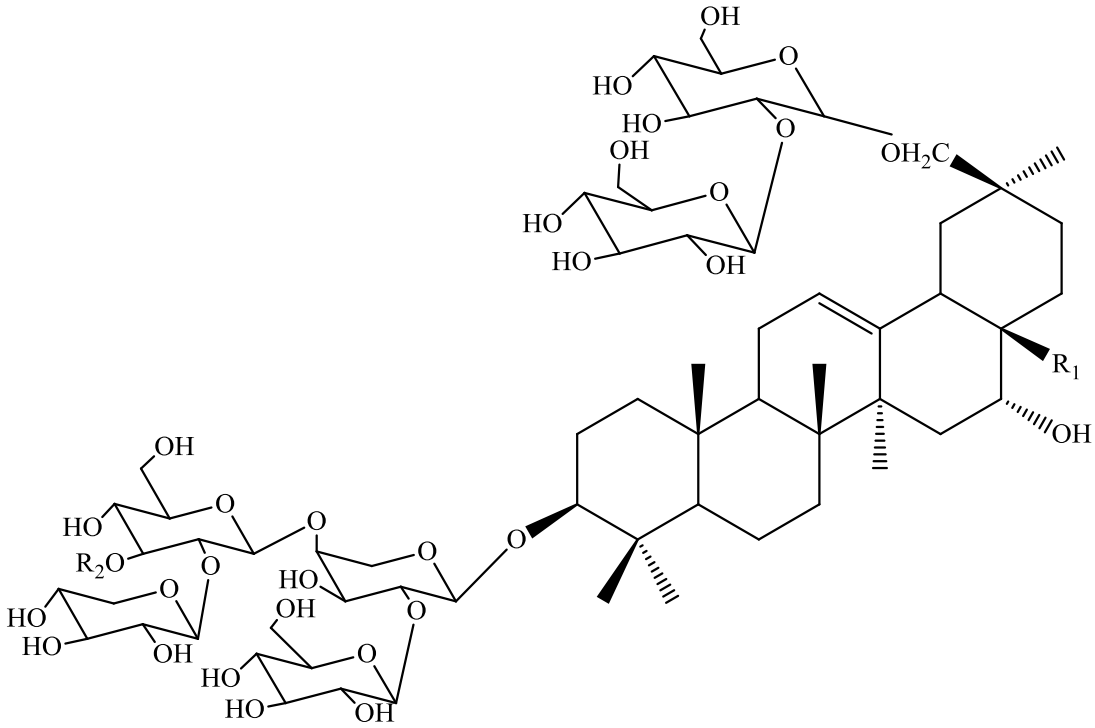

5 R_1 = CHO R_2 = H

6 R_1 = CH_2OH R_2 =

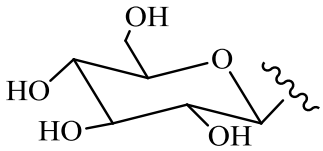

Figure 1.12 (cont.): Structure of triterpene saponins

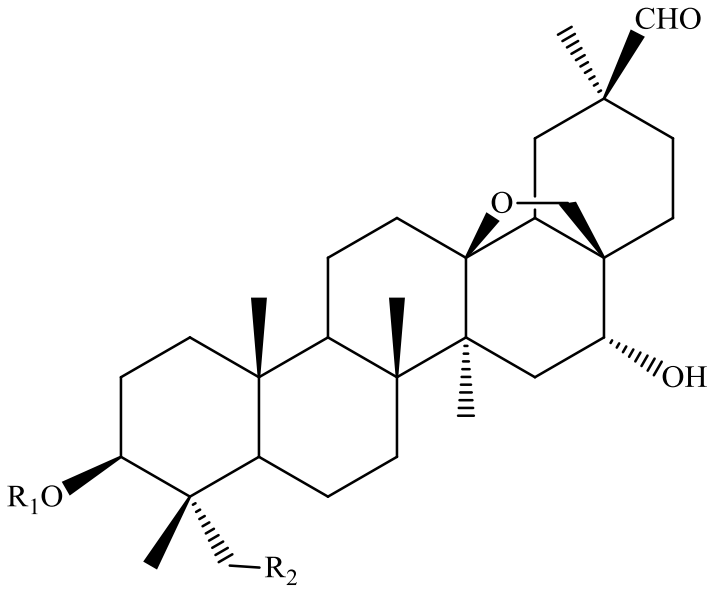

7 R_1 = a; R_2 = H
8 R_1 = b; R_2 = H
9 R_1 = b; R_2 = OH
10 R_1 = c; R_2 = H
11 R_1 = d; R_2 = H

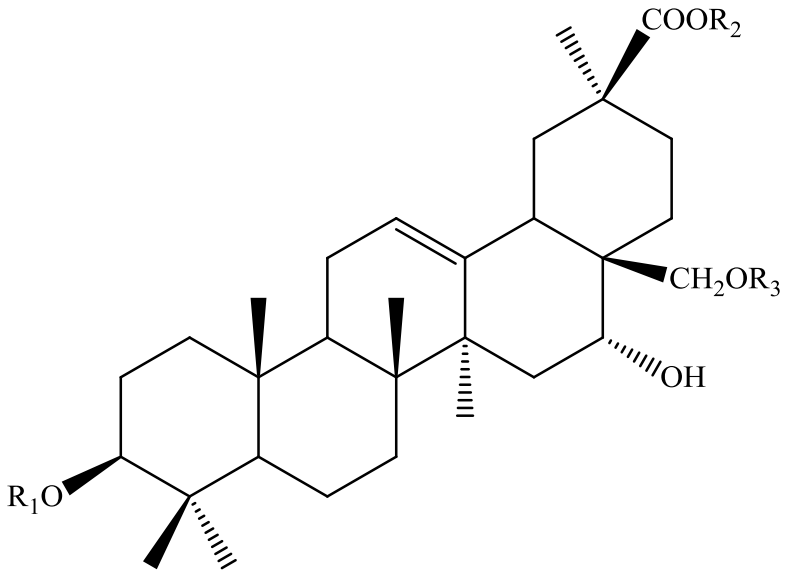

12 R_1 = d; R_2 = H; R_3 = H

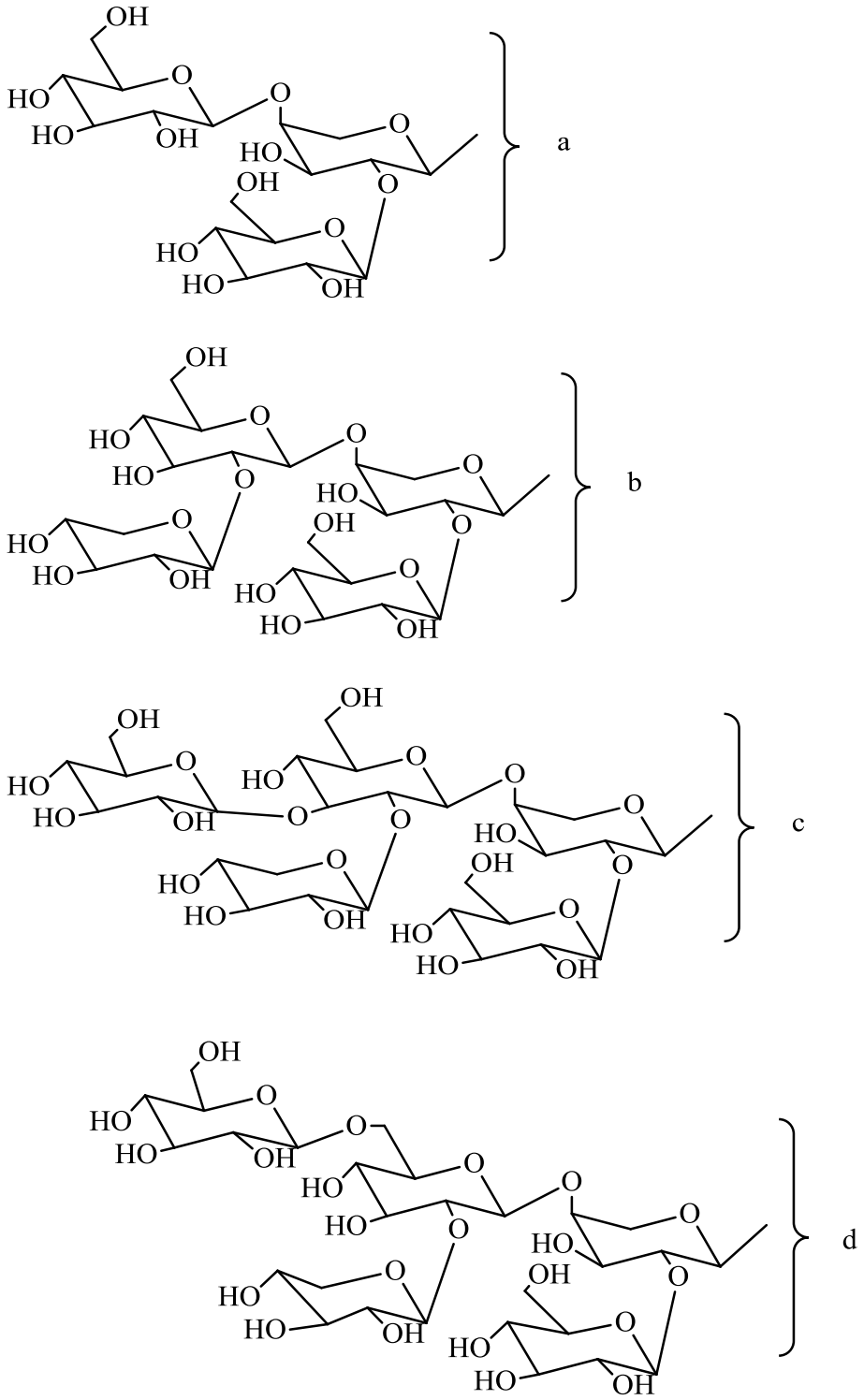

Figure 1.12 (cont.): Structure of triterpene saponins

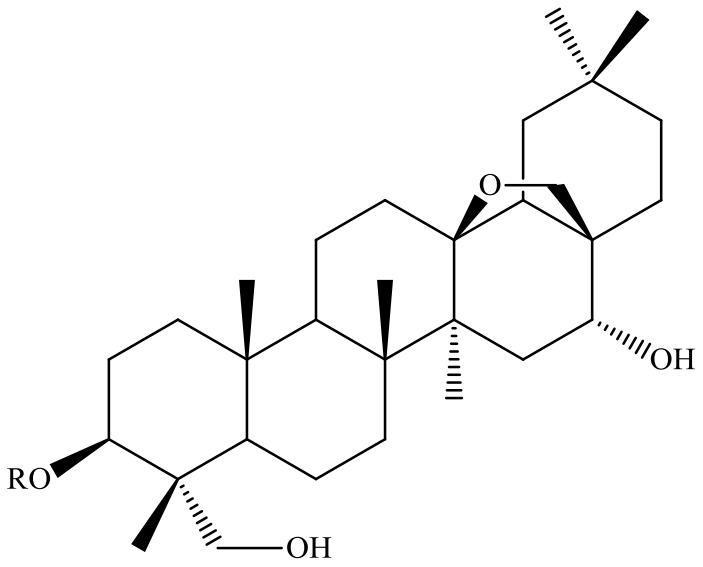
O
OH
RO
OH

13 **R =**

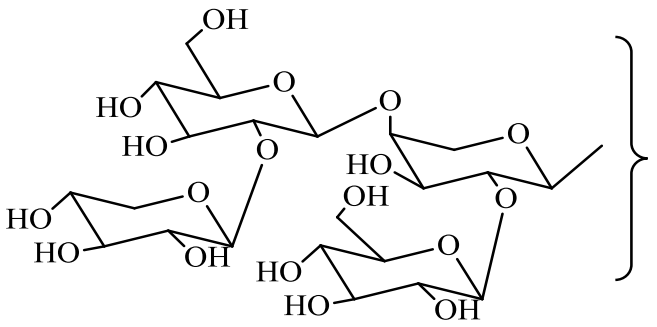
OH
HO
HO
O
O
O
O
HO
OH
O
HO
HO
OH
O
HO
HO
OH
O

14 **R =**

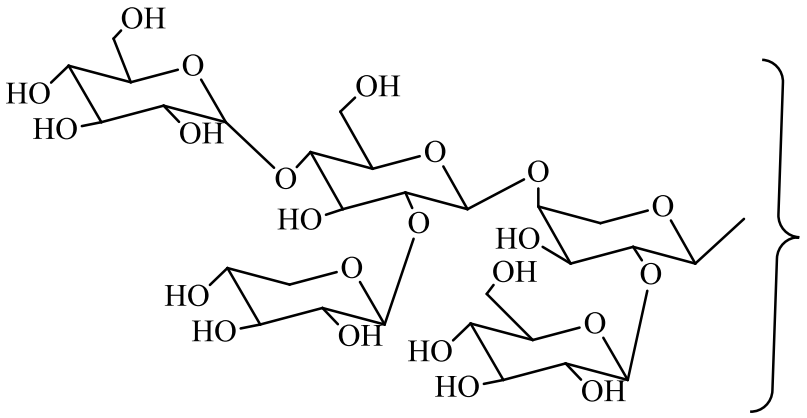
OH
HO
HO
OH
O
OH
O
O
O
HO
O
HO
O
O
HO
OH
O
HO
HO
OH
O
HO
HO
OH

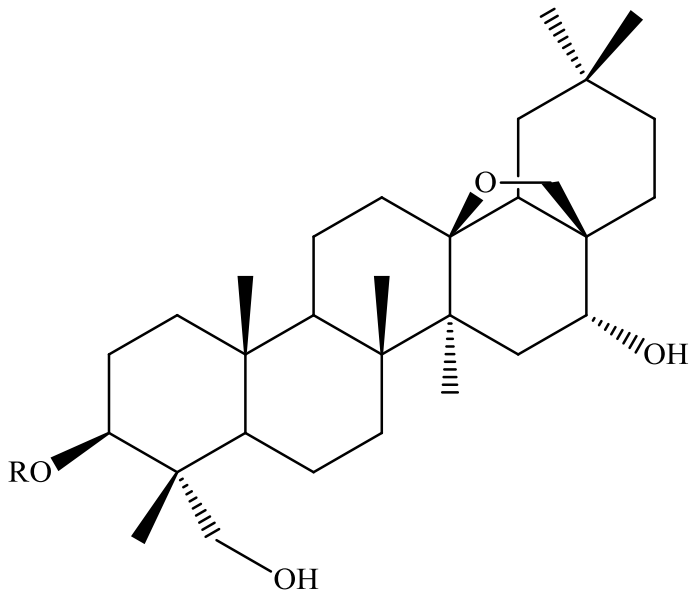

15 **R =** 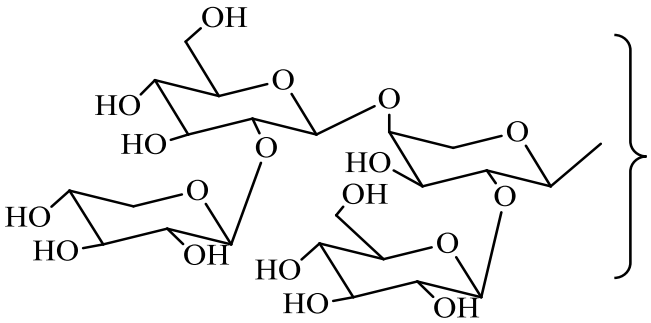

Figure 1.12 (cont.): Structure of triterpene saponins

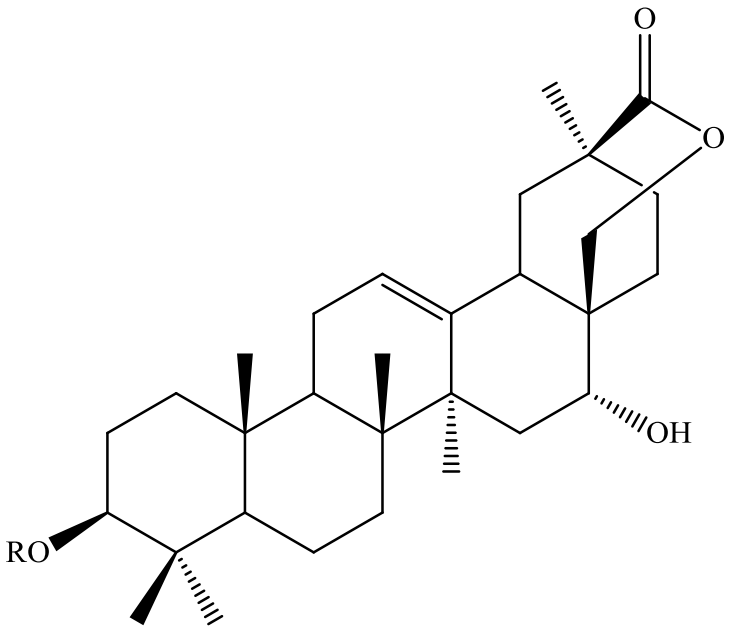
O
O
OH
RO

16 **R =**

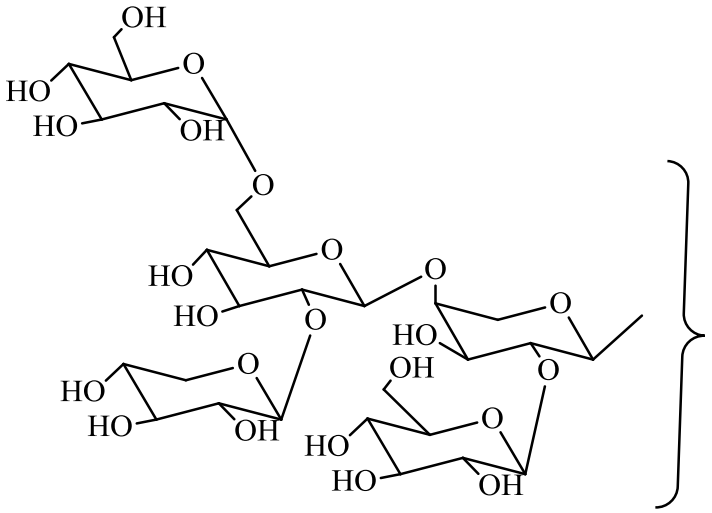
OH
O
HO
HO
OH
O
O
HO
HO
O
O
O
HO
OH
O
O
HO
HO
OH
O
HO
HO
OH

17 **R =**

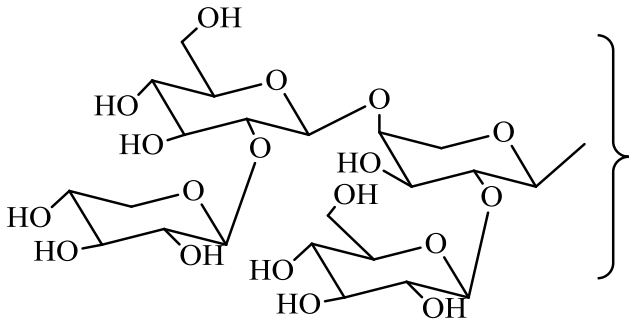
OH
O
HO
HO
O
O
O
HO
OH
O
O
HO
HO
OH
O
HO
HO
OH

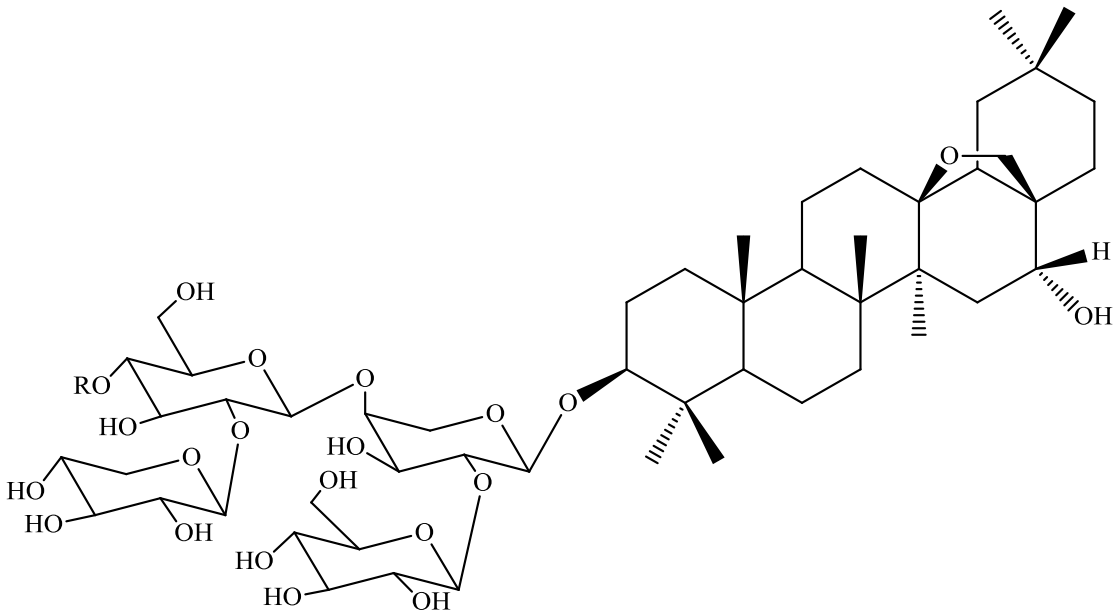

18 R =

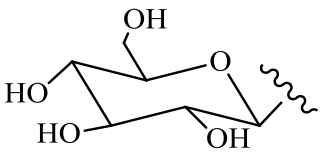

Figure 1.12 (cont.): Structure of triterpene saponins

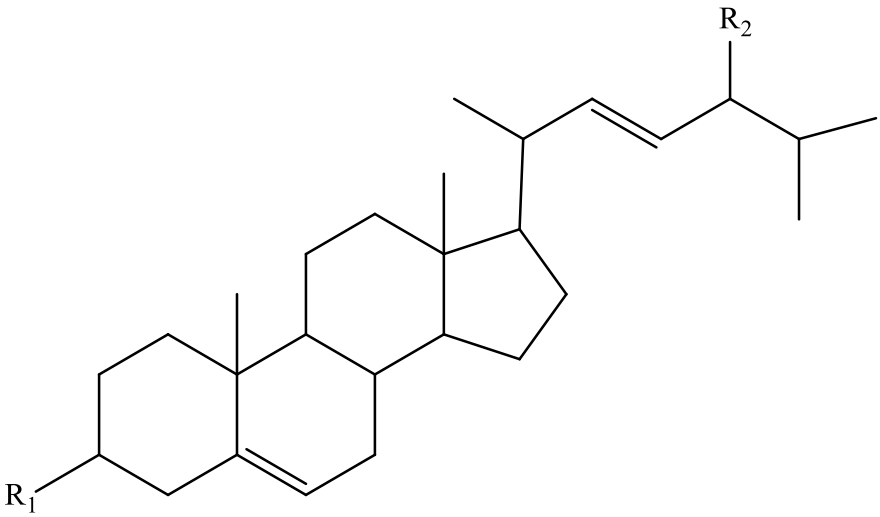

19 R_1 = OH R_2 = ⋯⋯ Et
20 R_1 = OH R_2 = ▬ Et
21 R_1 = H R_2 = -Et, Δ 3,5,22 triene
22 R_1 = H R_2 =-Et, Δ 3,5,7, 22 tetraen

Figure 1. 12: Structure of sterols

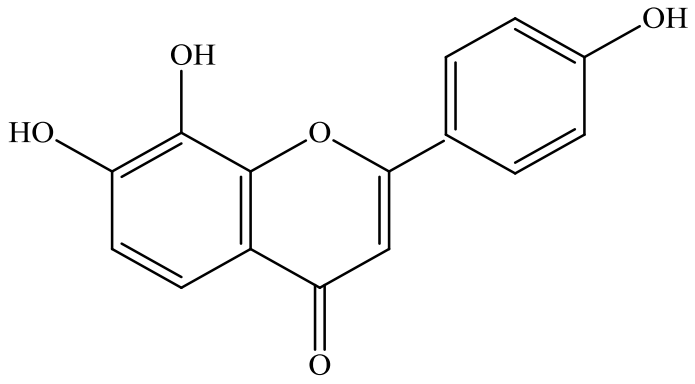

23

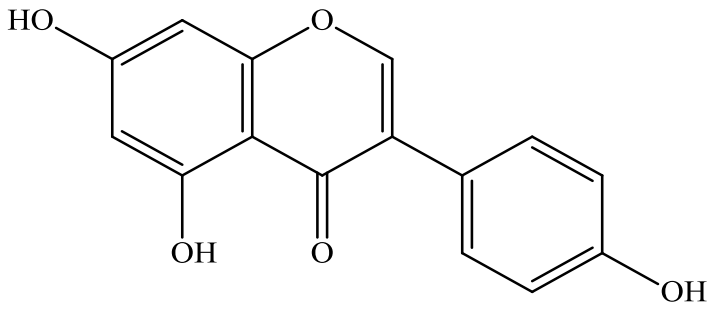

24

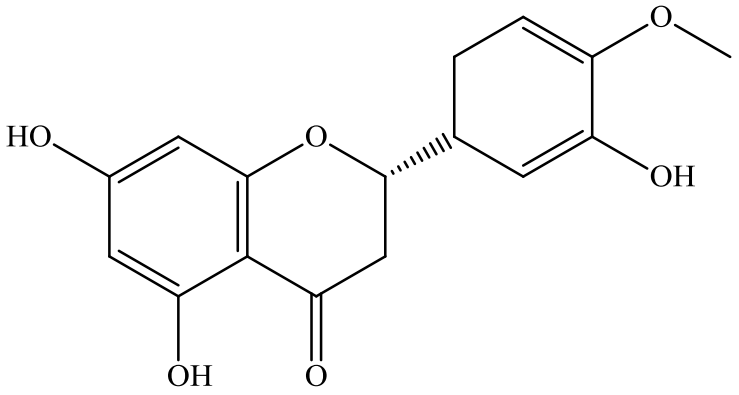

25

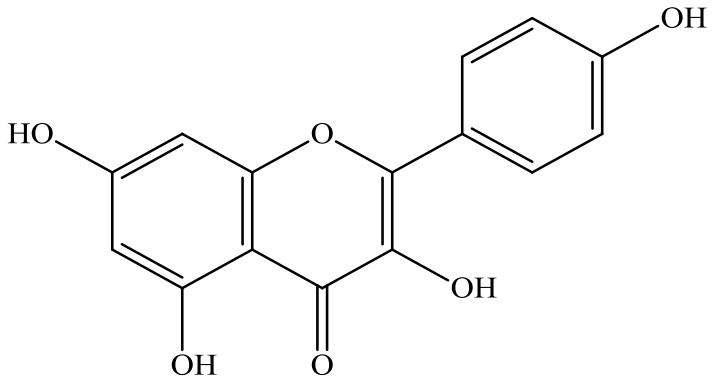

26

Figure 1. 13: Structure of flavonoids

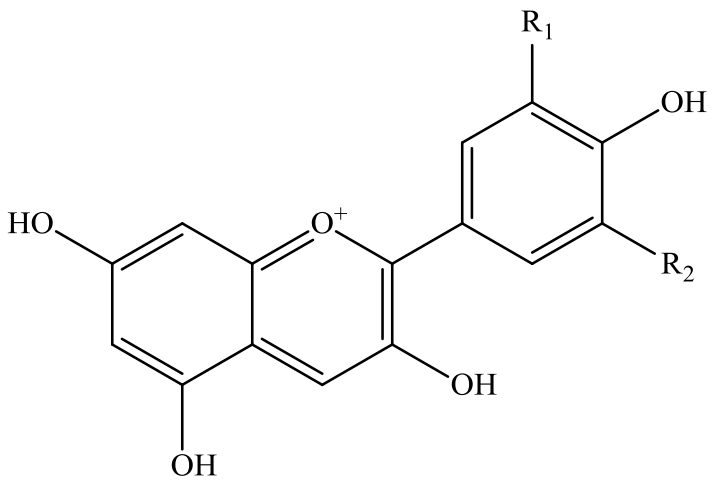

27	R_1 = OH	R_2 = H
28	R_1 = OCH_3	R_2 = H
29	R_1 = OH	R_2 = OH
30	R_1 = OCH_3	R_2 = OCH_3

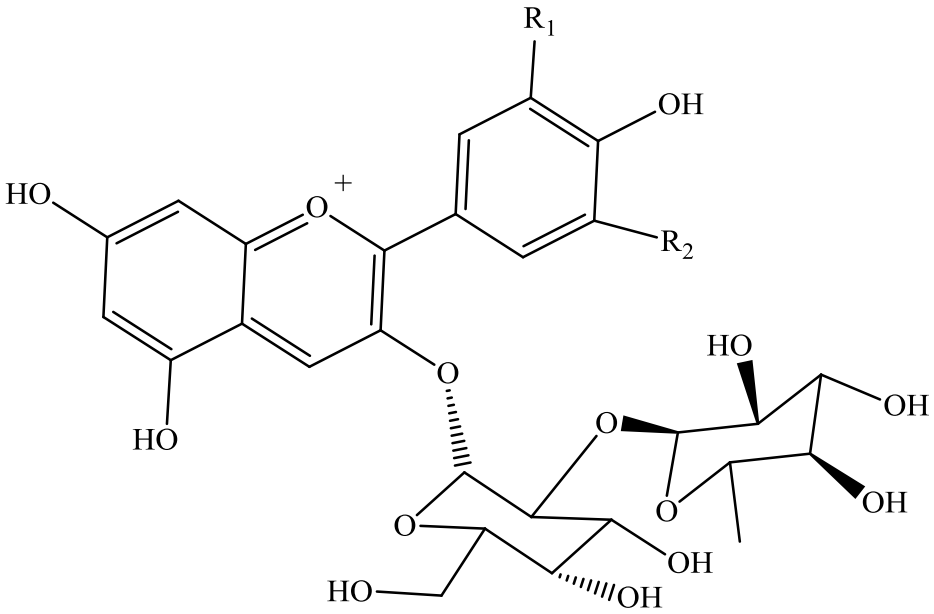

31 R_1 = OCH_3 R_2 = H
32 R_1 = OH R_2 = H
33 R_1 = H R_2 = H

Figure 1. 14: Structure of Anthocyanidins and anthocyanins

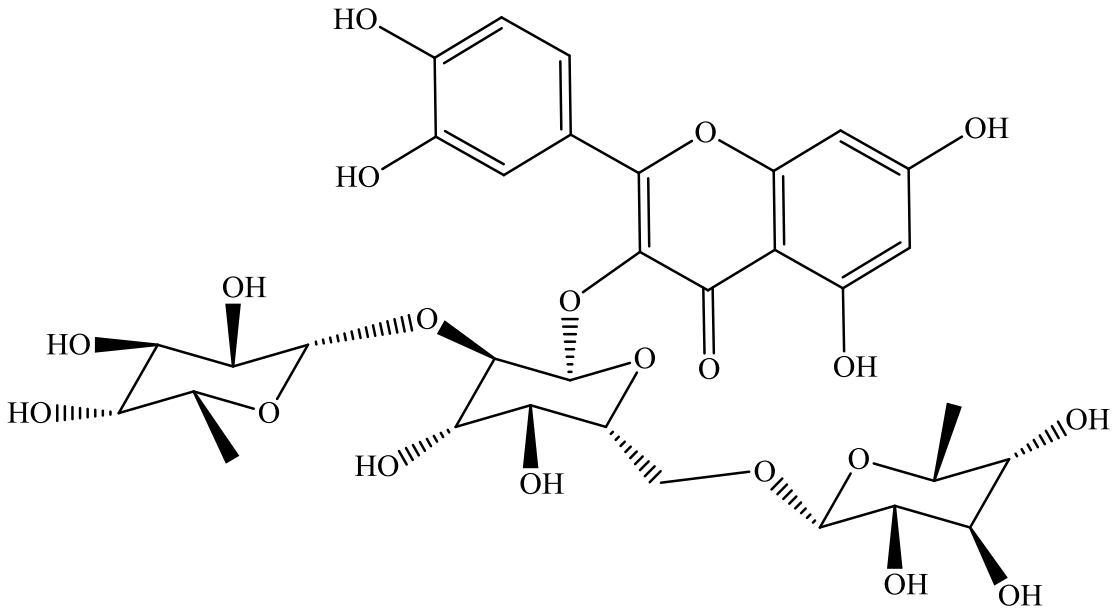

34

Figure 1. 16: Structure of Quercetin 3-*O*-2^{G}rhamnosylrutinoside

1.3.4 Previous pharmacological reports

The isolated triterpene saponins (**6**, **7**, **8**, **9**, **10** and **11**) from *C. mirabile* tubers were found to exhibit significant antifungal activity against *C. albicans, C. crusei, C. parapsilosis, C. pseudotropicalis, C. stellatoidea, C. tropicalis and C. neoformans*; compounds **6**, **7** and **9** showed stronger activity than the others as reported by Calis *et al*. (1997). Dall'Acqua *et al*. (2010) determined the anti-inflammatory activity of *C. repandum* and found that compounds **8**, **14** and **18** isolated from *C. repandum* tubers showed *in vitro* anti-inflammatory activity at 100µM by inhibiting LPS-induced IL-8 and TNF-α expression. Triterpenoid saponins **9** and **18** were demonstrated to have cytotoxic effects against various tumour cells - SK-BR-3 (breast adenocarcinoma cells), HT-29 (colon adenocarcinoma), HepG2/3A (hepatocellular carcinoma), NCI-H1299 (lung carcinoma), BXPC-3 (pancreatic carcinoma), and 22RV1 (prostate carcinoma). Both were shown to be cytotoxic at concentrations ranging from 0.18 to 0.84mM (El Hosry *et al.*, 2014). The methanol and water extracts of *C. coum* were found to induce cytotoxicity via apoptosis of both HeLa and human non-small cell lung carcinoma cell lines (Yıldız *et al.*, 2013) and the methanol, ethanol, acetone and petroleum benzine extracts of *C. graecum* tubers and leaves exhibited antioxidant activity using DPPH assay (Metin *et al.*, 2013).

1.4 Aims and objectives

The present work is aimed at carrying out a phytochemical investigation on the two Libyan plants, *Cynara cyrenaica* Maire &Weill and *Cyclamen. rohlfsianum* Aschers. Despite the long traditional use of *C. cyrenaica* and *C. rohlfsianum* as medicinal herbs, no biological work has been carried out on these potential medicinal plants. In addition, the abundant amounts of sesquiterpene and phenolic compounds in *Cynara* and triterpenoid saponins in *Cyclamen* species needs to be investigated in an attempt to isolate new constituents which may possess interesting biological activities. In particular, *Cynara* species (such as *C. scolymus* and *C. altilis*) have been used as medicine for cancer and diabetes for many years and *C. rohlfsianum* has been used traditionally as an antidiabetic. In addition, other *Cyclamen* species have shown potential cytotoxic activity against many cancer cell lines. This work aimed to investigate the crude hexane, ethyl acetate and methanol extracts along with the isolated compounds from both plants for antidiabetic potential as well as cytotoxicity.

The objectives of this work encompassed:

- Chapter 3 Phytochemical investigation: involving Soxhlet extraction using solvent of increasing polarity, followed by fractionation and isolationof compounds by various chromatographic techniques and identification by spectroscopic methods including 1D and 2D NMR spectroscopy.

- Chapter 4 Biological studies: *in vitro* screening of the crude extracts and isolated compounds using anti-diabetic assays (α-glucosidase, PTP1B and α-amylase) inhibition test, in the light of traditional use. Cytotoxicity assessment was made against the cancer cell lines: A375 (melanoma cell line), PANC-1 (human pancreatic carcinoma), and HeLa (human cervical cancer cells) compared with the normal cell line PNT2 (prostate cell line) for the purpose of screening the extracts along with the isolated compounds using an AlamarBlue® assay. Further examination of the most cytotoxic phytochemicals with an interesting core

structure was then carried out using PANC-1 cells as a model of inhibition of adhesion, invasion and migration.

CHAPTER II
2. MATERIALS AND METHODS

2.1 Materials

2.1.1 Solvents

Solvents listed below were obtained from Fisher Scientific UK Ltd, VWR International, and Sigma Aldrich. All the solvents were transferred to small glass bottles for routine use for different processes of extraction, chromatographic separation, analytical thin layer chromatography (TLC).

- Acetone (Analytical grade)
- Acetonitrile (HPLC grade)
- Chloroform (HPLC grade)
- Dichloromethane (HPLC grade)
- Ethyl acetate (HPLC grade)
- Formic acid (Analytical grade)
- Methanol (HPLC grade)
- n-Hexane (HPLC grade)

Solvents for NMR analysis: Below is the list of deuterated (99.9%) solvents obtained from Sigma Aldrich, UK.

- Acetone-*d6* ($(CD_3)_2CO$)
- Chloroform-*d* ($CDCl_3$)
- Dimethylsulphoxide-*d6* (DMSO-d_6)
- Methanol-*d5* (CD_3OD)
- Pyridine-d5 (C_5D_5N)

2.1.2 Reagents and chemicals

- α -glucosidase (Sigma-Aldrich, UK)
- α- Amylase (Sigma-Aldrich, UK)
- 4- nitrophenyl α-D-maltohexaside (Sigma-Aldrich, UK)
- 6,8-difluoro-4-methylumbelliferyl phosphate (Invitrogen Ltd)
- Acarbose (Sigma-Aldrich, UK)
- AlamarBlue®(Thermo Fisher, UK)
- Anti-bumping granules (Fisher Scientific, UK)
- Bis(4-Trifluoromethylsulfonamidophenyl)-1,4-diisopropylbenzine, (Calbiochem)
- Bovine serum albumin (Sigma-Aldrich, UK)

- Catalase (**H_2O_2**:H_2O_2 oxidoreductase) (Sigma-Aldrich, UK)
- Cotton wool (Fisher Scientific, UK)
- CytoSelect™ 48-Well Cell Adhesion, Collagen IV-Coated Assay Kit (Cambridge Bioscience Ltd, UK)
- CytoSelect™ 48-Well Cell Adhesion, Fibronectin-Coated Assay Kit (Cambridge Bioscience Ltd, UK)
- Dithiothreitol (Sigma-Aldrich, UK)
- Dimethylsulphoxide (Sigma-Aldrich, UK)
- Dulbecco's Modified Eagle's Medium (DMEM) (Sigma-Aldrich, UK)
- Ethylenediaminetetraacetic acid (Sigma-Aldrich, UK)
- Foetal bovine serum (FBS) (Biosera, South America)
- Hank's saline solution (Sigma-Aldrich, UK)
- HEPES (Sigma-Aldrich, UK)
- InnoCyte™ Cell Migration Assay kits (Millipore, UK)
- InnoCyte™ Cell Invasion Assay kits (Millipore, UK)
- L-glutamine (Sigma-Aldrich, UK)
- MEM Non-essential amino acid solution (Sigma-Aldrich, UK)
- *p*-Anisaldehyde (Sigma-Aldrich, UK)
- Penicillin/ Streptomycin (Cambrex, UK).
- *p*-nitrophenyl-α-D-glucopyranoside (Sigma-Aldrich, UK)
- Protein tyrosine phosphatase 1B (Sigma-Aldrich, UK)
- Poly-L-lysine precoated plates (VWR, UK)
- RPMI 1640 medium (Lonza Biowhittaker, Belgium)
- Sephadex LH-20 (Sigma-Aldrich, UK)
- Sodium phosphate monobasic dihydrate (Sigma-Aldrich, UK)
- Sodium phosphate dibasic heptahydrate (Sigma-Aldrich, UK)
- Sodium chloride (Sigma-Aldrich, UK)
- Sulphuric acid (VWR, UK Ltd)
- SYTOX® Green stain (Thermo Fisher, UK)
- TLC grade silica gel (60H, Merck, Germany)
- TLC silica gel 60 F_{254} pre-coated aluminium sheet (Merck, Germany)
- TripLE™ Express (Gibco®, Denmark)

2.1.3 Equipment

- 341 Polarimeter (PerkinElmer Inc, USA)
- 96-well plate (Sigma-Aldrich, UK)
- 96-well round-bottom clear plate (U-shape plate, Greiner bio-one, Germany)
- 25cm^2 and 75 cm^2 sterile flask (Thermo Fisher, UK)
- -80ºC freezer (Sanyo Electric Biomedical Co., Japan)
- CL2 centrifuge, 263 Aerocarrier rotor (Thermo Scientific, UK)
- Column: 55 x 2 cm (Sigma-Aldrich Ltd, UK)
- Cryogenic tubes (Nunc® Cryotubes)
- Decon Sanicator (Decon laboratories, UK)
- Edwards freeze dryer (Edwards, Crawley, UK)
- Haemocytometer (Hawksley, Lancing, UK)
- JEOL JNM LA400 NMR spectrophotometer (JEOL, UK).
- NMR tubes (5mm x 178mm, Sigma-Aldrich Ltd, UK)
- Orbitrap HRESI mass spectrometer (Thermo Fisher, Hemel Hempstead, UK)
- Rotary evaporator (Büchi, Switzerland)
- Shimadzu IRaffinity-1 FTIR
- Soxhlet apparatus (Quickfit, UK)
- SpectraMax M5 microplate reader (Molecular Devices Corporation, USA)
- UV-Lamp 254 nm and 364 nm UVGL-58 (UVP, USA)
- Water Bath (Grant Instruments, Royston, UK)

2.1.4 Plant material

*C. cyrenaic*a (flower heads, root, stem and leaf) and the tubers of *C. rohlfsianum* were collected from Libya from El-Jabal El-Akhdar region in the Wadi Alkuf in March 2014. Plants were identified by Dr Abdullsalam Mogasabe, Faculty of Science, Benghazi University. Plants were air dried to prevent mould or any type of degradation. The dried plant material was ground to a fine powder and stored in a fridge till investigated.

2.2 Methods

2.2.1 Plant extraction

The extraction of the ground plant materials was performed by sequential application of solvents of increasing polarity (n-hexane, ethyl acetate, and methanol) using a Soxhlet apparatus. The extraction process was carried out for 2-4 days with each solvent, then the extracts were filtered using filter paper and concentrated by evaporation using a rotary evaporator at a temperature of 40ºC.

2.2.2 Analytical techniques

2.2.2.1 Thin layer chromatography (TLC)

Thin layer chromatography (TLC) is one of the simplest forms of chromatographic techniques. This technique is essential for choosing suitable mobile phases for different separation methods such as column chromatography (CC), flash chromatography (FC), and vacuum liquid chromatography (VLC). It provides a quick way of analysing the components of a mixture or to compare samples with standards. TLC was also used to examine the purity of isolated compounds. Plant crude extracts, fractions or pure compounds were dissolved in a suitable solvent based on their solubility and spotted 1cm above the bottom edge of a TLC grade silica-coated aluminium sheet. A solvent or solvent mixture (known as the mobile phase) was added to the TLC tank and left for a while to saturate the tank environment. The filter paper was placed inside the tank to aid the saturation. Spotted TLC plates were then placed in the TLC tank to develop in an ascending direction. When the solvent reached about 1 cm below the top of the plate, the TLC plates were taken out of the tank, the solvent front was marked, and the plates air-dried immediately. They were then examined visually, and spots were detected as follows:

Detection by UV light: The spots were observed under UV light either at λ 254 nm as dark bands on a green background due to quenching fluorescence or at λ 366 nm where they fluoresced as coloured bands.

Detection by spray reagent: The TLC plates were sprayed with anisaldehyde-H_2SO_4 spray (5ml sulphuric acid, 85ml methanol, 10ml glacial acetic acid and 0.5ml anisaldeyde) and heated at 110°C for a minute to assist the colour development. R_f values were calculated. In addition, this technique was used to pool fractions with similar profiles together, which were then dried and further analysed by nuclear magnetic resonance (NMR) to elucidate the structure of the compounds.

2.2.2.2 Preparative thin layer chromatography (PTLC)

This technique was mostly used when compounds were required to be purified from fractions in low amounts. Samples were dissolved in a minimum volume of solvent and then applied 2cm from the bottom as a thin band across the entire width of the plate using a Pasteur pipette. The plates were developed as in section **2.2.2.1**. After that, the plate was observed under UV light (sometimes sprayed at one side with a suitable reagent) and the bands of interest were cut into strips along with the absorbent. The strips attributed to each separate component were further cut into small pieces and then soaked in a polar solvent overnight for maximum recovery, followed by filtration and evaporation. Finally, the recovered components were analysed by NMR spectroscopy.

2.2.2.3 Vacuum liquid chromatography (VLC)

A straight-sided sintered glass Büchner funnel was dry-packed with silica gel 60H under vacuum. Crude extract was adsorbed onto some silica, allowed to dry and then applied to the top of the VLC column. Elution was carried out with solvents of increasing polarity starting with n-hexane, n-hexane/EtOAc and EtOAc/MeOH. Then, the fractions were collected manually into a vacuum flask and were evaporated to dryness by rotary evaporation. After that, the fractions were examined by TLC to enable grouping of fractions with similar profiles (Coll and Bowden, 1986; Pelletier *et al.*, 1986).

2.2.2.4 Size -Exclusion Chromatography

This technique, also known as gel filtration chromatography, enables separation of molecules according to their size. The largest molecules elute from the column first followed by the smallest which tend to diffuse into porous gel particles contained within the column. A glass column of an appropriate size [2 cm (diameter) × 100 cm (height)] plugged with cotton wool was packed with Sephadex LH-20, which was prepared by suspending the stationary phase in 100% methanol overnight for polar fractions. Once the packed bed was settled, and the level of the solvent was just above the top of the bed, the sample to be fractionated was applied carefully using a Pasteur pipette after dissolving it in a minimum amount of the same solvent that was used to pack the column. Elution was commenced with 100% methanol and the fractions were collected in small vials about 1ml per fraction, and the fraction were left in a fume cupboard to dry (Kremmer and Boross, 1979).

2.2.2.5 Column Chromatography (CC)

This technique was applied to fractionate polar and non-polar components, using an open glass column plugged with cotton wool. The glass column was packed to 2/3 the length with silica gel 60 in the least polar system (usually n-hexane), (the quantity of silica gel 60 and the size of column used depended on the quantity of sample). The sample was dissolved in a minimum amount of a suitable solvent and pre-adsorbed onto silica gel 60 and was left in a fume cupboard to dry, before loading the sample. After that the adsorbed extract was introduced to the top of the column. The eluent was passed through the column with gradient elution starting with 100% hexane for hexane crude extract and with 90% hexane: 10% ethyl acetate in the case of the ethyl acetate crude extract and then the polarity was increased according to information derived from the TLC plates. The collected fractions were then examined by TLC and fractions with similar bands were combined and evaporated to dryness (Megalla, 1983).

2.2.3 Structure Elucidation

2.2.3.1 Nuclear Magnetic Resonance (NMR)

The NMR technique was used for structure elucidation of the isolated compounds. One and two-dimensional (1D and 2D) experiments were used to detect the type of compounds in fractions and to identify the structure of pure compounds. The NMR data were obtained on a JEOL (JNM LA400) spectrometer (400 MHz) at SIPBS and on a Bruker Avance 300 spectrometer at the Department of Pure and Applied Chemistry. About 10mg of each sample was dissolved in 500µl of deuterated solvents such as $CDCl_3$, DMSO-d_6, CD_3OD, ($(CD_3)_2CO$) or C_5D_5N based on the solubility of the compound obtained. The sample was then transferred to an NMR tube and from the resulting spectra, the structures of the compounds were elucidated. The NMR spectroscopic data were processed using MestReNova software 10 and ChemBioDraw Profesional 15.0 was used to draw compound structures.

2.2.3.1.1 One-Dimensional NMR (1D)

1D ^{1}H NMR experiment was used for the determination of the types of protons in the compounds and ^{13}C for providing data on the number and also the kinds of carbon atoms.

2.2.3.1.2 Two-Dimensional NMR (2D)

2D experiments were carried out because of their accurate assignments of the proton and carbon chemical shifts and for determining the relative stereochemistry.

Correlation Spectroscopy (COSY) experiments were used to indicate the connectivity between neighbouring protons. The ^{1}H-^{1}H correlations due to geminal (^{2}J) and vicinal (^{3}J) coupling appeared as cross-peaks symmetrically arranged about the diagonal. ^{1}H-detected Heteronuclear Single Quantum Coherence (HSQC) experiments were used to identify the ^{1}J ^{1}H-^{13}C correlations, whereas Heteronuclear Multiple Bond Coherence (HMBC) experiments were invaluable for determining the ^{1}H-^{13}C correlations via long range couplings (^{3}JCH and ^{2}JCH). Nuclear Overhauser Enhancement spectroscopy (NOESY) experiments were used to establish the relative stereochemistry of the pure compounds.

2.2.3.2 Mass Spectroscopy

This spectroscopic technique complements NMR spectroscopy, used in many different fields and is applied to pure samples as well as complex mixtures. It gives information about the molecular weight and molecular formula of the compounds under investigation. It is a very sensitive method since it can be carried out with a few micrograms of the sample. One mg of each sample was dissolved in 1ml methanol and 10µL of the solution was injected along with a direct infusion of 0.1% (v/v) formic acid in acetonitrile: water (90:10) at a flow rate of 200µl/m. Positive ion and negative ion mode ESI experiments were carried out on a Orbitrap HRESI mass spectrometer. MS data acquisition was carried out by Dr Tong Zhang (SIPBS, University of Strathclyde).

2.2.3.3 Infrared (IR) spectroscopy

The IR spectra of some isolated compounds were recorded on a Shimadzu IRaffinity-1 FTIR at the Department of Pure and Applied Chemistry, Strathclyde University by Dr. Abedawn Khalaf. A very small amount of the dry sample was loaded, and the spectrum was generated as a plot of absorbance against wave numbers (750-4500 cm^{-1} range).

2.2.3.4 Optical Rotation (OR)

The OR of some isolated compounds was measured using a 341 polarimeter at the Department of Pure and Applied Chemistry, Strathclyde University by Mr Gavin Bain. Variable concentrations of these compounds were prepared by dissolving them in $CHCl_3$ (spectrophotometric grade) to give 2ml test solutions in volumetric flasks. After that, the average of ten readings for each sample was taken and the optical rotation of the selected compounds was calculated using the following formula:

$$[\alpha]^{T}_{\lambda} = \frac{100 \text{ x } \alpha}{l \text{ x } c}$$

Where α is the average of the measured rotation (°), *l* is the path length in decimetres, *c* is the concentration of the solution in g/100ml, T is the temperature at which the measurement was taken (20°C), and *λ* is the wavelength in nanometres (*D*=589 nm).

2.2.4 Bioassays

2.2.4.1 In vitro antidiabetic assays

Initially, samples were tested at 30µg/ml as a preliminary screen. Subsequently, samples were tested at various concentrations based on the results from the preliminary screen.

2.2.4.1.1 Plant sample preparation

A stock concentration was prepared at 10mg/ml in dimethylsulfoxide (DMSO) solvent and stored at -20ºC. In all the enzyme assays, samples were screened at 30µg/ml in a 96-well round-bottom clear plate (U-shape plate, Greiner bio-one, Germany). Ten µl of the prepared sample was added to the enzyme and substrate in the enzyme assay plate. For active samples, different concentrations were assessed to obtain IC_{50}.

2.2.4.1.2 α-glucosidase assay

Buffer preparation

Phosphate buffer at a concentration of 0.1 mM was prepared by mixing 25.5ml of sodium phosphate monobasic dehydrate (solution A, 13.9g in 500ml distilled water) with 24.5ml of sodium phosphate dibasic heptahydrate (solution B, 26.8g in 500ml distilled water). The solution was made up to 100ml using distilled water and was calibrated to pH6.8 using a pH meter.

Enzyme preparation

Yeast α-glucosidase was purchased from Sigma (750 units). Stock glucosidase was made by dissolving the contents of one vial in 1ml of distilled water. Further stock of 75units/ml was prepared and stored at -20ºC. A working solution of enzyme of 0.2 units/ml was prepared by adding 13 µl (75units/ml) to 2.5ml of phosphate buffer.

Substrate preparation

4-nitrophenyl-α-D-glucopyranoside, stored at -20ºC was dissolved in phosphate buffer. A final concentration of 1mM was used.

Inhibitor preparation

Acarbose was used as a positive control and a standard curve was prepared to produce a final concentration range from 25mM to 10µM.

Assay

In a 96-half-well flat-bottom clear plate, 10µl of sample or reference standard (acarbose) was added to the well. Twenty µl of the enzyme was then added to each well incubated for 10min at 37ºC in an atmosphere containing 5% CO_2. After that, substrate (10µl) was then added to each well and incubated for another 10min at 37ºC in an atmosphere containing 5% CO_2. The absorbance was then read on a Spectramax plate reader at 405nm. Each sample was tested in triplicate and the results expressed as percent inhibition compared to the control. Statistical analysis was carried out using ANOVA with a Dunnet's post-test and graphs were plotted using GraphPad Prism version 5.0.

2.2.4.1.3 α-amylase assay

Buffer preparation

The assay buffer consisted of 50mM HEPES in water (5.96g dissolved in 500ml of distilled water) pH adjusted into 7.1.

Enzyme preparation

α-amylase from porcine pancreas was used and a stock concentration was made up with water to 250units/ml and kept at -20°C until required. A final concentration of 125units/ml was used.

Substrate preparation

4-nitrophenyl-α-D-maltohexaside purchased from Sigma 73681 (100mg), stored at 2-8°C was dissolved in water at 50mg/ml. The final concentration was required at 1.5 mM. A stock concentration of 6 mM was prepared by dissolving 6.66mg in 1ml buffer. Per plate 8.3mg of the substrate was dissolved in 1.25ml buffer.

Inhibitor preparation

Acarbose was used as a positive control and a standard curve was prepared to produce a final concentration range from 25mM to 10µM.

Assay

In a 96-half-well flat-bottom clear plate, 10µl of standard (acarbose) or samples were added to the plate, then 20µl of α-amylase was added to each well. The plate was incubated for 30min at 37ºC in an atmosphere containing 5% CO_2. Following incubation, 10µl of the substrate was added to the wells and then incubated for another

30 min at 37ºC in an atmosphere containing 5% CO_2. The absorbance was then read on a Spectramax plate reader at 405nm. Each sample was tested in triplicate and the results expressed as percent inhibition compared to the control. Statistical analysis was carried out using ANOVA with a Dunnet's post-test and graphs were plotted using GraphPad Prism version 5.0.

2.2.4.1.4 PTP1B assay

Buffer preparation

Buffer was prepared, composed of the following: 2975mg of HEPES (25mM), 146 mg of sodium chloride (50mM), 15.4mg of dithiothreitol (2mM), 36mg of ethylenediaminetetraacetic acid (EDTA 2.5 mM), 50µl of 10mg/ml of bovine serum albumin (BSA 0.01 mg/ml) and 12.5mg of catalase. All were dissolved in 50 ml of distilled water and the pH was adjusted to 7.2.

Enzyme preparation

The enzyme buffer was prepared using 595mg of HEPES (50mM), 38.5mg of dithiothreitol (5mM), 14.6mg of ethylenediaminetetraacetic acid (EDTA 1 mM), and 25µl of NP-40 (0.05%). All the components were added to 50 ml of distilled water and the pH was adjusted to 7.2. One hundred µl of the enzyme protein tyrosine phosphatase 1B was added to 25ml of the buffer and aliquoted into 1ml, then stored at -80ºC. A working solution of 1nM was needed; 100µl of the stock was added to 2.4ml of the buffer.

Substrate preparation

6,8-difluoro-4-methylumbelliferyl phosphate (DiFMUP) was prepared by dissolving 5mg in 1.71ml DMSO to give a concentration of 10mM. For 1 plate 5µl was added to 1.25ml buffer (10µM)**.**

Inhibitor preparation

Bis(4-trifluoromethylsulfonamidophenyl)-1,4-diisopropylbenzine (PTP inhibiter IV, TFMS) was used as a positive control. A serial dilution of TFMS was prepared to produce a final concentration range of 100µM to 0.03µM.

Assay

In a 96-half-well flat-bottom black plate, 10µl of the standard (TFMS) or samples were added. Then 20µl of the PTP1B enzyme was added to each well and incubated for 30 min at 37ºC in an atmosphere containing 5% CO_2. Ten µl of the substrate was added to the wells then incubated for another 10min. The reading was taken on a Spectramax plate reader at ex 355 nm/em 460 nm.

2.2.4.2 Cytotoxicity assays

2.2.4.2.1 Plant sample preparation

Crude extracts and pure compounds were dissolved in DMSO to give a stock solution of 10mg/ml and were kept at -20ºC. Further dilution to the required starting concentration was carried out using cell growth medium.

2.2.4.2.2 Cell lines and Growth Conditions

The growth medium (known as Complete Medium) for all cell lines was prepared in a sterile flow hood and stored at 4°C until required. A375, HeLa and PNT2 cells were cultured in RPMI 1640 cell culture media, supplemented with 10% (v/v) foetal bovine serum (FBS), 1% (v/v) L-glutamine, and 1% (v/v) penicillin/streptomycin. PANC-1 cells were cultured in DMEM, with 10% (v/v) FBS and 1% (v/v) penicillin/streptomycin and 1% (v/v) non-essential amino acid. All cell lines were grown in a humidified incubator at 37°C with 5% CO_2. The cells were kindly donated by Mrs Louise Young, SIPBS, Strathclyde University.

2.2.4.2.3 Cell culture

All cell lines were grown in Complete Medium until approximately 70-80% confluent before the cells were used. The nature of the cell lines used in this assay were adherent. The medium was discarded, and the cells were washed with Hank's balanced salt solution (HBSS) and incubated for 5min with 2ml TripLE™ Express dissociation reagent. The cells were viewed under a light microscope. Once fully dissociated, the cells were centrifuged at 1000×g for 2min. Then the medium was removed, and cell pellet resuspended in 10ml medium. After that, the cells were counted using a haemocytometer and seeded into clear 96-well cell culture plates at the optimum seeding density for all cell lines ($1x10^5$ cells/ml). The cell plates were then incubated overnight (24h) at 37ºC, 5% CO_2 and 100% humidity before the samples were added. The cell lines used were maintained in Complete Medium and the media was refreshed every 48h and passaged when 80-90% confluence was achieved.

2.2.4.2.4 SYTOX® Green assay

SYTOX® Green is a high-affinity nucleic acid stain which easily penetrates cells with compromised plasma membranes and does not penetrate living cells. Upon binding to cellular nucleic acids, the dye produces a large enhancement in fluorescence emission, which is monitored at fluorescein wavelengths (Jones and Singer, 2001; Roth *et al.*, 1997). The cells were seeded in a 96 well plate at $1x10^5$ cells per well in Complete Medium (100µl per well) and incubated for 24h. Following incubation, a serial

dilution of each sample was performed in a dilution plate and 100 µl of each sample was added to the cells to give a concentration range from 25 to 0.19µg/ml and incubated for 24h. SYTOX® Green was used at a final concentration of 5µM in each well and incubated for 20min at 37ºC, 5% CO_2 and 100% humidity. The fluorescence was measured at 485-535nm. Each sample was tested in triplicate and the results were calculated as a % viability compared with the control (untreated cells).

2.2.4.2.5 AlamarBlue® cytotoxicity assay

AlamarBlue® is based on resazurin which is blue in colour and a non-fluorescent compound. It is reduced in metabolically active cells to resorufin which is pink and highly fluorescent (O'Brien *et al.*, 2000; Erikstein *et al.*, 2010). The cells were seeded in a 96 well plate at $1x10^5$ cells per well in Complete Medium (100µl per well) and incubated 24h. Following incubation, a serial dilution of each sample was performed in a dilution plate and 100µl of each sample were added to the cells to give final concentration ranges from 25 to 0.19µg/ml. DMSO was used as a solvent control with concentrations ranging from 0.02% to 2.5% and staurosporine (5µM) was used as a positive control. The plate was incubated for 24h. Twenty µl of AlamarBlue® was added to each well and incubated for 4h. After that, the fluorescence readings were taken at 560-590nm. Each sample was tested in triplicate and the results were calculated as a % viability compared with the control (untreated cells).

2.2.4.2.6 Adhesion assay using a Cytoselect™ 48-well Collagen IV and Fibronectin adhesion assays

Following the manufacturer's instructions for collagen IV and fibronectin adhesion assay kits, both plates were allowed to warm up at room temperature for 10min, 150µl of a cell suspension containing $1x10^6$ cells/ml in serum free medium with the selected compounds for this assay - ll, 13-epoxysolstitialin coded CC5 (final concentrations of 5.9, 11.9, 23.9, 47.8 and 95.5µM) and the novel compound coded CC12 (final concentrations of 17.3, 34.5 and 69µM) were added to the inside of each well and incubated at 37ºC, 5% CO_2 and 100% humidity for 2h. Following incubation, the media from each well was discarded and the wells were washed with 250µl phosphate-buffered saline (PBS). The cells were extracted by adding 200µl of the extraction solution and quantified by measuring the absorbance at 560nm. The results were calculated as % adhesion of the untreated control (100%).

2.2.4.2.7 Poly-L-lysine adhesion assay

The cell number was adjusted to $5x10^5$ in serum free medium and 100µl of a cell suspension with CC5 (final concentrations of 5.9, 11.9, 23.9, 47.8 and 95.5µM) and CC12 (final concentrations of 17.3, 34.5 and 69µM) were added to the inside of each well and incubated at 37ºC in 5% CO_2 and 100% humidity for 2h. Following incubation, the media from each well was removed and the wells were washed with 200µl PBS. Cell detachment solution (100µl) was added to each well and incubated at 37ºC in 5% CO_2 and 100% humidity for 1h. The fluorescence readings were measured at 485-535nm. The results were calculated as % adhesion of the untreated control (100%).

2.2.4.2.8 Migration assay using an InnoCyte^{TM} Cell Migration Assay, 24-well plate

Following the manufacturer's instructions, 350µl of a cell suspension containing $8x10^5$ cells/ml in serum free medium with CC5 at final concentrations of 11.9µM and CC12 at a final concentration of 34.5µM were added to the inside of each polycarbonate membrane insert (migration chamber) with 8µm pore size. Culture medium (500µl) containing 20% (v/v) of FCS chemoattractant was added to the lower chamber of the migration plate and incubated at 37ºC in 5% CO_2 and 100% humidity 24h. Following incubation, the cell culture inserts were removed, and the remaining cells and the cell culture medium were discarded, then the cell culture inserts were placed in unused rows of the 24-well cell culture containing 0.5ml of detachment solution in each well and incubated at 37ºC in 5% CO_2 for 20min. After incubation, the inserts were removed from the 24-well cell culture plate and tapped gently against the bottom of the well to ensure that the cells were completely removed, then the 24-well plate containing dislodged cells was incubated for an additional 40 min. After that, 200µl of the dislodged cells were transferred to walls and the fluorescence readings were taken at 485-535nm a Spectramax plate reader. The results were calculated as % migration of the untreated control (100%).

2.2.4.2.9 Invasion assay using an InnoCyte^{TM} Cell Invasion Assay, 24-well plate

The difference between the invasion assay kit and the migration assay kit is that in the invasion assay kit the inserts are coated with a layer of dried basement membrane matrix extract which acts as a barrier to discriminate the invaded cells from the non-invaded. Following the manufacturer's instructions, the protocol was carried out as in section **2.2.4.2.8**, except that in the invasion assay the dried basement membrane matrix extract was rehydrated by adding 300µl of warm serum free medium to the

upper chambers and incubated for 1h at room temperature. The results were calculated as % invasion of the untreated control (100%).

CHAPTER III
3. RESULTS AND DISCUSSION
PART I: PHYTOCHEMICAL STUDIES

Preface

This chapter includes the phytochemical investigation and structural elucidation of isolated compounds from the plants, *C. cyrenaica* (flower heads, leaf, stem and root) and *C. rohlfsianum* (tuber). The biological results are provided in Chapter IV.

3.1 Phytochemical analysis of *C. cyrenaica*

3.1.1 Fractionation of C. cyrenaica flower heads crude extract

The hexane extract of *C. cyrenaica* flower heads (CHH, 20g) was fractionated by VLC (section **2.2.2.3**), fraction CC1(10mg) was isolated using 70% (v/v) hexane in ethyl acetate as a mobile phase and consisted of a white powder. The ethyl acetate extract of *C. cyrenaica* flower heads (CEH, 2g) was subjected to CC (section **2.2.2.5**) using Sephadex LH-20 (100% methanol as mobile phase) giving fractions CC2 (1mg) as a white powder and CC3 (1mg) as a yellow powder. The ^{1}H NMR spectrum of the methanol extract of *C. cyrenaica* flower heads (CMH) showed signals suggesting a mixture of compounds.

3.1.1.1 Characterisation of CC1 as taraxasterol

CC1 was observed as a pink spot on TLC (R_f value 0.94, using 50% (v/v) ethyl acetate in hexane as a mobile phase) after treatment with anisaldehyde-sulphuric acid reagent followed by heating.

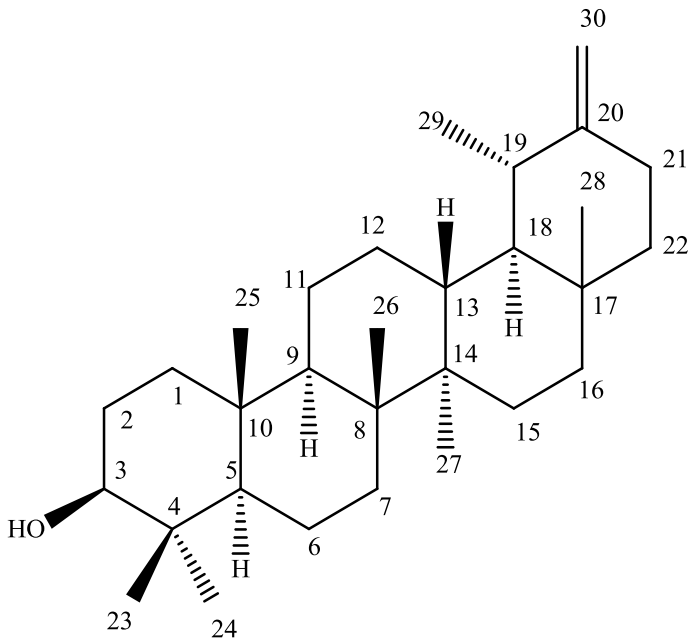

Figure 3. 1: Structure of taraxasterol

The mass spectrum in positive mode gave $[(M-H_2O) + H]^+$ at *m/z* 409.3825 suggesting a molecular formula of $C_{30}H_{50}O$. The pattern of the ^1H NMR spectrum (Figure 3.2, Table 3.1) indicated the presence of a triterpene compound. It displayed signals at δ_H 4.61 and 4.63 suggesting the presence of an exomethylene (H-30) and displayed a doublet of doublet at δ_H 3.20 indicating the presence of an oxymethine (H-3); this is a deshielded proton as a result of an OH group attached to its carbon C-3. The seven methyl groups were displayed in the spectrum by the presence of the following signals: 0.98 (Me-23), 0.78 (Me-24), 0.86 (Me-25), 1.02 (Me-26), 0.94 (Me-27), 0.87 (Me-28), and one methyl doublet at δ_H 1.03 attributed to Me-29. The spectrum also showed signals for the following protons: δ (ppm) 0.96/1.71 (2H-1), 1.61/1.65 (2H-2), 3.20 (H-3), 0.70 (H-5), 1.38/1.53 (2H-6), 1.39/1.40 (2H-7), 1.32 (H-9), 1.27/1.54 (2H-11), 1.13/1.68 (2H-12), 1.59 (H-13), 1.71/1.75 (2H-15), 1.18/1.24 (2H-16), 0.96 (H-18), 2.08 (H-19), 2.18/2.43 (2H-21), 1.43/1.45 (2H-22) and 4.61/ 4.63 (2H-30).

DEPTq135^{13}C NMR spectrum (Figure 3.3) showed 30 signals. δ (ppm) - 14.8 (C-27), 15.4 (C-24), 15.9 (C-26), 16.3 (C-25), 18.3 (C-6), 19.5 (C-28), 21.5 (C-11), 25.5 (C-29), 25.6 (C-21), 26.2 (C-12), 26.7 (C-15), 28.0 (C-23), 34.1 (C-7), 34.5 (C-17), 37.1 (C-10), 27.4 (C-2), 38.3 (C-16), 38.3 (C-1), 38.8 (C-4), 38.9 (C-22), 39.2 (C-13), 39.4 (C-19), 40.9 (C-8), 42.0 (C-14), 48.7 (C-18), 50.5 (C-9), 55.4 (C-5), 79.0 (C- 3). The peaks at 107.1 (C-30) and 154.6 (C-20) are related to olefinic carbons. The structural assignment was initiated from the long-range coupling networks observed between methyl protons and the adjacent carbons from the HMBC experiment (Figures 3.4 and 3.5), and the analysis was as following: the methyl groups at δ_H 0.98 (Me-23) and 0.78 (Me-24) showed ^2J correlation to the quaternary carbon at δ_C 38.8 (C-4), furthermore, Me-23 showed ^3J correlation to C-24 δ_C 15.4 and Me-24 also showed ^3J correlation to C-23 at δ_C 28.0. Thus, these were identified as geminal methyls. In addition, both Me-23 and Me-24 showed ^3J correlations to the C-3 and C-5 carbons at δ_C 79.0 and 55.4, respectively.

The signal at δ_H 0.86 (Me-25) showed ^3J correlations to the carbons C-5 and C-9 at δ_C 55.4 and 50.5, respectively. In addition, the methyl group at δ_H 1.02 (Me-26) showed ^2J correlation to the quaternary carbon at δ_C 40.9 (C-8) and ^3J correlations to the

carbons C-7, C-9, and C-14 at δ_C 34.1, 50.5 and 42.0, respectively. As well as the methyl group at δ_H 0.94 (Me-27) showed ^3J correlations to the carbons C-8, C-13, and C-15 at δ_C 40.9, 39.2 and 26.7, respectively. While the methyl at δ_H 0.87(Me-28) showed ^3J correlations to carbons at δ_C C-16, C-18 and C-22 at δ_C 38.3, 48.7 and 38.9, respectively and showed ^2J correlations to C-17 at δ_C 34.5, while Me-29 at δ_H 1.03 showed ^2J correlation to C-19 at 39.4 and ^3J correlations to C-18 and C-20 at δ_C 48.7 and 154.6, respectively. In addition, the exomethylene protons at δ_H 4.61/4.63 (2H-30) showed ^3J correlations to C-19 at δ_C 39.4 and C-21 at δ_C 25.6 and displayed ^2J correlation to an olefinic quaternary carbon at δ_C 154.6 (C-20). The HMBC spectrum also displayed that protons at δ_H 1.61/1.65 (2H-2) showed ^2J correlation to C-3 and ^3J correlation to C-4. H-6 at δ_H 1.38 showed ^2J correlation to C-5 and ^3J correlation to C-8 and H-9 at δ_H 1.32 showed ^3J correlation to C-25. H-11 at δ_H 1.54 showed ^3J correlation to C-10 and H-12 at δ_H 1.13 showed ^3J correlation to C-14 and C-18. Methylene protons at δ_H 1.71/1.75 (2H-15) showed ^2J correlation to C-16 and displayed ^3J correlation to C-27. H-19 at δ_H 2.08 showed ^3J correlation to C-21. In addition, protons at δ_H 1.43/1.45 (2H-22) showed ^2J correlation to C-17 and displayed ^3J correlation to C-18 and C-28. This led to the conclusion that CC1 had an oleanane skeleton. Based on the ^{1}H NMR and DEPTq135^{13}C along with the correlations observed from the HMBC spectrum, CC1 was identified as taraxasterol in agreement with a previous report (Shakeri and Ahmadian, 2014).

Table 3. 1: ^{1}H (400 MHz) and DEPTq-135 (100 MHz) data of CC1 in $CDCl_3$

Position	^{1}H δppm (m)	^{13}C δppm
1	0.96 (1H, *m*) 1.71 (1H, *m*)	38.3
2	1.61 (1H, *m*) 1.65 (1H, *m*)	27.4
3	3.20 (1H, *dd*, *J* = 11.2, 5. 0Hz)	79.0
4	-	38.8
5	0.70 (1H, *m*)	55.4
6	1.38 (1H, *m*) 1.53 (1H, *m*)	18.3
7	1.39 (1H, *m*) 1.40 (1H, *m*)	34.1
8	-	40.9
9	1.32 (1H, *m*)	50.5
10	-	37.1
11	1.27 (1H, *m*) 1.54 (1H, *m*)	21.5
12	1.13 (1H, *m*) 1.68 (1H, *m*)	26.2
13	1.59 (1H, *m*)	39.2
14	-	42.0
15	1.71 (1H, *m*) 1.75 (1H, *m*)	26.7
16	1.18 (1H, *m*) 1.24 (1H, *m*)	38.3
17	-	34.5
18	0.96 (1H, *m*)	48.7
19	2.08 (1H, *m*)	39.4
20	-	154.6
21	2.18 (1H, *m*) 2.43 (1H, *m*)	25.6
22	1.43 (1H, *m*) 1.45 (1H, *m*)	38.9
23	0.98 (3H, *s*)	28.0
24	0.78 (3H, *s*)	15.4
25	0.86 (3H, *s*)	16.3
26	1.02 (3H, *s*)	15.9
27	0.94 (3H, *s*)	14.8
28	0.87 (3H, *s*)	19.5
29	1.03 (3H, *d*, 4.2)	25.5
30	4.61(1H, *d*, *J* = 2.4 Hz) 4.63 (1H, *d*, 2.4 Hz)	107.1

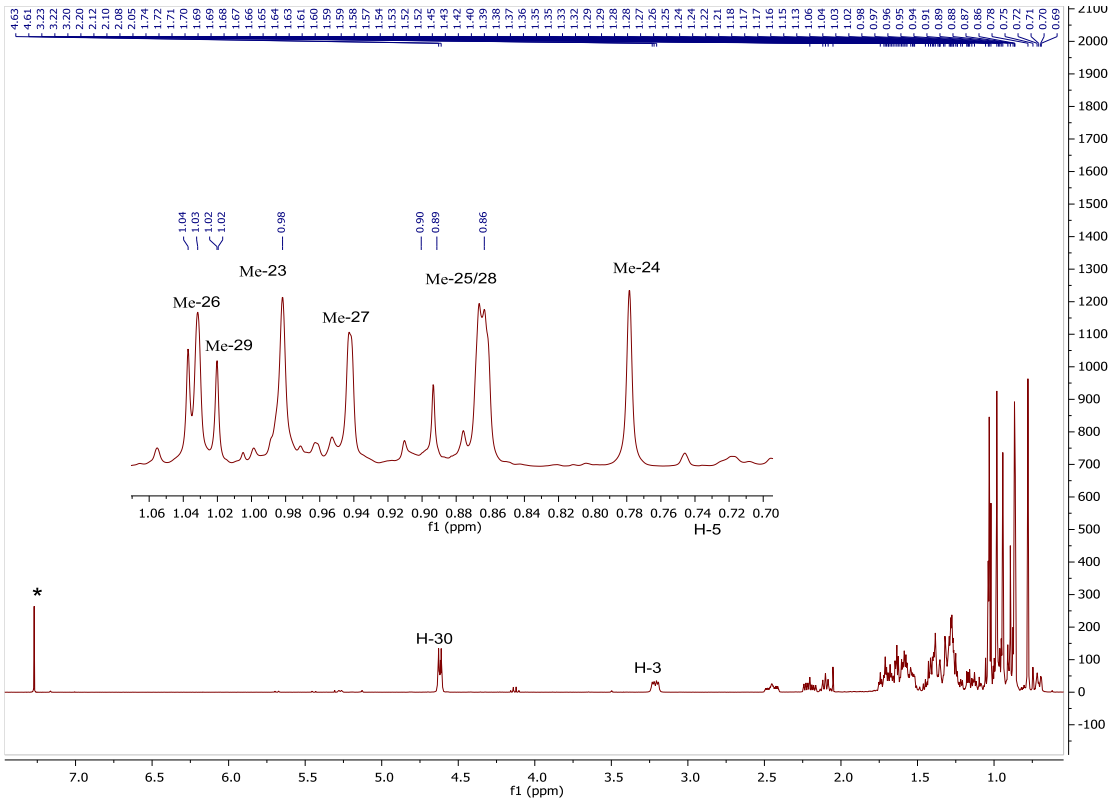

Figure 3. 2: ^{1}H NMR spectrum (400 MHz) of CC1 in $CDCl_3$

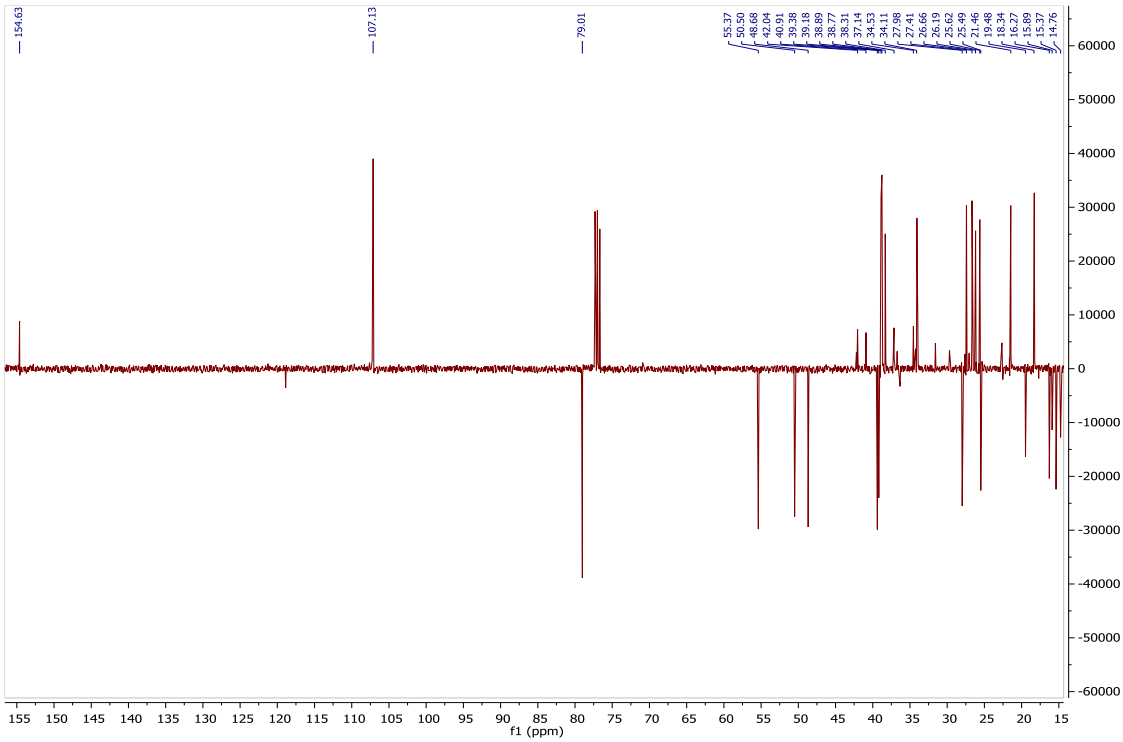

Figure 3. 3: DEPTq-135 spectrum (100 MHz) of CC1 $CDCl_3$

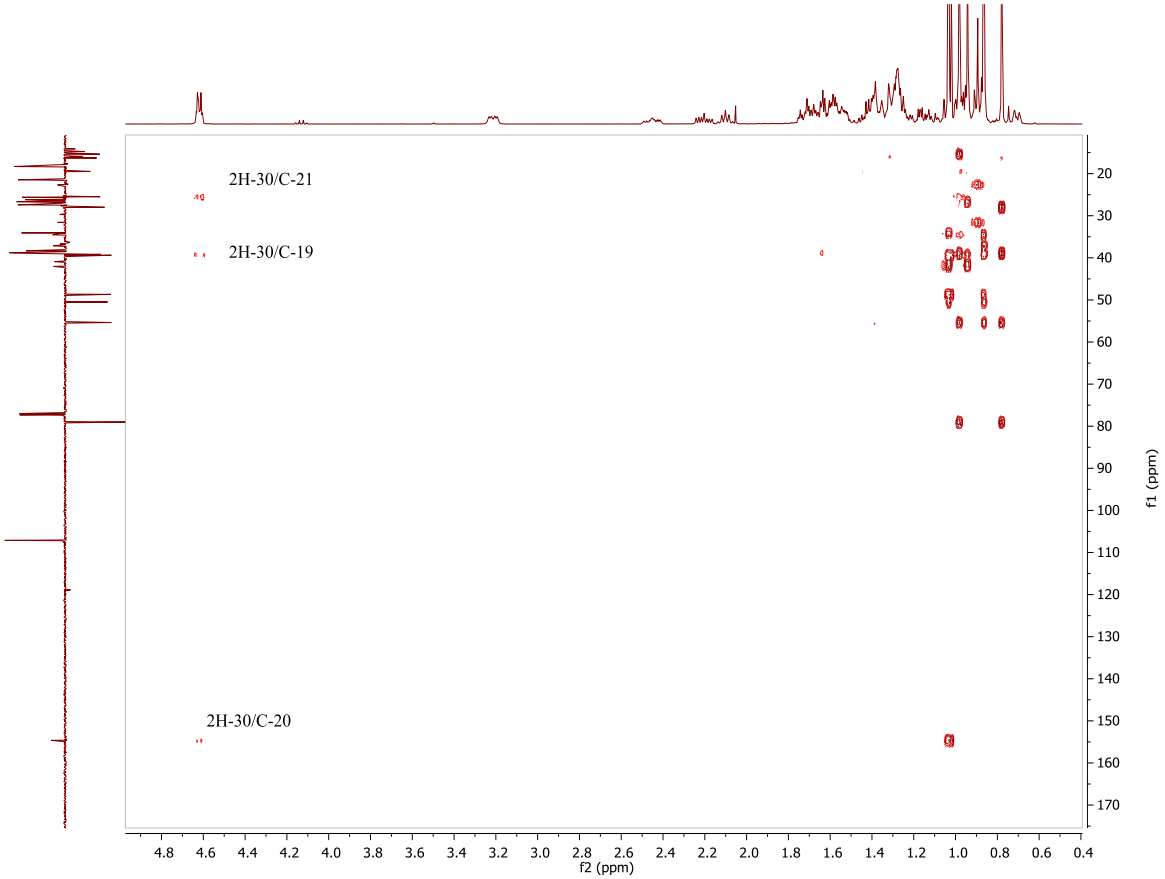

Figure 3. 4: HMBC spectrum of (400 MHz) of CC1 $CDCl_3$

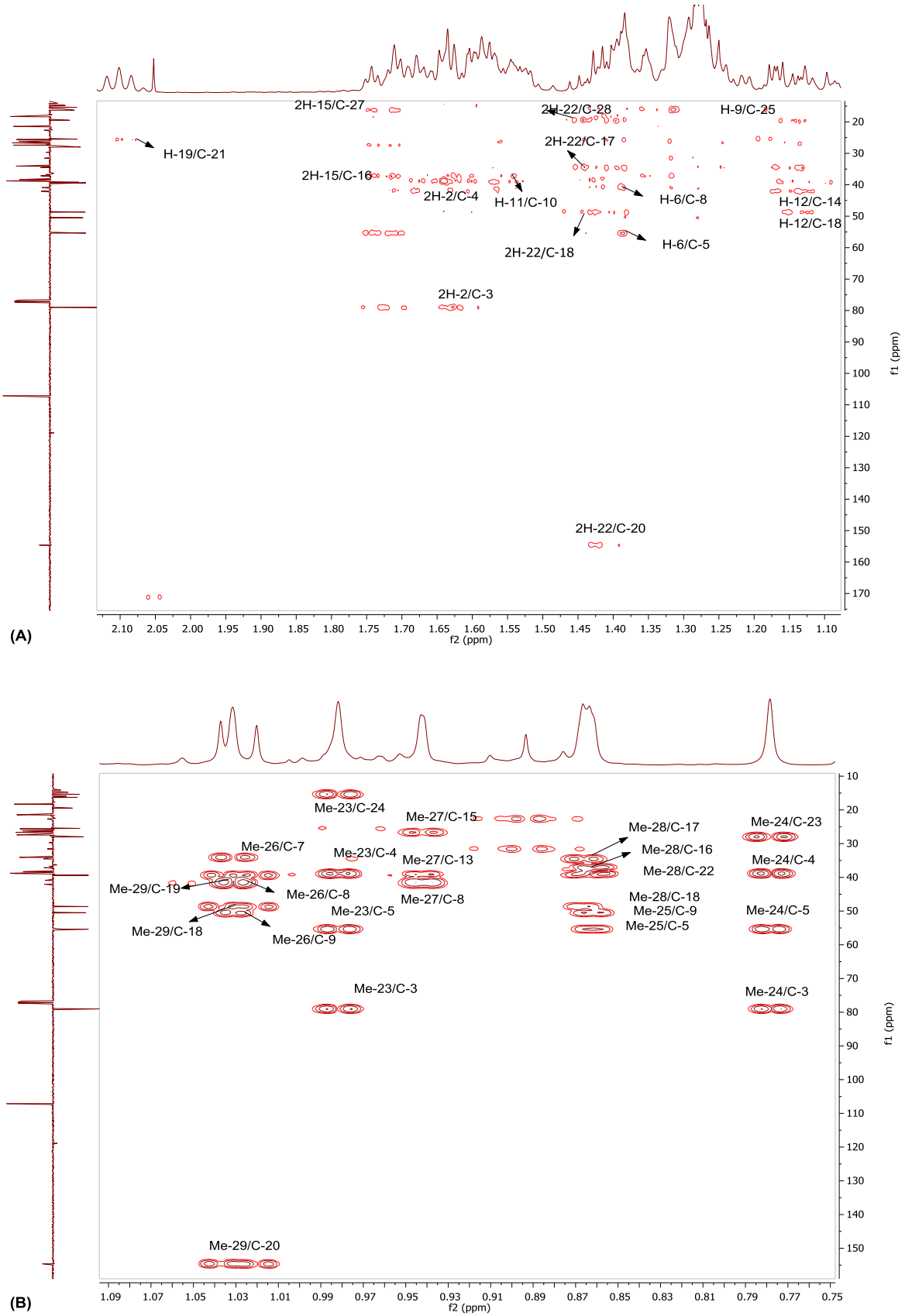

Figure 3. 5: (A) HMBC spectrum (400 MHz) of CC1 in the region 1.10 - 2.10 (B) Expansion of the region 0.75 - 1.09 ppm

3.1.1.2 Characterisation of CC2 as daucosterol

CC2 was revealed as a purple spot on TLC (R_f value 0.37, using 60% (v/v) ethyl acetate in hexane as a mobile phase) after treatment with anisaldehyde-sulphuric acid reagent followed by heating.

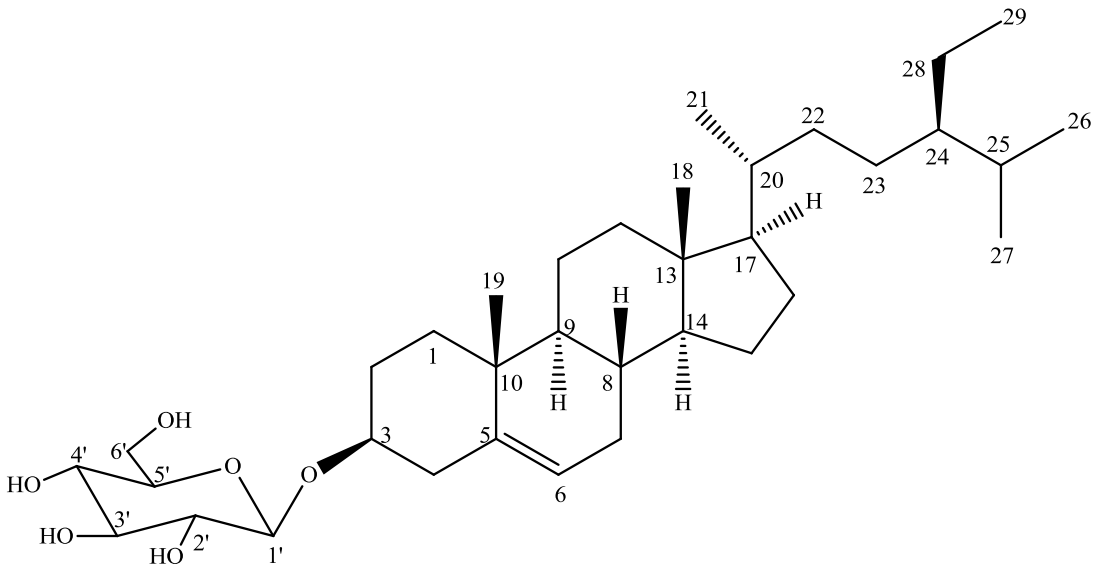

Figure 3. 6: Structure of daucosterol

The mass spectrum in positive ion mode gave $[M + H]^+$ at *m/z* 577.4099 suggesting a molecular formula of $C_{35}H_{60}O_6$. The ^1H NMR (Figure 3.7) indicated the presence of a phytosterol, which was suggested to be β-sitosterol with six methyl groups at δ_H 0.65 (3H, *s*, H-18), 0.79 (3H, *m*, H-29), δ0.80 (3H, *d*, H-27), δ0.96 (3H, *s*, H-19), δ0.91 (3H, *d*, *J* = 6.4 Hz, H-26) and δ_H 0.82 (3H, *d*, H-21). In addition, the spectrum also revealed distinctive the olefinic proton at δ_H 5.33 (H-6). Suggested the presence of a sugar unit which may be β-D-glucose with an anomeric proton δ_H 4.22 (1H, *d*, *J* = 7.74 Hz, H-1'). Moreover, the spectrum displayed signals at δ_H 2.88 - 3.15 (m, H-2`- H-5`), 3.41/3.62 (2 H-6`), 3.46 (H-3), 5.30 (H-6). The above data suggested that CC2 was daucosterol in agreement with a previous report (Mohammed, 2015).

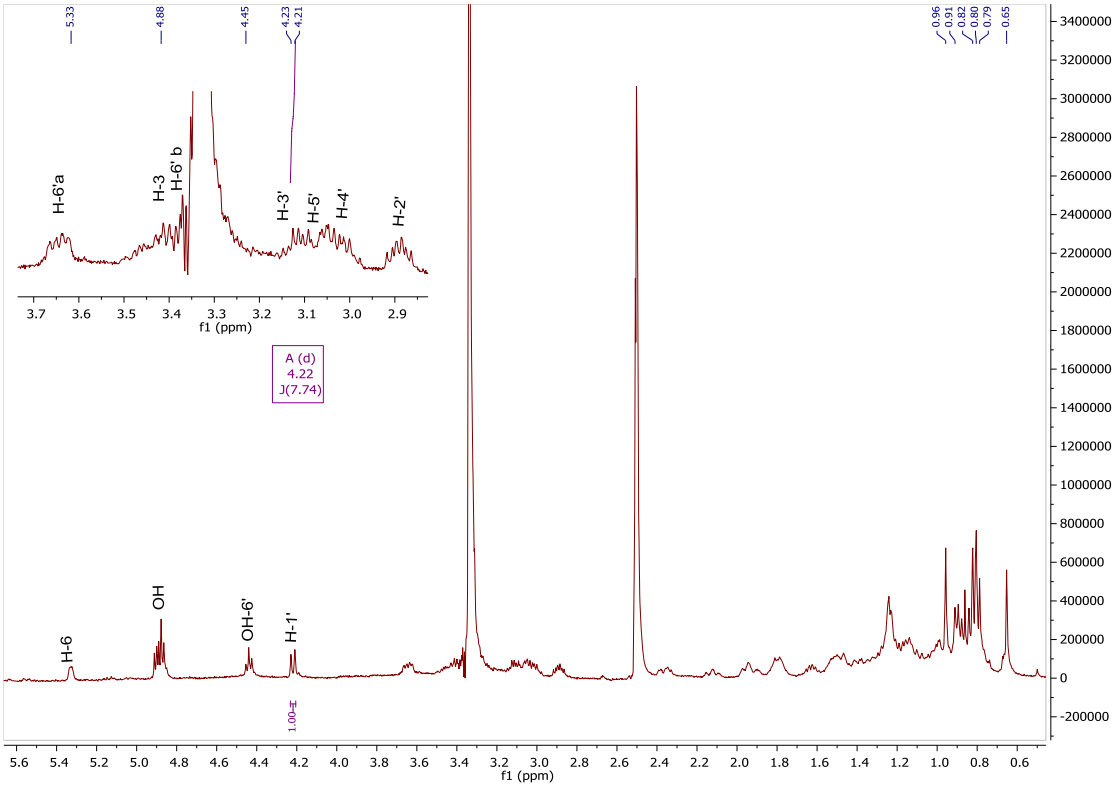

Figure 3. 7: ^{1}H NMR spectrum (400 MHz) of CC2 in DMSO-*d*$_6$

3.1.1.3 Characterisation of CC3 as 4´, 5, 7-trihydroxyflavone (apigenin)

CC3 revealed a yellow spot on TLC (R_f value 0.45, using 60% (v/v) ethyl acetate in hexane as a mobile phase), after treatment with anisaldehyde-sulphuric acid reagent followed by heating.

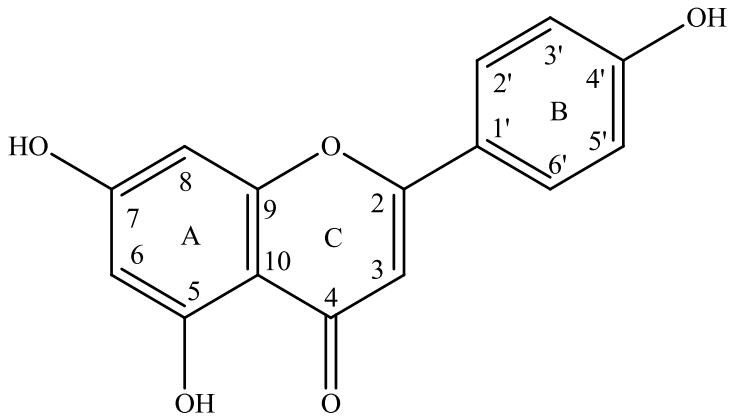

Figure 3. 8: Structure of 4´, 5, 7-trihydroxyflavone

The mass spectrum in positive ion mode gave $[M + H]^+$ at *m/z* 271.2273 suggesting a molecular formula of $C_{15}H_{10}O_5$. The pattern of the ^{1}H NMR spectrum (Figure 3.9, Table 3.2) displayed a signal at δ_H 13.02 (5-OH group) and showed the protons at δ_H 6.27 and 6.56 accounted for the A-ring as H-6 and H-8 protons, respectively and proton singlet at δ_H 6.65 of ring C as H-3. Also, the spectrum displayed the aromatic region of the protons signals of a typical AA'BB' system of ring B which attributed to H-3' and H-5' that appeared at δ_H 7.05 as well as H-2' and H-6' appeared at δ_H 7.95. The DEPTq135^{13}C NMR spectrum (Figure 3.10) indicated the presence of 15 carbons including a carbonyl at δc 182.3 (C-4) and seven methine carbons at δc 103.2 (C-3), 98.8 (C-6), 93.9 (C-8), including 2 carbons at δc 128.4 and 2 carbons at δc 116.0 for C-2'/C-6' and C-3'/C-5', respectively. Three phenolic carbons were observed at 164.1, 171.4, and 161.1 ppm (C-5, C-7, and C-4`, respectively) and four quaternary carbons at 122.3, 179.0, 147.5 and 108.6 (C-1', C-2, C-9 and C-10, respectively). The HMBC spectrum (Figure 3.12) showed ^2J correlation between H-3 at δ_H 6.65 and C-4 and ^3J correlation to C-1'. In addition, the proton at δ_H 13.02 (5-OH) showed ^2J correlation to C-5 and ^3J to C-6 and C-10. The proton at δ_H 6.27 (H-6) showed ^3J correlation to C-8. Furthermore, protons H-2'/H-6' displayed ^3J correlation to C-4' as

well as protons H3'/H-5' showed ^{3}J correlation to C-1' which indicated the presence of ring B. According to these data and through comparison with the literature (Tanjung *et al.*, 2008), CC3 was concluded to be 4´, 5, 7-trihydroxyflavone.

Table 3. 2: ^{1}H (600MHz) and ^{13}C (150MHz) data of CC3 in acetone-d_6

Position	^{1}H δppm (m, *J* Hz)	^{13}C
1	-	-
2	-	179.0
3	6.65 (1H, *s*)	103.2
4	-	182.3
5-OH	13.02 (*s*)	164.1
6	6.27 (1H, *d*, *J* = 2.1 Hz)	98.8
7-OH	9.90 (*br. s*)	171.4
8	6.56 (1H, *d*, *J* = 2.1 Hz)	93.9
9	-	147.5
10	-	108.6
1'	-	122.3
2'	7.95 (1H, *d*, *J* = 8.81 Hz)	128.4
3'	7.05 (1H, *d*, *J* = 8.80 Hz)	116.0
4'-OH	9.40 (*br. s*)	161.1
5'	7.05 (1H, *d*, *J* = 8.80 Hz)	116.0
6'	7.95 (1H, *d*, *J* = 8.81 Hz)	128.4

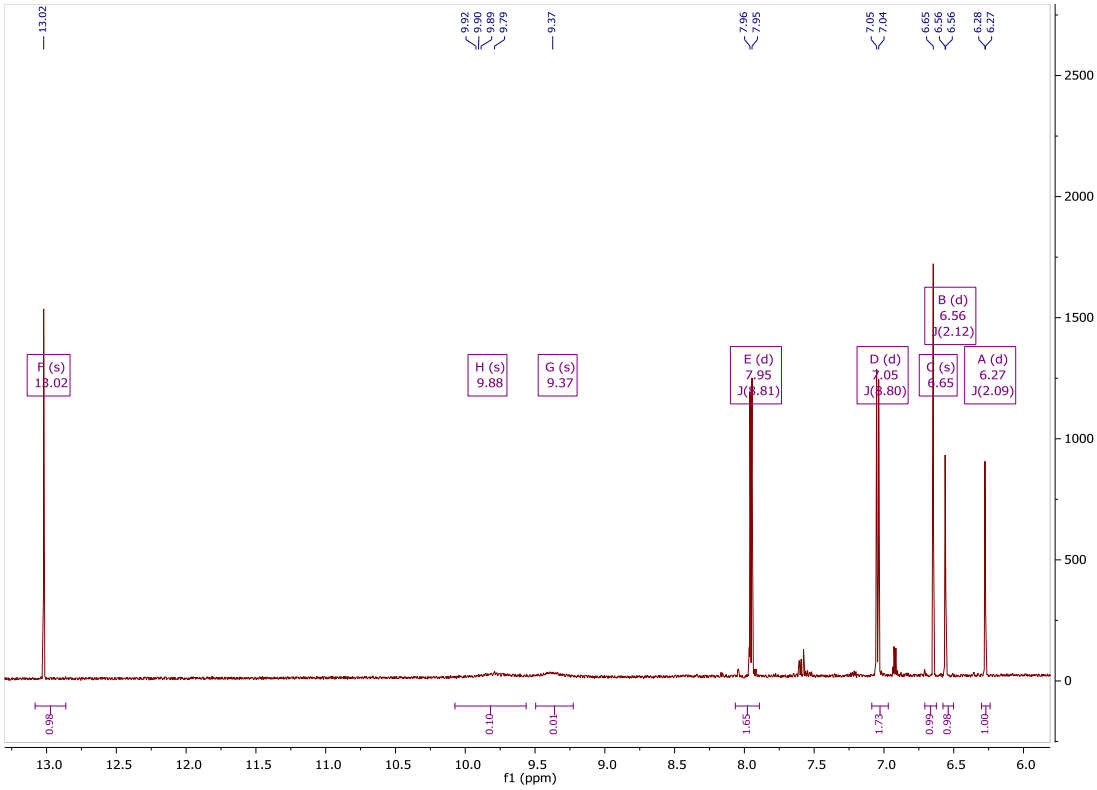

Figure 3. 9: Expanded ^{1}H NMR spectrum (600 MHz) of CC3 in acetone-*d*$_6$

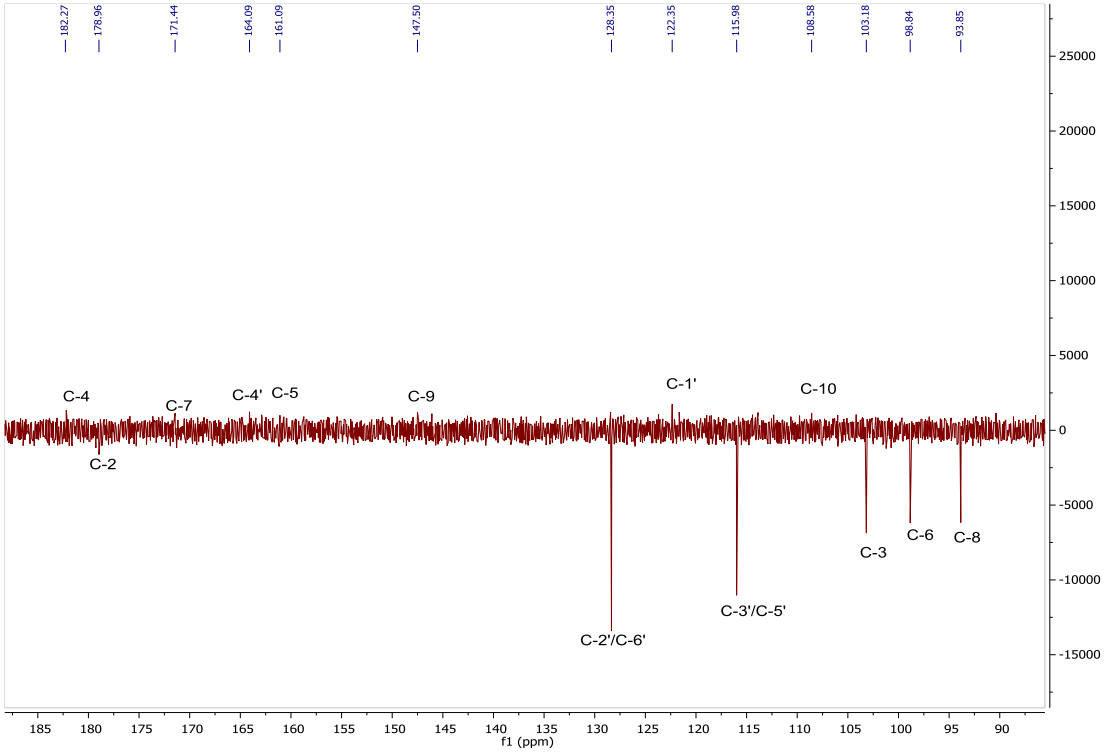

Figure 3. 10: DEPTq-135 spectrum (150 MHz) of CC3 in acetone-*d*$_6$

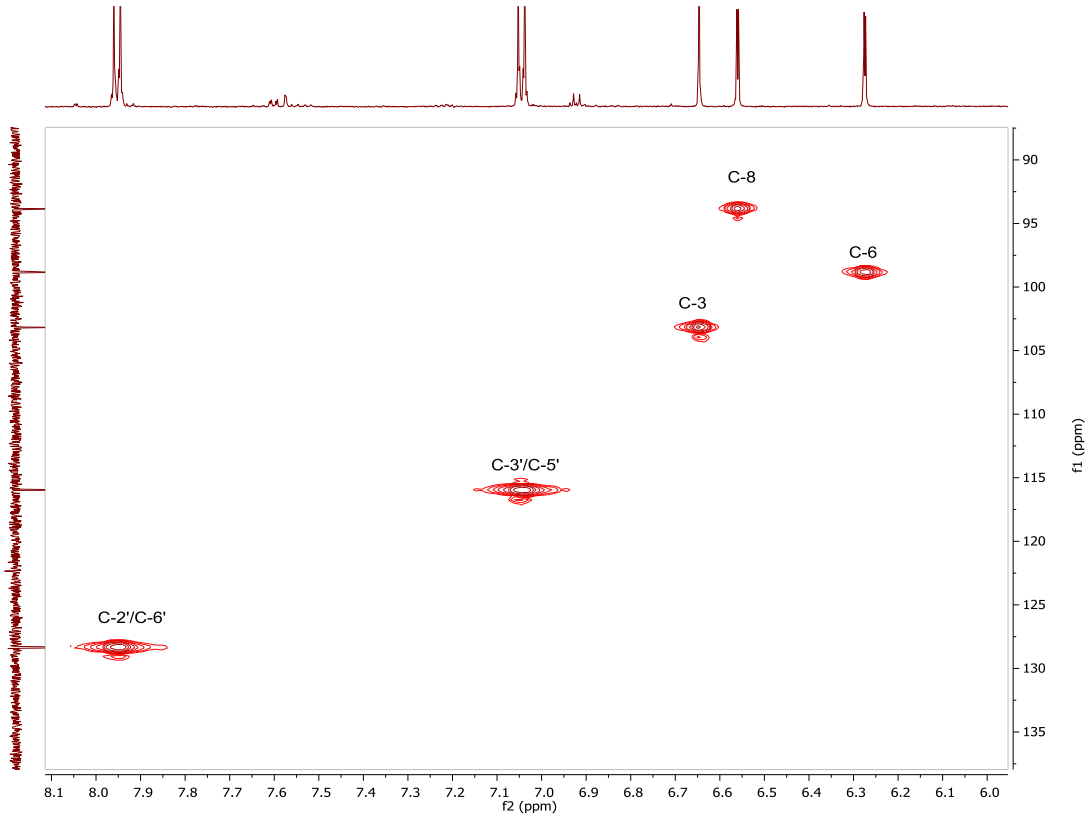

Figure 3. 11: HSQC spectrum (600 MHz) of CC3 in acetone-*d*$_6$

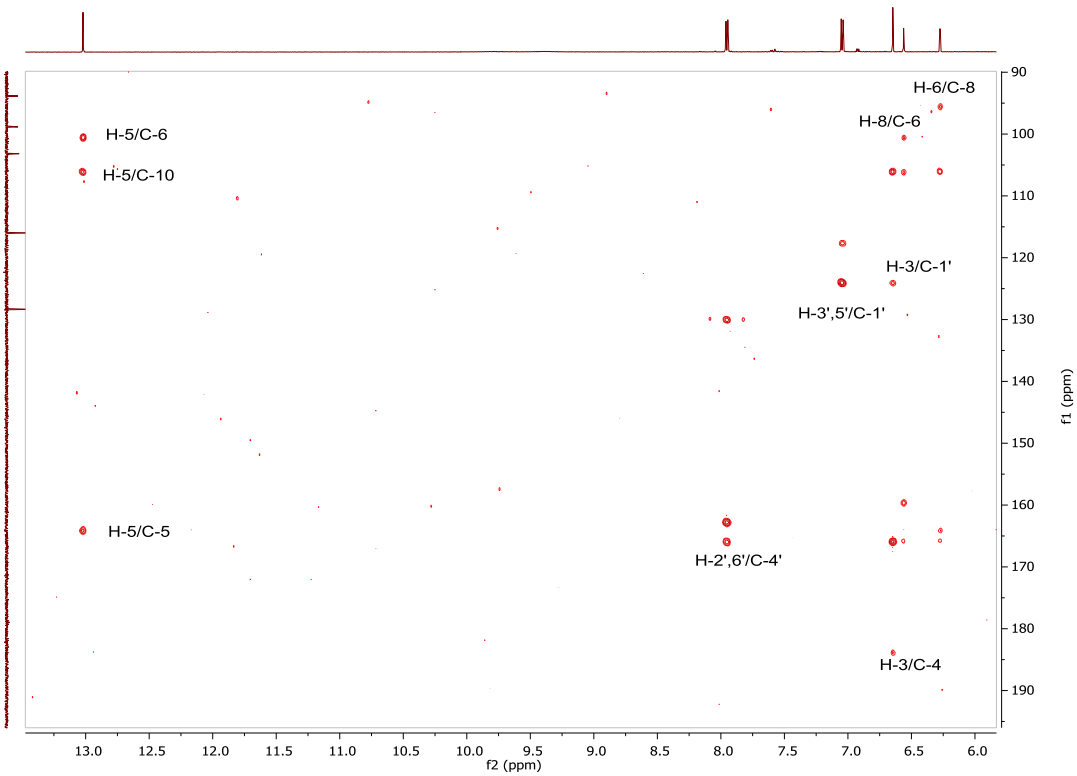

Figure 3. 12: HMBC spectrum (600 MHz) of CC3 in acetone-*d*$_6$

3.1.2 Fractionation of C. cyrenaica root crude extract

The hexane extract of *C. cyrenaica* root (CHR, 12g) was fractionated by column chromatography, fraction CC4 (2mg, white powder) was isolated using 50% hexane (v/v) in ethyl acetate and further purified by preparative thin layer chromatography using 80% hexane (v/v) in ethyl acetate as mobile phase. The ethyl acetate extract of *C. cyrenaica* root (CER, 5g) was fractionated using column chromatography, fraction CC5 (5mg, greenish powder) was isolated using 40% hexane (v/v) in ethyl acetate and further purified using size exclusion (100% methanol). The ^{1}H NMR spectrum of the methanol extract of *C. cyrenaica* root (CMR) showed signals suggesting a mixture of compounds.

3.1.2.1 Characterisation of CC4 as pseudotaraxasterol

CC4 revealed a dark pink spot on the TLC (R_f value 0.9 using 50% (v/v) ethyl acetate in hexane as a mobile phase), after treatment with anisaldehyde-sulphuric acid reagent followed by heating.

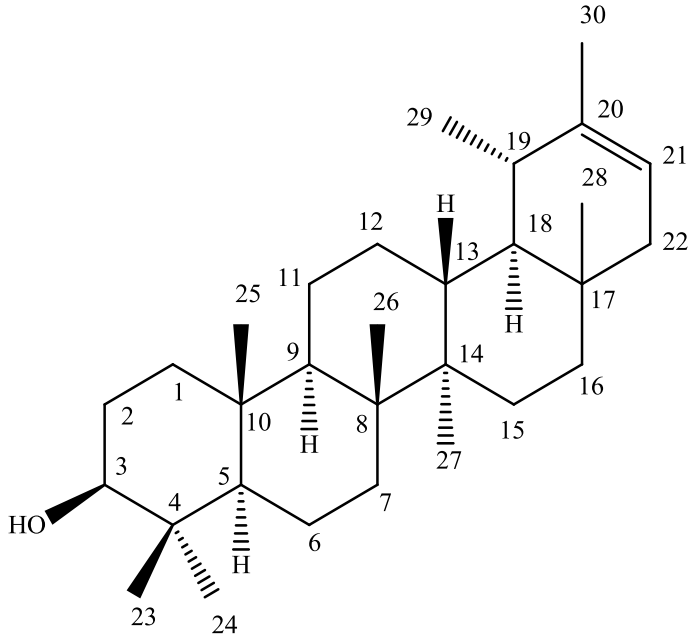

Figure 3. 13: Structure of pseudotaraxasterol

The mass spectrum in positive mode gave $[M\text{-}H_2O + H]^+$ at *m/z* 409.3828 suggesting a molecular formula of $C_{30}H_{50}O$. The pattern of the ^{1}H NMR spectrum (Figure 3.14, Table 3.3) indicated the presence of a triterpene compound. It displayed signal at δ_H

5.25 (H-21) suggesting the presence of methine and displayed a doublet of doublet at δ_H 3.20 (H-3) indicating the presence of an oxymethine, this is a deshielded proton as a result of OH group. The eight methyl groups were displayed in the spectrum by presence of the following signals: 0.96 (3H, H-23), 0.75 (3H, H-24), 0.86 (3H, H-25), 1.05 (3H, H-26), 0.94 (3H, H-27), 0.72 (3H, H-28), 1.64 (3 H, H-30), and one methyl doublet at δ_H 0.99 (3H, H-29) attributed to Me-29. CC4 is very similar to taraxasterol (CC1 in section **3.1.1.1)** as the data were in agreement with an oleanane skeleton of taraxasterol except that CC4 in the C-30 position has a methyl group which is confirmed by the signal at δ_C 21.7 (C-30) for 3H-30 at δ_H 1.64 whereas in CC1 the C-30 position has methylene carbon at δ_C 107.1 for 2H-30 at δ_H 4.61/4.63 ppm. According to these data and through comparison with the literature (Yang *et al.*, 2006), this compound was concluded to be pseudotaraxasterol.

Table 3. 3: ^{1}H (400 MHz) and ^{13}C (100 MHz) NMR data of CC4 in $CDCl_3$

Position	^{1}H δppm (m, *J* Hz)	^{13}C δppm
1	1.74 (1H, *m*), 0.96(1H, *m*)	38.8
2	1.65 (1H, *m*), 1.57(1H, *m*)	27.4
3	3.20 (1H, *dd*, *J* =11.2,5.2 Hz)	79.2
4	-	38.9
5	0.70 (*m*)	55.4
6	1.52 (1H, *m*), 1.38(1H, *m*)	18.4
7	1.41 (1H, *m*), 1.37(1H, *m*)	34.3
8	-	41.1
9	1.30 (1H, *m*)	50.5
10	-	37.2
11	1.58 (1H, *m*), 1.26 (1H, *m*)	21.6
12	1.62 (1H, *m*), 1.23 (1H, *m*)	27.7
13	1.61 (1H, *m*)	39.3
14	-	42.3
15	1.78 (1H, *m*), 1.01 (1H, *m*)	27.1
16	1.32 (1H, *m*),1.21 (1H, *m*)	36.8
17	-	34.5
18	1.03 (1H, *m*)	48.8
19	1.57 (1H, *m*)	36.4
20	-	139.9
21	5.25 (1H, *d*, *J* = 7.2 Hz)	118.9
22	1.72 (1H, *d*, *J* = 3.6 Hz), 1.55 (1H, *d*, *J* = 7.2 Hz)	42.2 (CH_2)
23	0.96 (3H, *s*)	28.1
24	0.75 (3H, *s*)	15.5
25	0.86 (3H, *s*)	16.4
26	1.05 (3H, *s*)	16.1
27	0.94 (3H, *s*)	14.8
28	0.72 (3H, *s*)	17.8
29	0.99 (3H, *d*, *J* = 5.9 Hz)	22.6
30	1.64 (3H, *m*)	21.7

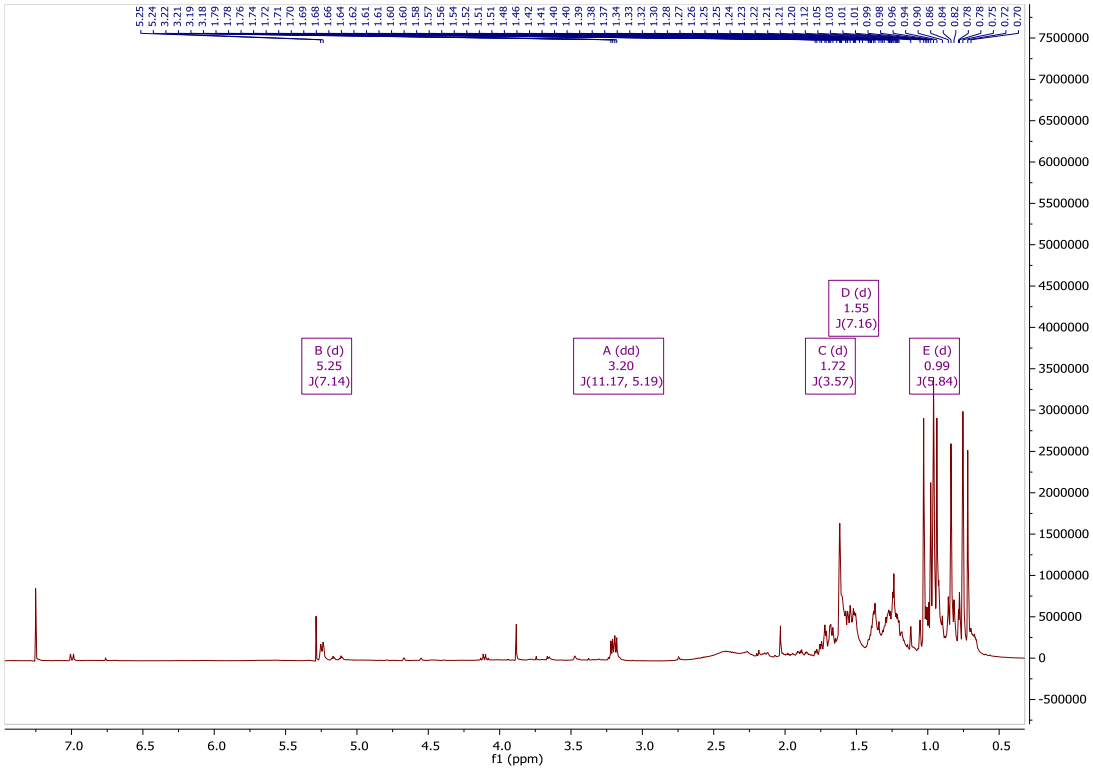

Figure 3. 14: ^{1}H NMR spectrum (400 MHz) of CC4 in $CDCl_3$

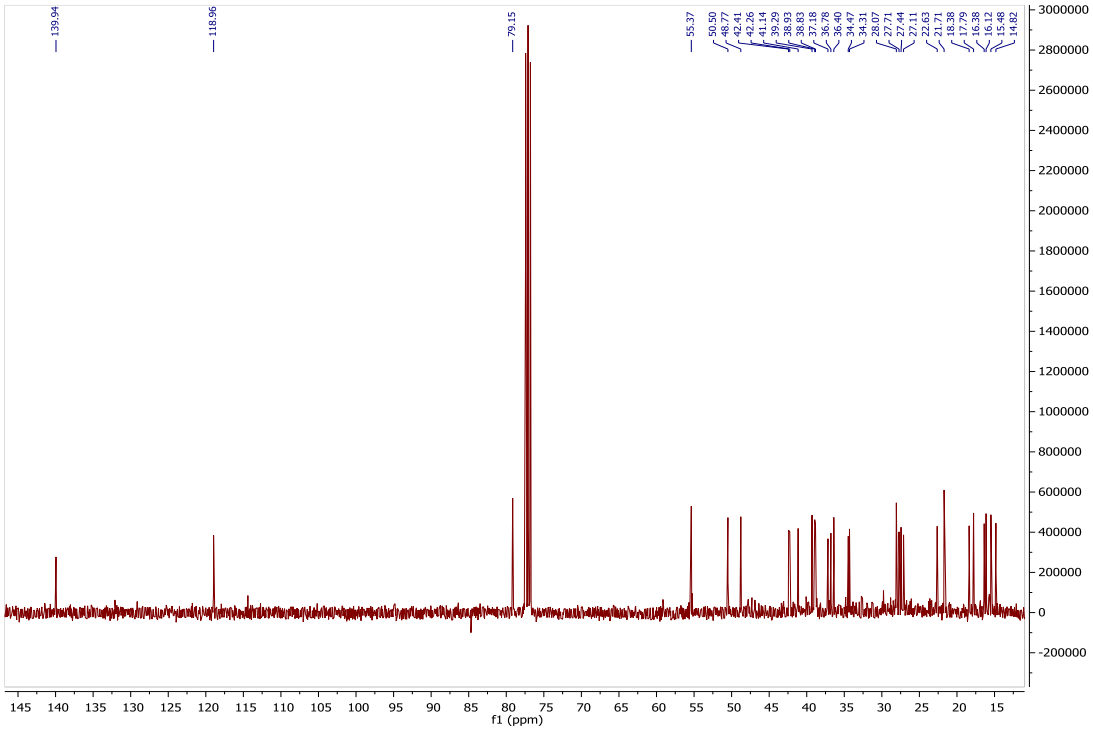

Figure 3. 15: ^{13}C NMR spectrum (100 MHz) of CC4 in $CDCl_3$

3.1.2.2 Characterisation of CC-5 as ll, 13-epoxysolstitialin

CC-5 revealed a dark pink spot on TLC (R_f value 0.88, using 10% (v/v) methanol in ethyl acetate as a mobile phase), after treatment with anisaldehyde-sulphuric acid reagent followed by heating.

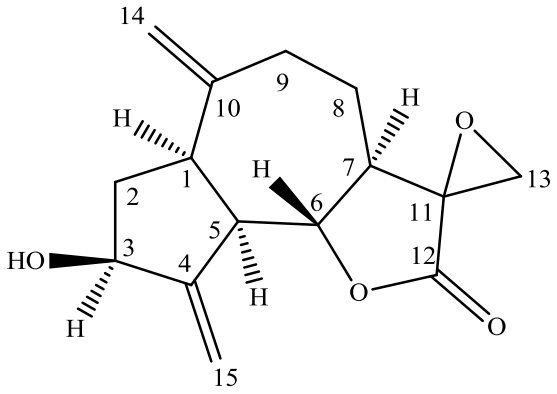

Figure 3. 16: Structure of ll, 13-epoxysolstitialin

The mass spectrum in positive ion mode gave $[M + H]^+$ at *m/z* 263.2370 suggesting a molecular formula of $C_{15}H_{18}O_4$. The ^1H NMR spectrum showed signal at δ_H 3.66 assigned to the C-13 suggesting the presence of an epoxide group. The spectral data showed the presence of a γ-lactone ring carbonyl of C-12 at δ_C 175.5. ^{13}C NMR showed the presence of four olefinic carbons C-4, C-15, C-10, and C-14 at δ_C 152.1, 111.4, 147.8, and 113.6, respectively (Table 3.4), one secondary carbon bearing oxygen at δ_C (81.9, C-6), and one tertiary carbon bearing oxygen (75.9, C-11). The ^1H NMR spectrum displayed signals at δ_H 5.00 and 5.02 for H-14 and at δ_H 5.37 and 5.43 for H-15 suggesting the presence of two exomethylene double bonds.

In the HMBC spectrum, H-1 proton at δ_H 2.92 showed ^2J correlation to a methine at δ_C 49.7 (C-5) and quaternary carbon at δ_C147.8 (C-10) and H-2 proton at δ_H 1.81 showed to ^2J correlations to a methine at δ_C 43.5 (C-1) and displayed ^3J correlation to quaternary C-10 at δ_C 147.8. In addition, H-2 at δ_H 2.38 showed ^3J correlation to the quaternary carbon C-4 at δ_C 152.1 and the C-5 at δ_C 49.7. H-5 at δ_H 2.88 showed ^2J correlations to C-1 (δ_C 43.5), C-4 (δ_C 152.1) and C-6 (δ_C 81.9). The methine proton (H-7) at δ_H 2.54 displayed ^2J correlations to a methine (C-6) at δ_C 81.9 and to quaternary carbon (C-11) at δ_C 75.9, also showed ^3J correlation to quaternary carbon (C-5) at δ_C 49.7. H-8 at δ_H 1.63 showed ^2J correlations to C-9 at δ_C 35.1 as well as H-

9 showed ^{2}J correlations to C-8 at δ_C 26.0 and quaternary carbon (C-10) at δ_C 147.8 and displayed ^{3}J correlations to methylene carbon (C-14) at δ_C 113.6. Proton H-13 at δ_H 3.66 showed ^{3}J correlations to C-7 and C-12 at δ_C 51.9 and 175.5, respectively and showed also ^{2}J correlation to C-11 at δ_C 75.9 which confirmed the presence of the epoxide group. Thus, these observations suggest that CC5 had a guaianolide carbon skeleton. In addition, the exomethylene protons 2H-14 at δ_H 5.0/5.02 showed ^{3}J correlations to C-1 and C-9 at δ_C 43.5 and 35.1, respectively, and showed ^{2}J correlation to the quaternary C-10 at δ_C 147.8. The exomethylene protons 2H-15 at δ_H 5.37/5.43 showed ^{3}J correlations to C-3 and C-5 at δ_C 73.1 and 49.7, respectively and showed ^{2}J correlation to the quaternary C-4 at δ_C 152.1. Hence these correlations confirm the presence of exomethylene protons 2H-14 and 2H-15. These serial HMBC correlations confirm the presence of a guaian-type sesquiterpene lactone. According to the data obtained from ^{1}H,^{13}C NMR and HMBC and through comparison with the literature (Reis *et al.*, 1992; Chhabra *et al.*, 1998) this compound was identified to be ll, 13-epoxysolstitialin. This compound was previously separated from the aerial parts of *C. humilis* (Reis *et al.*, 1992).

Table 3. 4:^{1}H (400 MHz) and ^{13}C (100 MHz) NMR data of CC5 in $CDCl_3$

Position	^{1}H δppm (m, *J* Hz)	^{13}C δppm
1	2.92 (1H, *m*)	43.5
2	1.81 (1H, *m*), 2.38 (1H, *dt*, *J* =13.41,7.5 Hz)	38.0
3	4.58 (1H, *br.t*, *J* = 7.6 Hz)	73.1
4	-	152.1
5	2.88 (1H, *m*)	49.7
6	4.27 (1H, *t*, *J* = 9.7 Hz)	81.9
7	2.54 (1H, *ddd*, *J* = 12.8, 10.02, 3.8 Hz)	51.9
8	1.63 (1H, *m*), 2.15 (1H, *m*)	26.0
9	2.03 (1H, *ddd*,13.00, 10.98,4.3 Hz), 2.62 (1H, *dt*, *J* = 13.04, 4.7 Hz)	35.1
10	-	147.8
11	-	75.9
12	-	175.5
13	3.66 (2H, *ABq*, *J* = 11.6 Hz)	43.5
14	5.00 (1H, *s*), 5.02 (1H, *s*)	113.6
15	5.37 (1H, *t*, *J* = 2.1Hz), 5.43 (1H, *t*, *J* = 2.1Hz)	111.4

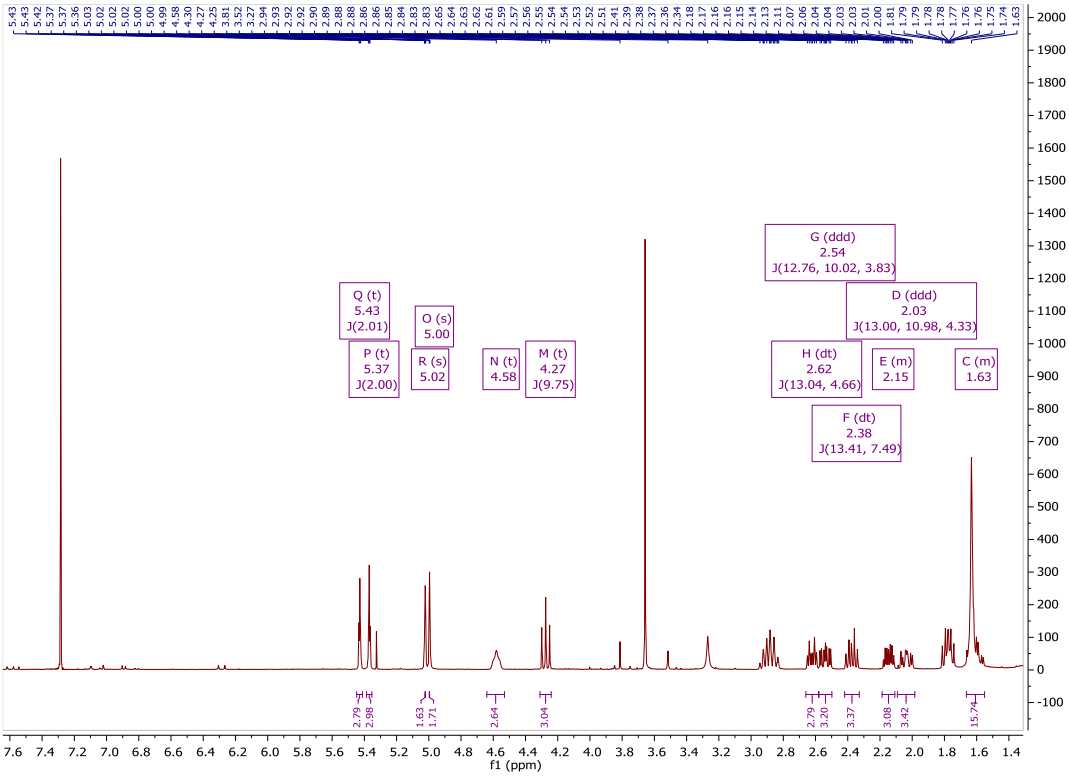

Figure 3. 17: ^{1}H NMR spectrum (400 MHz) of CC5 in $CDCl_3$

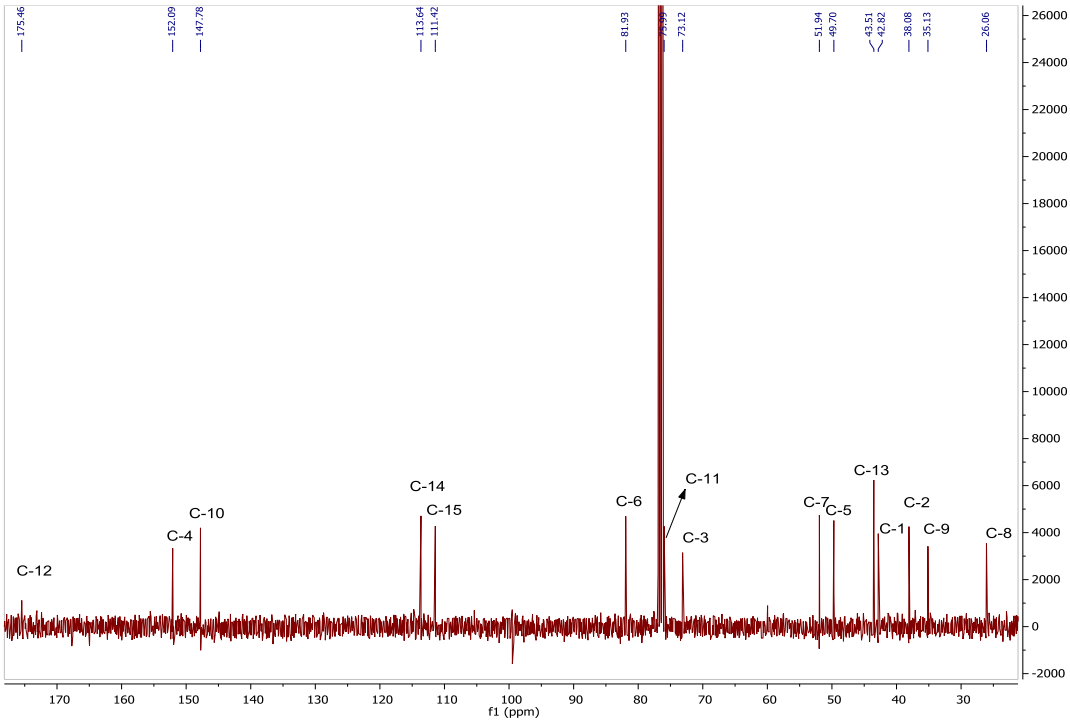

Figure 3. 18: ^{13}C NMR spectrum (100 MHz) of CC5 in $CDCl_3$

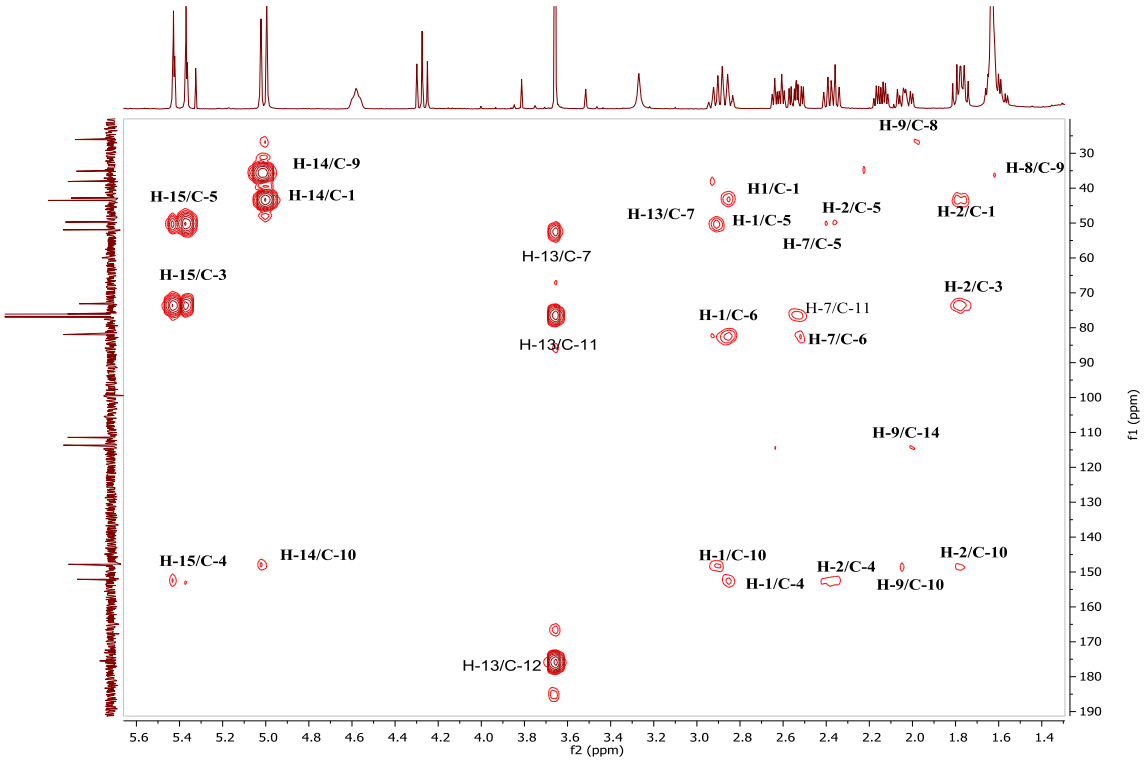

Figure 3. 19: HMBC spectrum of CC5 in $CDCl_3$

3.1.3 Fractionation of the crude extracts of C. cyrenaica leaves

The methanol extract of *C. cyrenaica* leaves (CML, 28g) was fractionated using VLC, fractions CC6 (1mg), CC7 (10mg) and CC8 (11mg) were separated as yellow powder using 10 %(v/v) hexane in ethyl acetate, 100% ethyl acetate and 10 % (v/v) methanol in ethyl acetate as mobile phase, respectively and they were further purified by size exclusion (100% methanol). The ^{1}H NMR spectrum of the hexane extract of *C. cyrenaica* leaves (CHL) and the ethyl acetate extract of *C. cyrenaica* leaves (CEL) showed signals suggesting a mixture of compounds.

3.1.3.1 Characterisation of CC6 as ferulic acid

CC6 revealed a pink spot on the TLC plate (R_f value 0.68, using 60% (v/v) ethyl acetate in hexane as a mobile phase), after treatment with anisaldehyde-sulphuric acid reagent followed by heating.

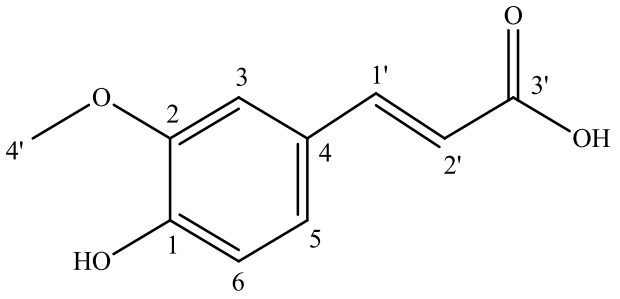

Figure 3. 20: Structure of ferulic acid

The mass spectrum in negative ion mode gave $[M - H]^-$ at *m/z* 193.0507 suggesting a molecular formula of $C_{10}H_{10}O_4$. ^{1}H NMR spectrum (Figure 3.21) showed three aromatic protons at δ_H 6.86, 7.00 and 7.07 which are characteristics for the H-6, H-5 and H-3 of the aromatic part of CC6. The presence of two proton doublets with J = 16 Hz at δ_H 6.26 (1H, *d*, J = 16Hz, H-2') and 7.57(1H, *d*, J = 16Hz, H-1') indicated the presence of H-2' and H-1' in the side chain of compound. The spectrum also displayed a signal for a methoxy group at δ_H 3.78 (3H, s, H-4'). DEPTq-135 spectrum showed three methine carbons at δ_C 122.0, 108.4 and 144.1 for H-3, H-5 and H-6, respectively, and one methyl at δ_C 51.1. The spectrum also showed signals for quaternary carbons at δ_C 146.4, 113.8 and 126.9 attributed for C-1, C-2 and C-4, respectively and one signal for carbonyl (C-3') at δ_C 171.2. The HMBC spectrum displayed ^{3}J correlation

between H-3 at δ_H 7.07 and C-1 and ^3J correlation between H-5 at δ_H 7.0 and C-1, furthermore, H-6 at δ_H 6.86 showed ^2J correlation to C-1 and ^3J correlation to C-4. Hence, these observations confirm the presence of the aromatic part of CC6. In addition, H-1' in the side chain at δ_H 7.57 showed ^2J correlation to C-2'. The above information led to the characterisation of CC6 as ferulic acid. The NMR data were in agreement with previously published data (Sajjadi *et al.*, 2012).

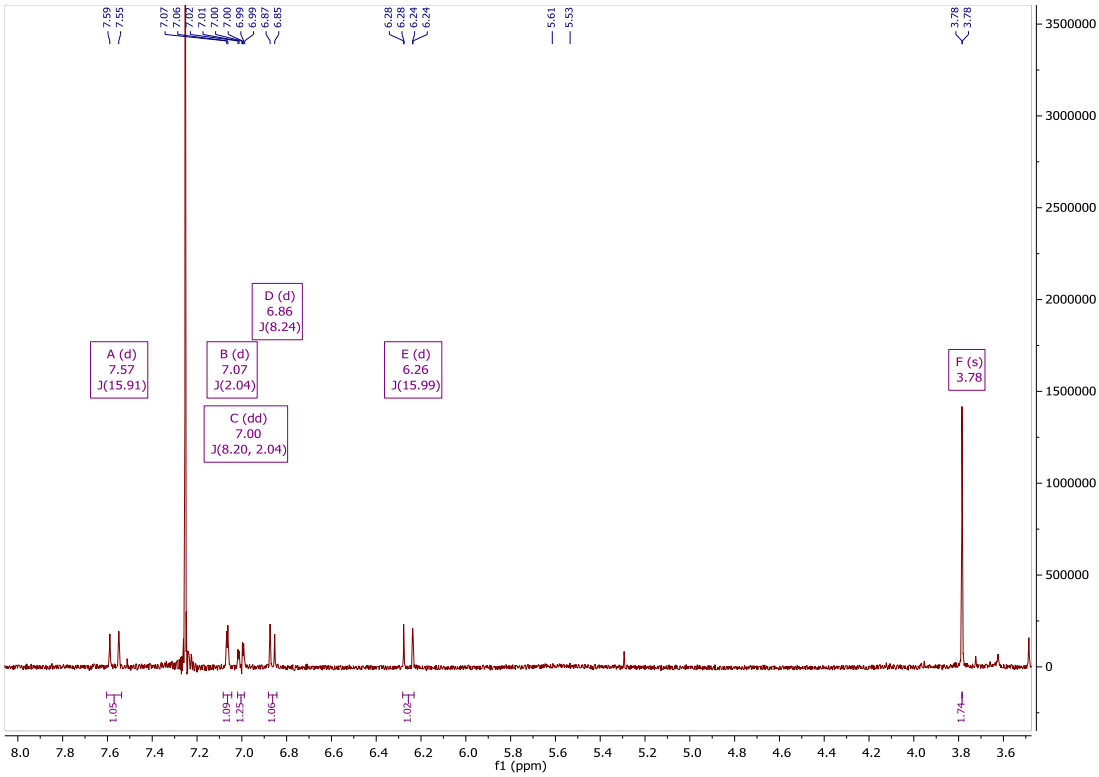

Figure 3. 21:^{1}H NMR spectrum (400 MHz) of CC6 in $CDCl_3$

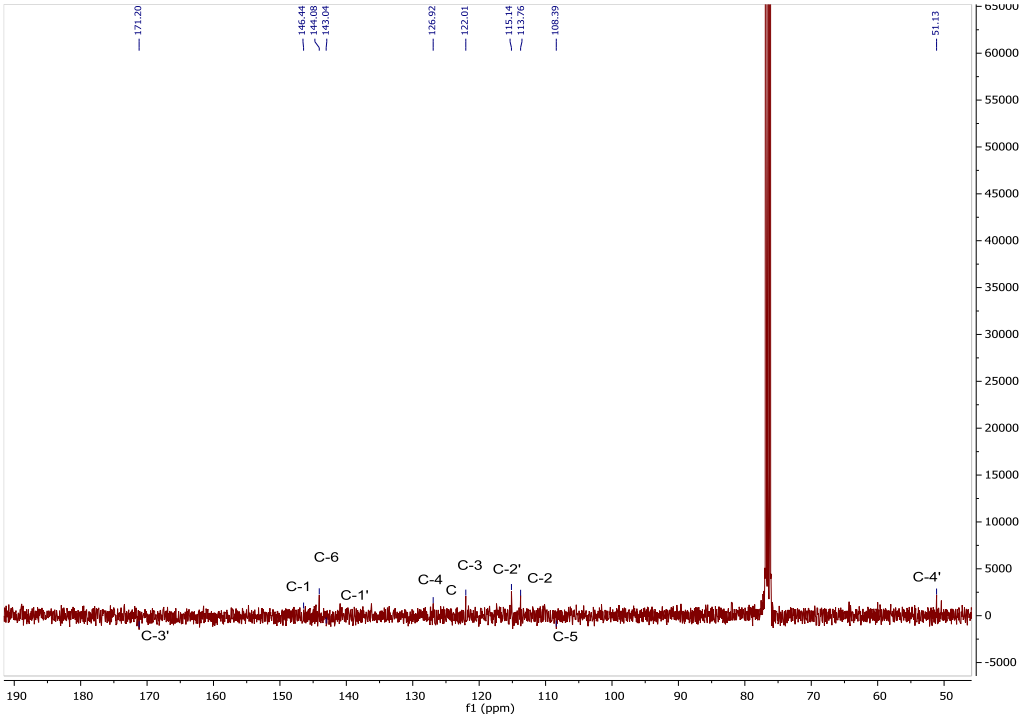

Figure 3. 22: DEPTq-135 spectrum (100 MHz) of CC6 in $CDCl_3$

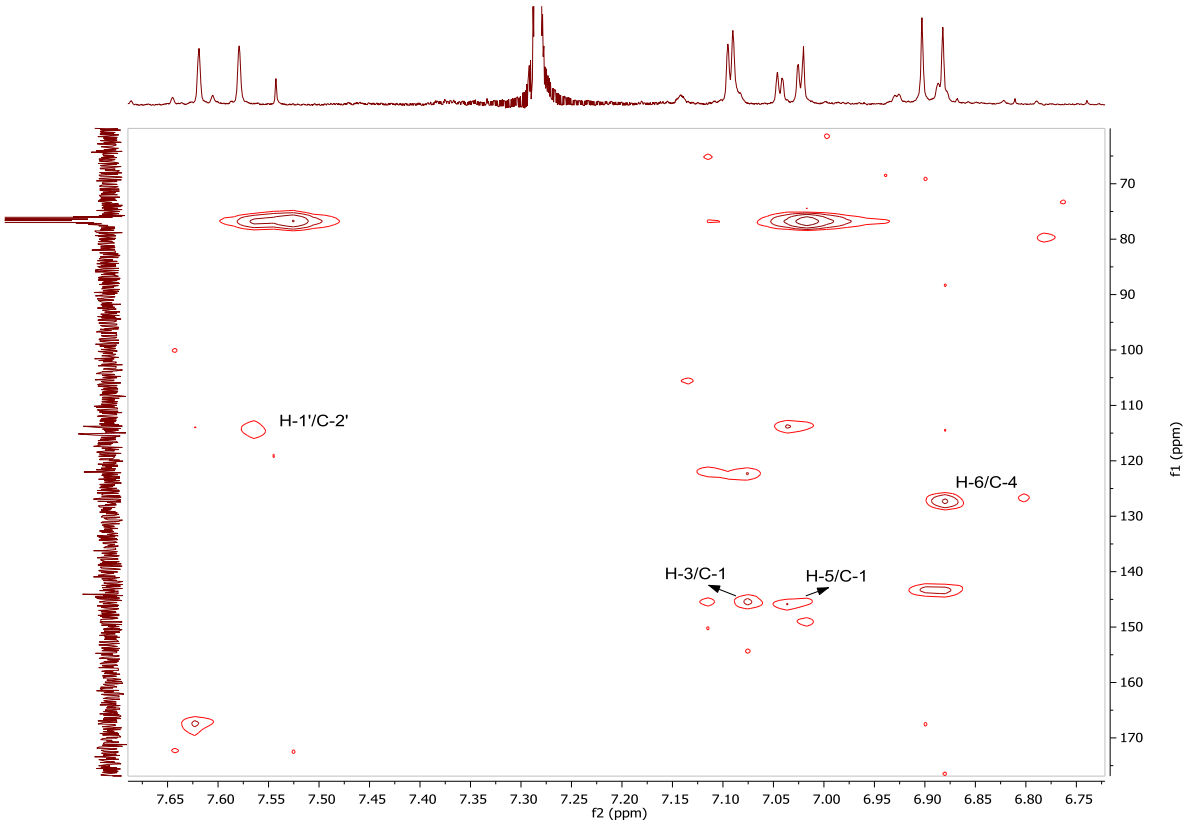

Figure 3. 23: HMBC spectrum (400 MHz) of CC6 in $CDCl_3$

3.1.3.2 Characterisation of CC7 as luteolin-7-O-β- D-glucopyranoside (cynaroside)

CC7 revealed a yellow spot on TLC (R_f value 0.72, using 10% (v/v) methanol in ethyl acetate as a mobile phase), after treatment with anisaldehyde-sulphuric acid reagent followed by heating.

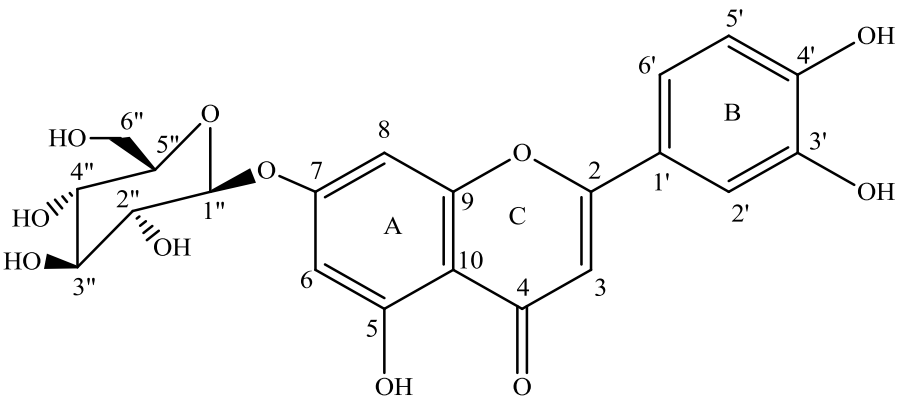

Figure 3. 24: Structure of luteolin-7-*O*-β-D-glucopyranoside

The mass spectrum in positive ion mode gave $[M+H]^+$ at *m/z* 449.1074 suggesting a molecular formula of $C_{21}H_{20}O_{11}$. The ^{1}H NMR spectrum (Figure 3.25, Table 3.5) gave a singlet at δ_H 12.97 indicating the presence of a chelated hydroxyl at C-5 position. It also showed aromatic protons of two *meta*–coupled doublets (J = 2.2Hz) at δ_H 6.45 and 6.80 attributed to H-6 and H-8 protons, respectively for ring A of a 5,7-dihydroxyflavonoid. A proton singlet at δ_H 6.75 was assigned to H-3 of the ring C. While H-2', H-5' and H-6' of ring B appeared at δ_H 7.42, 6.91 and 7.45, respectively which characteristic of a 1,3,4-trisubstituted phenyl unit. These spectral data revealed the presence of a luteolin skeleton. In addition, the ^{1}H NMR spectrum showed a series of signals between δ_H 3.21-3.72, attributable to a sugar moiety.

H-1" appeared at δ_H 5.07, while a series of signals between δ_H 3.21-3.51 attributed to H-2", 3", 4" and 5" (4H, m). 2H-6" appeared at δ_H 3.72/3.47. In addition, the proton located at δ_H 5.07 as well as the ^{13}C NMR chemical shifts of sugar at δ_C 99.8, 73.0, 77.0, 69.5, 76.3 and 60.5 indicated the presence of β-*O*-glucoside unit in luteolin-7-*O*-β-D-glucopyranoside as reported by (Chiruvella *et al.*, 2007). The ^{13}C NMR spectrum (Figure 3.26) indicated the presence of 21 carbons including a carbonyl at δc 181.8 (C-4) and six aromatic methines carbons at δc 103.0, 99.4, 94.7, 113.4, 115.9 and

119.1 (C-3, C-6, C-8, C-2`, C-5` and C-6`, respectively). Four phenolic carbons were observed at δc 161.0, 164.4, 145.7, and 149.9 (C-5, C-7, C-3` and C-4`, respectively) and four quaternary carbons at δc 162.8, 156.8, 105.2, and 121.2 (C-2, C-9, C-10 and C-1`, respectively). For glucopyranoside, the ^{13}C NMR spectrum showed five oxymethines carbons at δ_C 99.8, 73.0,77.0, 69.5 and 76.3 (C-1", C-2", C-3", C4" and C-5", respectively) and one oxymethylene carbon at δ 60.5 (C-6").

From HSQC spectrum (Figure 3.27) along with HMBC spectrum (Figure 3.28) a sequence of correlations was observed as following: the methine proton at δ_H 6.75 (H-3) of ring C displayed ^2J correlations to quaternary carbon (C-2) at δC 162.8 and carbonyl (C-4) at δ_C 181.8. The spectrum also showed ^3J correlations between H-3 and the quaternary carbon (C-10) at δ_C 105.2 and to C-1' of ring B at δ_C 121.2. In addition, H-6 of ring A showed ^2J correlations to C-5 and C-7 at δ_C 161.0 and 164.4, respectively and displayed ^3J correlations to C-8 and C-10 at δ_C 94.7 and 105.2, respectively as well as H-8 displayed ^2J correlations to C-7 and showed ^3J correlations to C-6 and C-10. Furthermore, H-2' proton of ring B at δ_H 7.42 showed ^2J correlations to C-3'at δ_C 145.7 and ^3J correlations to C-4' and C-6' at δ_C 149.9 and 119.1, respectively. In addition, H-5'at δ_H 6.91 showed ^3J correlations to C-1' and C-3'. H-6' also showed ^3J correlations to C-2 and C-2'. These correlations confirm the presence of luteolin unit. In addition, the HMBC spectrum, also showed a cross peak between the signal at δ_H 5.07 (H-1") and C-7 at δ_C 164.4 of ring A which indicated the attachment of sugar unit to luteolin moiety in the C-7 position. In addition, H-2" at δ_H 3.26 showed ^2J correlations to C-1" at δ_C 99.8 and H-3" at δ_H 3.33 displayed ^2J correlation to C-2". H-4" at δ_H 3.21 showed ^3J correlation to C-6" at δ_C 60.5. Furthermore, H-5" at δ_H 3.50 displayed ^3J correlation to C-3" at δ_C 77.0, and H-6"at δ_H 3.72 showed ^3J correlation to C-4".

Hence the above observations led to the conclusion that CC7 is a luteolin moiety attached to a sugar unit at C-7, thus CC7 was identified as luteolin-7-*O*-β-D-glucopyranoside in agreement with a previous report (Kurkin, 2015).

Table 3. 5: ^{1}H (400 MHz) and ^{13}C (100 MHz) NMR data of CC7 in DMSO-*d*$_6$

Position	^{1}H δppm (m, *J* Hz)	^{13}C δppm
1	-	-
2	-	162.8
3	6.75 (1H, *s*)	103.0
4	-	181.8
5-OH	12.97 (*br. s*)	161.0
6	6.45 (1H, *d*, *J* = 2.2Hz)	99.4
7	-	164.4
8	6.80 (1H, *d*, *J* = 2.2Hz)	94.7
9	-	156.8
10	-	105.2
1`	-	121.2
2`	7.42 (1H, *d*, *J* = 2.3 Hz)	113.4
3`	-	145.7
4`	-	149.9
5`	6.91 (1H, *d*, *J* =8.4 Hz)	115.9
6`	7.45 (1H, *dd*, *J* = 8.4, 2.3 Hz)	119.1
1”	5.07 (1H, *d*, *J* = 7.4 Hz)	99.8
2”	3.26 (1H, *m*)	73.0
3”	3.33 (1H, *m*)	77.0
4”	3.21 (1H, *m*)	69.5
5”	3.50 (1H, *m*)	76.3
6”	3.72 (1H, *m*), 3.47 (1H, *m*)	60.5

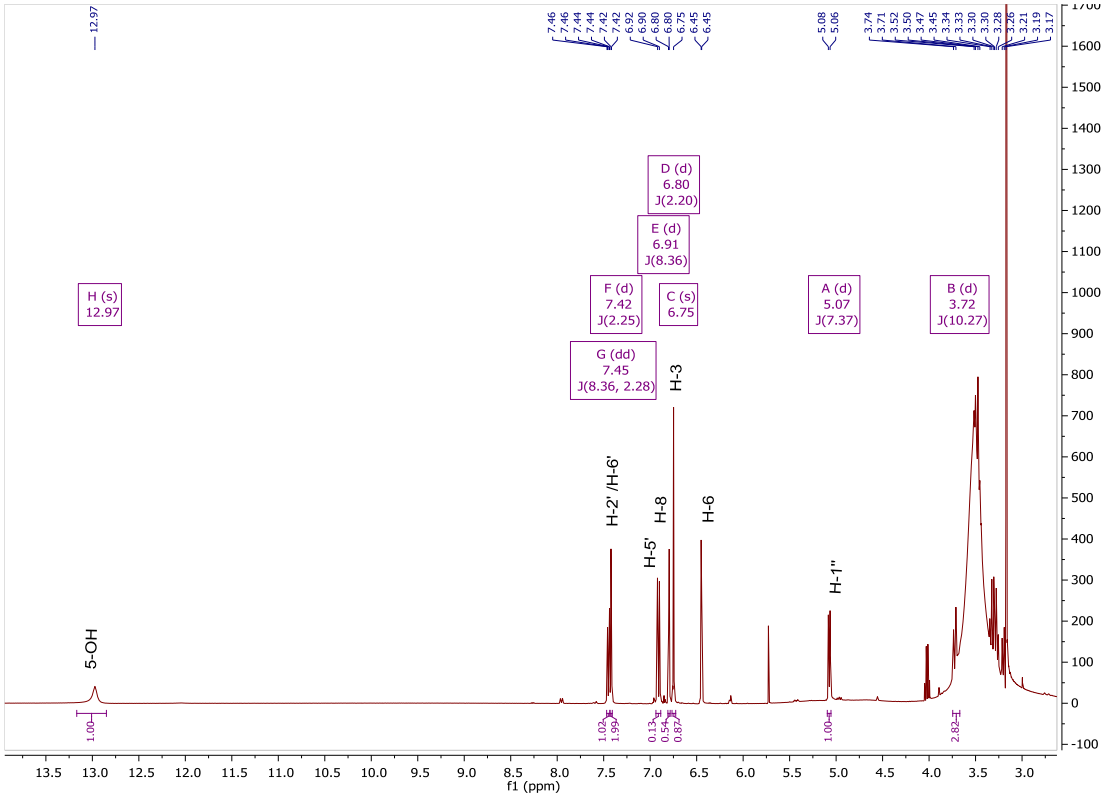

Figure 3. 25: ^{1}H NMR spectrum (400 MHz) of CC7 in DMSO-*d*$_6$

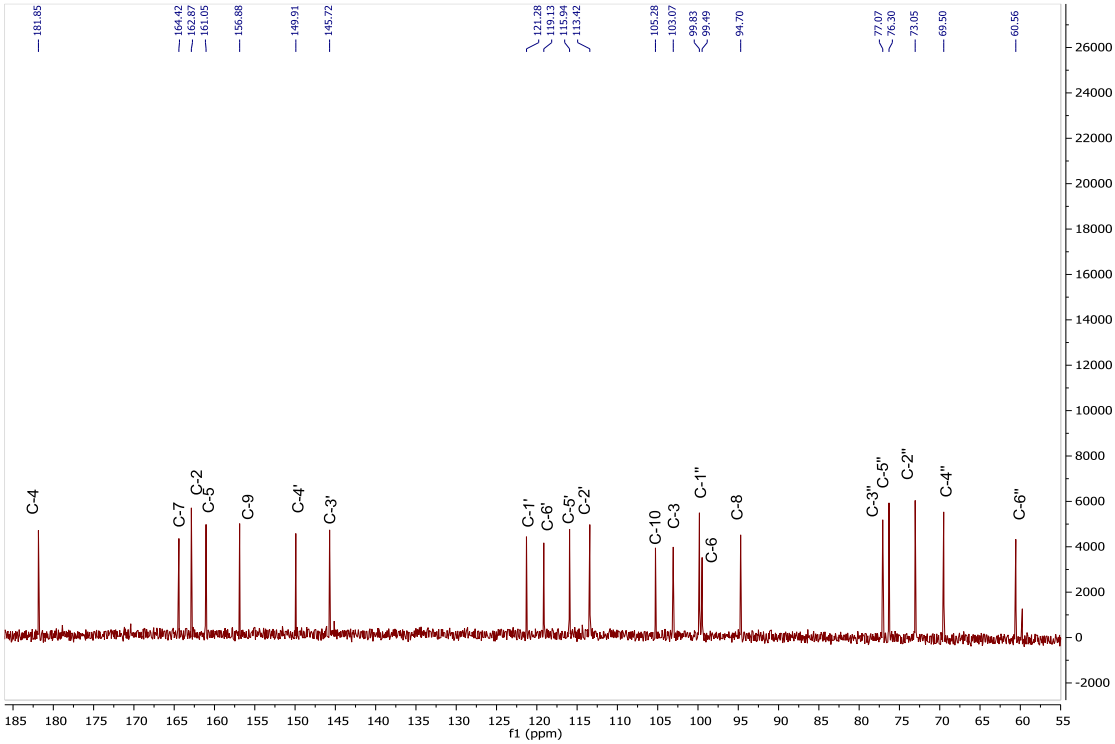

Figure 3. 26: ^{13}C NMR spectrum (100 MHz) of CC7 in DMSO-*d*$_6$

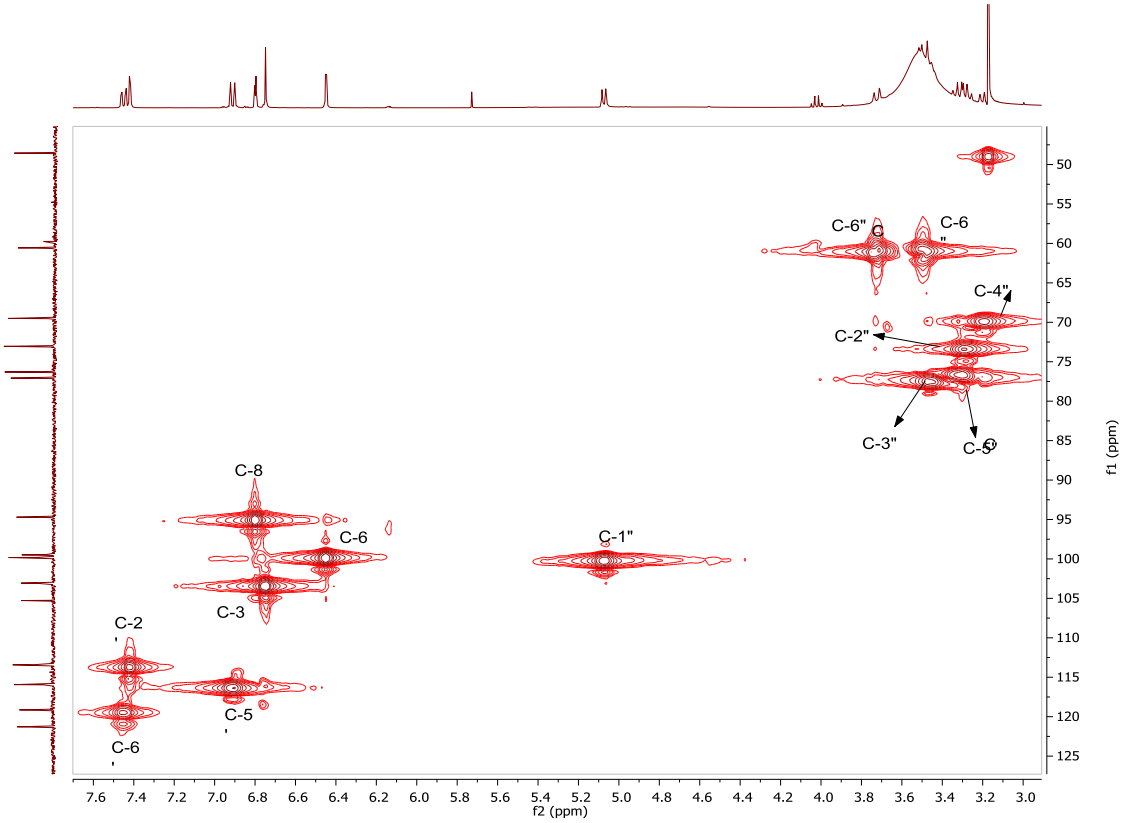

Figure 3. 27: HSQC spectrum (400 MHz) of CC7 in DMSO-*d*$_6$

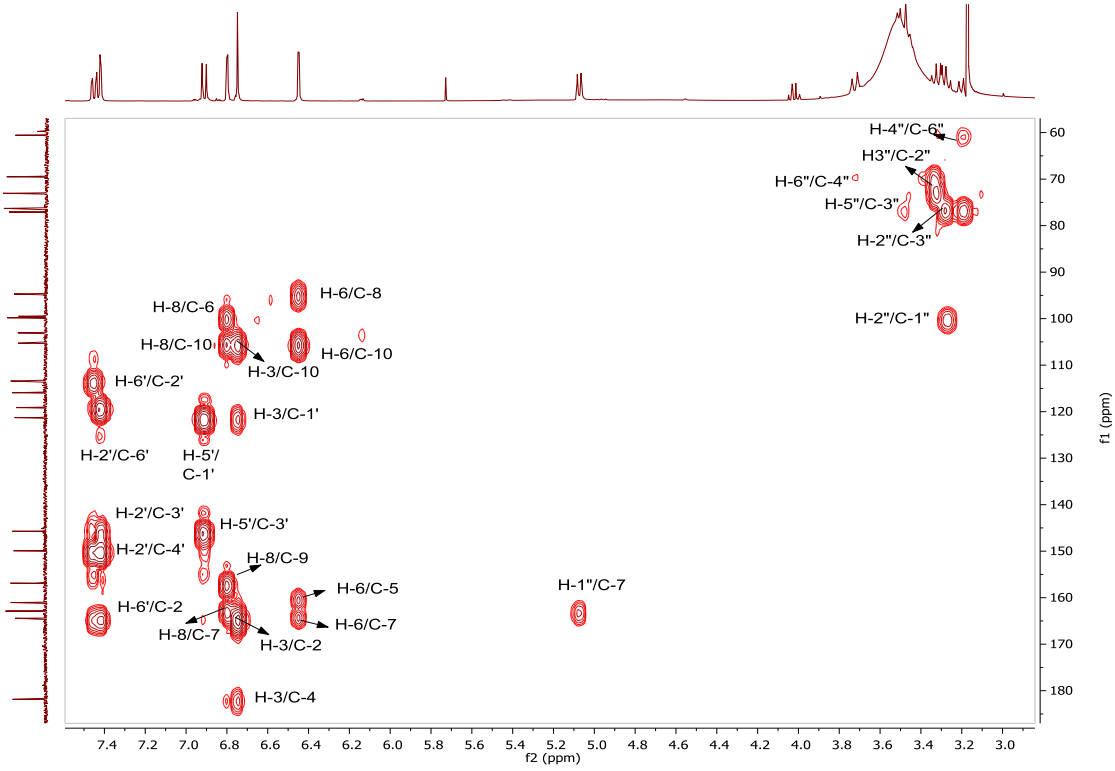

Figure 3. 28: HMBC spectrum (400 MHz) of CC7 in DMSO-*d*$_6$

3.1.3.3 Characterisation of CC8 as 1, 3-dicaffeoylquinic acid (cynarin)

CC8 revealed a yellow spot on TLC (R_f value 0.81, using 10% (v/v) methanol in ethyl acetate as a mobile phase), after treatment with anisaldehyde-sulphuric acid reagent followed by heating.

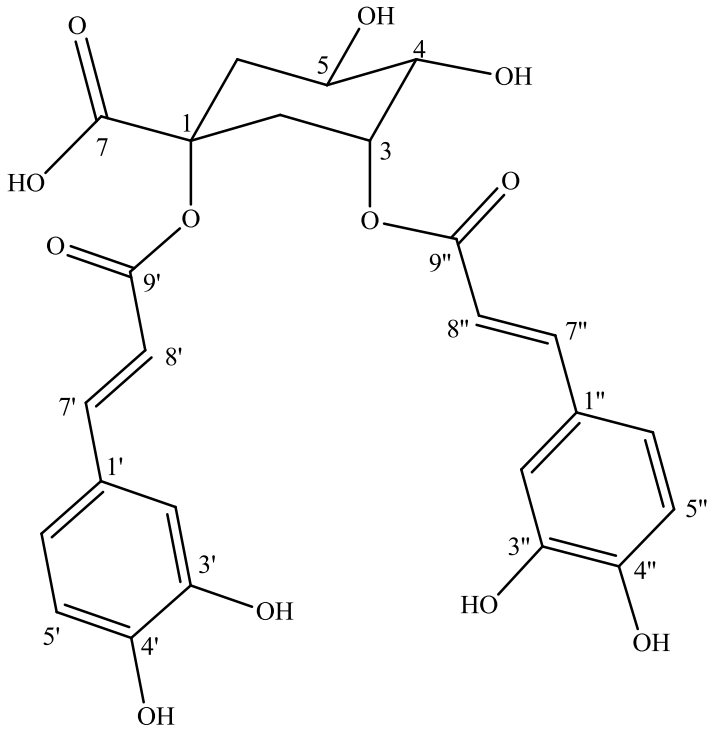

Figure 3. 29: Structure of 1, 3-dicaffeoylquinic acid

The mass spectrum in positive ion mode gave $[M+H]^+$ at *m/z* 517.1342 suggesting a molecular formula of $C_{25}H_{24}O_{12}$. The ^1H NMR spectrum (Figure 3.30, Table 3.6) showed three oxymethines at δ_H 5.42 (H-3), 3.76 (H-4) and 4.27 (H-5) and two methylenes at δ_H 2.04/2.65 (2-H2) and 2.27/2.49 (2-H6). These signals were similar to those of quinic acid. The presence of two caffeoyl groups was established with signals at δ_H 7.58 (H-7'/7"), 6.33 (H-8'), 6.29 (H-8"), 7.07 (H2'), 7.06 (2"), 6.94 (H-6'), 6.92 (6"), and δ_H 6.78 (H-5'/5"). DEPTq135^{13}C NMR spectral data (Table 3.6) showed 25 carbons including two carbonyls, four olefinic methines, six aromatic carbons from caffeoyl groups, three oxymethines, two methylenes and one carbonyl from quinic acid.

All protons were assigned with the aid of 2D spectra. In the HMBC spectrum (Figure 3.32), the proton at δ_H 5.42 (H-3) gave a ^3J HMBC correlation to the carbonyl at δ_C 169.2 (C-9") and this accounts for it being highly deshielded compared to H-4 and H-5, suggesting that the hydroxyl group at position 3 of quinic acid was substituted by a caffeoyl group. The proton at δ_H 3.76 (H-4) showed ^2J and ^3J correlations, respectively to one oxymethine at δ_C 71.8 (C-3) and one methylene at δ_C 36.7 (C-6). The proton at δ_H 4.27 (H-5) correlated via ^3J coupling to the methine at δ_C 71.8 (C-3) and one quaternary carbon at δ_C 83.6 (C-1) and ^2J coupling to the methine at δ_C 74.2 (C-4).

Two methylene protons at δ_H δ2.04/δ2.65 (2H-2) correlated via a ^2J coupling to the oxymethine at δ_C71.8 (C-3). The HMBC spectrum revealed another important correlation between the deshielded proton at δ_H 5.42 (H-3) and the carbonyl from one caffeoyl group at δ_C 169.2 (C-9"), which established that one caffeic acid unit was in C-3 of the quinic acid moiety. However, no correlation was observed between any other proton on the quinic acid moiety and the carbonyl at δ_C 168.4 (C-9'), suggesting that the second caffeic acid unit had to be attached to C-1 of the quinic acid moiety. In support of this, C-1 showed a chemical shift at δ_C 83.6 which a result of deshielded from the esterification, compared to the chemical shift of free OH at C-1 position which appear about δ_C 74.7 - 73.3 (Wan *et al.*, 2017).

Based on the above information, CC8 was identified as 1, 3-dicaffeoylquinic acid in agreement with a previous report (Danino *et al.*, 2009).

Table 3. 6: ^{1}H (400 MHz) and DEPTq-135 (100 MHz) NMR data of CC8 in CD_3OD

Position	^{1}H δppm (*J* Hz)	^{13}C δppm
1	-	83.6
2	2.04 (1H, *dd*, *J* =13.7,10.8 Hz)/δ2.65 (1H, *dd*,13.7,4.1 Hz)	38.1
3	5.42 (1H, *ddd*, *J* = 10.8, 9.3, 4.1 Hz)	71.8
4	3.76 (1H, *dd*, *J* = 9.3, 3.5Hz)	74.2
5	4.27 (1H, *q*, *J* = 3.5Hz)	70.8
6	2.27 (1H, *dd*, *J* = 15.5,3.5Hz)/δ2.49 (1H, *dd*, *J* = 15.5,3.5Hz)	36.7
7	-	177.8
1’	-	127.9
2’	7.07 (1H, *d*, *J* = 2.04 Hz)	115.2
3’	-	146.6
4’	-	149.3
5’	6.78 (1H, *d*, *J* = 8.2 Hz)	116.6
6’	6.94 (1H, *dd*, *J* = 8.2, 2.04 Hz)	122.9
7’	7.58 (1H, *d*, *J* = 15.9 Hz)	146.8
8’	6.33 (1H, *d*, *J* = 15.9 Hz)	115.3
9’	-	168.4
1”	-	128.2
2”	7.06 (1H, *d*, *J* = 2.04 Hz)	116.5
3”	-	146.7
4”	-	149.5
5”	6.78 (1H, *d*, *J* = 8.2 Hz)	116.6
6”	6.92 (1H, *dd*, *J* = 8.2,2.04 Hz)	123.0
7”	7.58 (1H, *d*, *J* = 15.9 Hz)	147.0
8”	6.29 (*d*, *J* = 15.9 Hz)	115,5
9”	-	169.2

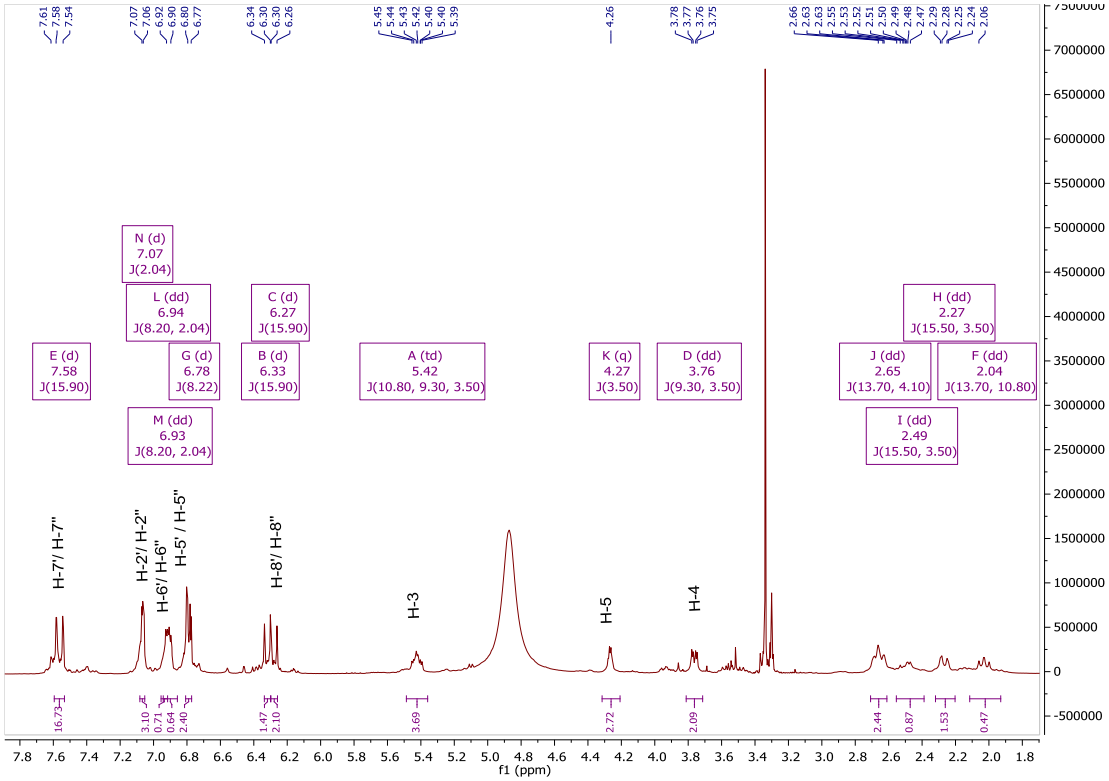

Figure 3. 30: ^{1}H NMR spectrum (400 MHz) of CC8 in CD_3OD

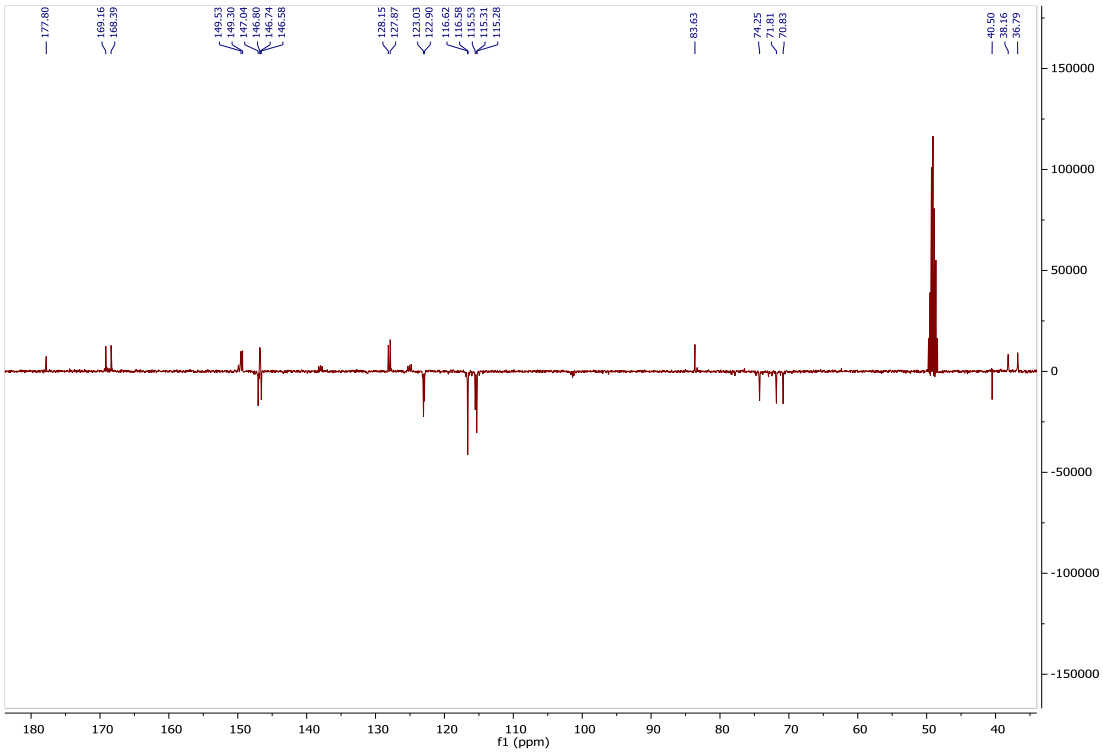

Figure 3. 31: DEPTq-135 spectrum (100 MHz) of CC8 in CD_3OD

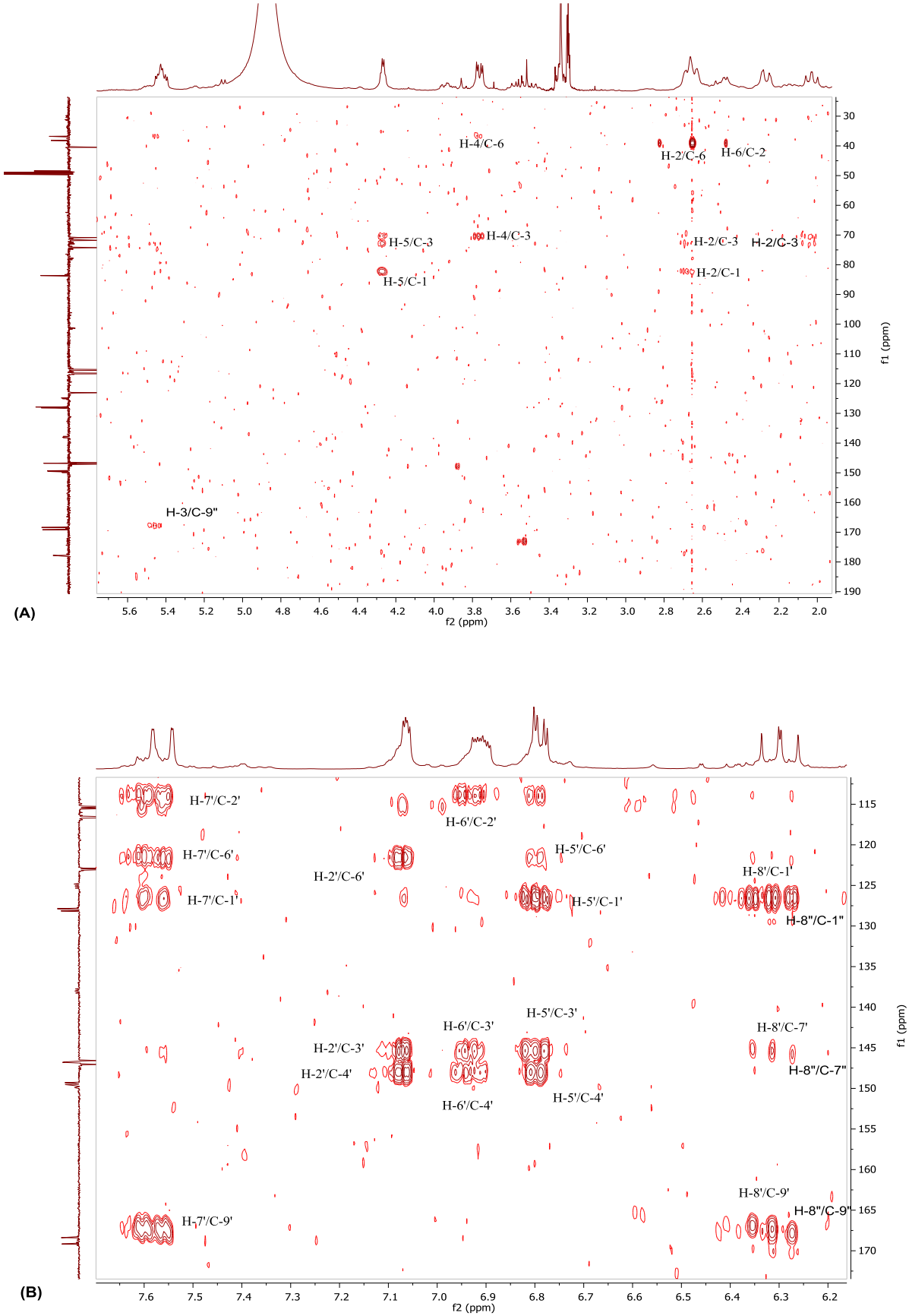

Figure 3. 32:(A) HMBC spectrum (400 MHz) of CC8 in CD_3OD the region 2.0 - 5.6ppm (B) Expansion in the region of 6.2 - 7.3 ppm

3.1.4 Fractionation of C. cyrenaica stem extract

The methanol extract of *C. cyrenaica* stem (CMS, 30g) was fractionated by VLC, fractions CC9 (4mg) separated as a yellow powder and CC10 (7mg) as a greenish powder using 80% (v/v) ethyl acetate in hexane and 100% ethyl acetate as mobile phase, respectively. The ethyl acetate extract of *C. cyrenaica* stem (CES, 5g) was fractionated by CC, fractions CC11 (5mg), CC12 (6mg) and CC13 (2mg) were separated as greenish powder using 80% (v/v) ethyl acetate in hexane as a mobile phase. The ^{1}H NMR spectrum of the hexane extract of *C. cyrenaica* stem (CHS) showed signals suggesting a mixture of compounds.

3.1.4.1 Characterisation of CC9 as 3`, 4`, 5, 7-tetrahydroxyflavone (luteolin).

CC9 revealed a yellow spot on TLC (R_f value 0.56, using 60% (v/v) ethyl acetate in hexane as a mobile phase), after treatment with anisaldehyde-sulphuric acid reagent followed by heating.

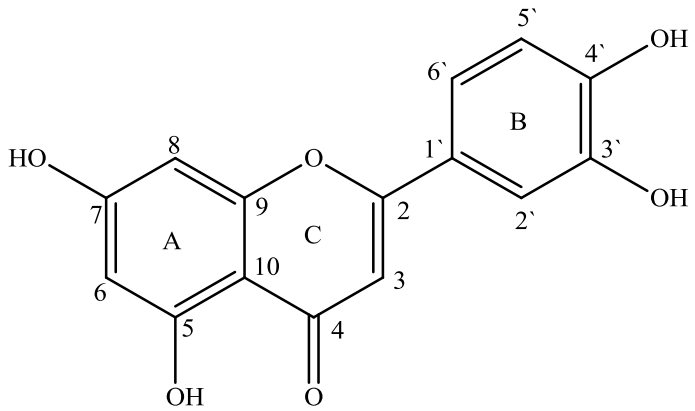

Figure 3. 33: Structure of luteolin

The mass spectrum in negative ion mode gave $[M-H]^-$ at *m/z* 285.0408 suggesting a molecular formula of $C_{15}H_{10}O_6$. The ^{1}H NMR spectrum (Figure 3.34) showed a proton singlet at δ_H 13.04 (1H, *s*, 5-OH group), and signals at δ_H 6.26 and 6.54 attributed to the A-ring as H-6 and H-8 protons, respectively and a proton singlet at δ_H 6.59 (1H, *s*) of ring C as H-3. While H-2', H-5' and H-6' of ring B appeared at δ_H 7.51, 7.01 and 7.48, respectively. The DEPTq135^{13}C NMR spectrum (Figure 3.35) indicated the presence of 15 carbons including a carbonyl at δc 182.1 (C-4) and six methines carbons at δ_C 103.2, 98.8, 93.8, 113.2, 115.8 and 119.2 (C-3, C-6, C-8, C-2`, C-5` and

C-6`, respectively). Four phenolic carbons were observed at $\delta_C$ 162.5, 164.3, 145.7, and 149.5 (C-5, C-7, C-3` and C-4`, respectively) and four quaternary carbons at $\delta_C$ 164.1, 157.9, 104.4, and 122.7 (C-2, C-9, C-10 and C-1`, respectively).

The HMBC spectrum (Figure 3.37) displayed ^2J correlation between H-3 in the C-ring at δ_H 6.59 and C-2 and C-4 at δ_C 164.1 and 182.1, respectively and showed ^3J correlation to C-1' and C-10 at δ_C 122.7 and 104.4, respectively. H-6 in the A-ring at δ_H 6.26 showed ^2J correlation to C-5 δ_C 162.5 and ^3J correlation to C-8 and C-10 at δ_C 93.8 and 104.4, respectively as well as H-8 at δ_H 6.54 displayed ^2J correlation to C-7 and C-9 at δ_C 164.3 and 157.9, respectively and showed ^3J correlation to C-6 and C-10 at δ_C 98.8 and 104.4, respectively. In addition, B-ring also showed ^2J correlation between H-2' at δ_H 7.51 and C-3'at δ_C 145.7 and showed ^3J correlation to C-4' and C-6' as well as to C-2 in the C-ring at δ_C 149.5,119.2 and 164.1, respectively. Furthermore, H-5' at δ_H 7.01 showed ^2J correlation to C-4' at δ_C 149.5 and ^3J correlation to C-1'and C-3' at δ_C 122.7 and 145.7, respectively. The HMBC spectrum also showed ^3J correlation between H-6' at δ_H 7.48 and C-2' and C-4' at δ_C 113.2 and 149.5, respectively, hence this sequence of correlations confirmed the structure of CC9 as 3`, 4`, 5, 7-tetrahydroxyflavone.

From 1D NMR spectra and HSQC data along with the sequence of HMBC correlations observed, CC9 was identified as luteolin. In addition, the ^{1}H &^{13}C NMR spectral data are in agreement with those previously reported (Özgen *et al.*, 2011).

Table 3. 7: ^{1}H (400 MHz) and DEPTq-135 (100 MHz) NMR data of CC9 in acetone-*d*$_6$

Position	^{1}H δppm (*J* Hz)	^{13}C δppm
1	-	-
2	-	164.1
3	6.59 (1H, *s*)	103.2
4	-	182.1
5	13.04 (-OH)	162.5
6	6.26 (1H, *d*, *J* = 2.14 Hz)	98.8
7	-	164.3
8	6.54 (1H, *d*, *J* = 2.10 Hz)	93.8
9	-	157.9
10	-	104.4
1`	-	122.7
2`	7.51 (1H, *d*, *J* = 2.22 Hz)	113.2
3`	-	145.7
4`	-	149.5
5`	7.01 (1H, *d*, *J* = 8.29 Hz)	115.8
6`	7.48 (1H, *dd*, *J* = 8.35,2.24 Hz)	119.2

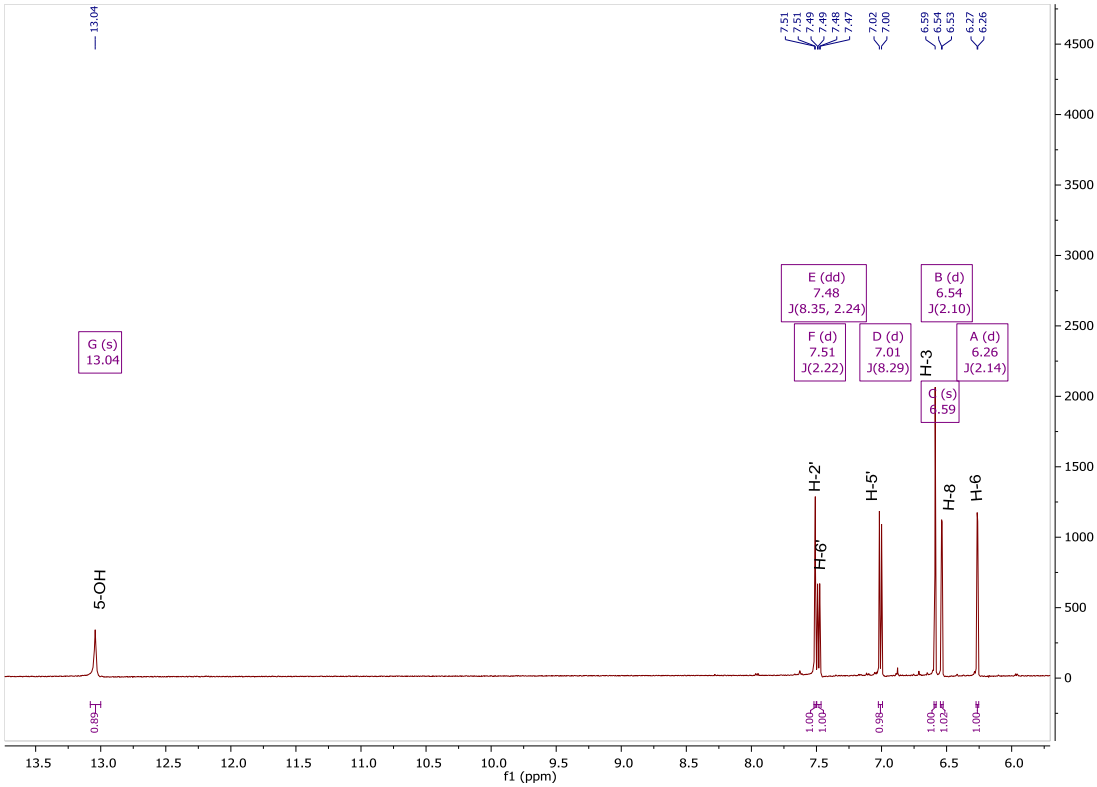

Figure 3. 34: ^{1}H NMR spectrum (400 MHz) of CC9 in acetone-*d*$_6$

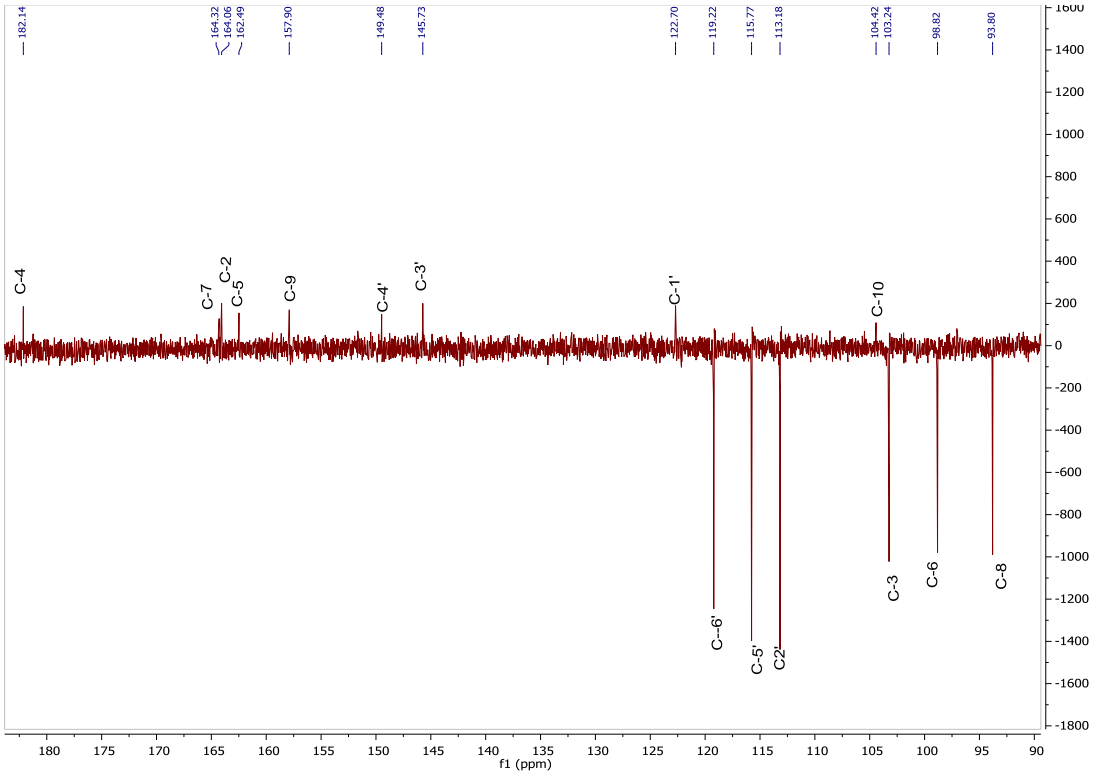

Figure 3. 35: DEPTq-135 NMR spectrum (100 MHz) of CC9 in acetone-*d*$_6$

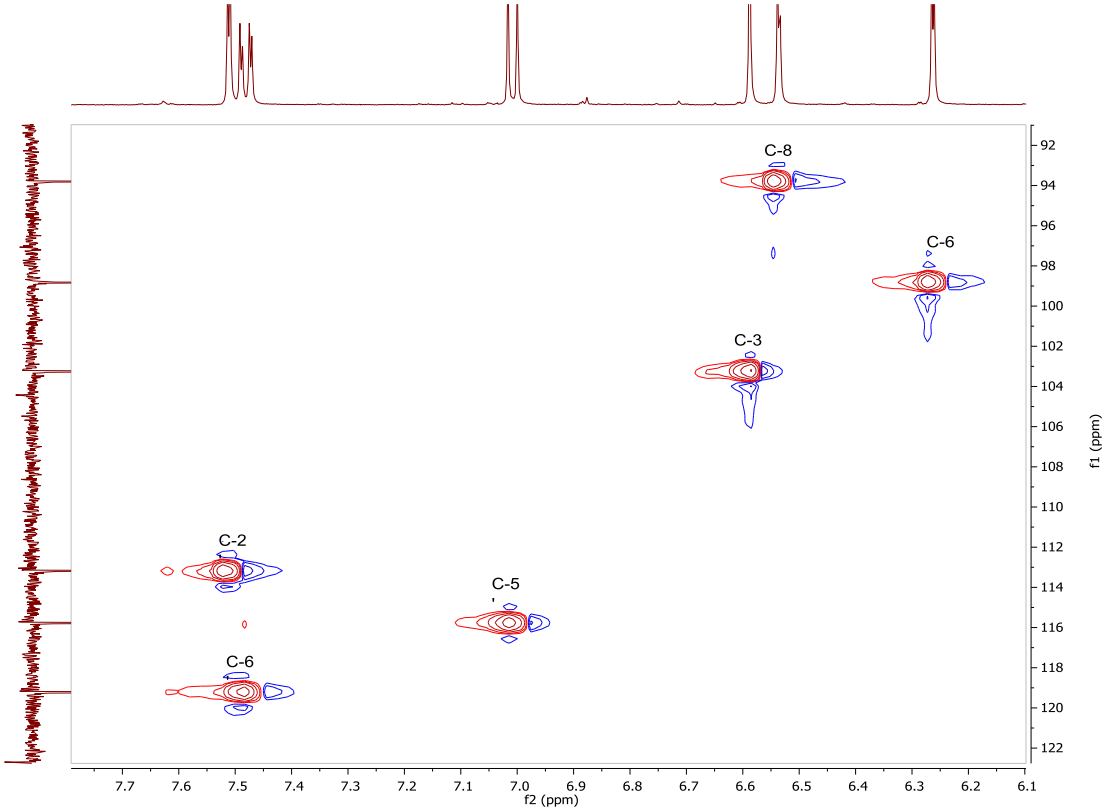

Figure 3. 36: HSQC spectrum (400 MHz) of CC9 in acetone-*d*6

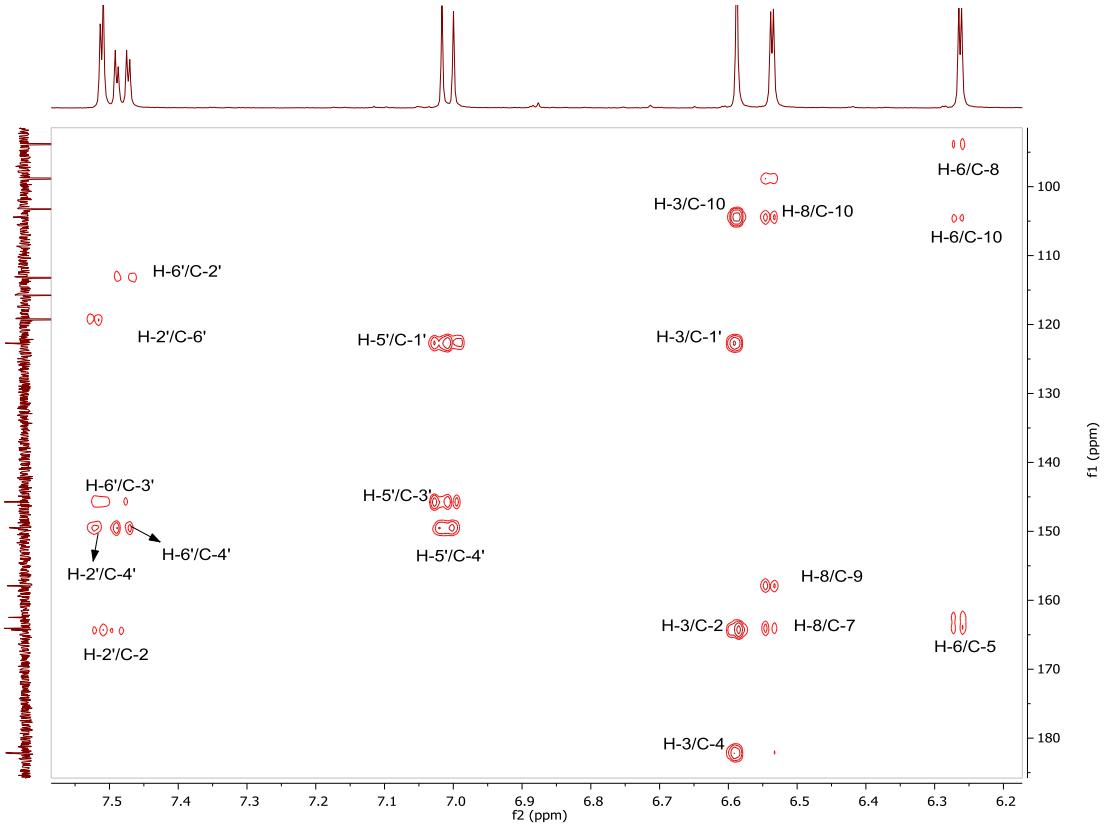

Figure 3. 37: HMBC spectrum (400 MHz) of CC9 in acetone-*d*6

3.1.4.2 Characterisation of CC10 as catechin 7-O-gallate

CC10 revealed a dark brown spot on TLC (R_f value 0.83, using 10% (v/v) methanol in ethyl acetate as a mobile phase), after treatment with anisaldehyde-sulphuric acid reagent followed by heating.

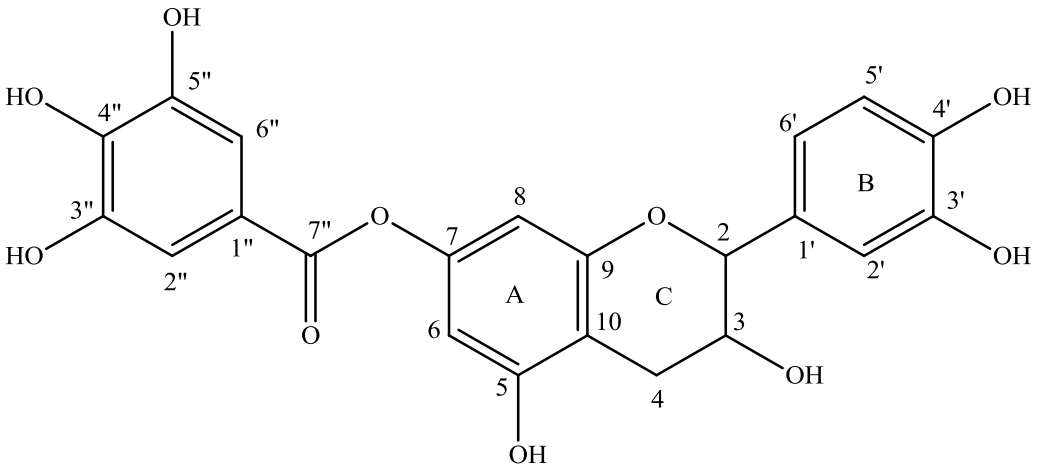

Figure 3. 38: Structure of catechin 7-*O*-gallate

The mass spectrum in negative ion mode gave $[M - H]^-$ at *m/z* 441.0832 suggesting a molecular formula of $C_{22}H_{18}O_{10}$. The ^{1}H NMR spectrum (Figure 3.39) showed signals at δ_H 4.69, 4.10 and 2.65/3.0 which attributed to H-2, H-3, and 2H-4, respectively. Signals at δ_H 6.26 and 6.35 accounted for the A-ring as H-6 and H-8 protons, respectively. While H-2', H-5' and H-6' of ring B appeared at δ_H 6.93,6.82 and 6.79, respectively. For a galloyl moiety, proton at δ_H 7.25 (2H, s) assigned to H-2”and H-6”. The ^{13}C NMR spectrum (Figure 3.40) showed peaks at δc 27.3(C-4), 66.5 (C-3), 81.5(C-2), 100.7(C-6), 100.5 (C-8), 113.8 (C-2'), 114.3 (C-5'), 118.6 (C-6') and other aromatic carbons showed peaks at δ_C 105.5, 130.5, 144.3, 144.4, 150.1, 155.2 and 155.5. Galloyl moiety showed peaks assigned as following: 163.8 (C-7”), 144.8 (C-3”), 144.9 (C-5”), 138.0 (C-4”), 119.7 (C-1”), 108.9 (C-2”,6”).

The HMBC spectrum displayed ^2J correlation between 2H-4 (δ_H 2.65/3.0) and C-3 and C-10 at δ_C 66.5 and 105.5, respectively as well as it showed ^3J correlation to C-2 and C-9 at δ_C 81.5 and 155.2, respectively. In addition, H-2 at δ_H 4.69 showed ^2J correlation to C-1’ (δ_C 130.5) and C-3 (δ_C 66.5) and ^3J correlation to C-2’ (δ_C 113.8) and C-4 (δ_C 27.3). The spectrum also displayed long-range ^{1}H-^{13}C correlations between H-2 and C-9 at δ_C 155.2. Both H-6 at δ_H 6.26 and H-8 at δ_H 6.35 showed ^2J

correlation to quaternary carbons C-5 (δ_C 155.5) and C-7(δ_C 150.1), repectively and displayed ^3J correlation to C-10 (δ_C 105.5). In addition, H-5' at δ_H 6.82 showed ^2J correlation to C-4' (δ_C 144.3) and ^3J correlation to C-1' (δ_C 130.5). H-2' at δ_H 6.93 showed ^3J correlation to C-2(δ_C 81.5) and C-6' (δ_C 118.6) and ^2J correlation to C-3' (δ_C 144.4). H-2" in the galloyl moiety showed ^2J correlation to quaternary carbons C-1"and C-3" at δ_C 119.7 and 144.8, respectively and ^3J correlation to C-4", C-6" and C-7" at δ_C 138.0,108.9 and 163.8, respectively, hence these serial correlations led to the conclusion that this compound consists of catechin with a galloyl moiety attached to C-7. The location of the galloyl group in CC10 was deduced to be at C-7 OH of the catechin moiety, from the ^{1}H NMR spectrum, in which signals due to the C-6 proton and C-8 proton appeared deshielded at lower field at δ_H 6.26 and 6.35, respectively than those observed in catechin moiety at δ_H 6.0 and 5.8 for H-6 and H-8, respectively (Davis *et al.*, 1996), which as a result from esterification of OH at C-7 with a galloyl moiety.

Based on the above data 1D and 2D NMR, CC10 was identified as catechin 7-*O*-gallate in agreement with those reported (Tanaka *et al.*, 1983).

Table 3. 8: ^{1}H (400 MHz) and ^{13}C (100 MHz) NMR data of CC10 in acetone-d_6

Position	^{1}H δppm (m, *J* Hz)	^{13}Cppm
1	-	-
2	4.69 (*d*, *J* = 7.6 Hz)	81.5
3	4.10 (*td*, *J* = 8.1, 5.5 Hz)	66.5
4	2.65 (*dd*, *J* = 16.5, 8.3 Hz, H-4) 3.0 (*dd*, *J* = 16.5, 5.4 Hz, H-4)	27.3
5	-	155.5
6	6.26 (*d*, *J* = 2.2	100.7
7	-	150.1
8	6.35 (*d*, *J* = 2.2 Hz),	100.5
9	-	155.2
10	-	105.5
1’	-	130.5
2’	6.93 (*d*, *J* = 1.8 Hz),	113.8
3’	-	144.4
4’	-	144.3
5’	6.82 (*d*, *J* = 8.1 Hz)	114.3
6’	6.79 (*dd*, *J* = 8.3 Hz, 1.8 Hz)	118.6
1”	-	119.7
2”	7.25 (*s*)	108.9
3”	-	144.8
4”	-	138.0
5”	-	144.9
6”	7.25 (*s*)	108.9
7”	-	163.8

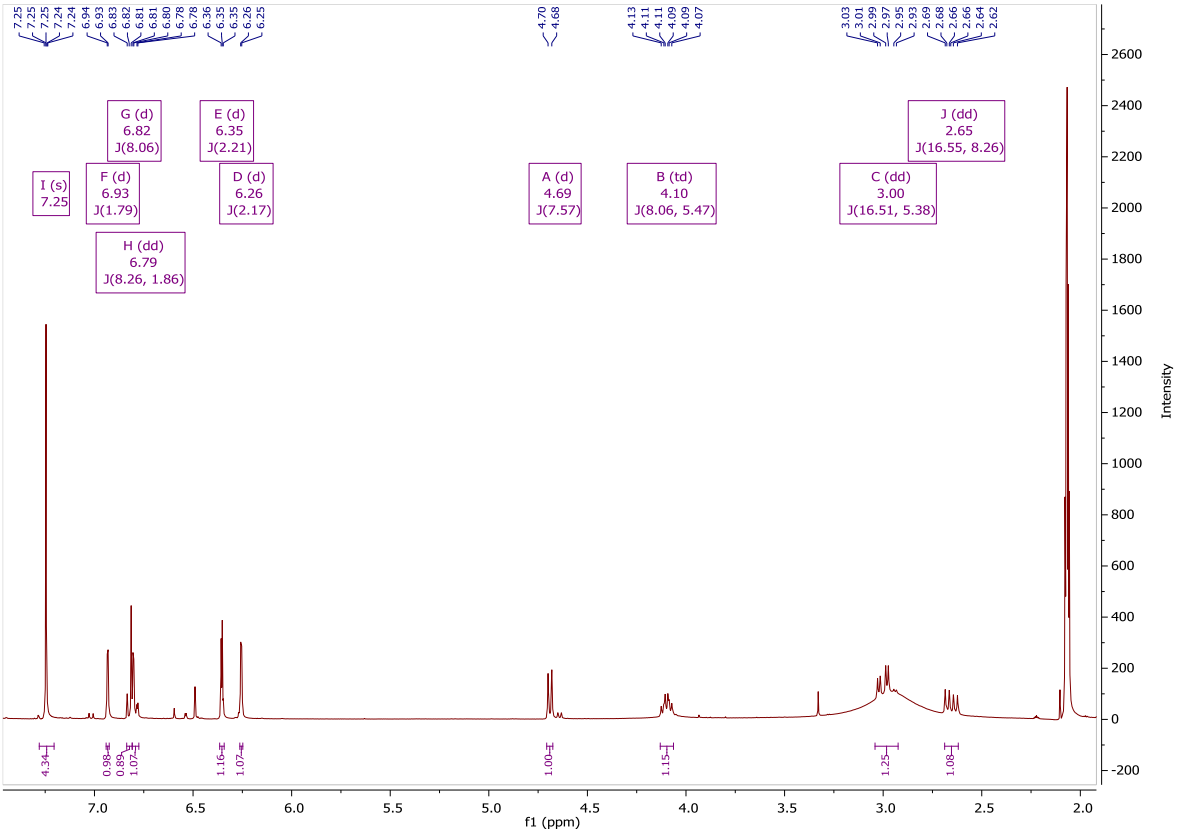

Figure 3. 39: ^{1}H NMR spectrum (400 MHz) of CC10 in acetone-d_6

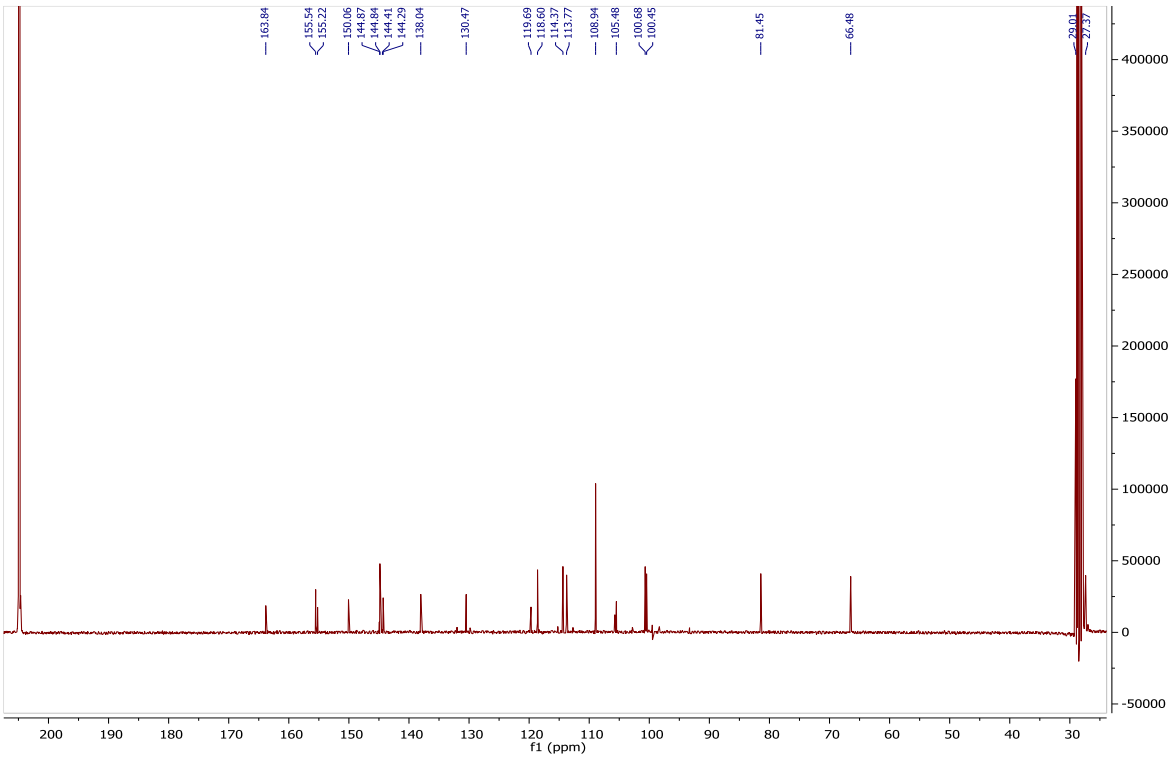

Figure 3. 40: ^{13}C NMR spectrum (100 MHz) of CC10 in acetone-d_6

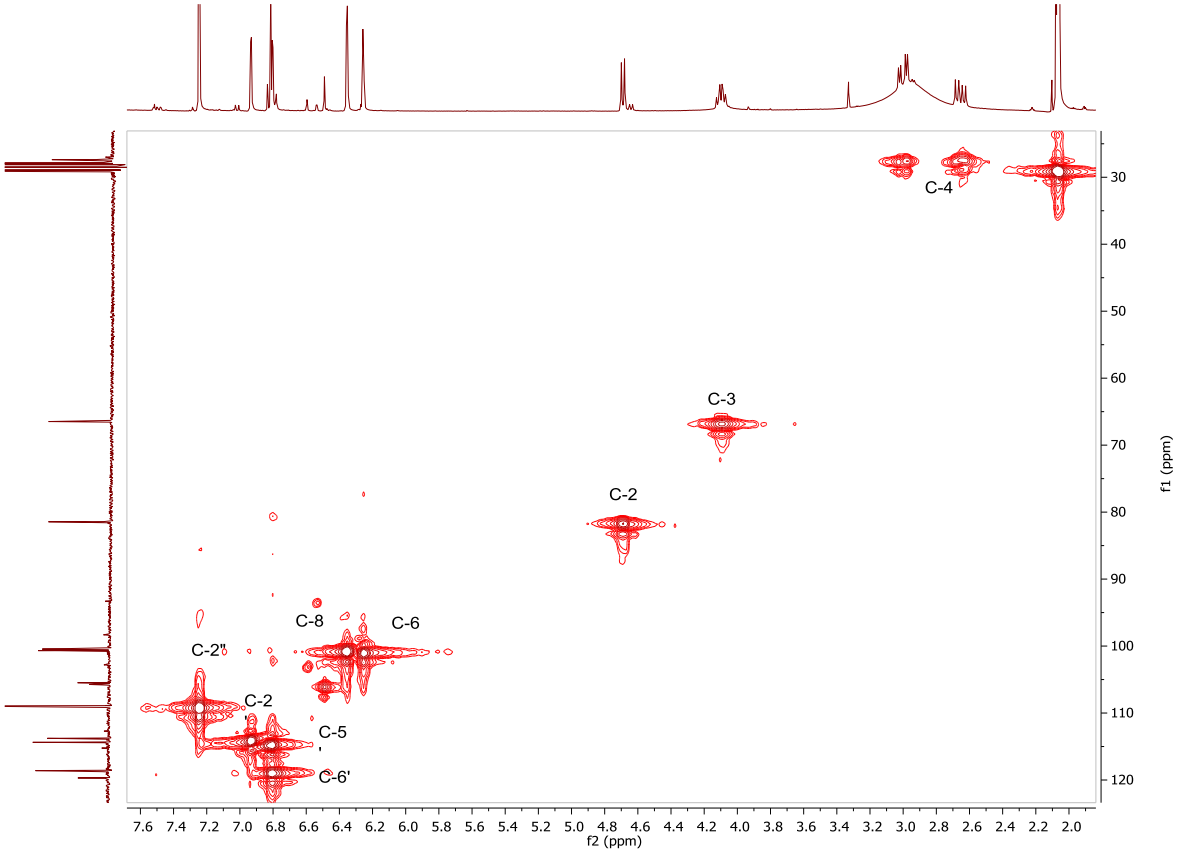

Figure 3. 41: HSQC spectrum (400 MHz) of CC10 in acetone-d_6

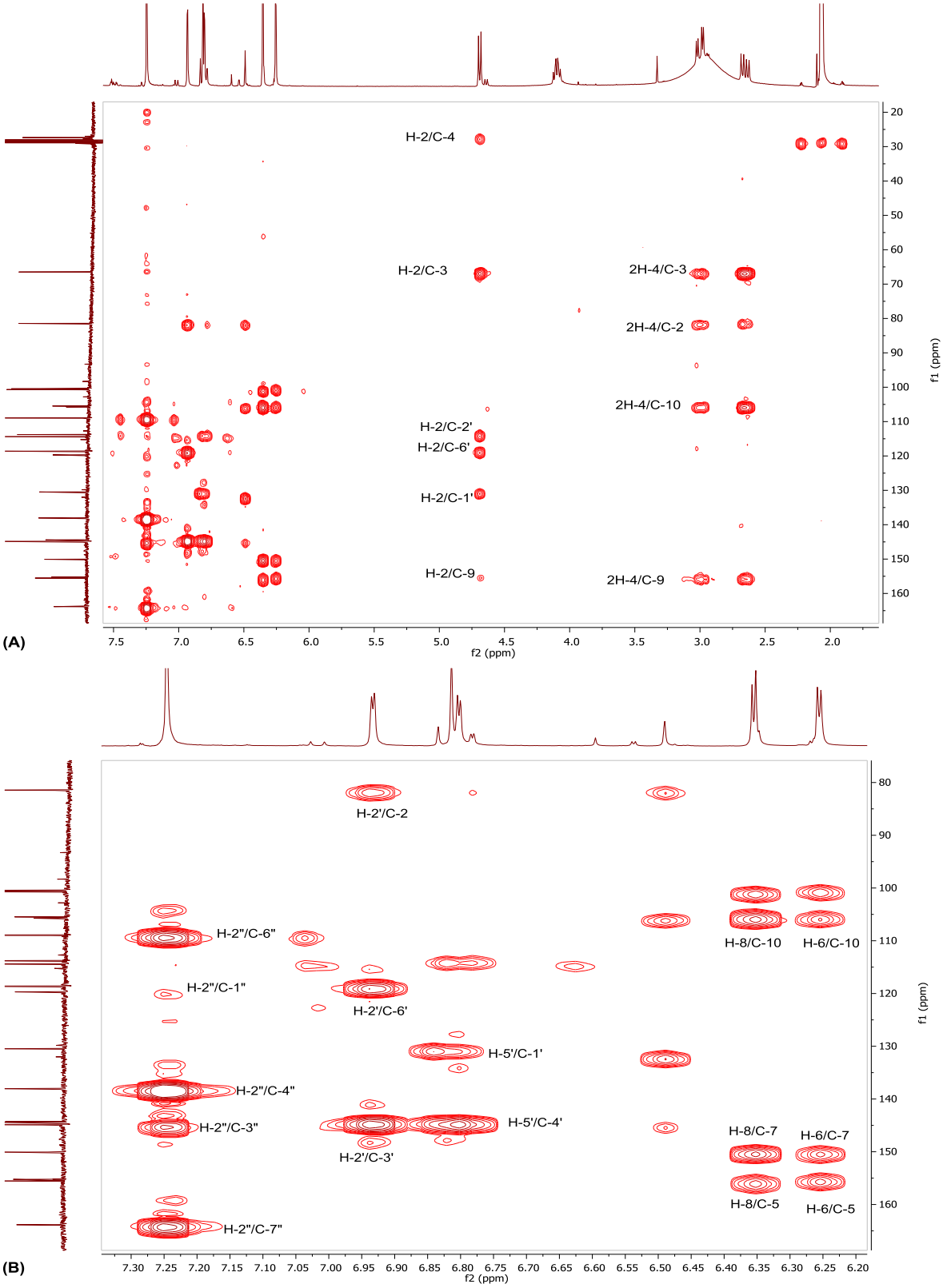

Figure 3. 42: (A) HMBC spectrum (400 MHz) of CC10 in acetone-d_6
(B) selected expansion in the region of 6.2 - 7.3 ppm

3.1.4.3 Characterisation of CC11 as 1-monoacetyl glycerol

CC11 revealed a green spot on TLC (R_f value 0.51, using 60% (v/v) ethyl acetate in hexane as a mobile phase), after treatment with anisaldehyde-sulphuric acid reagent followed by heating.

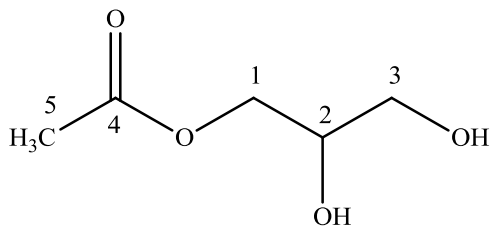

Figure 3. 43: Structure of 1-monoacetylglycerol

The mass spectrum in positive ion mode gave $[M + H]^+$ at *m/z* 135.0650 suggesting a molecular formula of $C_5H_{10}O_4$.The ^{1}H NMR spectrum (Figure 3.44) displayed a sharp singlet at δ_H 2.09 (3H) typical for methyl protons of an acetyl group (Me-5). The spectrum also showed protons signals at δ_H 3.59 (1H, *dd*, *J* = 3.9, 11.5 Hz) and 3.69 (1H, *dd*, *J* = 3.9, 11.5 Hz) attributed for oxymethylene protons (2H-3) and signals at δ_H 4.17 and 4.20 attributed for oxymethylene protons (2H-1). A multiplet accounting for one proton was observed at δ_H3.93 for H-2.

DEPTq135^{13}C NMR spectrum (Figure 3.45) spectrum showed one methyl at δ_C 20.82, two oxymethylenes at δ_C 63.33 and δ_C 65.6, one oxymethine at δ_C 70.2 and a carbonyl at δ_C 171.50. The HMBC spectrum (Figure 3.46) showed ^2J correlation between 2H-1 at δ_H 4.17 and 4.20 and C-2 at δ_C 70.2 and between H-2 at δ_H 3.93 and C-1 at δ_C 65.6. The spectrum also displayed long-range ^{1}H-^{13}C correlations between 2H-1 and C-4 at δ_C 171.5. In addition, 3H-5 showed ^2J correlation to C-4. This led to the characterisation of CC11 as 1-monoacylglycerol in agreement with previously published data (Hatzakis *et al.*, 2011).

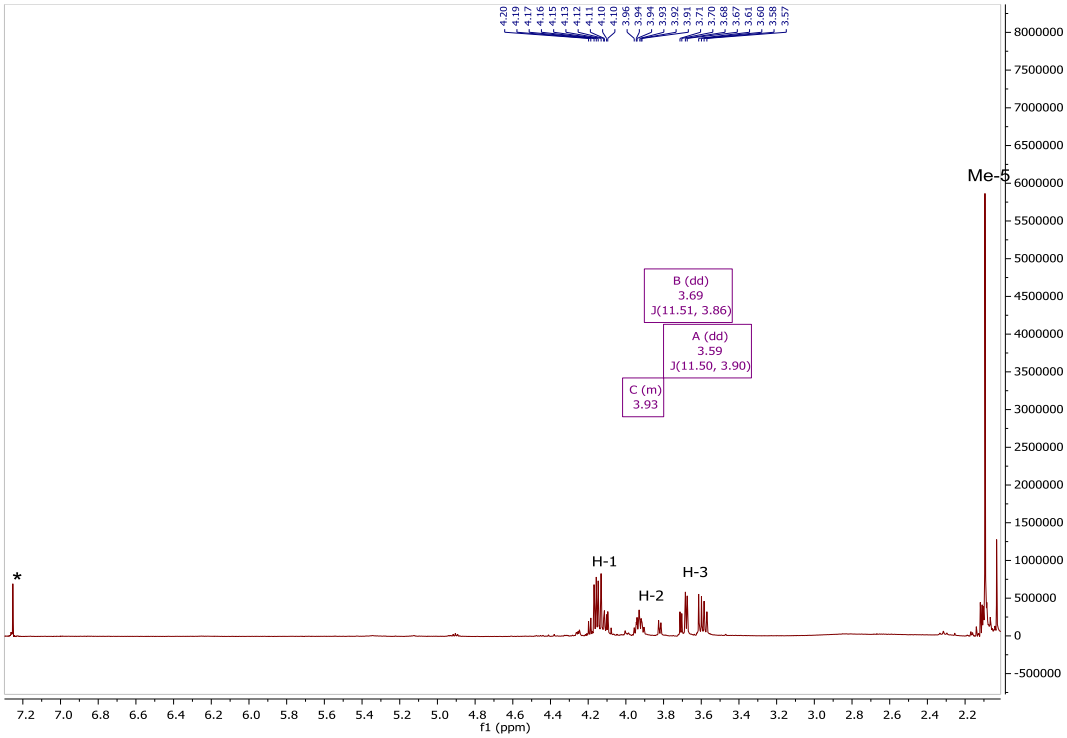

Figure 3. 44: ^{1}H NMR spectrum (400 MHz) of CC11 in $CDCl_3$

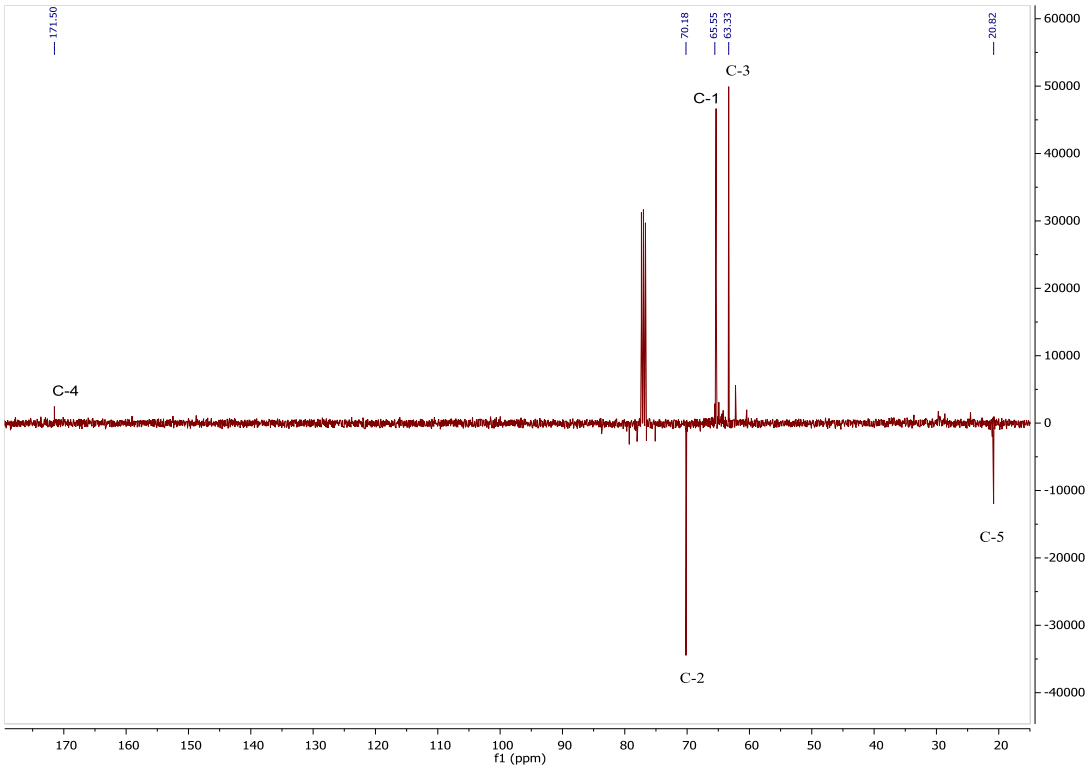

Figure 3. 45: DEPTq 135 13C NMR spectrum (100 MHz) of CC11 in $CDCl_3$

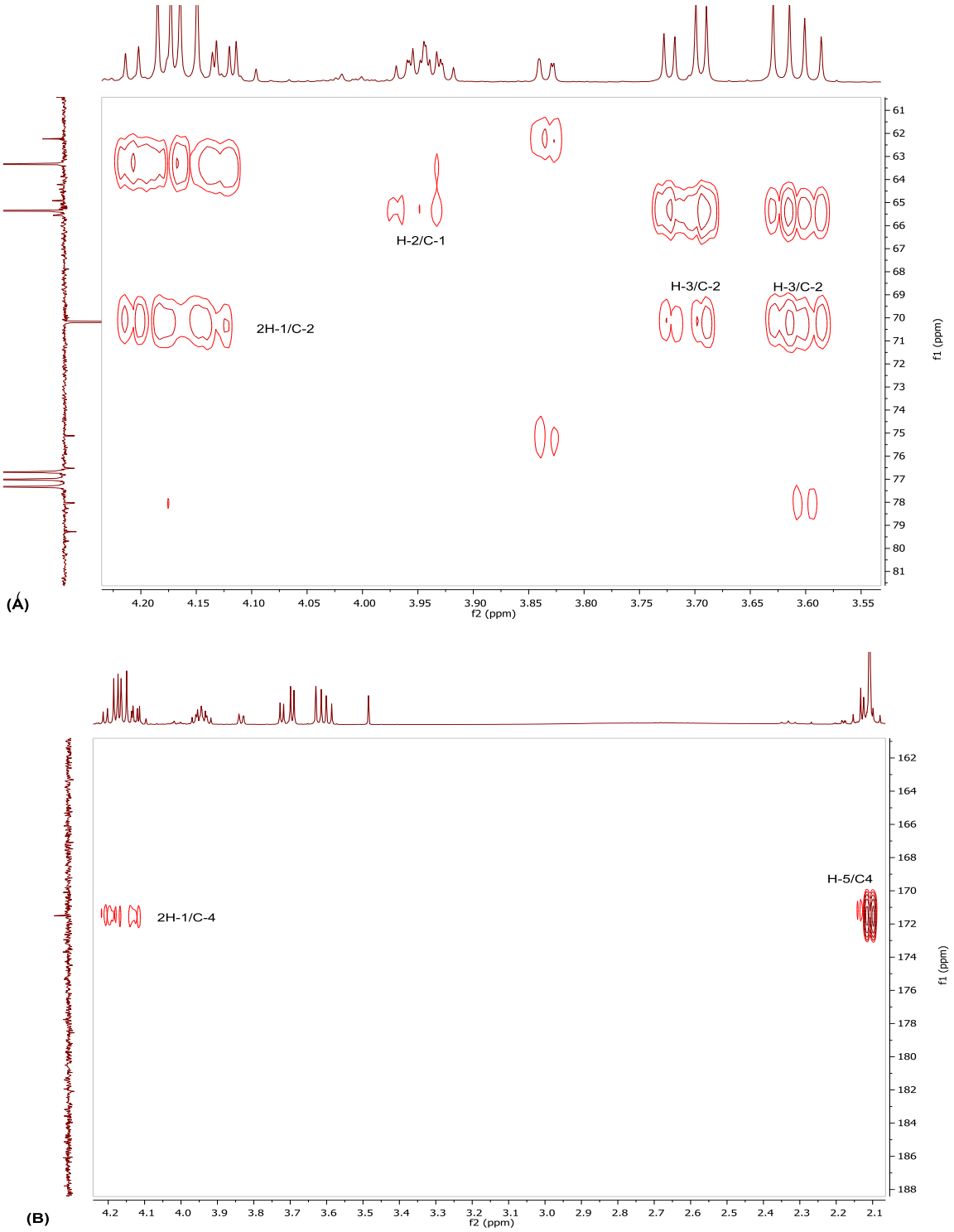

Figure 3. 46:(A) HMBC spectrum (400 MHz) of CC11 in $CDCl_3$ in the region 3.55-4.20ppm (B) Expansion in the region of 2.1 - 4.2 ppm

3.1.4.4 Characterisation of CC12 as a novel sesquiterpene lactone named 3β-hydroxy-8α-[(S)-4-hydroxy-3-methylbutanyloxy]-guaian-4(15),10(14),11(13)-trien-1α, 5α, 7α, 6βH-12, 6-olide.

CC12 revealed a dark purple spot on TLC (R_f value 0.81, using 10% (v/v) methanol in ethyl acetate as a mobile phase), after treatment with anisaldehyde-sulphuric acid reagent followed by heating.

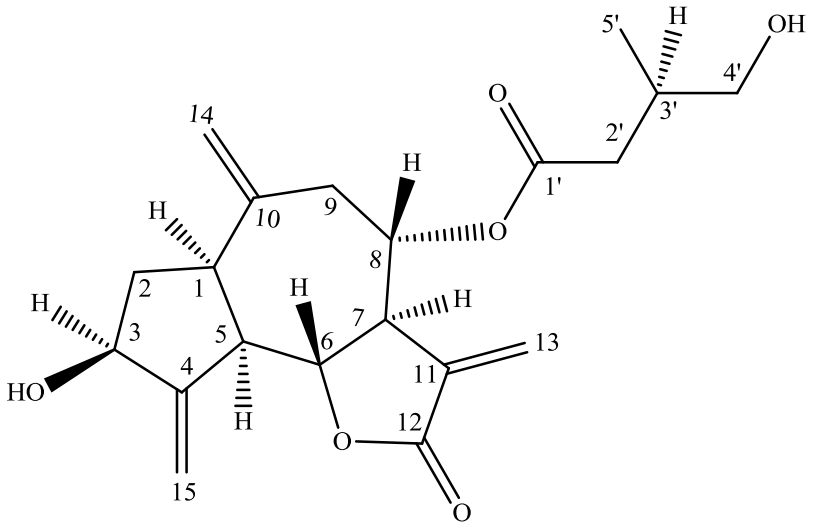

Figure 3. 47: Structure of CC12

The mass spectrum in positive ion mode gave $[M + H]^+$ at *m/z* 363.1798 suggesting a molecular formula of $C_{20}H_{26}O_6$. The IR spectrum showed absorptions at cm^{-1} 1734 indicated the presence of γ-lactone (C=O stretch), 1233 (CH_3), 2928 (C═CH_2 Stretch), 1044 (C─O Stretch) and 2872 (C-H Stretch). In addition, optical rotation $[\alpha]_D^{20}$ was +53 (*c*=0.1, $CHCl_3$). The ^1H NMR spectrum (Figure 3.49, Table 3.9), showed two doublets at δ_H 5.70 and 6.25 attributed to 2H-13 for C-13 (δ_C 122.6) methylene protons, indicating the presence of an α-methylene-γ-lactone moiety. In addition, the ^1H NMR spectrum also showed signals of the other two exomethylenes at δ_H 5.16, 4.97 (each 1H) and 5.52,5.38 (each 1H) attributed to H-14 and H-15 methylene protons, respectively. In addition, the ^1H NMR spectrum showed three oxygenated methines at δ_H 4.58 (H-3), 4.22 (H-6), and 5.06 (H-8), as well as the signals of an oxygenated methylene at δ_H 3.67/3.50 which attributed to H-4'. Furthermore, the spectrum also displayed a signal for a methyl doublet at δ_H 1.04 attributed to H-5'.

The chemical shifts of all hydrogen-bearing carbons were assigned from the HSQC and HMBC spectra combined with the COSY experiment. The DEPTq135^{13}C spectrum (Table 3.9) exhibited signals for 20 carbons including one methyl, seven methylenes (including three olefinics, one oxygenated), seven methines (including three oxygenated), and five quaternary carbons (three olefinics, two carbonyls). The HMBC spectrum (Figure 3.51) showed a sequence of correlations as following: exomethylene protons 2H-13 at δ_H 5.70 and 6.25 showed ^3J correlations C-7, furthermore 1H-13 at δ_H 6.25 ^2J correlation to C-11 and ^3J correlation to C-12 which suggested the presence a carbonyl of a α-methylene-γ-lactone moiety. H-14 at δ_H 4.97 showed ^3J correlation to C-9 and H-14 at δ_H 5.16 showed ^3J correlation with C-1, the H-15 proton at δ_H 5.38 showed ^3J correlation to C-3 while H-15 (δ_H 5.52) showed ^3J correlation to C-5, hence these correlations confirm the presence of the exomethylene protons of H-14 and H-15. The HMBC spectrum also showed ^3J correlation between H-2 at δ_H 2.26 and C-5. H-8 at δ_H 5.06 showed ^3J correlations to C-6 and to quaternary carbons C-10 and C-11. The spectrum also showed ^2J correlation between 2H-9 (δ_H 2.39 and 2.71) and quaternary carbon C-10, moreover, H-9 at δ_H 2.71 showed ^3J correlation to C-1. Furthermore, in the HMBC spectrum a cross peak was seen between the signal at δ_H 4.22 (H-6) and C-12. This sequence of correlations indicates the existence of a sesquiterpene lactone core structure. In addition, the HMBC spectrum showed correlations in a 5-carbon ester side chain, H-2’ at δ_H 2.55 showed ^2J correlation to methine carbon (C-3’). H-3’ at δ_H 2.32 displayed ^2J correlation to the methylene carbon (C-4’), furthermore H-4’ at δ_H 3.67showed ^3J correlation to the methylene carbon (C-2’), in addition, H-5’ at δ_H 1.04 displayed ^2J correlation to methine carbon (C-3’) and ^3J correlation to the two methylene carbons C-2’ and C-4’. These observations were further supported by the COSY which displayed a vicinal coupling between H-2’ at δ_H 2.29 and the adjacent proton H-3’ at δ_H 2.32 and showed a coupling between H-2’ and H-5’ at δ_H 1.04. In addition, 2H-4’ protons at δ_H 3.67 and 3.50 showed vicinal coupling with the adjacent proton at δ_H 2.32 (H-3’). Hence, along with the observations in the HMBC experiment, the above data established the presence of H-2’protons (δ_H 2.29 and 2.55) at δ_C 38.8 (C-2’) which is unique protons for this compound. In addition, in the HMBC spectrum a cross peak was seen between the signal at δ_H 5.06 (H-8) and δ_C 172.6 (C-1') which confirmed the attachment position of a 5-carbon ester side chain to the C-8 of sesquiterpene lactone molecule. Furthermore, the COSY spectrum displayed a sequence of ^{1}H-^{1}H coupling in the

sesquiterpene lactone molecule. H-1 at δ_H 2.99 displayed coupling to the adjacent protons at δ_H 1.75 and 2.26 (H-2) which in turn showed coupling to the adjacent proton at δ_H 4.58 (H-3). H-5 at δ_H 2.85 showed coupling to H-6 at δ_H 4.22 which in turn showed coupling to H-7 at δ_H 3.13 which also in turn showed coupling to H-8 at δ_H 5.06 and an allylic coupling with the exomethylene protons at δ_H 5.70 and 6.25 (2H-13). H-8 proton also displayed coupling to methylene protons at δ_H 2.39 and 2.71 (2H-9). The exomethylene protons at δ_H 5.52 and 5.38(2H-15) showed allylic coupling to the adjacent protons at δ_H 4.58 and 2.85 for H-3 and H-5, respectively, hence these observation, along with the results from HMBC experiment, indicate the presence of a sesquiterpene lactone with a 5-carbon ester side chain attached to C-8 at δ_C 73.9.

Analysis of the HMBC, HSQC, 1H - 1H COSY and NOESY spectra permitted full assignments of the ^{1}H and ^{13}C NMR data of CC12 and indicated a close structural similarity to a guaianolide isolated from the aerial parts of *Centaurea pabotii* (Figure 3.48) and named as 3β-hydroxy-8α-[(S)-3-hydroxy-2-methylpropionyloxy] guaian-4(15), 10(14), 11(13)-trien-1α, 5α, 6βH-12, 6-olide (Marco *et al.*, 1992), however the only significant difference between this compound and CC12 was the methylene that was attributed to H-2' (δ_H 2.29 and 2.55) at δ_C 38.8 (C-2') in a 5-carbon ester side chain attached in C-8 and with a molecular formula of $C_{20}H_{26}O_6$. Hence, based on the data obtained from ^{1}H and ^{13}C NMR, COSY, and HMBC, CC12 was identified to be a novel sesquiterpene lactone named 3β-hydroxy-8α-[(S)-4-hydroxy-3-methylbutanyloxy]-guaian-4(15), 10(14), 11(13)-trien-1α, 5α, 7α ,6βH-12, 6-olide.

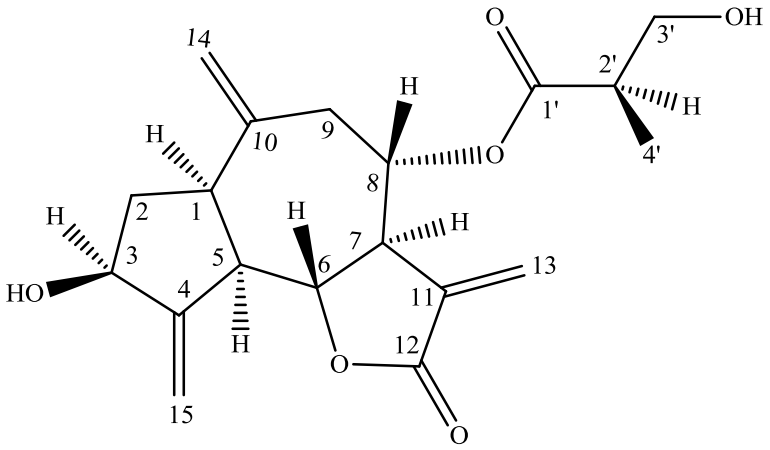

Figure 3. 48: Structure of 3β-hydroxy-8α-[(S)-3-hydroxy-2-methylpropionyloxy] guaian-4(15), 10(14), 11(13)-trien-1α, 5α, 6βH-12, 6-olide

The relative stereochemistry of CC12 was identified with a NOESY experiment. The NOESY spectrum (Figure 3.53) showed that the two methine protons H-1 (δ_H 2.99) and H-5 (δ_H 2.85) had mutual correlations to each other and the proton H-1 correlated to H-14 (δH 5.16). H-2 at δ_H 2.26 correlated with H-1 and H-3, furthermore H-7 at δ_H 3.13 correlated to H-5. In addition, methylene protons (2H-2') in the side chain at δ_H 2.29 and 2.55 correlated with H-5' at δ_H 1.04. Moreover, H-2'at δ_H 2.29 correlated with H-4' (δ_H 3.67). H-5' (δ_H 1.04) showed NOE correlation to H-3' and to H-4' at δ_H 3.50. The exomethylene proton at δ_H 5.52 (H-15) correlated with H-5 (δ_H 2.85) and 5.38 (H-15) correlated with H-3 (δ_H 4.58). These NOE correlations led to the conclusion that H-1/H-2 (2.26)/H-3/H-5/H-7/H-14 (5.16) and 2H-15 as well as 2H-2'/H-3'/H-4' and H-5'were all placed on the α side of the molecule. On the other hand, H-6 at δ_H 4.22 correlated with H-2 at δ_H 1.75. H-8 (δ_H 5.06) correlated to 2H-9 (δ_H 2.39 and 2.71) as well as H-9 at δ_H 2.71 correlated with H-2 (δ_H 1.75) which in turn correlated with H-6 (δ_H 4.22), this led to the conclusion that H-2 (δ_H 1.75)/H-6/H-8 and 2H-9 were located on the β side.

Table 3. 9: ^{1}H (600 MHz) and DEPTq-135 (150 MHz) NMR data of CC12 in $CDCl_3$

Position	^{1}H δppm (m, *J* Hz)	^{13}C
1	2.99 (1H, *dt*, *J* = 10.7, 8.2 Hz)	45.3
2	1.75 (1H, *ddd*, *J* = 13.3,10.9,7.4 Hz)/2.26 (1H, *dt*, *J* = 13.1, 7.1 Hz)	39.1
3	4.58(1H, *tt*, †)	73.7
4	-	152.2
5	2.85 (1H, *ddt*, *J* = 10.4,9.1,1.4 Hz)	51.3
6	4.22 (1H, *m*)	78.5
7	3.13 (1H, *tt*, *J* = 9.4,3.2 Hz)	47.6
8	5.06 (1H, *ddd*, *J* = 3.2, 5.2, 4.0Hz)	73.9
9	2.39 (1H, *dd*, *J* = 14.5, 4.0 Hz)/2.71 (1H, *dd*, *J* = 14.5, 5.2 Hz)	37.2
10	-	141.7
11	-	137.3
12	-	169.1
13	5.70 (1H, *d*, *J* = 3.4 Hz) 6.25 (1H, *d*, *J* = 3.1 Hz)	122.6
14	4.97 (1H, *br. s*) 5.16 (1H, *br. s*)	118.1
15	5.38 (1H, *br. s*) 5.52 (1H, *br. s*)	113.5
1`	-	172.6
2`	**2.29 (1H, *m*)/ 2.55 (1H, *dd*, *J* = 15.1, 6.6 Hz)**	**38.8**
3`	2.32 (1H, *m*)	32.9
4`	3.67 (1H, *dd*, *J* = 10.7, 5.0 Hz)/3.50 (1H, *dd*, *J* = 10.7, 7.1 Hz)	67.5
5`	1.04 (3H, *d*, *J* = 6.7Hz)	16.7

(†) Unassigned coupling constants due to overlapping.

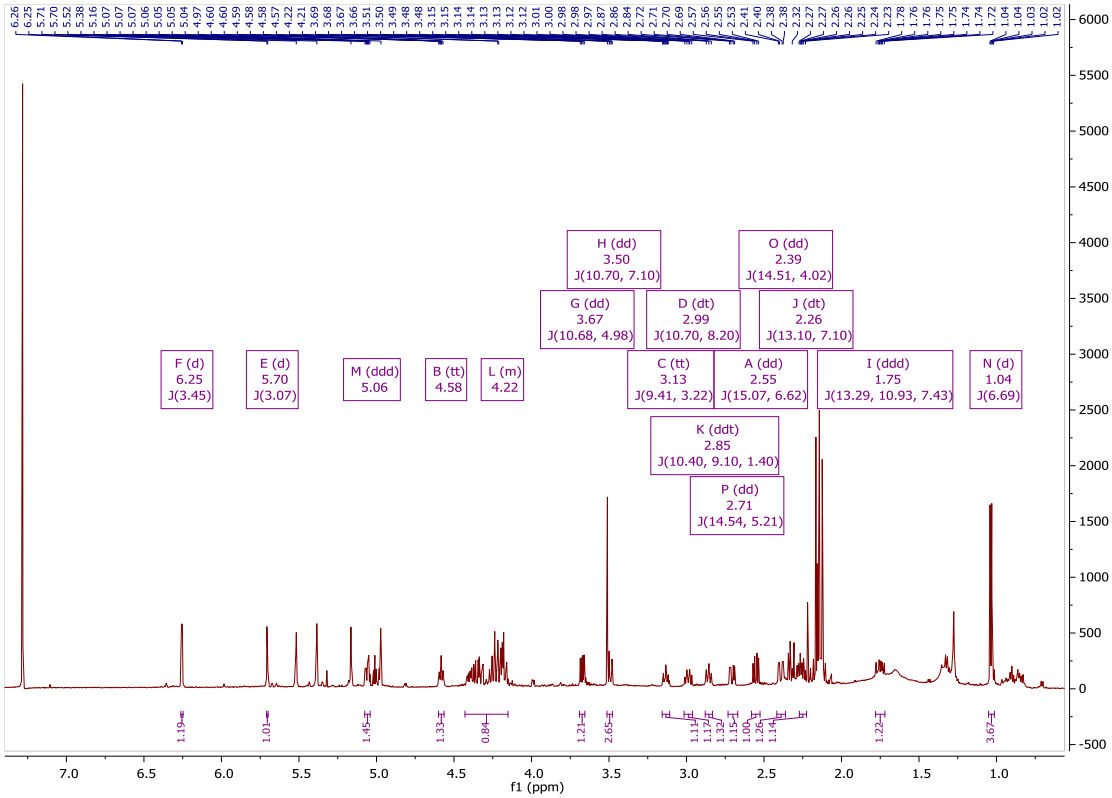

Figure 3. 49: ^{1}H NMR spectrum (600 MHz) of CC12 in $CDCl_3$

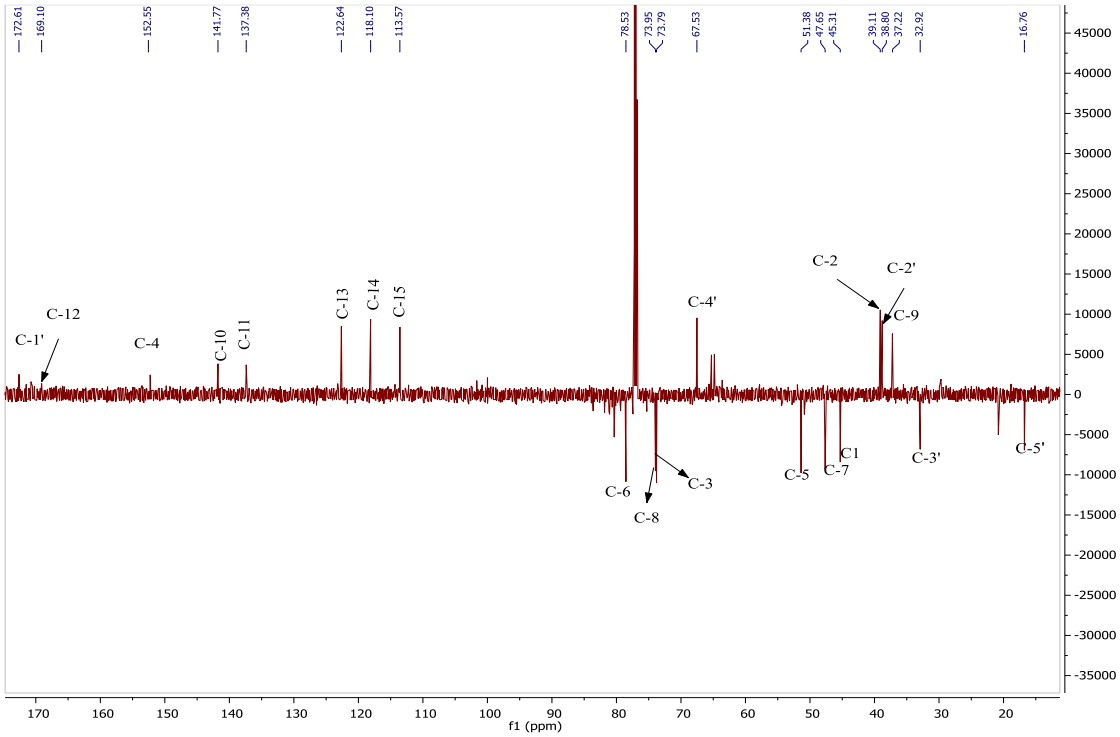

Figure 3. 50: DEPTq-135 NMR spectrum (150 MHz) of CC12 in $CDCl_3$

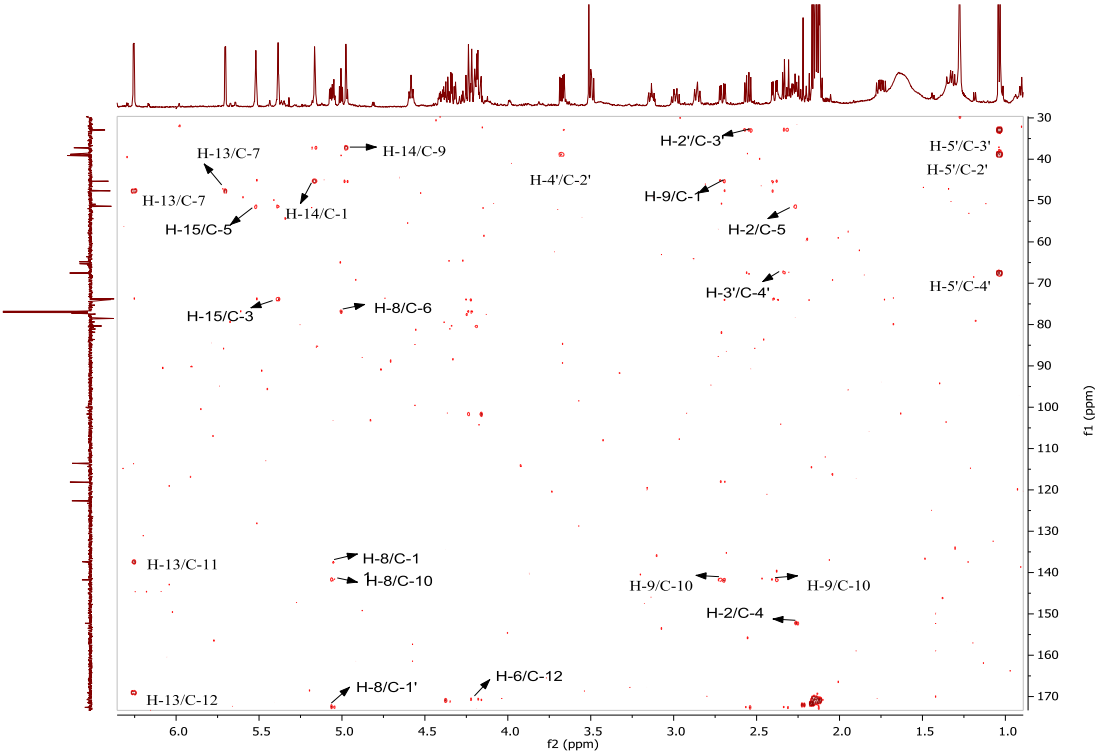

Figure 3. 51: Full HMBC spectrum (600 MHz) of CC12 in $CDCl_3$

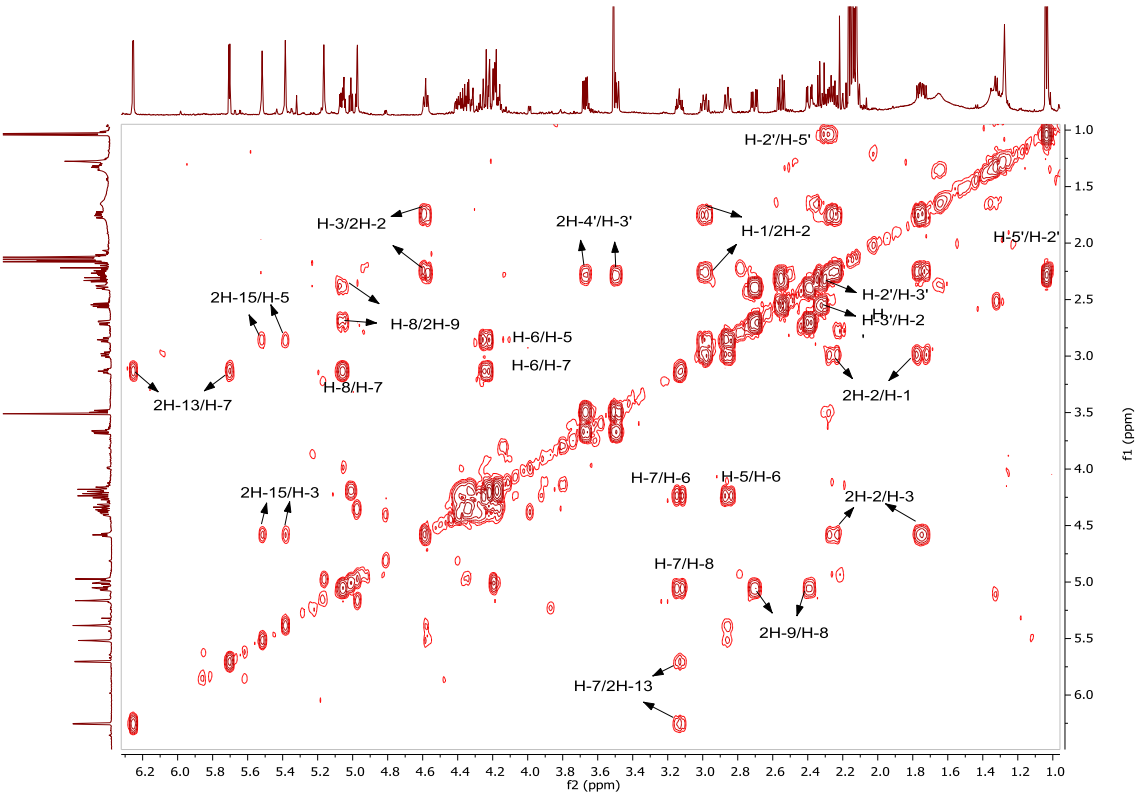

Figure 3. 52: 1H-1H COSY spectrum (600 MHz) of CC12 in $CDCl_3$

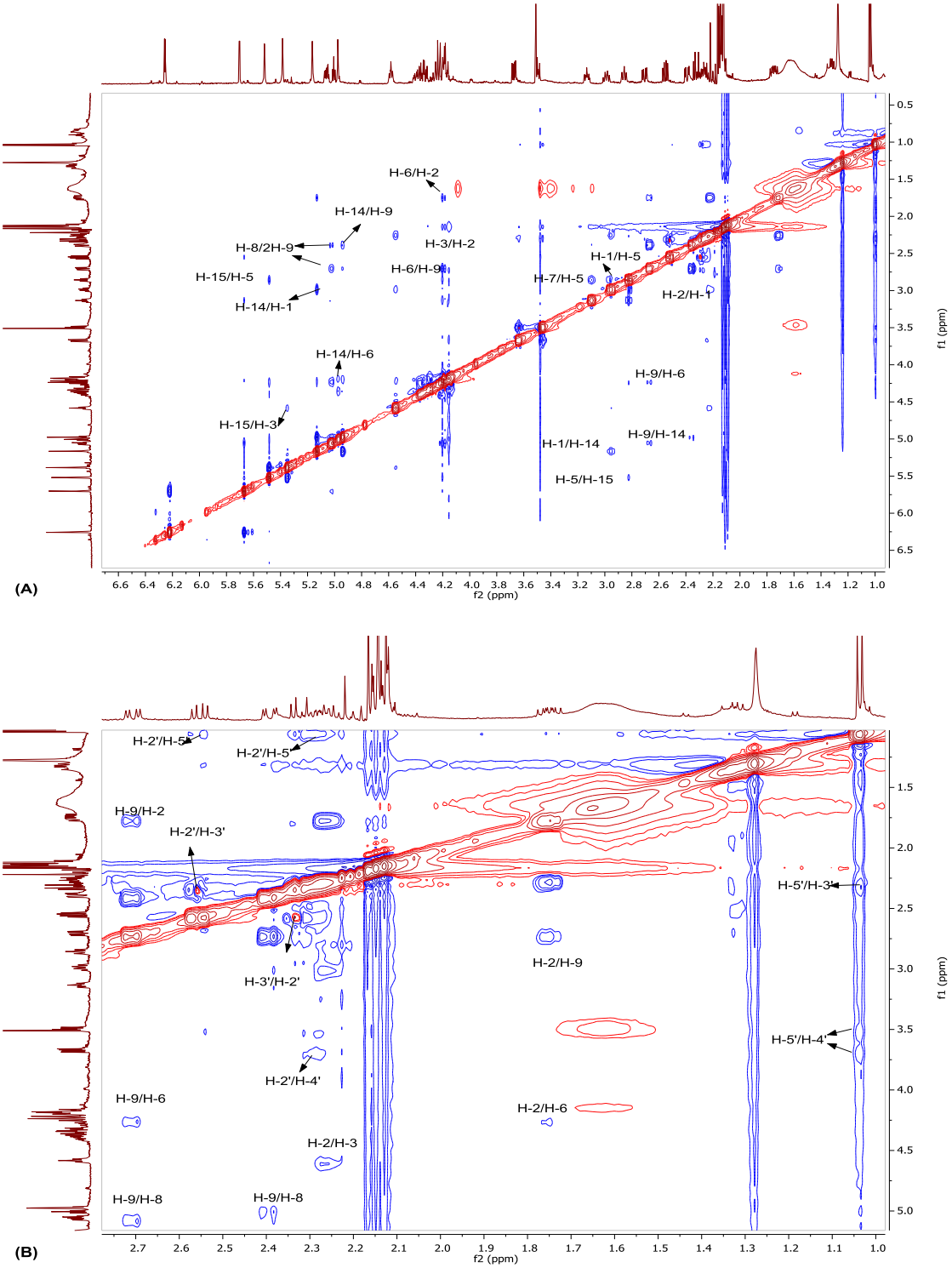

Figure 3. 53:(A) NOESY spectrum (600 MHz) of CC12 in $CDCl_3$
(B) Selected expansion in the region of 1.0 - 2.7 ppm

3.1.4.5 Characterisation of CC13 as a novel sesquiterpene lactone named 11, 13 epoxy-guaian-4(15), 10(14)-dien-1α, 5α, 7α, 6βH-12, 6-olide-3-yl acetate

CC13 revealed a dark purple spot on TLC (R_f value 0.89, using 10% (v/v) methanol in ethyl acetate as a mobile phase), after treatment with anisaldehyde-sulphuric acid reagent followed by heating.

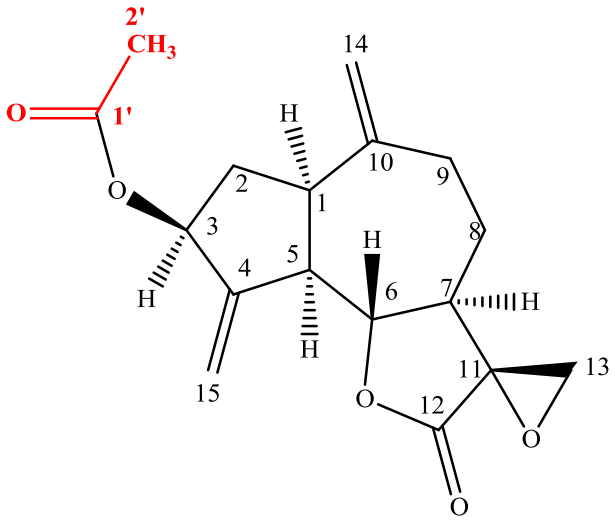

Figure 3. 54: Structure of CC13

The mass spectrum in positive ion mode gave $[M + H]^+$ at *m/z* 305.1380 suggesting a molecular formula of $C_{17}H_{20}O_5$.The IR spectrum indicated the presence of two distinctive bands in the carbonyl region at 1778 cm^{-1} from a γ-lactone and 1734 cm^{-1} from an acetate group and also showed the following absorption bands at 2859 and 2926 cm^{-1} for (C═CH_2 Stretch), 1071 cm^{-1} for (C─O Stretch) and 2872 cm^{-1} for (C-H Stretch) and 1242 cm^{-1} for (CH_3). In addition, optical rotation $[\alpha]_D^{20}$ was +34.5 (*c*=0.04, $CHCl_3$).^{1}H NMR spectrum (Figure 3.55) displayed of an AB quartet signal at δH 3.65,3.66 (2H, *ABq*) assigned to the C-13 protons which suggest the presence of an epoxide group. The spectral data also showed the presence of a γ-lactone ring carbonyl of C-12 at δ_C 175.7 and one secondary carbon bearing oxygen at δ_C (82.2, C-6), and one tertiary carbon bearing oxygen (76.4, C-11). In addition, ^{1}H NMR and HSQC, HMBC spectra confirm the presence of methyl singlet at δ_H 2.13 (H-2') and a low field signal δ_C at 21.2 (C-2') as well as carbonyl at δ_C 170.5 which attributed to acetate group.

DEPTq135^{13}C NMR spectrum showed the presence of four olefinic carbons C-4, C-15, C-10 and C-14 at δ_C 147.7,114.0, 148.1, and 114.3, respectively. The ^{1}H NMR spectrum displayed signals at δ_H (2H, 4.97/4.99) for H-14 and (2H, 5.34/5.46) for H-15 suggesting the presence of two exomethylene double bonds. The HMBC spectrum showed a sequence of correlations as following: H-2 proton at δ_H 1.83 showed ^2J correlation to C-3 at δ_C 74.7 and ^3J correlation to C-10 (δ_C 148.1). H-8 at δ_H 2.15 showed ^2J correlations to C-7 and C-9 and H-6 at δ_H 4.25 showed ^3J correlation to C-8. H-9 proton at δ_H 2.61 showed ^3J correlation to C-1 and C-7, also showed ^3J correlation to the exomethylene carbon at δ_C 114.3 (C-14) and exomethylene protons 2H-14(δ_H 4.97,4.99) showed ^3J correlations to C-1 and C-9, hence these correlations confirm the presence of exomethylene protons (2H-14). Furthermore, H-9 showed ^2J correlations to C-8 at δ_C 26.5 and to quaternary carbon (C-10) at δ_C 148.1. These observations suggest that CC13 had a guaianolide carbon skeleton. In addition, the 2H-13 protons at δ_H 3.65 and 3.66 showed ^2J and ^3J correlations to C-11 and C-12 respectively, moreover, 2H-13 at δ_H 3.65 and 3.66 showed ^3J correlations to C-7 at δ_C 52.1, thus these correlations confirm the presence of the epoxide group. The HMBC spectrum also demonstrated the ^2J correlation of methyl proton at δ_H 2.13 (H-2') to C-1' at δ_C 170.5 which suggesting the presence of an acetate group. Hence, the above data with serial HMBC correlations confirm the characteristics of a guaian-type sesquiterpene lactone compound which was further supported by the COSY observations that confirmed the position of the two exomethylene double bonds, since, in the COSY spectrum (Figure 3.58) protons at δ_H 5.57 (H-3) and 2.86 (H-5) showed an allylic coupling with the exomethylene protons at δ_H 5.34/5.46 (2H-15). Furthermore, proton at δ_H 2.95 (H-1) also showed an allylic coupling with the exomethylene protons (2H-14). In addition, the 1H- 1H COSY spectrum showed correlations between H-1/2H-2; H-3/2H-2, H-6/H-5; H-6/H-7;.H-7/H-8 and H-9/H-8.

The NOESY spectrum (Figure 3.59) showed that the two methine protons H-5 (δ_H 2.86) and H-3 (δ_H 5.57) had mutual correlations to each other and the proton H-5 correlated to H-1 (δH 2.95) which in turn correlated to H-7 (δ_H 2.54) indicating that these protons were all on the same face. The spectrum also showed NOE correlation between H-1 (δ_H 2.95), H-2 (δ_H 2.49) and H-9 (δ_H 2.05), in addition, H-7 (δ_H 2.54) correlated with H-8 (δ_H 2.15) as well as H-9 (δ_H 2.05), hence these NOE correlations led to the conclusion that H-1/ H-2 (δ_H 2.49) /H-3/ H-5/ H-7/ H-8 (δ_H 2.15) and H-9

(δ_H 2.05) were all placed on the α side of the molecule. On the other hand, H-6 (δ_H 4.25) showed NOE correlations with H-8 (δ_H 1.61) and H-2 (δ_H 1.83). Furthermore, H-6 NOE with H-13 at δ_H 3.66 which also in turn correlated to H-8 at δ_H 1.61, furthermore H-13 at δ_H 3.65 also correlated with H-8 at δ_H 2.15. In addition, H-9 at δ_H 2.61 correlated H-8 at δ_H1.61, hence all these protons were placed on the β side. The NOESY spectrum also displayed the NOE effects of exomethylene protons H-14 and H-15. H-14 proton at δ_H 4.97 correlated with H-2 (δ_H 1.83) and H-14 proton at δ_H 4.99 correlated with H-9 (δ_H 2.61) This led to the conclusion that 2H-14 protons were placed on the β side of the molecule. Furthermore, H-3 at δ_H 5.57 correlated with H-15 (δ_H 5.34) which placed on the on the α side, moreover, H-6 at δ_H 4.25 showed NOE correlation with H-15 (δ_H 5.46) which located on the β side.

The nature of the guaianolide skeleton of this compound and the sequence of correlations were determined by a combination of COSY, NOESY, DEPT, HMBC and HSQC. Starting from the coupling of each proton with the adjacent was identified using COSY, the corresponding ^{13}C resonances were assigned by HSQC and further confirmed by HMBC. The inter guaianolidic linkages were established from HMBC and NOESY experiments.

Analysis of the 1H-1H COSY, HMBC, and HSQC spectra permitted full assignments of the ^{1}H and ^{13}C NMR data, which revealed that CC13 is very similar to CC5 a known sesquiterpene lactone isolated from the aerial parts of *C. humilis* (section **3.1.2.2**) as the data were in agreement with guaianolide skeleton of CC5 except that CC13 in the C-3 position has an OAc group which is confirmed by the signals at δ_C170.5 (C-1') for the carbonyl and the presence of the acetate group which was confirmed in the ^{1}H NMR spectrum by a singlet of three protons at δ_H 2.13 (H-2'). In support, H-3 signal in CC5 appears at δ_H 4.58, whereas in CC13 exists at δ_H 5.57 because of the esterification, hence the acetate group at C-3 is a unique for CC13. Based on the above data CC13 was identified to be a novel sesquiterpene lactone named 11,13 epoxy-guaian-4(15), 10(14)-dien-1α, 5α, 7α, 6βH-12, 6-olide-3-yl acetate.

Table 3. 10: ^{1}H (600MHz) and DEPTq-135 (150 MHz) of CC13 in $CDCl_3$

Position	^{1}H	^{13}C
1	2.95 (1H, *q*, *J* = 8.2 Hz)	43.8
2	1.83 (1H, *ddd*, *J* = 14.1, 7.4,6.7 Hz), 2.49 (1H, *dt*, *J* = 14.1, 7.9 Hz)	36.0
3	5.57 (1H, *br. t*, *J* = 7.66 Hz)	74.7
4	-	147.7
5	2.86 (1H, *br.t*, *J* = 9.6 Hz)	50.6
6	4.25 (1H, *t*, *J* = 9.8 Hz)	82.2
7	2.55 (1H, *m*)	52.1
8	1.61 (1H, *m*)/2.15 (1H, *m*)	26.5
9	2.05 (1H, *m*)/2.61 (*dt*, *J* = 13.1, 4.6 Hz)	35.6
10	-	148.1
11	-	76.4
12	-	175.7
13	3.66/3.65 (2H, *ABq*, *J* = 11.7 Hz)	43.9
14	4.97 (1H, *s*)/4.99 (1H, *s*)	114.3
15	5.34 (1H, *s*)/5.46 (1H, *s*)	114.0
1’	-	170.5
2’	2.13 (3H, *s*)	21.2

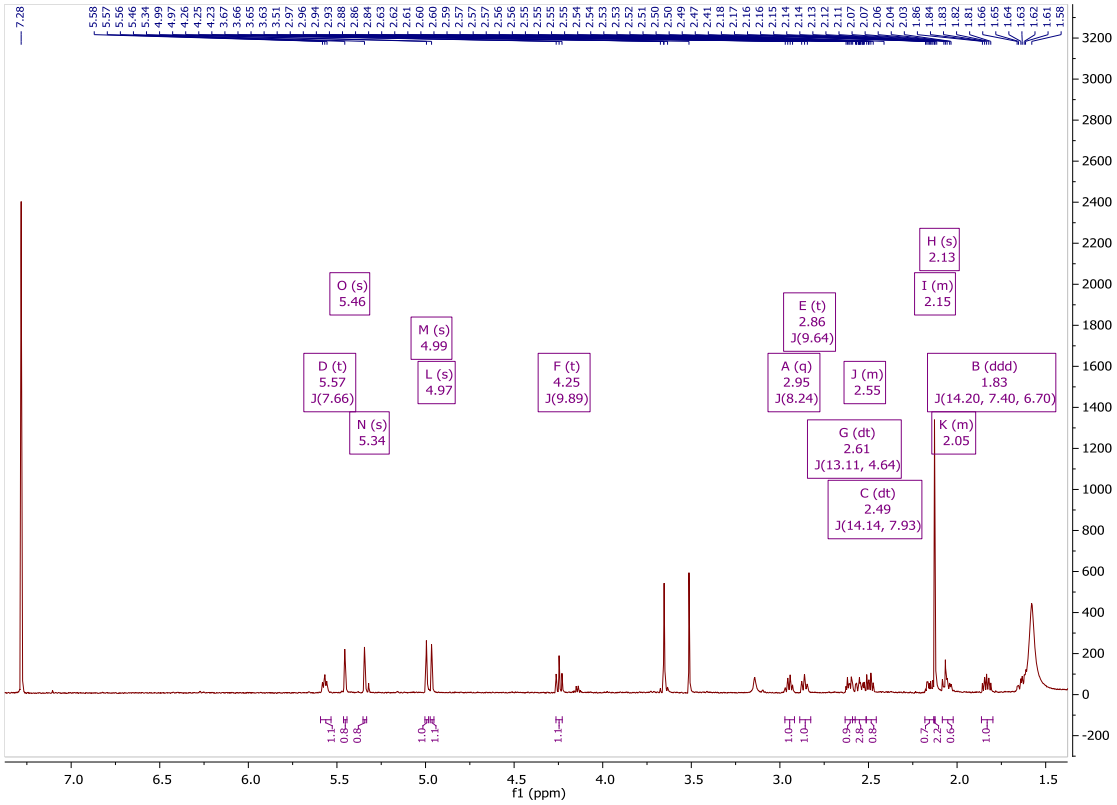

Figure 3. 55: ^{1}H NMR spectrum (600 MHz) of CC13 in $CDCl_3$

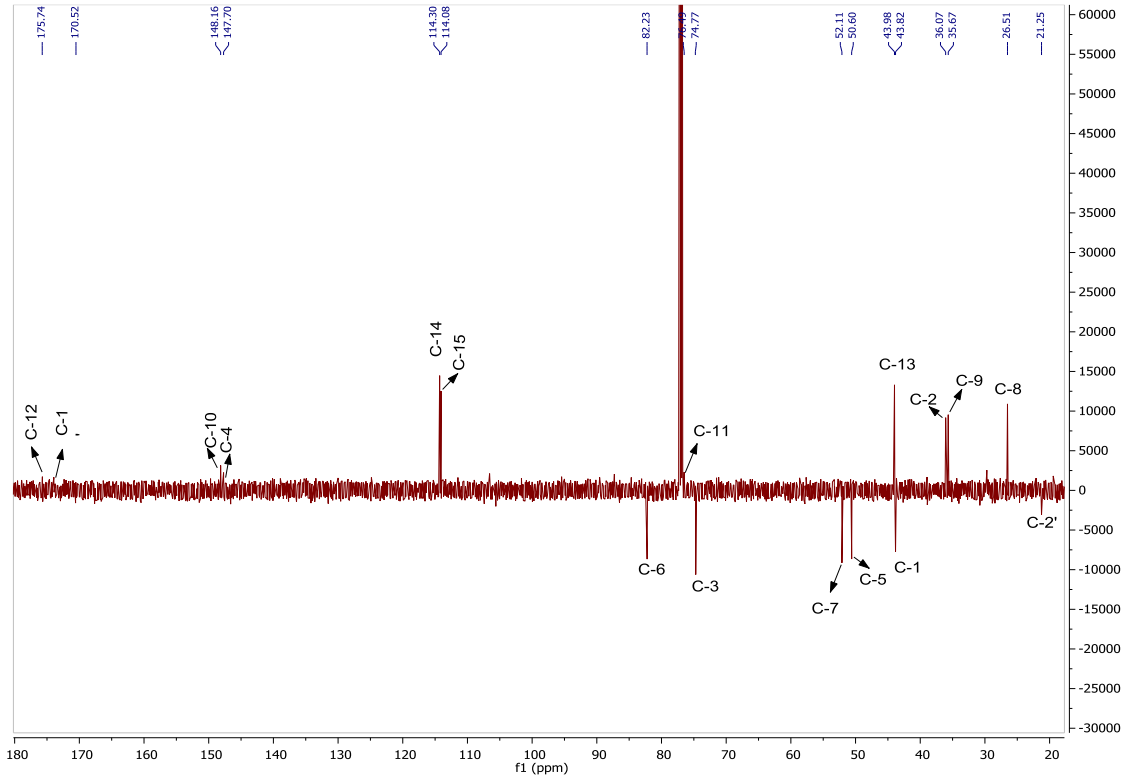

Figure 3. 56: DEPTq-135 NMR spectrum (150 MHz) of CC13 in $CDCl_3$

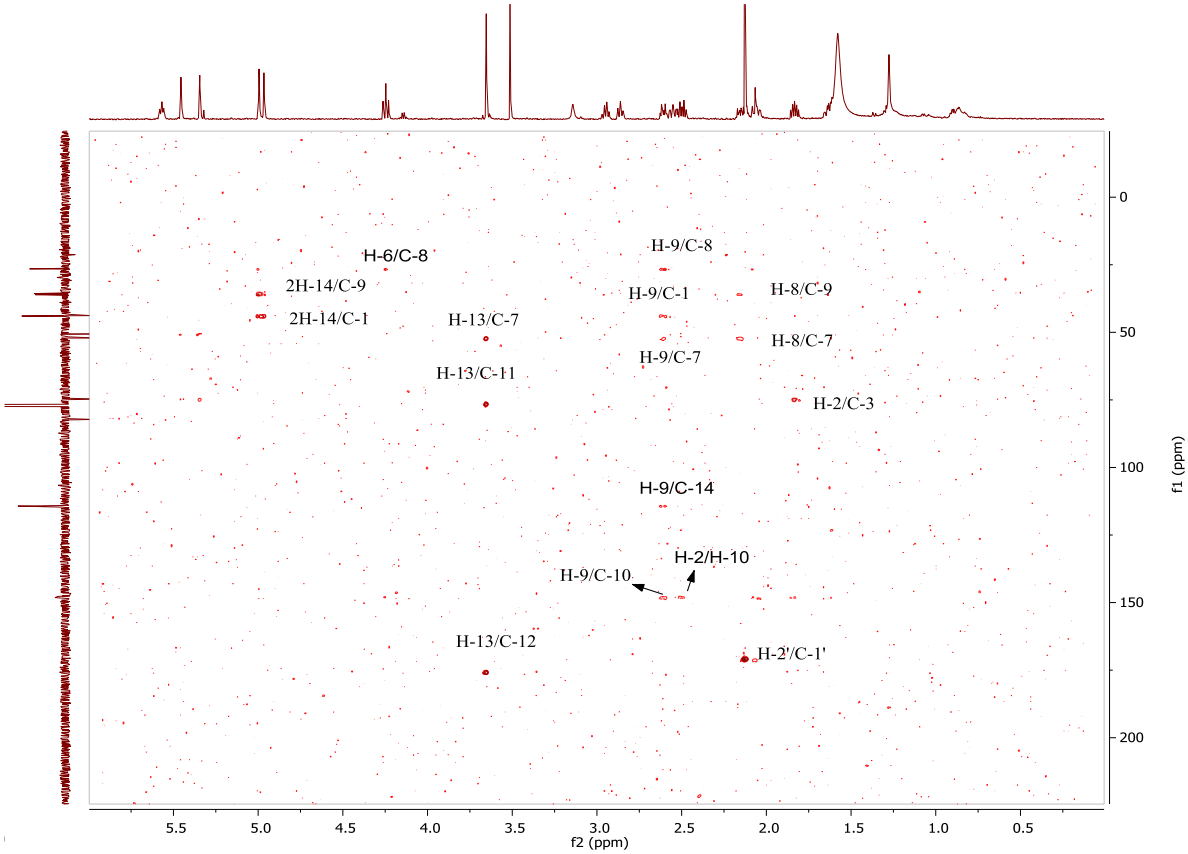

Figure 3. 57: HMBC spectrum (600 MHz) of CC13 in $CDCl_3$

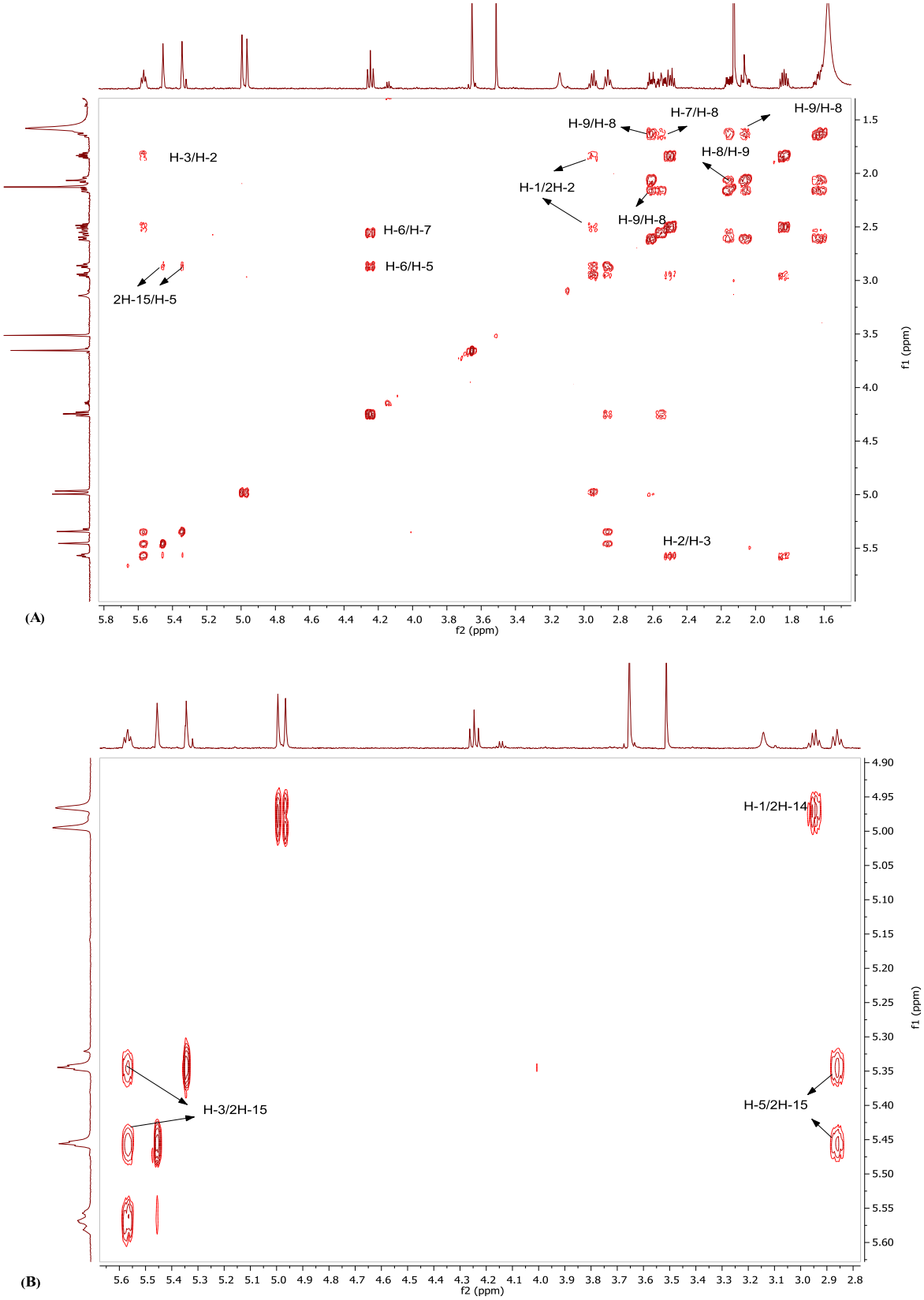

Figure 3. 58:(A) 1H-1H COSY spectrum (600 MHz) of CC13 in $CDCl_3$
(B)Selected expansion in the region of 2.8 - 5.6 ppm

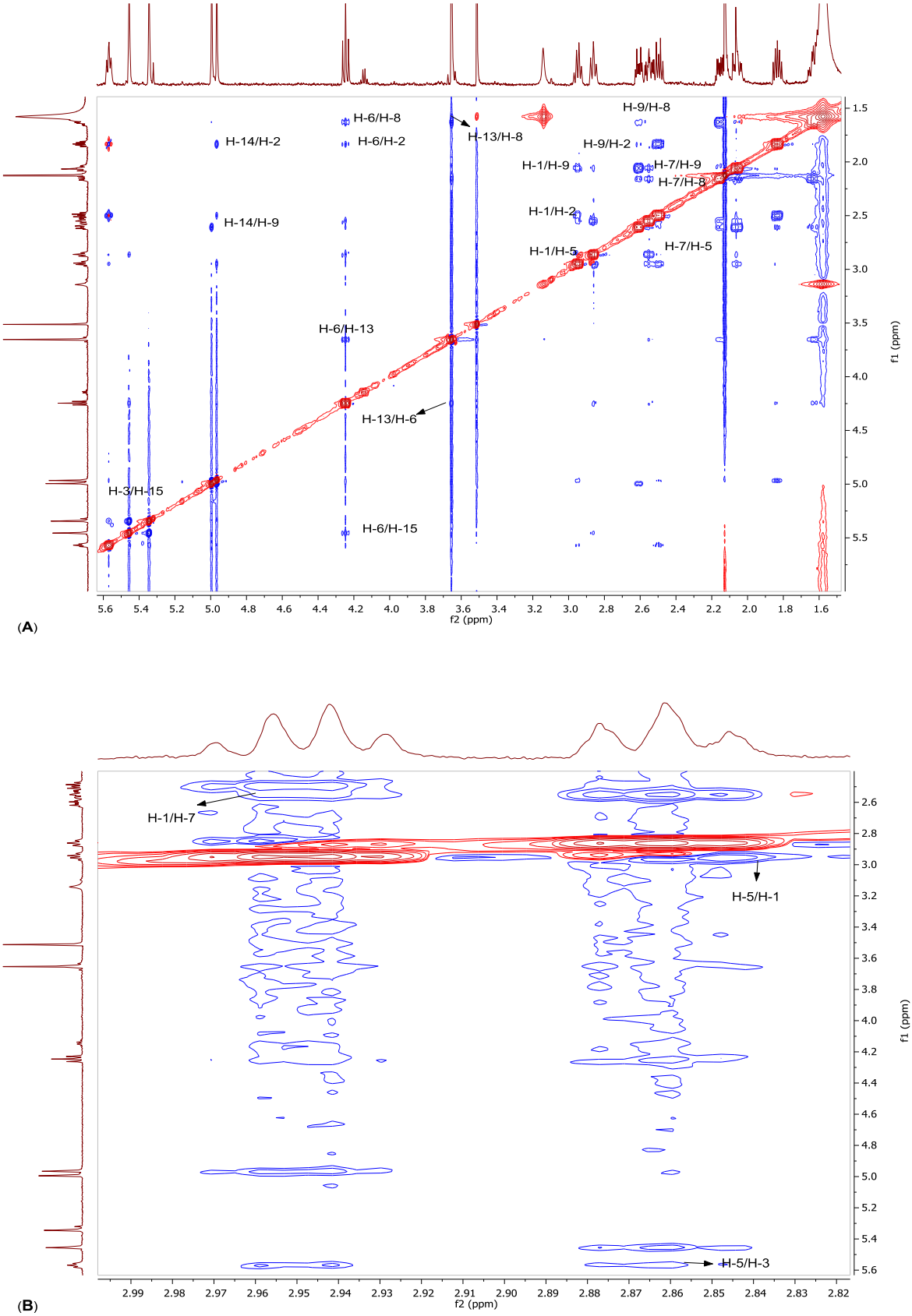

Figure 3. 59:(A) NOESY spectrum (600 MHz) of CC13 in $CDCl_3$
(B) Selected expansion in the region of 2.82 - 2.99 ppm

3.2 Phytochemical analysis of *C. rohlfsianum*

3.2.1 Fractionation of C. rohlfsianum tuber

The methanol extract of *C. rohlfsianum* tuber (CYMT, 30g) was fractionated by VLC, fraction CY1 (10mg) was separated as brown crystals using 90% ethyl acetate in methanol and further purified by size exclusion chromatography using 100% methanol as a mobile phase. The hexane extract of *C. rohlfsianum* tuber (CYHT) and the ethyl acetate extract of *C. rohlfsianum* tuber (CYET) were not fractionated due to limitations in time.

3.2.1.1 Characterisation of CY1 as 3-O-{β-D-xylopyranosyl-(1→2)-β-D-glucopyranosyl-(1→4)-[β-D-glucopyranosyl-(1→2)]-α-L-arabinopyranosyl}-cyclamiretin A

CY1 revealed a brown spot on TLC (R_f value 0.77, using: chloroform:methanol:water:formic acid in a 6:3.2:8:1.2 ratio as the mobile phase), after treatment with anisaldehyde-sulphuric acid reagent followed by heating.

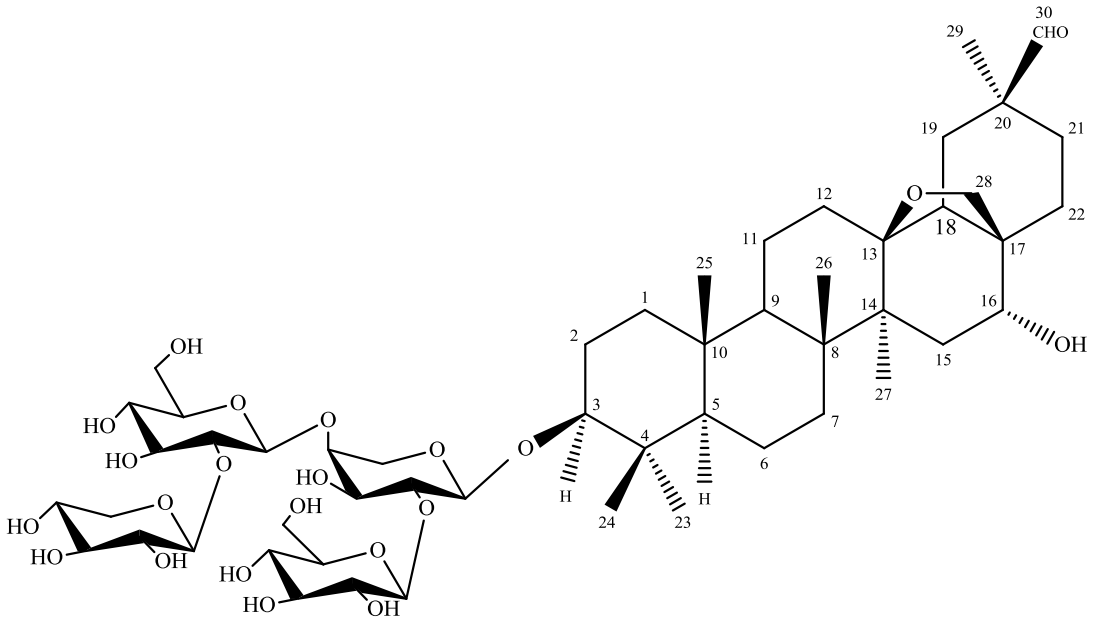

Figure 3. 60: Structure of CY1

The result of mass spectrum in negative ion mode and NMR analysis indicated a molecular formula $C_{52}H_{84}O_{22}$. The ^{1}H NMR spectrum (Figure 3.62) showed signals of six tertiary methyl groups at δ_H 0.82, 1.01, 1.07, 1.21, 1.28 and 1.54, the corresponding methyl carbons were assigned by HSQC, at δ_C 16.2, 23.9, 16.4, 27.9, 18.3 and 19.6. Moreover, in the lower field region of the ^{1}H NMR spectrum a proton signal due to a formyl group at δ_H 9.62 (δ_C 207.4) and signals of four sugar anomeric protons at δ_H 5.46, 4.98, 4.89 and 4.78 were seen. Among the 30 carbons of the triterpene aglycone in the ^{13}C NMR spectrum as was disclosed by the DEPTq135 experiment, six were methyls, eleven were methylenes, six were methines and seven were quaternary carbons including one oxygen-bearing methylene (δ_C 77.4), three oxygen-bearing methines (δ_C 76,7, 88.9, 207.4) and one oxygen-bearing quaternary carbon (δ_C 86.1) (Table 3.11). The structural assignment was initiated from the long - range coupling networks observed between methyl protons and the adjacent carbons from the HMBC experiment (Table 3.12).

This analysis indicated that the aglycone of CY1 had an oleanane skeleton with an oxygen bridge between C-13 (δ_C 86.1) and C-28 (δ_C 77.4), a formyl group at C-30 (δ_C 207.4) and a hydroxyl at C-16 (δ_C 76.7). The α configuration of the hydroxyl group at C-16 was evident from the chemical shift in comparison to literature data (16 α OH at about δ_H 76.6) (Huang *et al.*, 2000, Jia *et al.*, 1994) and from the NOESY results, as spatial proximities were observed between H-16 and H-28. The orientation of the hydroxyl at C-3 could be deduced from the spatial proximities observed between H-3 (δ_H 3.17) and H-23 (δ_H 1.21) as well as H-3 and H-5 (δ_H 0.67) (Table 3.13).

The above data for the aglycone part of CY1 corresponded well with cyclamiretin A (3β,16α-dihydroxy-13β,28-epoxy-30-oleanal), which was further confirmed by comparison of NMR data with the literature (Mahato and Kundu, 1994, Jia *et al.*, 1994). The attachment of the sugar chain was indicated by the low field shift of C-3 (δ_C 88.9). The mass fragmentation pattern suggested that the chain was branched: $[M - H]^-$ ion at *m/z* 1059.5355 and fragments corresponding to an independent loss of a pentose unit $[(M - H) -132]^-$ at *m/z* 927.4951, and a hexose unit $[(M- H) - 162]^-$ at *m/z* 897.1533 and to a loss of a pentose-hexose unit $[(M -H) - (132 +162)]^-$ at *m/z* 765.5546. The nature of the monosaccharides and the sequence of a tetrasaccharide chain was determined by a combination of COSY, NOESY, DEPT, HMBC and HSQC spectra.

Starting from the anomeric protons of each sugar the hydrogens within each spin system were identified using COSY, the corresponding ^{13}C resonances were assigned by HSQC and further confirmed by HMBC.

The interglycosidic linkages were established from the HMBC and NOESY experiments. In the HMBC spectrum a cross peak was seen between the signal at δ_H 4.78 (H-1 of arabinose) and 88.9 (C-3 of the aglycone) which confirmed the attachment position of the sugar chain. Other key cross peaks were observed between: H-1 glucose (G) and C-4 arabinose (A); H-1 of glucose'(G') and C-2 arabinose (A); H-1 of xylose (X) and C-2 glucose (G) (Table 3.12). The same conclusion was drawn from the NOESY experiment. All these observations confirm the identity of CY1 as 3-*O*-{β-D-xylopyranosyl- (1→2)-β-D-glucopyranosyl-(1→4)-[β-D-glucopyranosyl-(1→2)]-α-L-arabinopyranosyl}-cyclamiretin A and the data were in agreement with those reported (Podolak *et al.*, 2007). The compounds of such structure were previously isolated from *Ardisia crenata* as ardisiacrispin A (Jia *et al.*, 1994) and from *Androsace umbellate* as saxifragifolin B (Zhang *et al.*, 2007) and in the genus *Cyclamen* under the name of deglucocyclamin that was isolated from tubers of *C. mirabile* (Calis *et al.*, 1997) and tubers of *C. repandum* (Speroni *et al.*, 2007).

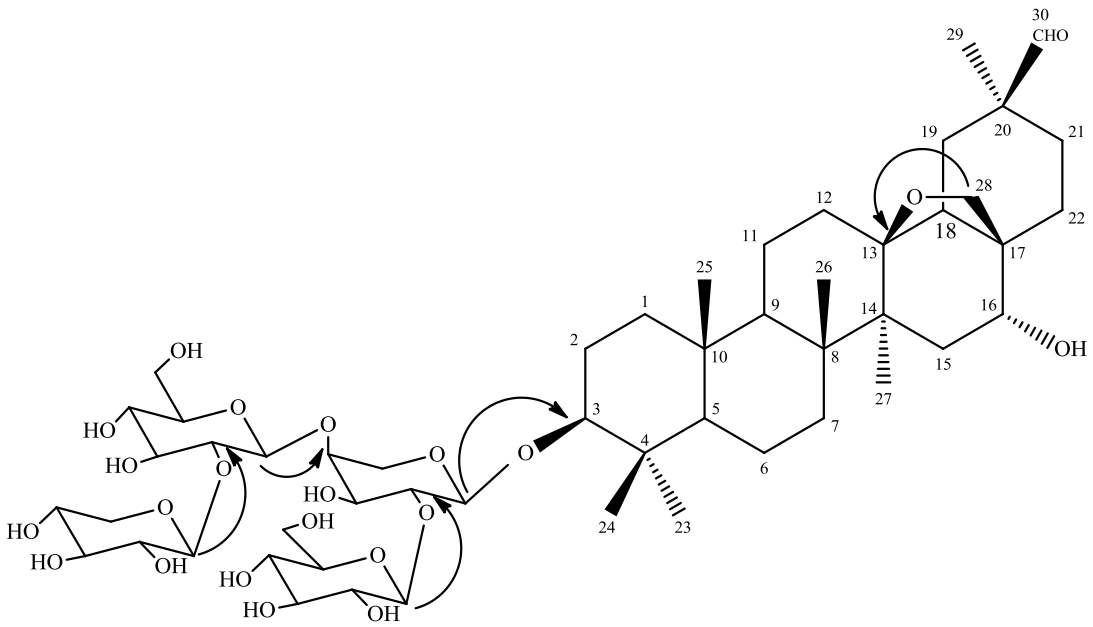

Figure 3. 61: Characteristic long-range ^{1}H - ^{13}C correlations observed in the HMBC experiment for CY1

Table 3. 11:^{1}H NMR and DEPTq-135 NMR spectral data of CY1 in pyridine-d_5.

Aglycone	^{1}H δppm (m, *J* Hz)	^{13}C	Sugar	^{1}H	^{13}C
			Arabinose (A)		
1	0.84 (1H, *m*), 1.64 (1H, *m*)	39.0			
2	1.81 (1H, *m*), 2.01 (1H, *m*)	26.4	A-1	4.78(1H, *d*, *J* = 6.1Hz)	104.5
3	3.17 (1H, *dd*, *J* =11.2, 4.0Hz)	88.9	A-2	4.54(1H, *m*)	79.5
4	-	39.5	A-3	4.27(1H, *m*)	73.1
5	0.67 (1H, *d*, *J* = 11.6 Hz)	55.5	A-4	4.26(1H, *m*)	78.0
6	1.32 (1H, *m*), 1.43 (1H, *m*)	17.7	A-5	3.69(1H, *m*), 4.62(1H, *m*)	64.5
7	1.18 (1H, *m*), 1.53 (1H, *m*)	34.1	**Glucose (G) terminal**		
8	-	42.3	G-1	5.46(1H, *d*, *J* = 7.6 Hz)	104.0
9	1.25 (1H, *m*)	50.2	G-2	4.07(1H, *m*)	76.7
10	-	36.6	G-3	4.20(1H, *m*)	77.3
11	1.45 (1H, *m*), 1.71 (1H, *m*)	18.9	G-4	4.30(1H, *m*)	70.9
12	1.41 (1H, *m*), 2.09 (1H, *m*)	32.5	G-5	4.06(1H, *m*)	77.7
13	-	86.1	G-6	4.41(1H, *m*), 4.56(1H, *m*)	62.1
14	-	43.8	**Glucose (G') inner**		
15	1.49(1H, *m*), 2.20(1H, *dd*, *J* = 14.3, 4.4Hz)	36.7	G'-1	4.98(1H, *d*, *J* = 7.8Hz)	104.6
16	4.22 (1H, *m*)	76.7	G'-	3.89(1H, *m*)	85.1
17	-	44.4	G'-	4.0(1H, *m*)	77.4
18	1.38 (1H, *m*)	53.1	G'-	4.19(1H, *m*)	71.6
19	2.11(1H, *m*), 2.84 (1H, *t*,13.6, 13.3)	33.2	G'-	4.26(1H, *m*)	77.9
20	-	48.1	G'-	4.28(1H, *m*), 4.63(1H, *m*)	62.8
21	2.06 (1H, *m*), 2.53 (1H, *td*)	30.3	**Xylose (X)**		
22	1.56 (1H, *m*), 1.96 (1H, *m*)	32.1	X-1	4.89(1H, *d*, *J* = 7.1Hz)	107.4
23	1.21 (3H, *s*)	27.9	X-2	4.01(1H, *m*)	76.0
24	1.07 (3H, *s*)	16.4	X-3	4.24(1H, *m*)	78.4
25	0.82 (3H, *s*)	16.2	X-4	4.11(1H, *m*)	70.5
26	1.28 (3H, *s*)	18.3	X-5	3.70(1H, *m*), 4.55(1H, *m*)	67.2
27	1.54 (3H, *s*)	19.6			
28	3.15 (1H, *q*), 3.54 (1H, *d*, *J* = 7.8Hz)	77.4			
29	1.01 (3H, *s*)	23.9			
30	9.62 (1H, *s*)	207.4			

Table 3. 12: Selected HMBC correlations of CY1 in pyridine-d_5.

Position	Selected HMBC correlations (H→C)
1	H-1/C-4, C-5, C-10
2	H-2/C-3, C-4
	H-2/C-3
3	H-3/C-1, C-2, A-1 arabinose
4	-
5	H-5/C-4, C-10, C-25
6	H-6/C-7, C-8
7	
8	-
9	H-9/C-10
10	-
11	H-11/C-13
12	H-12/C-11
13	-
14	-
15	H-15/C-13, C-16, C-17
	H-15/C-8, C-14, C-27
16	H-16/C-14, C-17, C-18, C-22
17	-
18	
19	H-19/C-18, C-20, C-29, C-30
20	-
21	H-21/C17, C-20, C-22, C-30
	H-21/C-20, C-22, C-29, C-30
22	H-22/C-16, C-17, C-18, C-20, C-21
	H-22/C-28
23	H-23/C-3, C-4, C-5, C-24
24	H-24/C-3, C-4, C-5, C-23
25	H-25/ C-1
26	H-26/C-7, C-8, C-9, C-14
27	H-27/C-8, C-13, C-15
28	H-28/C-13, C-16, C-17, C-22
29	H-29/C-19, C-20, C21, C-30
30	H-30/C-20, C-21
Glucose	H-1(G)/C-4 arabinose
Glucose’	H-1(G’)/C-2 arabinose
Xylose	H-1(X)/C-2 glucose

Table 3. 13: Selected data from NOESY experiment of CY1 in pyridine-d_5.

proton-proton connectivities between:	
3.17 (H-3 aglycone)	0.84 (H-1 aglycone)
3.17 (H-3 aglycone)	0.67 (H-5 aglycone)
3.17 (H-3 aglycone)	1.21 (H-23 aglycone)
4.22 (H-16 aglycone)	1.28 (H-26 aglycone)
4.22 (H-16 aglycone)	3.15 (H-28 aglycone)
3.17 (H-3 aglycone)	4.78 (H-1 arabinose)
5.46 (H-1 glucose)	4.26 (H-4 arabinose)
5.98 (H-1 glucose’)	4.54 (H-2 arabinose)
4.89 (H-1 xylose)	4.07 (H-2 glucose)

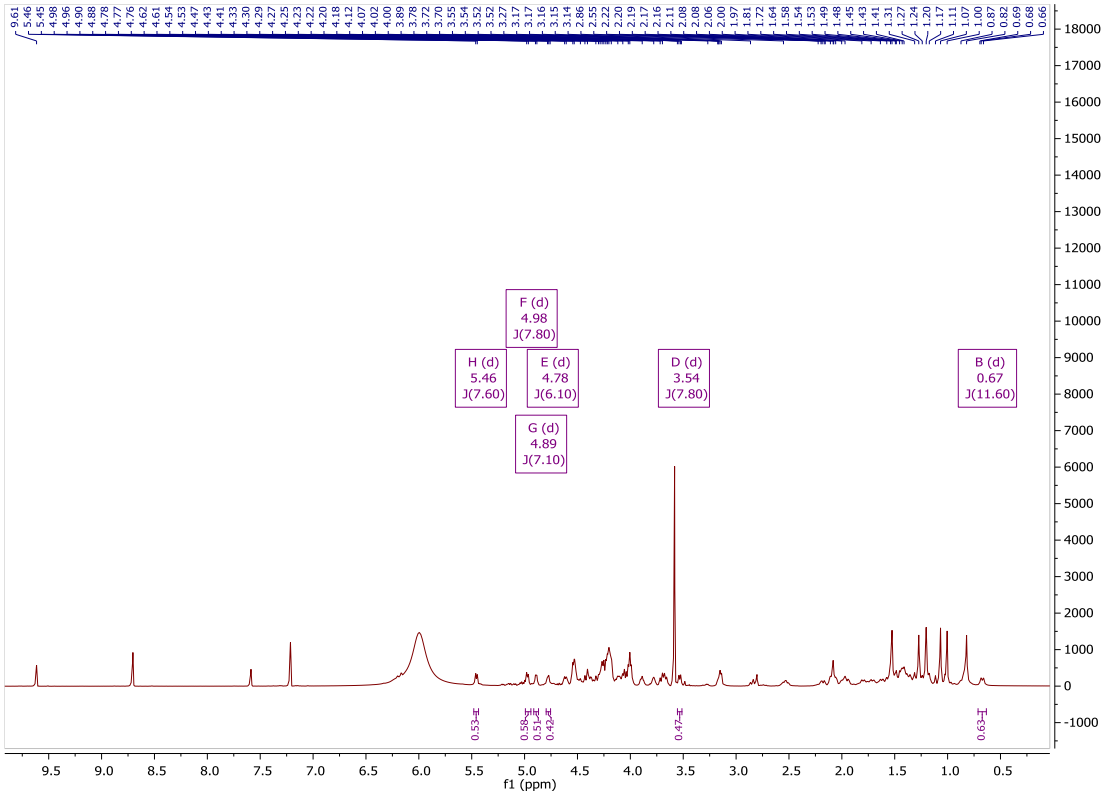

Figure 3. 62: ^{1}H NMR spectrum (400 MHz) of CY1 in pyridine-*d*$_5$

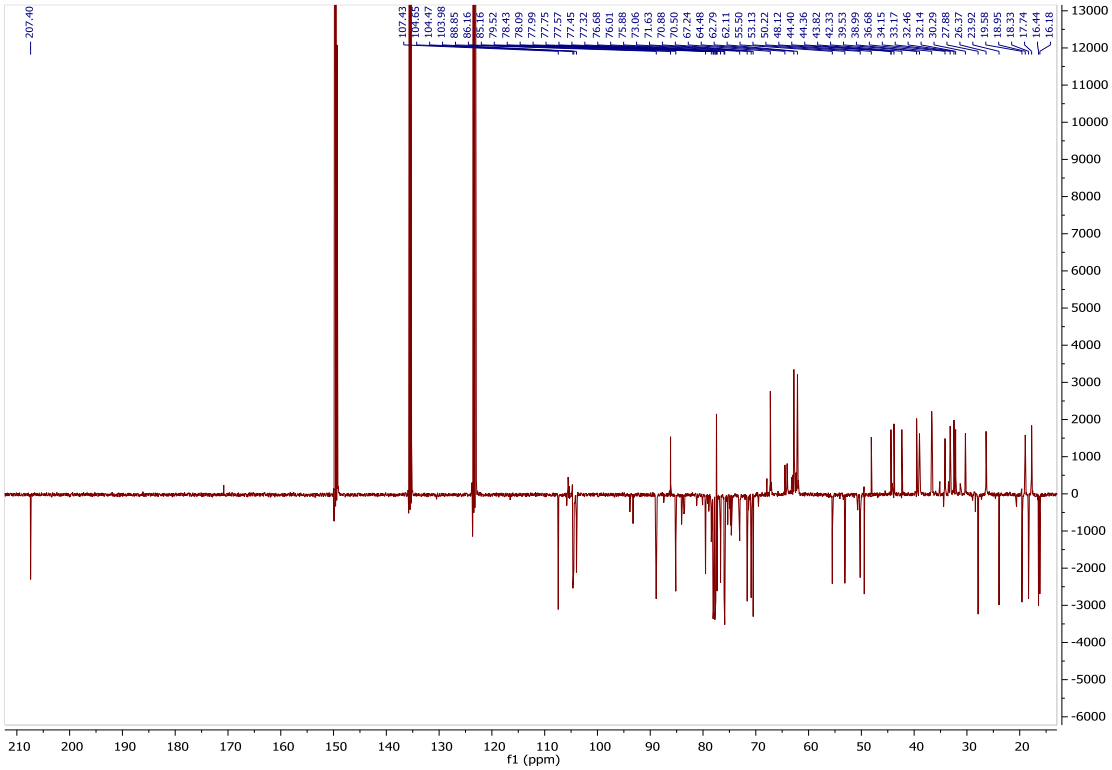

Figure 3.63: DEPTq-135 NMR spectrum (100 MHz) of CY1 in pyridine-*d*$_5$

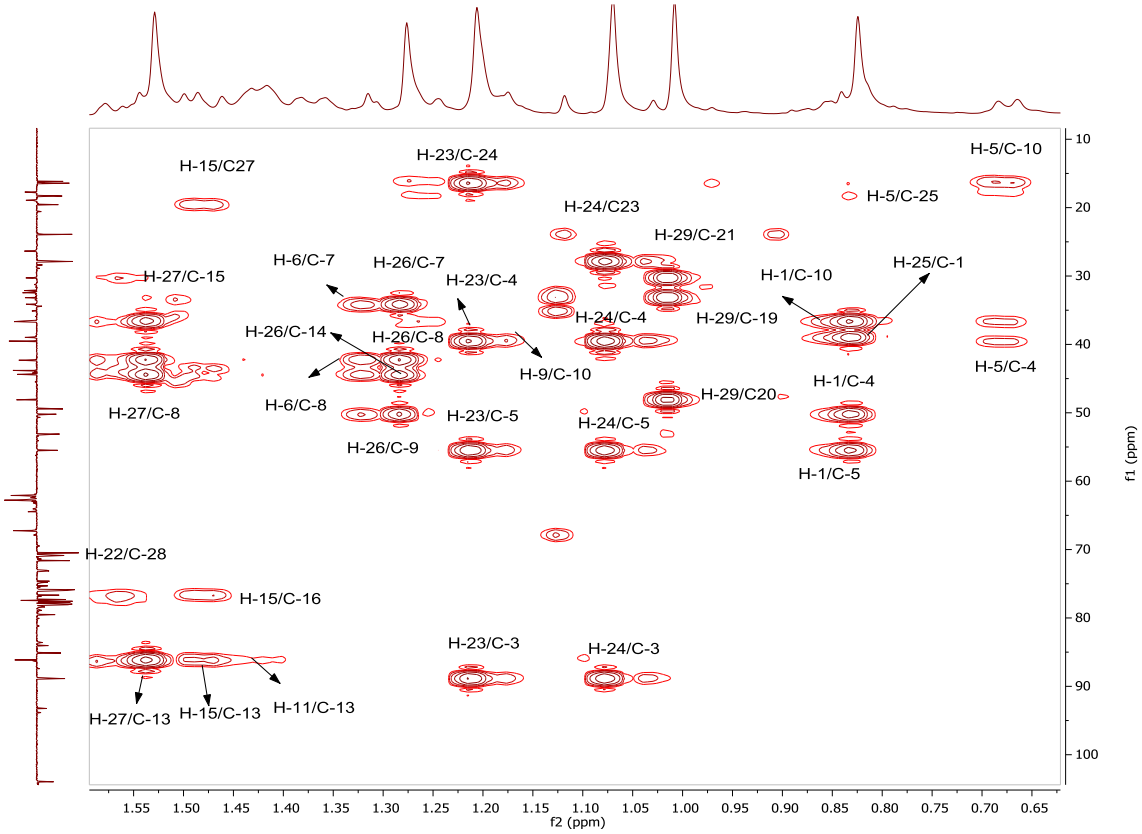

Figure 3. 64: HMBC spectrum (400 MHz) of CY1 in the region 0.56 - 1.55 ppm

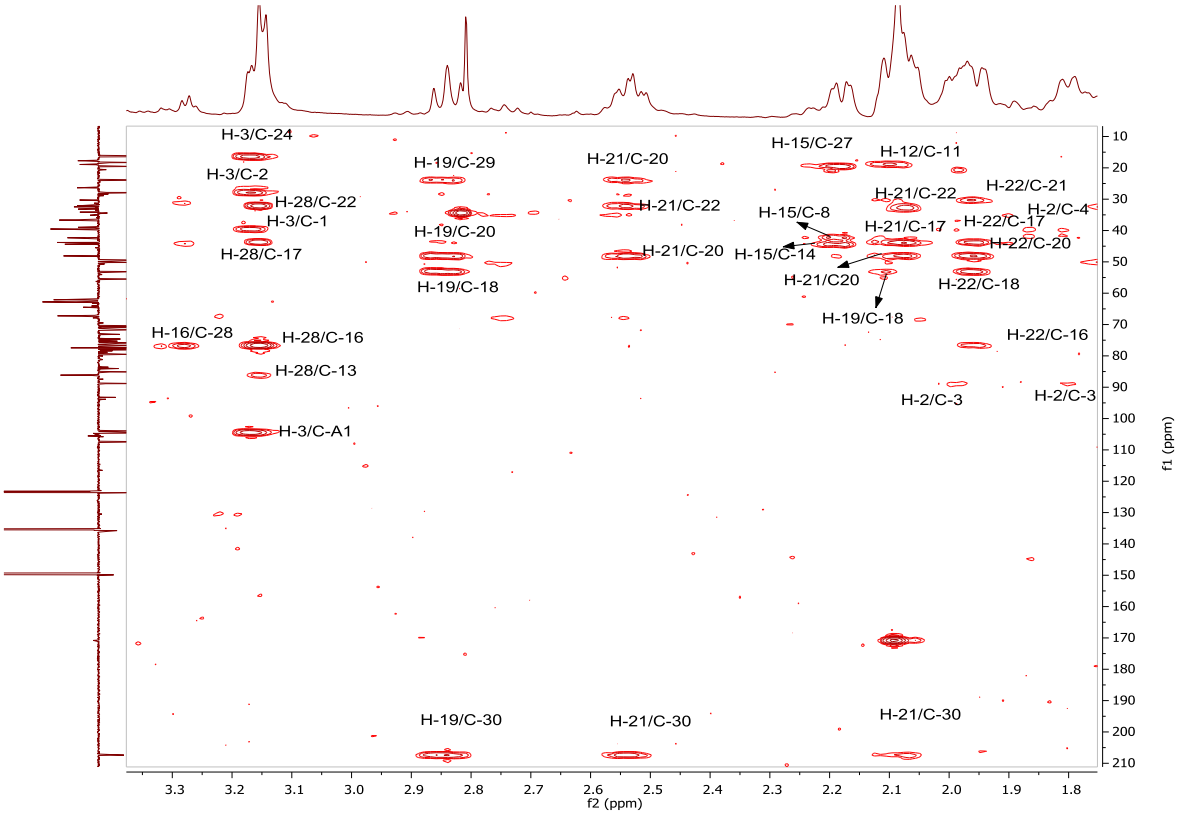

Figure 3.65: HMBC spectrum (400 MHz) of CY1 in the region 1.8 - 3.3 ppm

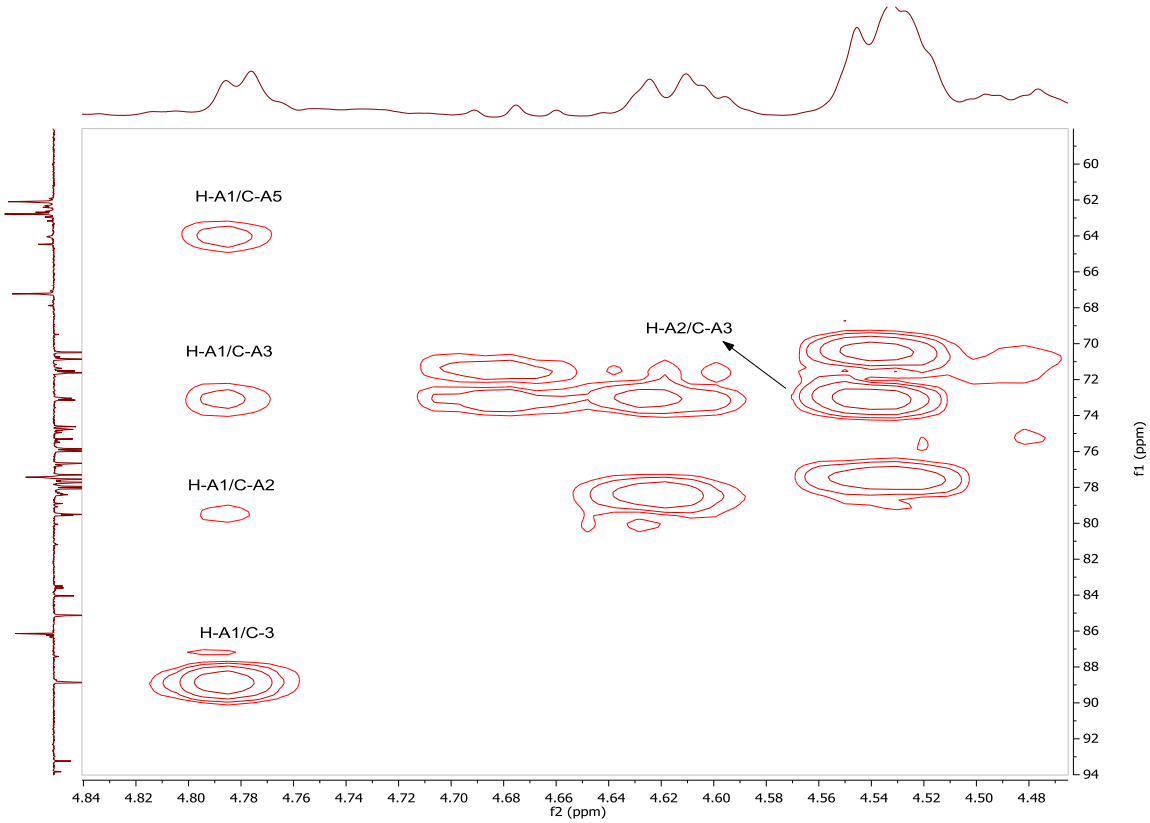

Figure 3.66: HMBC spectrum (400 MHz) of CY1 in the region 4.48 - 4.84ppm

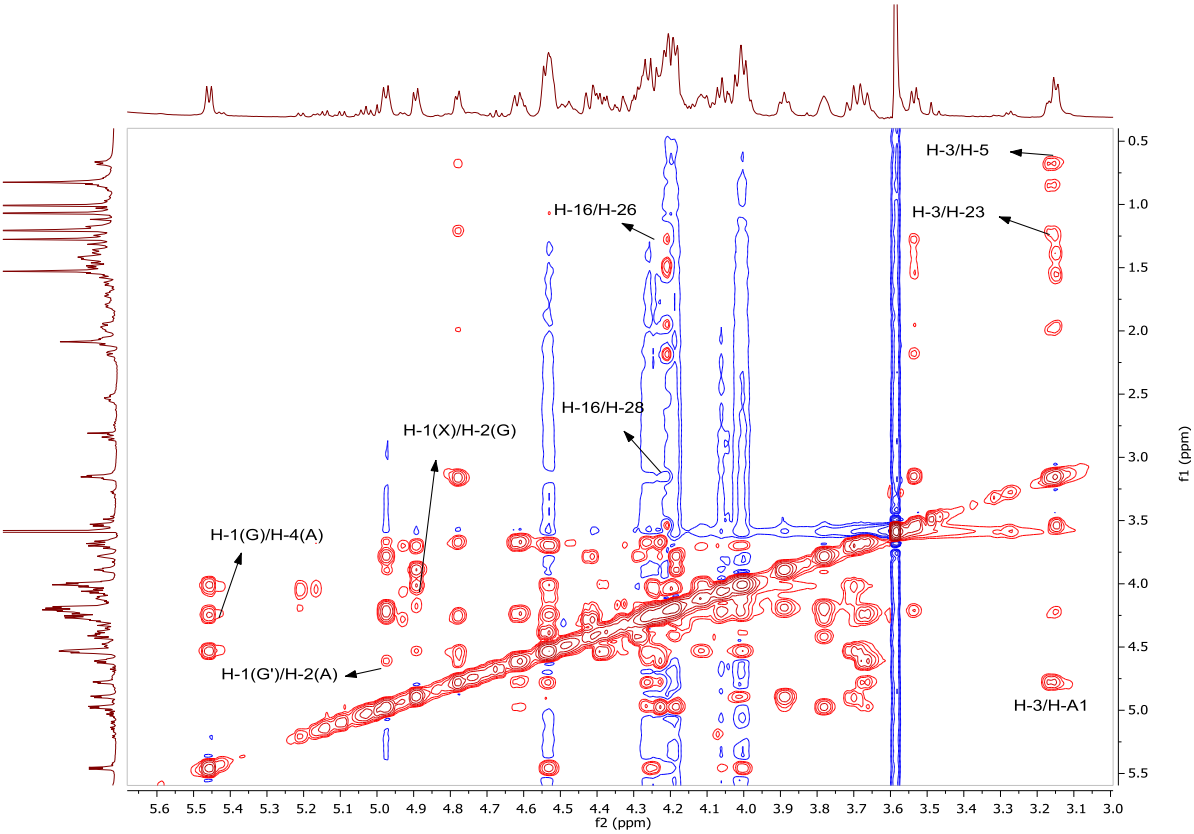

Figure 3. 13: NOESY spectrum (400 MHz) of CY1 in the region 3.0-5.6ppm

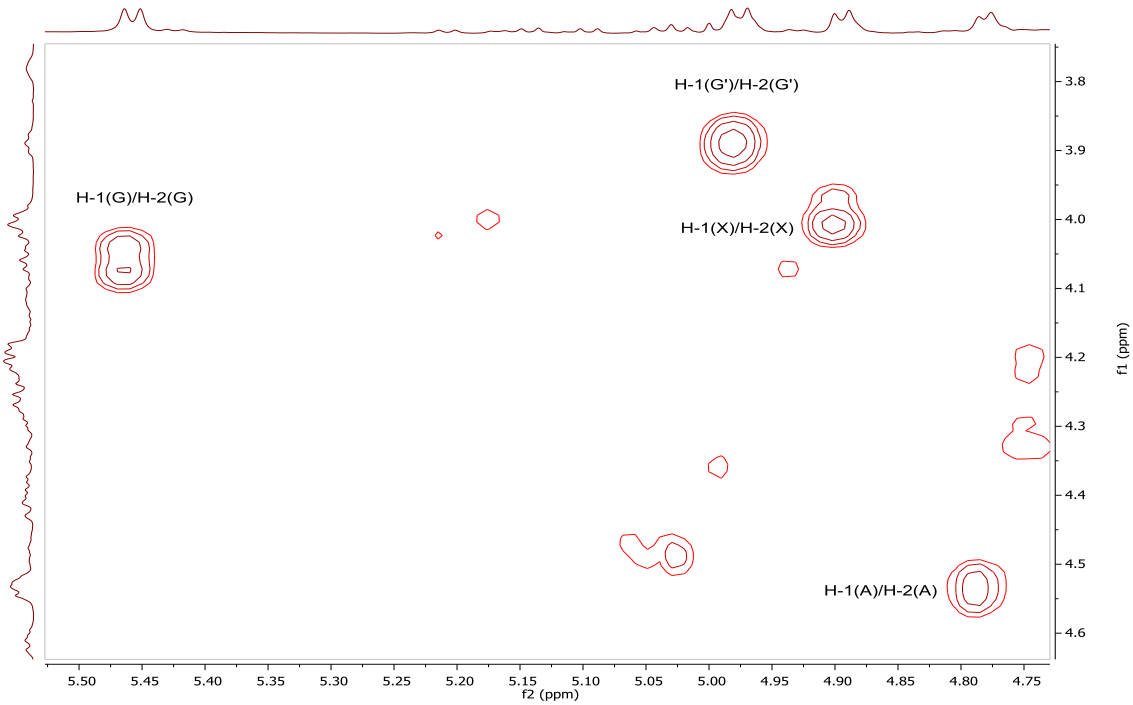

Figure 3.68: COSY spectrum (400 MHz) of CY1 in the region 4.75 - 5.50 ppm

A total 14 compounds were isolated in the current work - 13 were isolated from *C. cyrenaica* which underwent phytochemical investigation for the first time for all plant parts (flower heads, root, leaf and stem). Among the 13 compounds, two were identified as novel (CC12 and CC13). One compound (CY1) was separated from *C. rohlfsianum* tuber, which had previously been isolated from *C. mirabile* tubers (Calis *et al.*, 1997) and tubers of *C. repandum* (Speroni *et al*., 2007). Fractionation of the hexane extract of *C. cyrenaica* flower heads led to the isolation of CC1 which was previously isolated from *C. cardunculus* L. var. *altilis* and *C. scolymus* L (Ramos *et al.*, 2013; Shakeri and Ahmadian, 2014). Fractionation of the ethyl acetate extract of *C. cyrenaica* flower heads led to the isolation of CC2 which was isolated for the first time from *Cynara* and CC3 which was isolated before from *C. scolymus* L. (Lattanzio *et al.*, 2009). The ^{1}H NMR spectrum of the methanol extract of *C. cyrenaica* flower heads (CMH) showed signals suggesting a mixture of aromatic compounds and fats. CC4 was isolated from fractionation of the hexane extract of *C. cyrenaica* root and was isolated previously from *C. cardunculus* L. var. *altilis* (Ramos *et al.*, 2013). Fractionation of the ethyl acetate extract of *C. cyrenaica* root led to the isolation of sesquiterpene lactone (CC5), which was isolated previously from the aerial parts of *C. humilis* L (Reis *et al.*, 1992), and had not studied before for biological activity.

The ^{1}H NMR spectrum of the methanol extract of *C. cyrenaica* root (CMR) showed signals suggesting a mixture of aromatic compounds and fats. Fractionation of the methanol extract of *C. cyrenaica* leaves led to the isolation of CC6 along with CC7 and CC8 which were previously isolated from *C. scolymus* L (Lattanzio *et al.*, 2009; Jacociunas *et al.*, 2014; Nassar *et al.*, 2013). The ^{1}H NMR spectrum of the hexane extract of *C. cyrenaica* leaves (CHL) and the ethyl acetate extract of *C. cyrenaica* leaves (CEL) showed signals suggesting a mixture triterpene compounds and fats. Fractionation of the methanol extract of *C. cyrenaica* stem led to the isolation of CC9 which was isolated before from *C. scolymus* L (Lattanzio *et al*., 2009; Jacociunas *et al*., 2014; Nassar *et al*., 2013) and CC10 which was isolated for first time from *Cynara.* Fractionation of the ethyl acetate extract of *C. cyrenaica* stems led to the isolation of CC11, CC12 and CC13. The ^{1}H NMR spectrum of the hexane extract of *C. cyrenaica* stem (CHS) showed signals suggesting a mixture of fats. For *C. rohlfsianum,* the only phytochemical study on this plant was carried out by Elabbar *et al*. (2014) and revealed the presence of oleanolic acid (**1**), 7, 8, 4`-trihydroxyflavone (**23**), genistein (**24**),

hesperetin (**25**), kaempferol (**26**). The phytochemical investigation in the current work was carried out on the tuber in an attempt to isolate the phytochemical(s) that could be responsible for antidiabetic activity in the light of traditional use. The results from the phytochemical investigation of *C. rohlfsianum* tuber revealed the isolation of CY1.

CHAPTER IV

4. RESULTS AND DISCUSSION PART II: BIOLOGICAL STUDIES

4.1 *In vitro* anti-diabetic activity assessment

The aim of this part of the chapter was to determine the potential of the crude extracts along with some of the isolated compounds from *C. cyrenaica and C. rohlfsianum* in the treatment of diabetes. This was achieved by investigating the antidiabetic activity *in vitro* using α-glucosidase, PTP1B and α-amylase inhibition tests. Samples that showed 40% or less of the control (more than 60% inhibition) were considered to be potentially active.

4.1.1 Effect of the extracts and the isolated compounds from C. cyrenaica and C. rohlfsianum on α-glucosidase inhibition test

As can be seen from Figure 4.1 the standard acarbose inhibitor produced a concentration-dependent inhibition (IC_{50} 728.4 ± 1.17µM). *C. cyrenaica* and *C. rohlfsianum* crude extracts were screened at 30µg/ml (Figure 4.2 **A** and **B**).

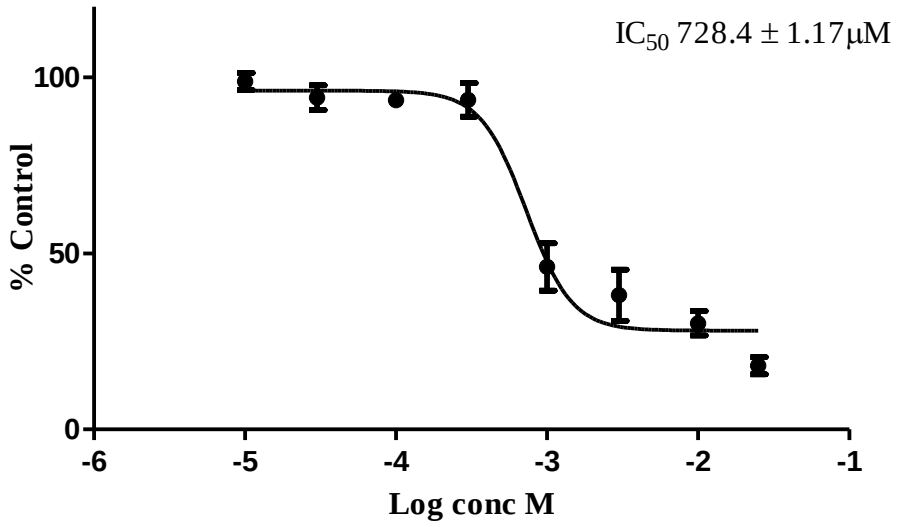

Figure 4. 1: Effect of acarbose on the α-glucosidase assay in the presence of 4-nitrophenyl-glucopyranoside (substrate). Acarbose at different concentrations (25mM to 10µM) was incubated with α-glucosidase for 10min at 37ºC in an atmosphere containing 5% CO_2. 4-nitrophenyl-glucopyranoside (4mM) was then added and incubated for 10min at 37ºC. The absorbance readings were taken at 405nm. Data points represent the mean ± SEM of α-glucosidase hydrolysis (% control) of 3 values.

For *C. rohlfsianum* tuber crude extracts, the only significant ($p < 0.001$) inhibition was found with the methanol extract (CYMT) at 30µg/ml, which exhibited 82.1% of enzyme inhibition (Figure 4.2 **A**). According to the results obtained, CYMT contains potential antidiabetic compound(s) that are responsible for this inhibition. This crude extract was fractionated and CY1 was isolated (section **3.2.1.1**). CY1 was tested for potential antidiabetic effects and found to also potentially be active as it showed significant ($p < 0.001$) inhibitory effect on α-glucosidase (98.9% of enzyme inhibition) (Figure 4.2 **B**).

From the results obtained, *C. cyrenaica* crude extracts did not show any inhibition. However, the only compound that displayed inhibitory activity was CC10 that was isolated from the methanol extract of *C. cyrenaica* stem (section **3.1.4.2**). CC10 exhibited significant ($p < 0.001$) inhibition on α-glucosidase (98.3% of enzyme inhibition) (Figure 4.2 **B**).

The experiment was carried out again (Figures 4.3 and 4.4 **A**, **B** and **C**) as CC10 along with CY1, and CYMT were further tested, in order to determine if there was concentration-dependent inhibition. The results showed that the standard acarbose inhibitor produced a concentration-dependent inhibition with an IC_{50} value of 512.19 ± 1.36µM. CC10, CY1, and CYMT produced a concentration-dependent inhibition of the enzyme with IC_{50} 3.94 ± 1.1µM, 5.53 ± 1.1µM, and 3.46 ± 1.13µg/ml, respectively.

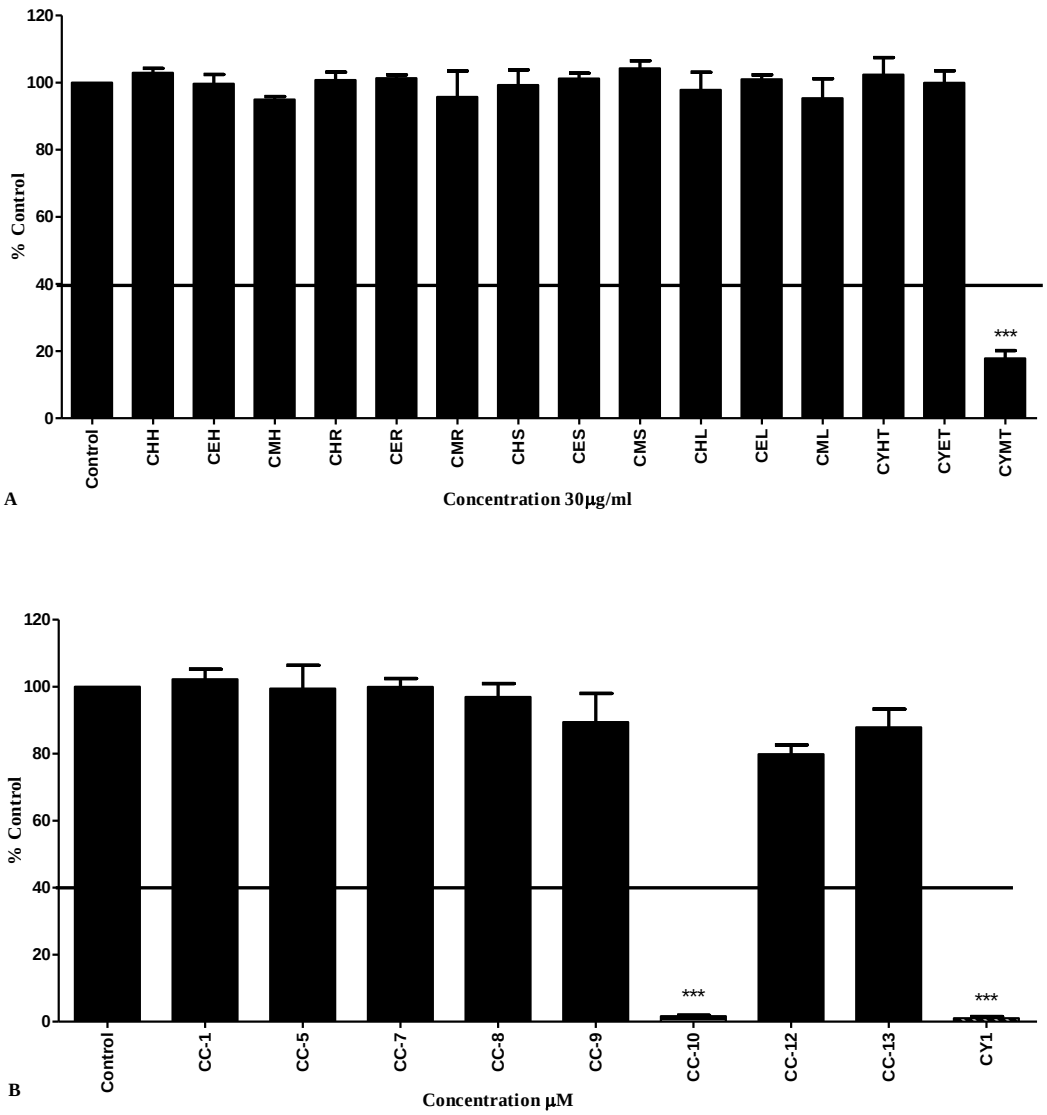

Figure 4. 2: Effect of (A) *C. cyrenaica* (flower heads, root, stem and leaf) crude solvent extracts and (B) *C. rohlfsianum* (tuber) crude solvent extracts on α-glucosidase inhibition. The samples were incubated with α-glucosidase for 10min at 37ºC. Then 4-nitrophenyl-glucopyranoside was added and incubated for 10min at 37ºC. The absorbance readings were taken at 405nm. Data points represent the mean ± SEM of α-glucosidase hydrolysis (% control) of three independent experiments. The data were analysed by Dunnett post-test, ***P value < 0.001 versus control.

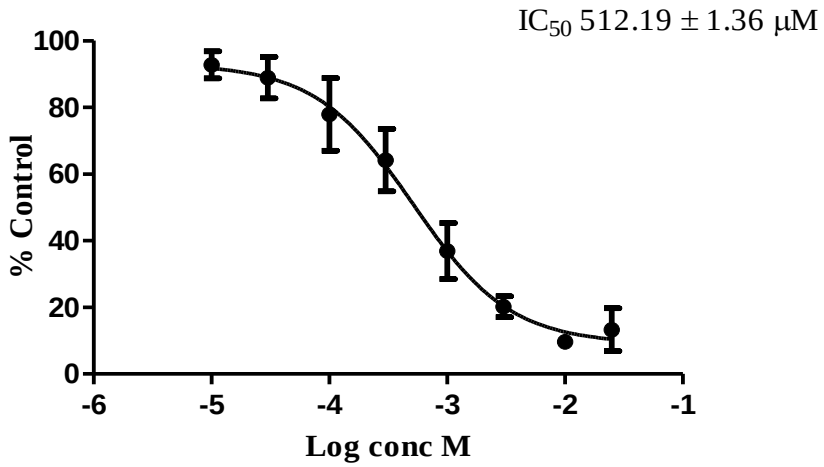

Figure 4. 3: Effect of various concentrations of acarbose standard on the α-glucosidase in the presence of 4-nitrophenylglucopyranoside (substrate). Acarbose at different concentrations (25mM to 10μM) was incubated with α-glucosidase for 10min at 37ºC in an atmosphere containing 5% CO_2. 4-nitrophenyl-glucopyranoside was then added and incubated for 10min at 37ºC. The absorbance readings were taken at 405nm. Data points represent the mean ± SEM of α-glucosidase hydrolysis (% control) of three experiments.

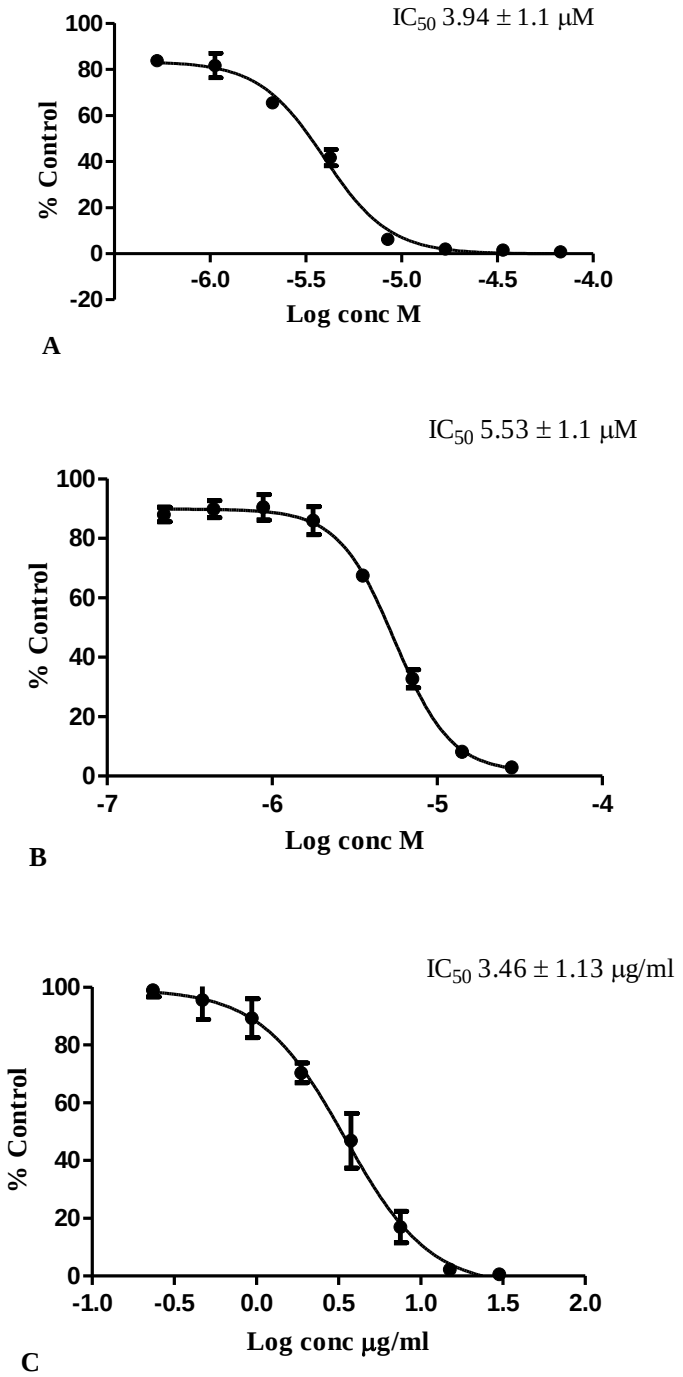

Figure 4. 4: The effect of different concentrations of (A) CC10, (B) CY1, (C) CYMT on α-glucosidase inhibition. Samples were incubated with α-glucosidase for 10min at 37ºC in an atmosphere containing 5% CO_2. 4-nitrophenyl-glucopyranoside was then added and incubated for 10min at 37ºC. The absorbance readings were taken at 405nm. Data points represent the mean ± SEM of α-glucosidase hydrolysis (% control). n=3.

4.1.2 Effect of the extracts and the isolated compounds from C. cyrenaica and C. rohlfsianum on α-amylase inhibition test

For the α-amylase assay, the standard inhibitor, acarbose, produced a concentration-dependent inhibition of α-amylase enzyme with an IC_{50} 781.1 ± 1.57µM (Figure 4.5). According to the results obtained, none of the extracts or separated compounds from both plants were considered to be active on α-amylase (Figure 4.6 **A** and **B**)

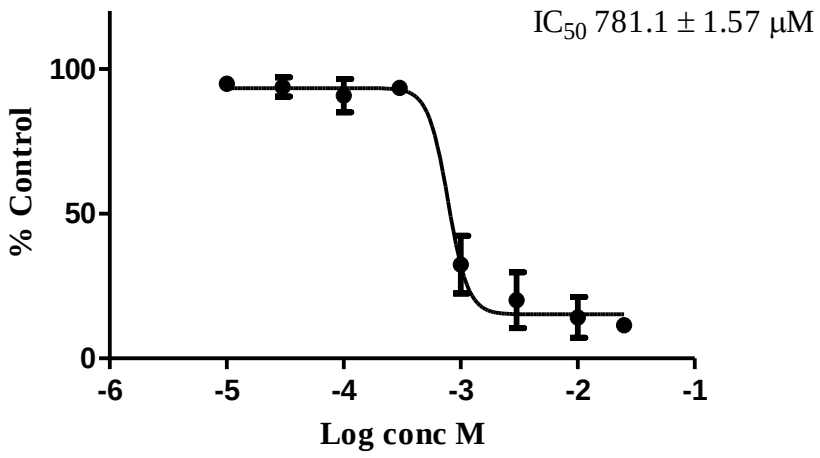

Figure 4. 5: Effect of various concentrations of acarbose standard on α-amylase activity in the presence of 4-nitrophenyl-α-D-maltohexaside. Acarbose at different concentrations (25mM to 10µM) was incubated with α-amylase for 30min at 37ºC in an atmosphere containing 5% CO_2. 4-nitrophenyl-α-D-maltohexaside (1.5mM) was then added and incubated for 30min at 37ºC. The absorbance readings were taken at 405nm. Data points represent the mean ± SEM of α-amylase enzyme hydrolysis (% control) of three experiments.

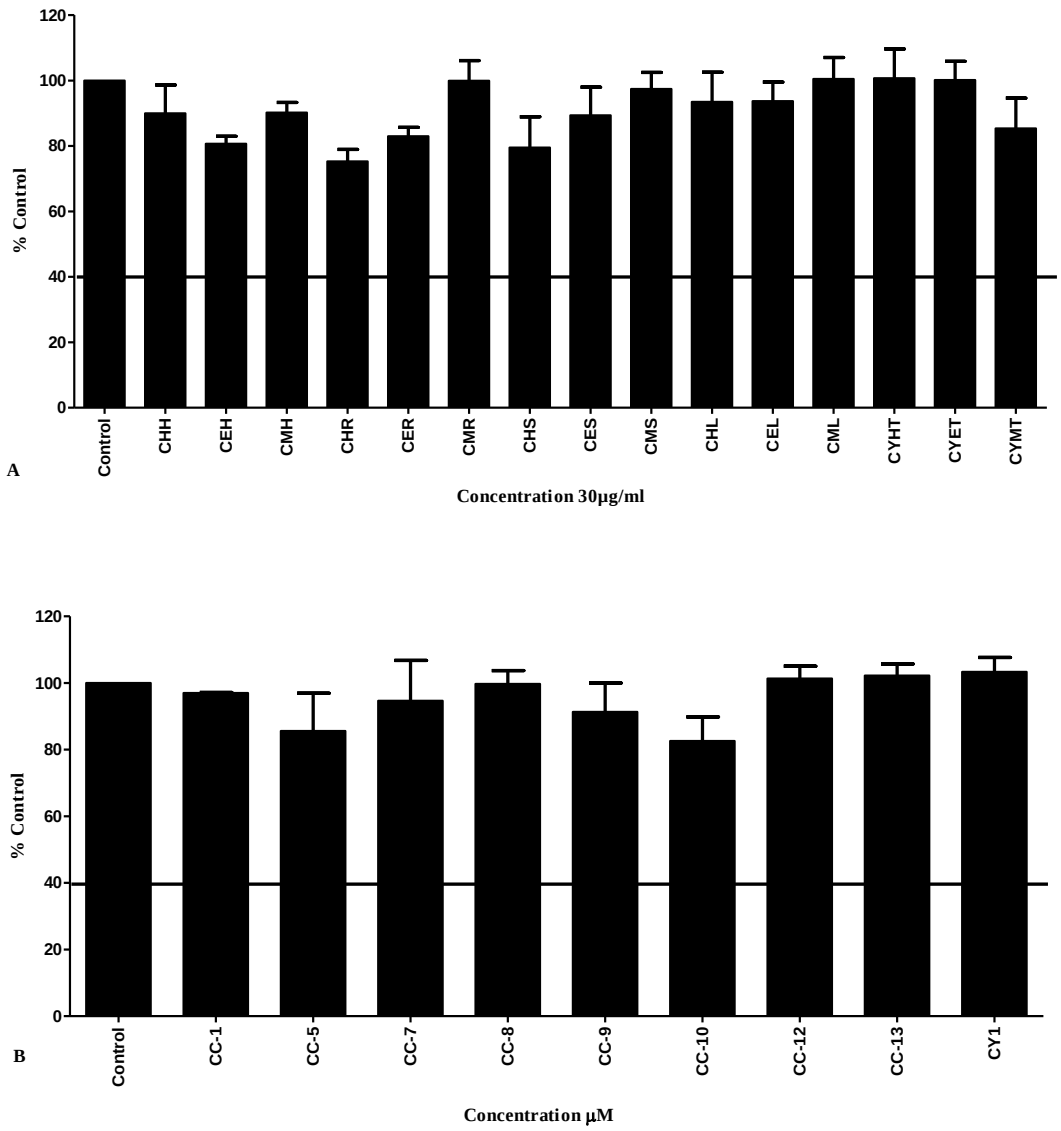

Figure 4. 6: Effect of crude solvent extracts (A) and isolated compounds (B) of both plants on α-amylase inhibition in the presence of 4-nitrophenyl-α-D-maltohexaside substrate. The samples prepared at 30µg/ml were incubated with α-amylase for 30min at 37ºC in an atmosphere containing 5% CO_2. 4- nitrophenyl-α-D-maltohexaside (1.5mM) was then added and incubated for 30min at 37ºC. The absorbance readings were taken at 405nm. Data points represent the mean ± SEM of enzyme hydrolysis (% control) of three independent experiments. The data were analysed by Dunnett post-test.

4.1.3 Effect of the extracts and the isolated compounds from C. cyrenaica and C. rohlfsianum on PTP1B enzyme

The standard inhibitor, TFMS, produced a concentration-dependent inhibition (IC_{50} 9.1 ± 1.17µM) (Figure 4.7). The plant extracts and compounds were tested in the PTP1B enzyme assay compared with the standard inhibitor.

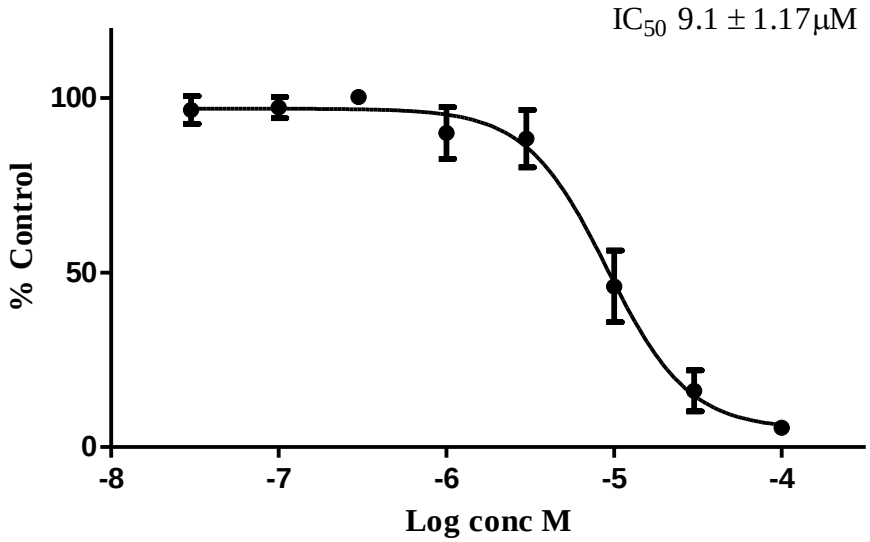

Figure 4. 7: Effect of TFMS standard at different concentrations (100µM – 0.03µM) on PTP1B enzyme in the presence of DiFMUP substrate. TFMS standard at different concentrations (100µM – 0.03µM) were incubated with PTP1B enzyme for 30min at 37ºC in an atmosphere containing 5% CO_2. DiFMUP (10µM) was then added and incubated for 10min at 37ºC. The fluorescence intensity was measured at 355/460nm. Data points represent the mean ± SEM of PTP1B enzyme hydrolysis (% control) of three independent experiments.

As can be seen from Figure 4.8 **A**, none of the extracts from both plants were considered to be active against PTP1B enzyme, however, CC-9 showed significant ($p < 0.001$) inhibition accounted for 72.61% (Figure 4.8 **B**) and produced a concentration-dependent inhibition of the enzyme with IC_{50} value of 15.94 ± 1.12µM.

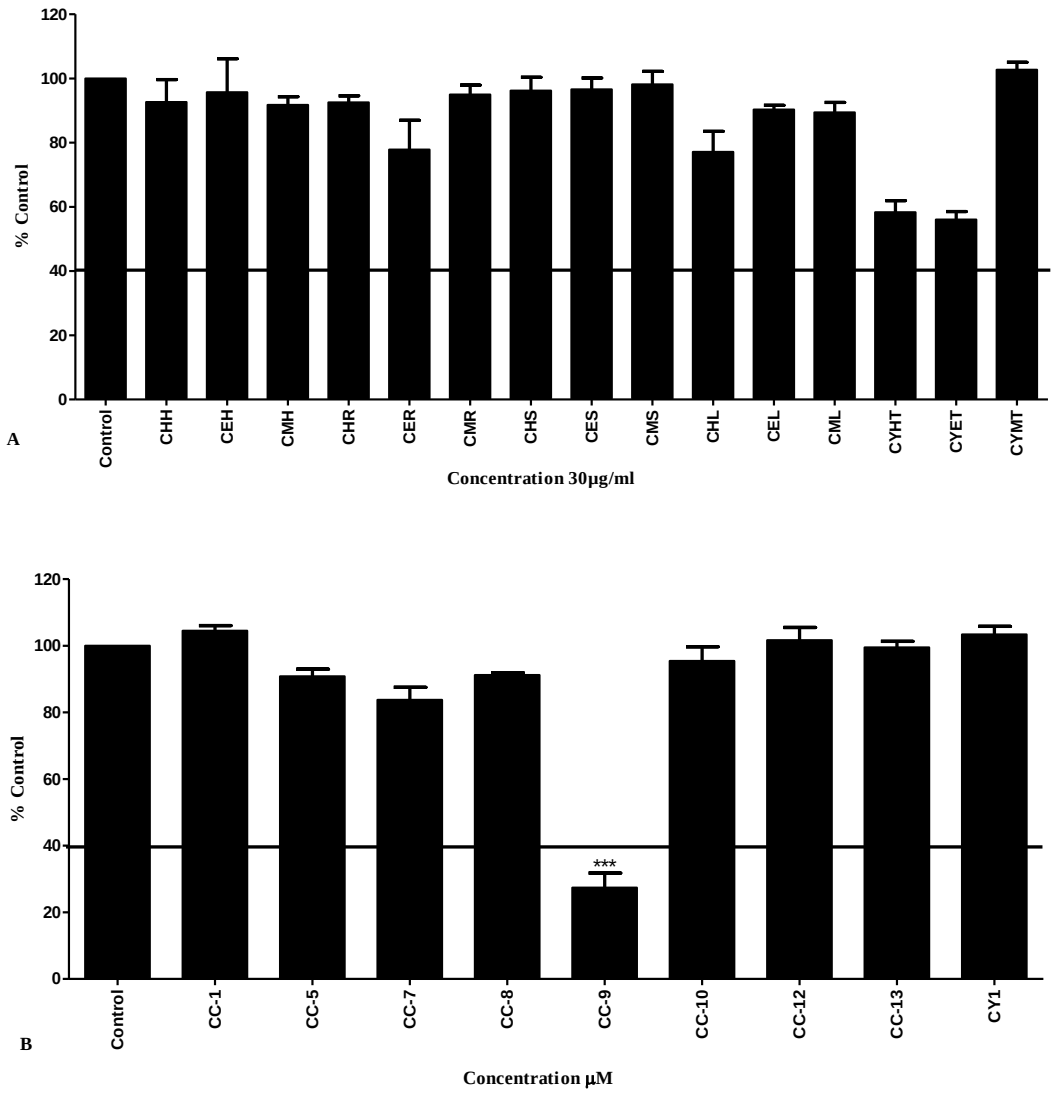

Figure 4. 8: Effect of crude solvent extracts (A) and the isolated compounds (B) of both plants on PTP1B enzyme in the presence of DiFMUP substrate. The samples were incubated with PTP1B enzyme for 30min at 37ºC in an atmosphere containing 5% CO_2. DiFMUP (10µM) was then added and incubated for 10min at 37ºC. The fluorescence intensity was measured at 355/460nm. Data points represent the mean ± SEM of PTP1B enzyme hydrolysis (% control) of three independent experiments. The data were analysed by Dunnett's post-test. ***P value < 0.001 versus control.

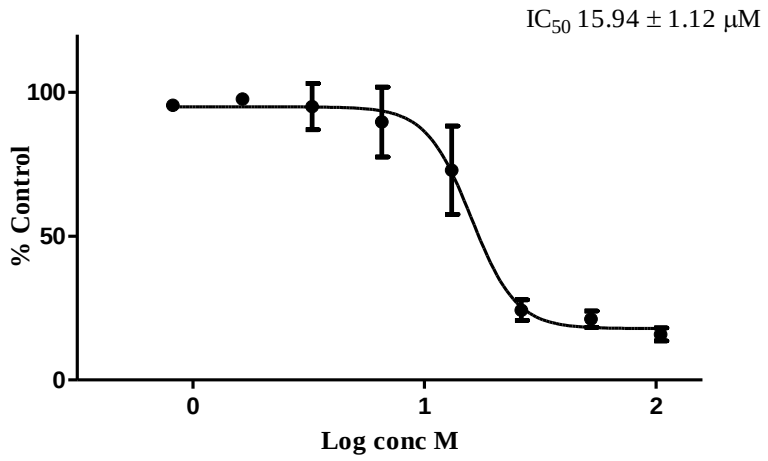

Figure 4. 9: The effect of different concentrations of CC9, on PTP1B enzyme. The sample was incubated with PTP1B enzyme for 30min at 37ºC in an atmosphere containing 5% CO_2. DiFMUP (10μM) was then added and incubated for 10min at 37ºC. The fluorescence intensity was measured at 355/460nm. Data points represent the mean ± SEM of PTP1B enzyme hydrolysis (% control) of three independent experiments.

Based on the results obtained from the inhibitory activity screen of the extracts along with some of the isolated compounds of *C. cyrenaica* and *C. rohlfsianum* on three enzymes; PTP1B, α-glucosidase and α-amylase, there was no inhibition observed from both plants on α-amylase. For the PTP1B assay, the only compound that showed inhibition was CC9 separated from *C. cyrenaica* and produced significant ($p < 0.001$) inhibitory activity. CC9 also produced a dose-dependent effect with an IC_{50} value of 15.94 ± 1.12µM. For α-glucosidase, only CC10 from *C. cyrenaica* was found to be active and evidenced significant ($p < 0.001$) inhibition with a concentration-dependent inhibition with an IC_{50} value of 3.94 ± 1.1µM. For *C. rohlfsianum*, CYMT and the pure compound CY1 isolated from it showed significant ($p < 0.001$) inhibition on α-glucosidase, suggesting that CY1 was the likely component responsible for this activity. Both CYMT and CY1 displayed dose-dependent inhibition with IC_{50} values of 3.46 ± 1.13µg/ml and 5.53 ± 1.1µM, respectively compared to acarbose specific inhibitor (IC_{50} 512.19 ± 1.36µM). On searching the literature neither *C. rohlfsianum* nor any other *Cyclamen* species have been studied for their potential antidiabetic effects even though *C. rohlfsianum* has been used tradionally as an antidiabetic. Thus, the results obtained from this work supported the traditional use of this plant as an antidiabetic. Therefore, natural α-glucosidase inhibitors from *C. cyrenaica* and *C. rohlfsianum* could be an attractive source for further study.

Diabetes mellitus, particularly type 2 diabetes (T2D) mellitus has been on the increase and accounts for 90% of the cases of diabetes around the world. T2D is characterized by hyperglycemia that is associated with a gradual decline in insulin sensitivity and/or insulin secretion (Jiang *et al.*, 2012). Controlling postprandial hyperglycemia has been found to be an efficient approach to manage diabetes, by retarding the two key enzymes α-amylase and α-glucosidase in the digestive system that are linked to the adsorption of glucose (Gao *et al.*, 2013). Natural therapies from plant origin have been known since ancient times, and herbal medicines are used widely because of the belief that they incur fewer side effects, higher effectiveness and lower costs (Elberry *et al.*, 2015). Many herbal medicines and active phytochemicals have been studied for their efficiency to treat diabetes and its complications, by a variety of cellular and molecular mechanisms that have the effect of delaying the development of diabetic complications and changing the metabolic abnormality (Arulselvan *et al.*, 2014).

Many phytochemicals responsible for antidiabetic effects have been isolated from plants and can be used as alternative medicine. More than 80 anti-diabetic phytoconstitiuents isolated from various plant species have been recently reviewed by (Upadhyay, 2016). As a result, scientific attention has been directed to search for medicinal plants that have antihyperglycemic effects and can be consumed along with food (Arulselvan *et al.*, 2014). As a recommendation from a WHO expert committee on diabetes, therapeutics derived from natural sources should be further studied because they are frequently considered to be free from toxicity and have fewer side effects. Therefore, the search for more effective and safe bioactive chemicals continues to be an important biomedical drug development research with respect to this disease (Arulselvan *et al.*, 2014).

Natural α-amylase inhibitors from plant sources are an attractive therapeutic strategy in the management of post-prandial hyperglycemia by reducing the glucose release from starch and delaying carbohydrate absorption. Therefore, these compounds are potentially useful in control of diabetes due to the ability of these compounds on inhibition of the activity of the carbohydrate hydrolysing enzymes in the small intestine (Safamansouri *et al.*, 2014). Salem *et al.* (2017) revealed that an ethanol extract of the leaves of *C. scolymus* had inhibitory activity on α- amylase with an IC_{50} value of 50.18 ± 0.58μg/mL compared to acarbose (IC_{50} = 31.05 ± 0.08μg/mL).

Many studies have shown the potential of α-glucosidase inhibitors from plant extracts. It has been reported that natural products have being used as potential inhibitors against carbohydrate hydrolysing enzymes to treat diabetes mellitus. Liu *et al.* (2016) reported that qingzhuan tea extracts revealed potent inhibitory effects against α-glucosidase, which was likely attributed to the presence of epigallocatechin gallate and epicatechin gallate. Fu *et al*. (2017) reported that, the number of hydroxyl groups on the bioactive compounds play an essential role for α-glucosidase inhibition. Therefore, the structure of the gallate group that esterified catechin moiety is important, as the gallated catechin such as catechin gallate, gallocatechin gallate, epicatechin gallate, and epigallocatechin gallate showed stronger inhibitory activity than their corresponding ungallated compounds such as - catechin, epicatechin, gallocatechin and epigallocatechin. Yilmazer-Musa *et al.* (2012) suggested that the presence of a gallate group esterified to the 3-position of the C-ring of catechin moiety

was important for the interaction of flavan-3-ols with the enzyme, as the results revealed that catechin 3-gallates strongly exhibited α-glucosidase inhibition, unlike nongallated catechins which showed poor enzyme inhibition (Yilmazer-Musa *et al.*, 2012). These observations support the findings of the current work for catechin 7-*O*-gallate (CC10) isolated from the methanol extract of *C. cyrenaica* stem that showed a marked inhibitory effect on α-glucosidase in a dose-dependent manner and suggests that the activity of CC10 could be attributed to the presence of gallate esterified at the 7-position of the A-ring of the catechin moiety.

Luo *et al*. (2008) reported the strong inhibitory activity of triterpenoid saponins isolated from *Gypsophila oldhamiana* on α-glucosidase. Compounds 1 - 4 (Figure 4.10) exhibited more potent α-glucosidase inhibitory activities (IC_{50} 23.1 ± 1.8, 78.5 ± 7.1,65.5 ± 4.5 and 15.2 ± 1.8µM, respectively) than that of acarbose (IC_{50} 388.0 ± 9.6µM). These findings correlate and support the results of the current work, which demonstrated that triterpenoid saponin (CY1) isolated from CYMT exhibited stronger α-glucosidase inhibitory activity (IC_{50} 5.53 ± 1.1µM) than that of acarbose (IC_{50} 512.19 ± 1.36µM).

,

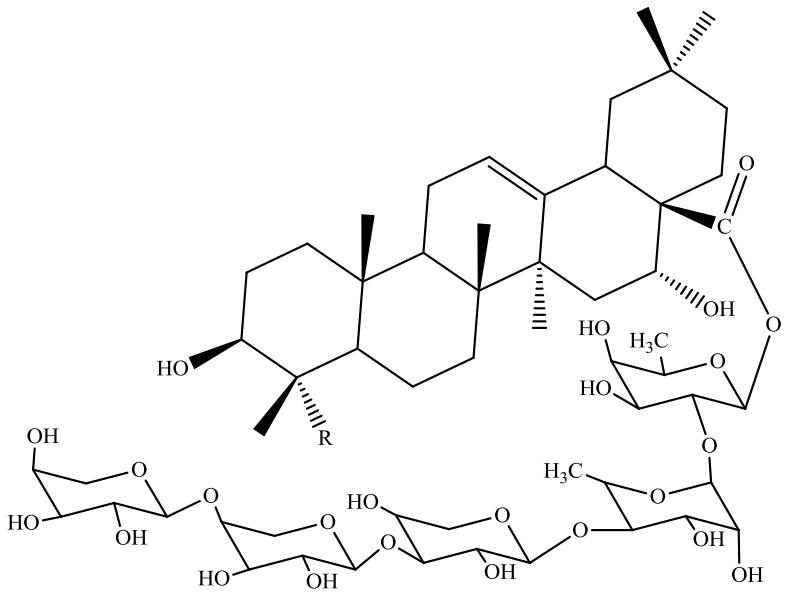

1 R = OH
2 R = CHO

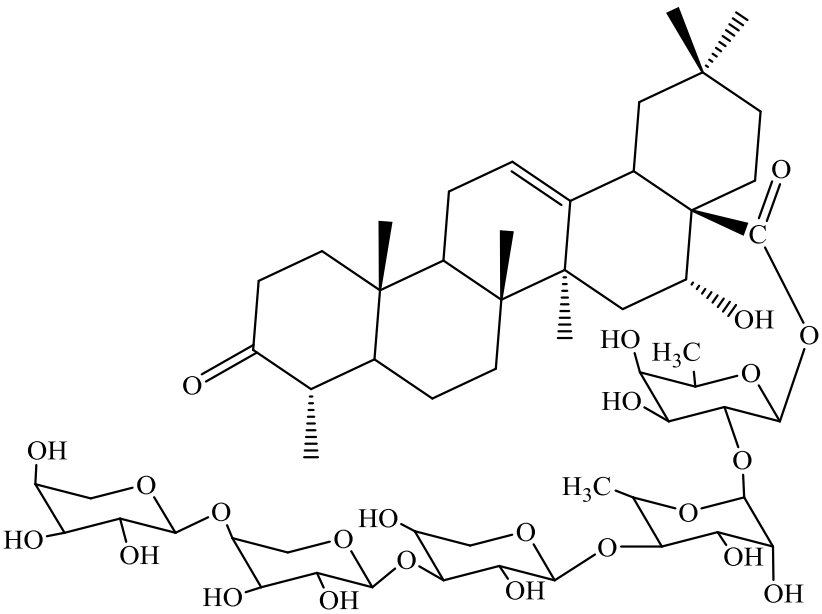

3

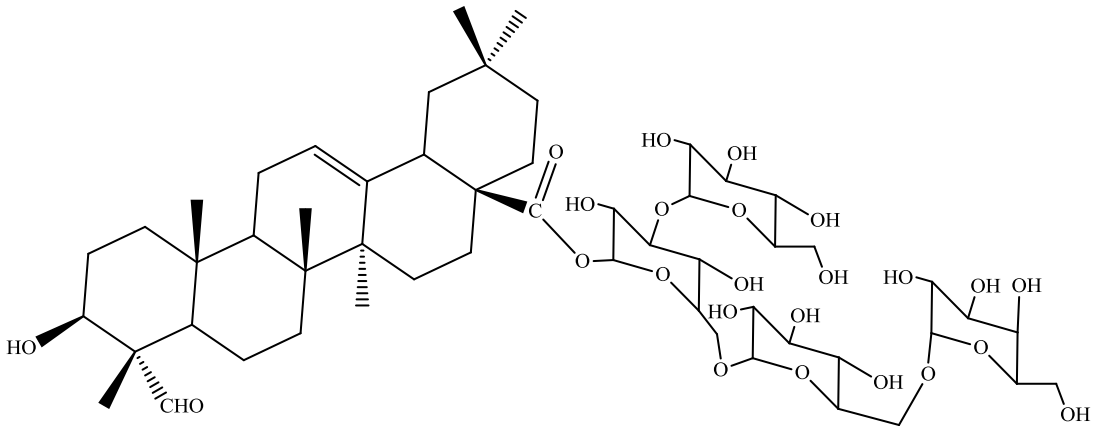

4

Figure 4. 10: Structure of triterpenoid saponins isolated from *Gypsophila oldhamiana*

On searching the literature, several studies have shown the potential of *Cynara* species extracts as antidiabetic agents. *C. scolymus* flowering heads were also found to be active in lowering post-prandial glycemia in normal and obese rats. The rats were treated with a purified extract of *C. scolymus* flowering heads (500–1500mg/kg) by gavage one hour prior to access to food. Glycemia was recorded 60, 120 and 360 min

after food presentation. The results showed a significant decrease of post-prandial glycemia in both rat strains (Fantini *et al.*, 2011). In another study, Ahmid (2011) reported the antidiabetic effects of an aqueous extract of *C. cornigera* root in alloxan-induced experimental diabetes mellitus. Hyperglycemia was induced by intraperitoneal injection of alloxan at a single dose of 150mg/kg. Diabetic rats received 1.5g/kg of *C. cornigera* extract and 10mg/kg of glibenclamide orally using an intra-gastric tube once daily for 30 days, 5 days after alloxan treatment. The results showed a significant ($p < 0.05$) decrease in blood glucose levels (from 330.80 ± 10.11mg dL^{-1} to 229.70 ± 7.94 and 195.50 ± 6.53mg dL^{-1} for the extract and glibenclamide, respectively).

On searching the literature, more than 300 natural products were found to exhibit PTP1B inhibitory activity reviewed by Jiang *et al.* (2012). Increased PTP1B activity results in the development of insulin resistance, leading to T2D (Kim *et al.*, 2016). Choi *et al*. (2014) reported the anti-PTP1B effects of luteolin and its derivatives, orientin and isoorientin. Luteolin was found to be the most potent PTP1B inhibitor, with an IC_{50} value of 6.70 ± 0.03µM, compared to the positive control ursolic acid (IC_{50} value of 8.20 ± 0.55µM). In addition, isoorientin exhibited inhibition of PTP1B, with an IC_{50} value of 24.54 ± 0.48µM, while orientin exhibited a much weaker PTP1B inhibition (57.11 ± 0.69µM) than luteolin. This correlates with the results of the current work, which demonstrated that luteolin separated from the methanol extract of *C. cyrenaica* stem showed an anti-PTP1B effect and produced a dose-dependent effect compared to the standard inhibitor TFMS.

The current study has opened up a new area of research particularly with respect to the methanolic extract from *C. rohlfsianum* and the pure compound CY1 isolated from it as well as CC10 from *C. cyrenaica.* This could be a new target for possible therapeutic applications for the treatment of T2D as their potential activity on α-glucosidase inhibition would be a key achievement of testing their activity on blood glucose in non-insulin-dependent diabetics in *in vivo* studies.

4.2 *In vitro* cytotoxicity assessment

The aim of this part of the chapter was to determine the cytotoxic effect of the crude and isolated compounds from *C. cyrenaica* and *C. rohlfsianum* against A375, PANC-1, and HeLa cancer cell lines as well as their effects on a normal cell line (PNT2). These aims were met through the use of two different assays, AlamarBlue® and

SYTOX® Green, based on the detection of metabolic activity and membrane integrity of the cell lines, respectively, following treatment with the compounds.

4.2.1 Cytotoxicity screen of crude extracts and isolated compounds from C. cyrenaica and C. rohlfsianum on cell viability of A375, HeLa, and PANC-1 cell lines using an AlamarBlue® assay

Samples that caused a decrease of cell metabolic activity to less than 50% was considered to be cytotoxic and the concentration-dependent inhibition (IC_{50}) of such samples was then calculated. Staurosporin (5µM) was used as a positive control and showed cytotoxicity of 13.2 %, 28.9 % and 25.4 % for A375, HeLa and PANC-1, respectively. Several tumour cell lines are sensitive to staurosporine-induced apoptosis (Nakano and Omura, 2009; Belmokhtar *et al.*, 2001) and is a potent protein kinase inhibitor (Yoshizawa *et al.*, 1990).

In addition, the effect of DMSO on cell viability at the equivalent DMSO content in the wells for each cell line used was tested at different percentages starting at 0.02% to 2.5 % (Figure 4.11), although it is well known that DMSO is toxic to cells, the actual percent varies from one cell line to another.

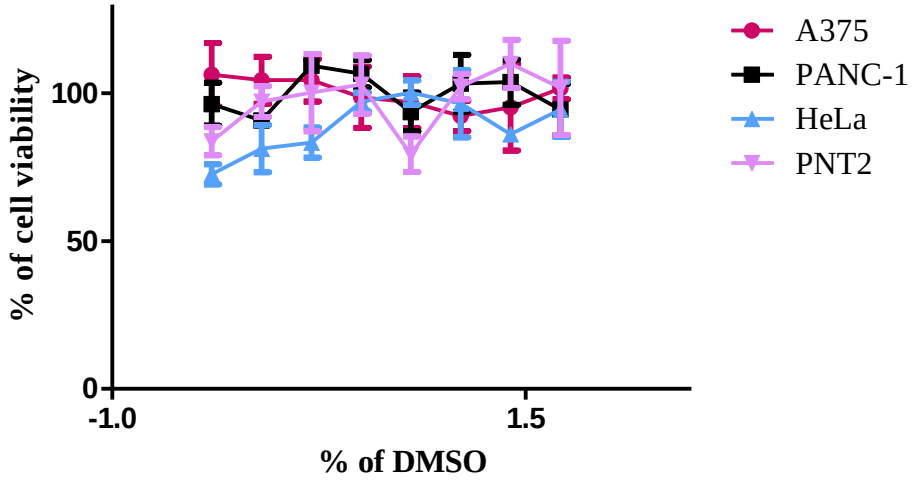

Figure 4. 11: Effect of DMSO on cell metabolic activity at the equivalent DMSO content in the wells for each cell line used. Cells were prepared $1x10^5$ cells/ml in Complete Medium, incubated for 24h. Followed by adding DMSO which was prepared at different percentages starting at 0.02% to 2.5 % then incubated for 24h at 37ºC in an atmosphere containing 5% CO_2. AlamarBlue® was used at 20µl in each well and incubated for 4h at 37ºC. A SpectraMax M5 plate reader was used to measure the fluorescence intensity at 560 - 590 nm.

Based on the results obtained from the cytotoxicity screen (Table 4.1), only CHH CEH, CER and CEL crude extracts from *C. cyrenaica* showed cytotoxic effects against A375 cells at 25µg/ml. For *C. rohlfsianum*, only CYMT extract showed cytotoxicity against A375 cells in a concentration-dependent manner with an IC_{50} value of 6.35 ± 1.09µg/ml. Among the tested compounds, CC5, CC9 and CC12 showed cytotoxicity against A375 cells with IC_{50} values of 16.53 ± 1.10, 64.76 ± 1.69 and 43.55 ± 1.63µM, respectively. CY1 also displayed concentration-dependent cytotoxicity with an IC_{50} value of 5.34 ± 1.22µM.

For the HeLa cell line, CHH, CEH, CER, CHS, CHL and CEL were found to be active at 25µg/ml, while amongst the *C. rohlfsianum* crude extracts only CYMT exhibited concentration-dependent inhibition with an IC_{50} value of 42.37 ± 1.13µg/ml. For the tested compounds, only CC1 and CC12 were active at the highest concentration of 58.6 and 69µM, respectively whereas CC5, CC9 and CY1 produced IC_{50} values of 31.24 ± 1.62, 12.25± 1.07 and 3.94 ± 1.23µM, respectively.

For the cytotoxicity screen against the PANC-1 cell line, CHH, CEH, CER, CHS, CES, CEL and CYMT showed concentration-dependent inhibition with IC_{50} values of 11.00 ± 1.15, 11.07 ± 1.07, 2.73 ± 1.18, 7.97 ± 1.12, 1.40 ± 1.87, 0.004 ± 1.02 and 4.19 ± 1.11µg/ml, respectively. Among the tested compounds, CC13 (novel compound) was found to be active at the highest concentration of 82.2µM and the quantity of this compound was not enough to carry out more studies. CC5, CC9, CC12 and CY1 exhibited IC_{50} values of 4.70 ± 1.06, 40.34 ± 1.42, 24.43 ± 1.32 and 3.93 ± 1.10µM, respectively.

For the PNT2 cell line, CER, CYMT and CES crude extracts in particular were found to be toxic to normal cells with IC_{50} values of 3.79 ± 1.98, 3.16 ± 1.08 and 9.76 ±1.26 µg/ml, respectively. This is could be linked to presence of sesquiterpene lactones - CC5 in CER, CC12 in CES and saponin CY1 in CYMT which also showed cytotoxic effects against the normal cells with IC_{50} values of 43.16 ± 1.04, 40.51 ± 1.9 and 2.62 ± 1.07µM, respectively. In addition, CHH, CEH, CHS, and CHL crude extracts were also found to be toxic to normal cells with various ranges of IC_{50} (Table 4.1).

Table 4. 1: Summary of the cytotoxicity effects (IC_{50} values) of crude extracts and their constituents from *C. cyrenaica and C. rohlfsianum*.

Sample code	A375 cells IC_{50} (µg/ml), n=3	HeLa cells IC_{50} (µg/ml), n=3	PANC-1 cells IC_{50} (µg/ml), n=3	PNT2 cells IC_{50} (µg/ml), n=3
CHH	ND	ND	11.00 ± 1.15	12.80 ± 1.32
CEH	ND	ND	11.07 ± 1.07	4.57 ±1.43
CMH	NA	NA	NA	NA
CHR	NA	NA	NA	NA
CER	ND	ND	2.73 ± 1.18	3.79 ± 1.98
CMR	NA	NA	NA	NA
CHS	NA	ND	7.97± 1.12	13.73 ±1.5
CES	NA	NA	1.40 ± 1.87	9.76 ±1.26
CMS	NA	NA	NA	NA
CHL	NA	ND	ND	10.71 ± 1.30
CEL	ND	ND	0.004 ± 1.02	ND
CML	NA	NA	NA	NA
CYHT	NA	NA	NA	NA
CYET	NA	NA	NA	ND
CYMT	6.35 ± 1.09	42.37 ± 1.13	4.19 ±1.11	3.16 ± 1.08
		IC_{50} (µM), n=3		
CC1	NA	ND	NA	NA
CC5	16.53 ± 1.10	31.24 ± 1.62	4.70 ± 1.06	43.16 ± 1.04
CC7	NA	NA	NA	NA
CC8	NA	NA	NA	NA
CC9	64.76 ± 1.69	12.25 ± 1.07	40.34 ± 1.42	NA
CC10	NA	NA	NA	NA
CC12	43.55 ± 1.63	ND	24.43 ± 1.32	40.51 ± 1.9
CC13	NA	NA	ND	ND
CY1	5.34 ± 1.22	3.94 ± 1.23	3.93 ± 1.10	2.62 ± 1.07

NA: not active, ND: not determined (active only at highest concentration)
The highlighted compound showed selectivity to HeLa cells.

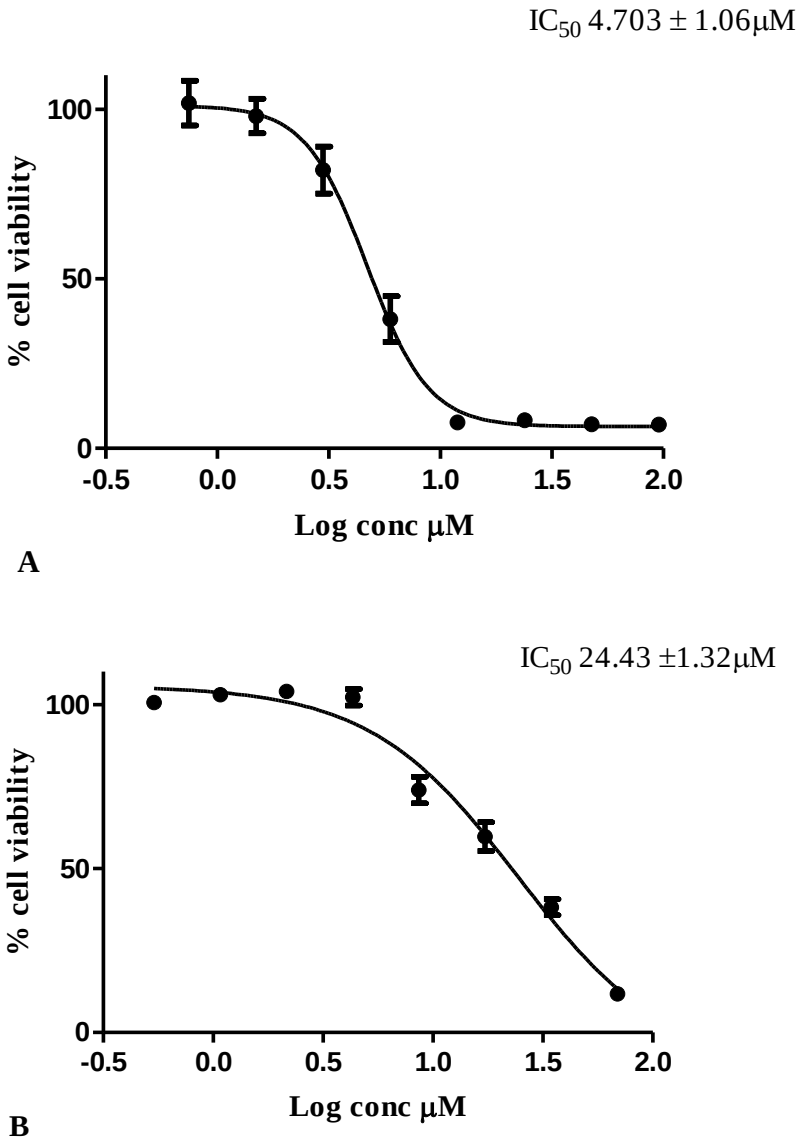

Figure 4. 12: Effect of compounds (A) CC5 and (B) CC12 on the metabolic activity of PANC-1 cells. Cells were seeded in a 96 well plate at a density of 1 x 10^5 cells per well in Complete Medium and incubated overnight at 37ºC in an atmosphere containing 5% CO_2. After which, CC5 and CC12 were prepared and added to the wells and incubated overnight. AlamarBlue® was added in each well and incubated for 4h at 37°C. The fluorescence intensity was measured at 560-590nm. Values represent the mean ± SEM of 3 values.

4.2.2 Effect of CC5 and CC12 on membrane integrity of PANC-1 and PNT2 cells line

Based on the results from the cytotoxicity screen using the AlamarBlue® assay, CC5 was the most active against PANC-1 cells and CC12 also showed marked inhibition activity against PANC-1 cancer cells and both produced dose-dependent inhibition (Figure 4.12). Hence, both were further tested for their activity on membrane integrity of PANC-1 cancer cells and PNT2 cells using a SYTOX®Green assay. As can be seen from Figures 4.13 **A** and **B**, CC5 showed dose-dependent inhibitory activity against PANC-1 cancer cells with IC_{50} value of 3.25 ± 1.14µM while CC12 showed inhibitory activity with IC_{50} value of 13.71 ± 1.08µM. For PNT2 cell, as can be seen from Figures 4.14 **A** and **B** both CC5 and CC12 appeared to have cytotoxic effect against PNT2 only at the highest concentrations of 95.5 and 47.8µM (CC5) and 69µM (CC12).

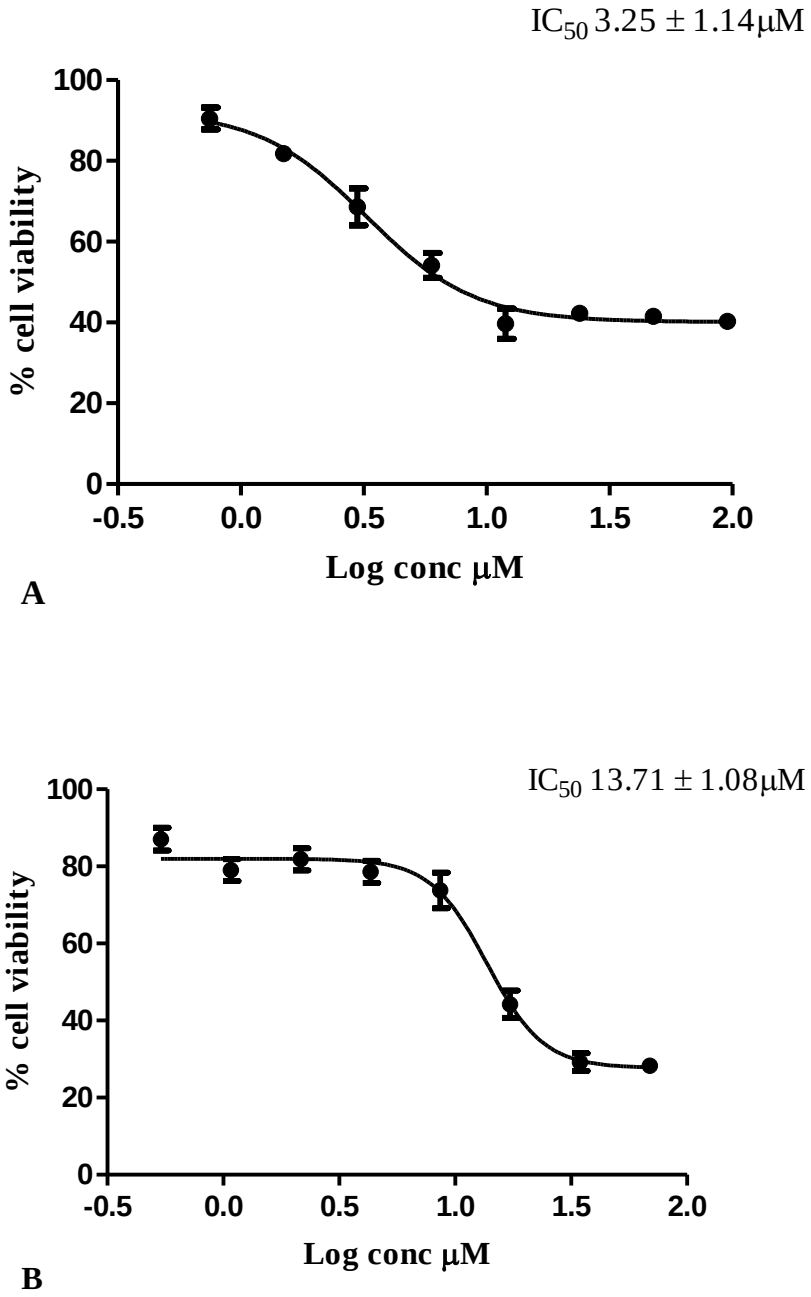

Figure 4. 13: Effect of compounds (A) CC5 and (B) CC12 on the membrane integrity of PANC-1 cells. Cells were seeded in a 96 well plate at a density of 1 x 10^5 cells per well in Complete Medium and incubated overnight at 37ºC in an atmosphere containing 5% CO_2. After which, CC5 and CC12 were prepared and added to the wells and incubated overnight. SYTOX®Green was used at a final concentration of 5μM in each well and incubated for 15 min at 37°C. The fluorescence intensity was measured at 485-535nm. Values represent the mean ± SEM of 3 values.

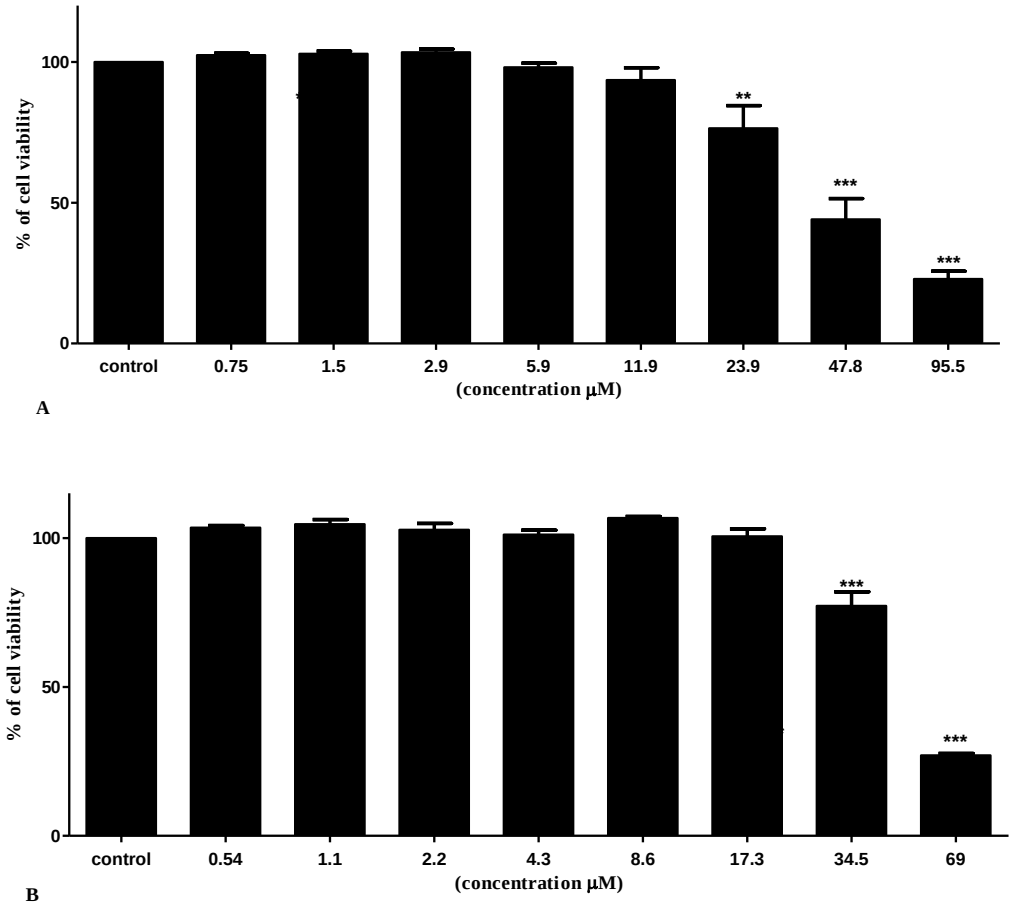

Figure 4. 14: Effect of compounds (A) CC5 and (B) CC12 on membrane integrity of PNT2 cells. Cells were seeded in a 96 well plate at a density of 1 x 10^5 cells per well in Complete Medium and incubated overnight at 37ºC in an atmosphere containing 5% CO_2. After which, CC5 and CC12 were prepared and added to the wells and incubated overnight. SYTOX®Green was used at a final concentration of 5µM in each well and incubated for 15 min at 37°C. The fluorescence intensity was measured at 485-535nm. Values represent the mean ± SEM of 3 values. Statistical analysis was carried out using one way ANOVA with Dunnett's post-hoc test. ** and *** indicate significant differences ($p < 0.01$, $p < 0.001$) compared with the untreated control.

Cytotoxicity assessment is a necessary step to determine the toxicity and effects of each sample on various cell lines and this is an important step for anticancer drug development. The results (section **4.2.1**) showed that the crude extracts and some of the isolated compounds from both plants had different ranges of cytotoxicity against cancer cell lines. Among the tested compounds only CC5, CC9, CC12 and CY1 were found to be active against all investigated cancer cell lines, however, CY1 was very toxic to normal cells with an IC_{50} value 2.62 ± 1.07µM. In addition, CC1 was also shown to be active only against HeLa cells with no toxic effect on normal cells, which suggests that this compound possesses selective activity against the HeLa cancer cell line. Dai *et al*. (2001), reported the cytotoxic effect of taraxasterol against HeLa cancer cells and revealed an IC_{50} 117 117.3 ± 4.6µg/ml using a MTT [3-(4, 5-dimethylthiazol-2-yl)-2, 5-diphenyltetrazolium bromide] assay which is based on reduction of MTT to the water insoluble pink formazan product, by mitochondrial dehydrogenases (Nemudzivhadi and Masoko, 2014). In the current study, the IC_{50} for CC1 was not determined as CC1 was active only at 58.6µM.

George *et al*. (2013) reported the cytotoxic effects of luteolin against A375 cancer cells and revealed an IC_{50} 115.1µM using a XTT (2, 3-bis[2-methoxy-4-nitro-5-sulfophenyl]-5-[(phenylamino) carbonyl]-2H-tetrazolium hydroxide) reagent which is metabolically reduced by mitochondrial dehydrogenase enzyme in viable cells to a water-soluble formazan orange product which is measured spectrophotometrically; this correlates with the current work for CC9 which also showed cytotoxicity against A375 cells with IC_{50} value of 64.76 ± 1.69µM.

Another study assessed the cytotoxicity of luteolin on human pancreatic carcinoma cells including PANC-1 using a MTT assay and the results showed that luteolin treatment significantly ($p < 0.05$) inhibited the growth of pancreatic carcinoma cells (Cai *et al.*, 2012). In this study, luteolin was assessed at four concentrations of 20, 40, 60 and 80µM at different intervals (12, 24, 48 and 72h). The study concluded that at a given duration of treatment, the number of viable cells decreased as the concentration of luteolin increased (Cai *et al.*, 2012). This correlates with the current study which demonstrated that CC9 showed cytotoxicity against PANC-1 cancer cells with an IC_{50} value of 40.34 ± 1.42µM.

Kim *et al*. (2014) also assessed the effects of luteolin on HeLa cells by MTT assay and the results showed significant reduction in the growth of HeLa cells with an IC_{50} value of 15.41µM. In addition, luteolin was previously tested against other cancer cell lines. Farid *et al.* (2015) showed that luteolin isolated from *Arum palaestinum* (Araceae) was significantly active against four human tumour cell lines with IC_{50} (µg/ml) values of – 9.98 Hep2 (epidermal carcinoma of the larynx), 16 HeLa (cervical cancer cells), 17.80 HepG2 (liver cancer) and 21.80 MCF7 (breast cancer), however, the cytotoxicity assay used in this study was a sulforhodamine-B (SRB) assay which is not the same as in the current study. SRB is a protein stain that binds to the amino groups of intracellular proteins. It consists of a bright pink aminoxanthrene dye with two sulphonic groups. Another study, demonstrated the cytotoxic effect of luteolin on HeLa cells with an IC_{50} value of 4.0µg/ml using a MTT assay (Mori *et al.*, 1988). This correlates with the result of the current work for CC9 which had inhibitory effects on HeLa cells and produced an IC_{50} value of 12.25 ± 1.07µM.

These studies revealed that luteolin (CC9) in the current work isolated from *C. cyrenaica* shows potential cytotoxicity on many cell lines. Lin *et al*. (2008) inferred that luteolin was also able to inhibit the proliferation of cancer cells derived from nearly all types of cancers.

In the current study, CY1 which is a type of triterpenoid saponin isolated from *C. rohlfsianum* and identified as 3-*O*-{β-D-xylopyranosyl-(1→2)-β-D-glucopyranosyl-(1→4)-[β-D-glucopyranosyl-(1→2)]-α-L-arabinopyranosyl}-cyclamiretin A and also called ardisiacrispin A (section **3.2.1.1**) showed potent cytotoxicity against all the cell lines investigated. On searching the literature another analogue of CY1 named ardisiacrispin B was active against many types of cancer cell lines. Li *et al*. (2008) assessed the cytotoxicity of a mixture of ardisiacrispin A and B against Bel-7402 (human hepatoma cells), KB (nasopharyngeal carcinoma cells), HeLa (uterine cervix carcinoma cells), SKOV-3 (ovarian carcinoma cells) , BGC- 823 (gastric carcinoma cells) , and MCF-7 (breast carcinoma cells) - the results showed that the mixture was potent towards all the investigated cell lines with IC_{50} (µg/ml) values – of 0.9 (Bel-7402), 2.0 (KB), 2.3 (HeLa) , 5.0 (SKOV-3), 6.2 (BGC-823), and 6.5 (MCF-7) (Li *et al*., 2008). This correlates with the current work for CY1 which was cytotoxic against HeLa cells with an IC_{50} value of 3.94 ± 1.23µM. It has also been reported that

ardisiacrispin A showed cytotoxicity against P388 (murine leukemia) cells with an IC_{50} value of 7.0µg/ml (Bloor and Qi, 1994). Another study assessed the cytotoxic activity of ardisiacrispin A on sarcoma XC (murine cancer cell line) with an ED50 value of 4.5µg/ml (Podolak *et al.*, 2007). Finally, another report examined ardisiacrispin B activity against HCT-8 (human ileocecal carcinoma), Bel7402 (human hepatocellular cancer), BGC-823 (stomach adenocarcinoma), A549 (human lung carcinoma), A2780 (ovary adenocarcinoma), and KETR3 (human renal carcinoma) using the MTT test. The results showed that ardisiacrispin B showed strong cytotoxicity against the investigated cell lines with IC_{50} (µg/ml) values – of 1.59 (HCT-8), 1.67 (Bel7402), 1.78 (BGC-823), 1.78 (A549), 2.05 (A2780), and 1.64 (KETR3) (Zheng *et al.*, 2008).

Of the sesquiterpene lactones CC5 and CC12, CC5 had not been studied before and CC12 is a novel compound. Both showed marked effects on all the cancer cell lines examined compared with the control (untreated cells). Numerous studies have reported the cytotoxic activities of sesquiterpene lactones against many cancer cell lines. Toyang *et al.* (2013) isolated two active sesquiterpenes (vernopicrin and vernomelitensin) from the leaves of *Vernonia guineensis* Benth. (Asteraceae) and both compounds demonstrated *in vitro* activity against ten human cancer cell lines - MDA-MB-231 and MCF-7 (breast), HCT-116 (colon), HL-60 (leukemia), A549 (lung), A375 (melanoma), OVCAR3 (ovarian), Mia-paca (pancreas) PC-3 and DU-145 (prostate) with IC_{50} values ranging from 0.35–2.04µM ($P < 0.05$) for vernopicrin and 0.13–1.5µM ($P < 0.05$) for vernomelitensin. Xie *et al.* (2007), reported cytotoxic sesquiterpene from *Inula cappa* named inulacappolide against HeLa cells with an IC_{50} value of 1.2µM**.** These results correlate with the current work for the sesquiterpene lactones CC5 and CC12 which also demonstrated cytotoxicity against A375, PANC-1 and HeLa cells.

Saúde-Guimarães *et al.* (2014) studied the cytotoxicity of sesquiterpene lactones (lychnopholide and eremantholide C) separated from *Lychnophora trichocarpha* Spreng. (Asteraceae). The isolated compounds were evaluated for their *in vitro* antitumor activity in the National Cancer Institute, USA (NCI, USA), against a panel of 52 human tumour cell lines of major human tumours derived from nine cancer types (leukemia, lung, colon, melanoma, CNS, ovarian, renal, prostate and breast cancers). The results revealed that lychnopholide demonstrated significant activity against 30

cell lines of seven cancer types with IC_{100} (total growth concentration inhibition) values between 0.41µM and 2.82µM. Eremantholide C showed significant activity against 30 cell lines of eight cancer types with IC_{100} values between 21.40µM and 53.70µM. Lychnopholide showed values of lethal concentration 50 % (LC_{50}) for 30 human tumour cell lines between 0.72 and 10.00µM, whereas eremantholide C presented values of LC_{50} for 21 human tumour cell lines between 52.50 and 91.20µM. The current work revealed that compounds CC5 and CC12 were found to possess cytotoxic activity towards all examined cell lines. Hence, from the results of the current work it is thought that the structural differences of the sesquiterpene lactones could affect the cytotoxic activity. Numerous studies reported the importance and the correlation of the α-methylene-γ-lactone (αMγL) group with the cytotoxicity activity of sesquiterpene lactones (Chadwick *et al.*, 2013; Maldonado *et al.*, 2014; Dey *et al.*, 2016). Dey *et al*. (2016) reported that, an α-methylene-γ-lactone ring and an epoxide group are able to interact with the nucleophilic sites of biological molecules particularly with cysteine thiol groups in a michael addition reaction, and this leads to depletion of thiols and induces oxidative stress. Hence, this could correlate with the cytotoxicity findings of the current work for CC5 as it has an epoxide group (section **3.1.2.2**) and CC12 which has a αMγL group (section **3.1.4.4**).

4.3 Effects of CC5 and CC12 on the dissemination of PANC-1 cells

Based on the results from the cytotoxicity screen assays (section **4.2.1**), CC5 and CC12 were selected for further studies as they showed the most cytotoxic effects on PANC-1 cancer cells compared with the other cell lines. CC5 had not been studied before and in the current study showed inhibitory effects in a dose-dependent manner, while CC12 the novel compound showed marked cytotoxic effects against PANC-1 cells compared with the control (untreated cells). In addition, both were the most abundant compounds in *C. cyrenaica*. Furthermore, the core structure of these compounds as sesquiterpene lactone type underscores the importance of investigating their action against the adhesion, migration and invasion (processes of metastasis) in the PANC-1 cancer cell line. PANC-1 cells selected for subsequent experiments as the metastatic potential of this cell line needs to be studied and to understand the properties of cancer cell adhesion which basically determines the dissemination potential of cancer cells and effects the tumour growth. Pancreatic cancer is known to develop chemoresistance and very few approved chemotherapeutics are available (Ma *et al.*, 2011) and early metastasis is a hallmark of pancreatic cancer and responsible for 90% of the deaths

(Ren *et al*., 2011). On searching the literature, the apoptotic morphology of PANC-1 cancer cells was observed as cell shrinkage (Ma *et al*., 2011) and granular, punctate and bubble- like morphologies (Ren *et al.*, 2011). Hence, the findings from the current work (Figures 4.15 and 4.16) showed the cytotoxic effects of CC5 and CC12 on PANC-1 cancer cells morphology as shrinkage in the cells and granular like morphologies was observed. As a result of this, these observations suggest that CC5 and CC12 induced apoptotic effect on PANC-1 cells.

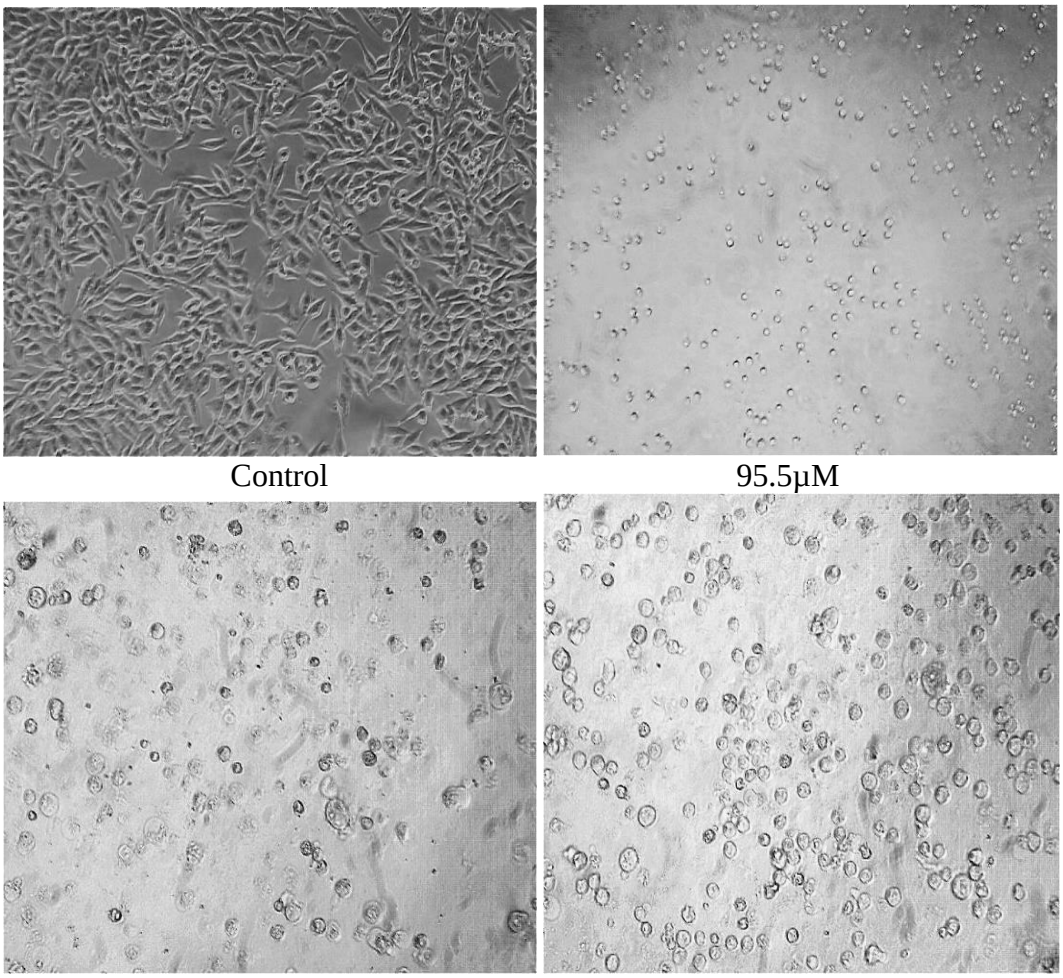

Figure 4. 15: Effect of different concentrations of CC5 on PANC-1 cells morphology. Objective lens X10

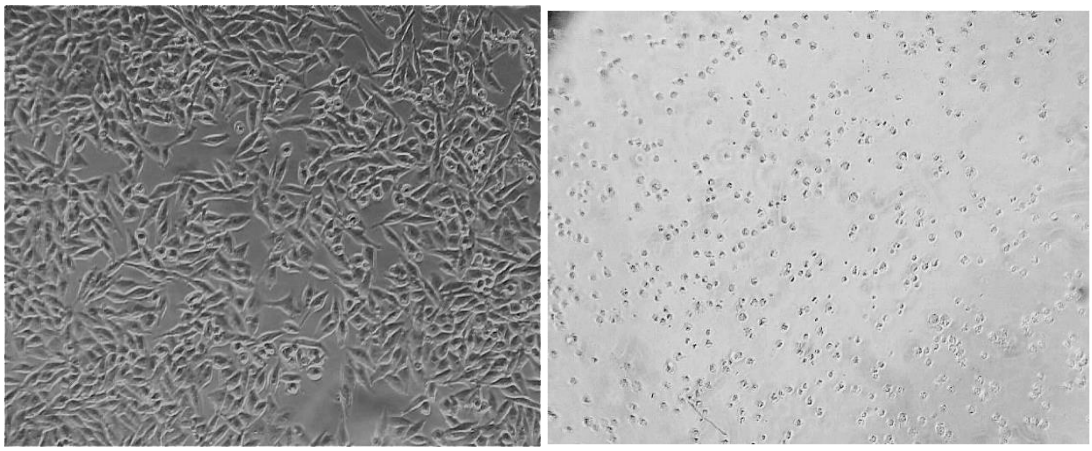

Control 69µM

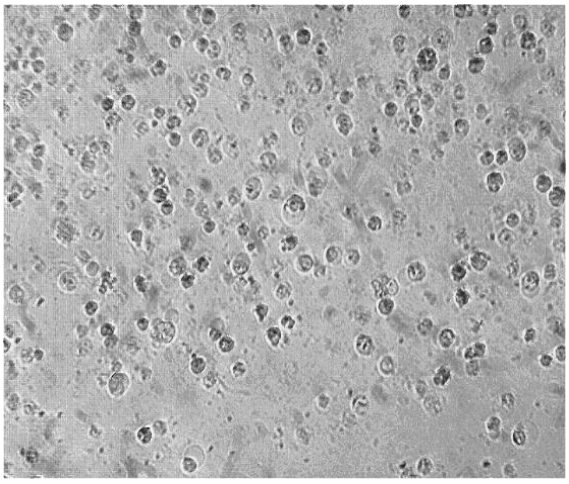

34.5µM

Figure 4. 16: Effect of different concentrations of CC12 on PANC-1 cells morphology. Objective lens X10

4.3.1 Effects of CC5 and CC12 on adhesion of PANC-1 cells to collagen IV, fibronectin and poly-L-lysine

This experiment was carried out to assess the effect of CC5 and CC12 on adhesion of PANC-1 cancer cells and to investigate whether CC5 and CC12 is specific for binding to the integrin family of adhesion receptors or not. The current work utilised the extra cellular matrix (ECM) such as fibronectin and collagen IV and a non-integrin dependent matrix poly-L-lysine in the presence of BSA as a negative control. As can be seen from Figure 4.17 **A**, CC5 had activity against the adhesion of PANC-1 cells on collagen IV, but not fibronectin and poly-L-lysine (Figures 4.18 **A** and 4.19 **A**), unlike C12 which had a significant ($p < 0.05$, $p < 0.01$, $p < 0.001$) effect on adhesion to all the substrates (Figures 4.17 **B**, 4.18 **B** and 4.19 **B**).

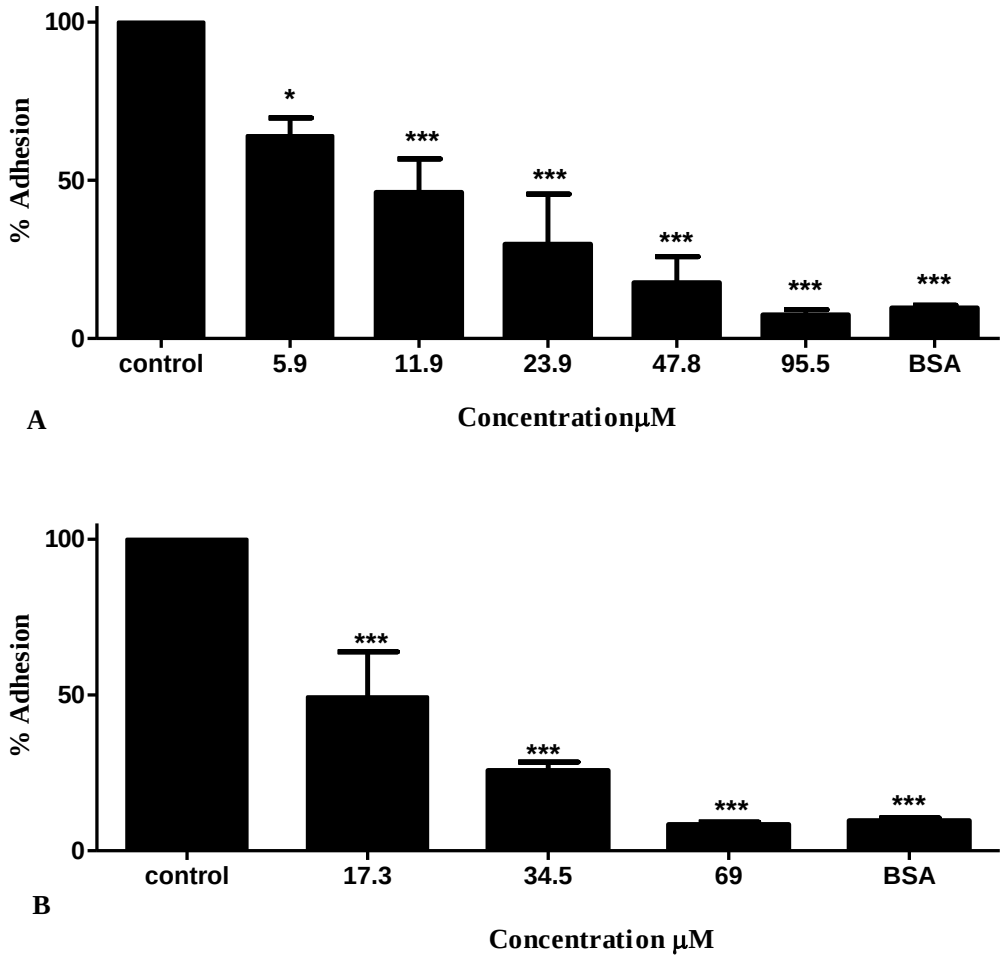

Figure 4. 17: Effect of (A) CC5 and (B) CC12 on adhesion of PANC-1 cells to collagen IV using a Cytoselect^{TM} 48-well collagen IV assay. The cells were adjusted to $1x10^6$ cells /ml in serum free DMEM medium and seeded onto the collagen IV pre-coated plate, incubated for 2h with various concentrations of CC5 and CC12 at 37ºC in an atmosphere containing 5% CO_2, then absorbance readings were taken at 560 nm. The values are means ± SEM of 3 values. Statistical analysis using one way ANOVA with Dunnett's post-hoc test. * and *** indicates significant differences ($p < 0.05$, $p < 0.001$) compared with the control.

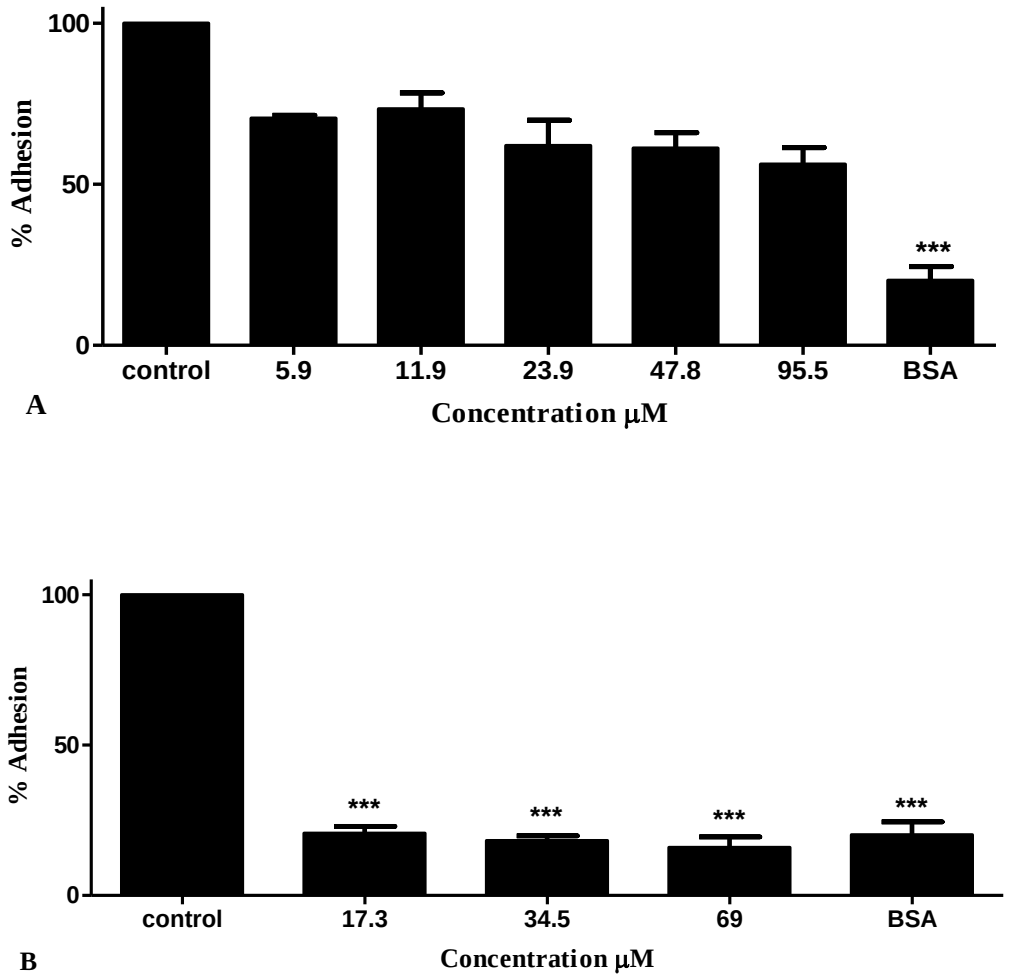

Figure 4. 18: Effect of (A) CC5 and (B) CC12 on adhesion of PANC-1 cells to fibronectin using a Cytoselect^{TM} 48-well fibronectin. The cells were adjusted to $1x10^6$ cells /ml in serum free DMEM medium and seeded onto fibronectin pre-coated plate, incubated for 2h with various concentrations of CC5 and CC12 at 37ºC in an atmosphere containing 5% CO_2, then absorbance readings were taken at 560 nm. The values are means ± SEM of 3 values. Statistical analysis using one way ANOVA with Dunnett's post-hoc test. *** indicates significant differences ($p < 0.001$) compared with the control.

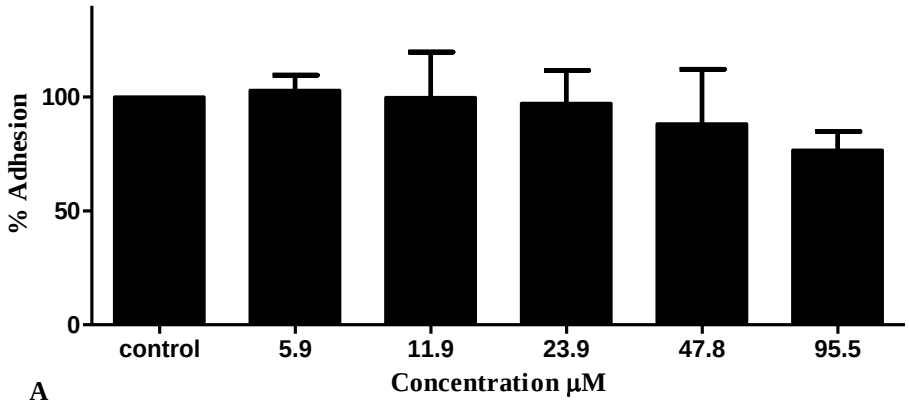

A

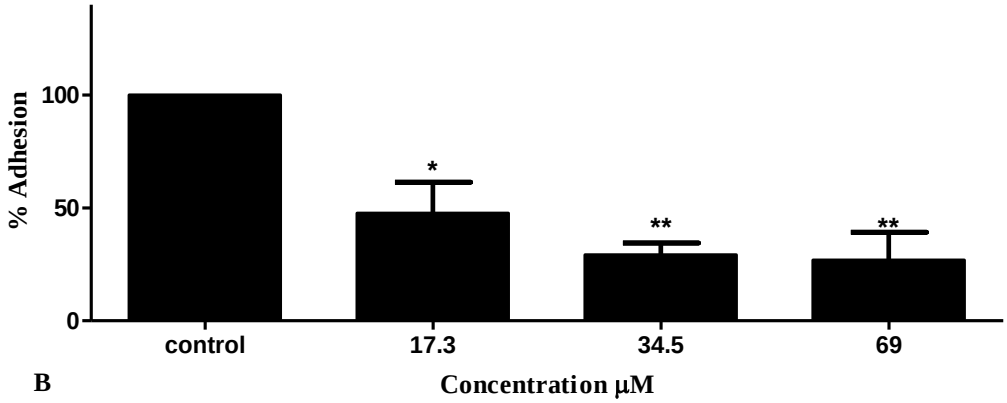

B

Figure 4. 19: Effect of (A) CC5 and (B) CC12 on adhesion of PANC-1 cells to poly-L-lysine. The cells were adjusted to $5x10^5$ cells /ml in serum free DMEM medium and seeded onto poly-L-lysine pre-coated plate, incubated for 2h with various concentrations of CC5 and CC12 at 37ºC in an atmosphere containing 5% CO_2, then fluorescence readings were taken at 485 - 538 nm. The values are means ± SEM of 3 values. Statistical analysis using one way ANOVA with Dunnett's post test. * and ** indicates significant differences ($p < 0.05$, $p < 0.01$) compared with the control.

4.3.2 Effects of CC5 and CC12 on migration and invasion of PANC-1 cells

To further clarify the actions of CC5 and CC12 on PANC-1 cells, migration and invasion were examined at non-toxic concentrations to normal cells in the presence of Latrunculin A (3µM) as a positive antimigratory control. As can be seen from Figure 4.20 **A** and **B** both CC5 and CC12 have inhibited the migration of PANC-1 cells, however, CC12 was found to be more active than CC5 and showed inhibition of migration by 73.31% compared with the control (untreated cells). For invasion, both CC5 and CC12 had inhibited invasion across the basement membrane. CC5 at 11.9 showed significant ($p < 0.001$) inhibition of invasion by 70.36 % compared with the control (untreated cells). CC12 at 34.5µM showed inhibition of invasion by 74.7% compared with the control.

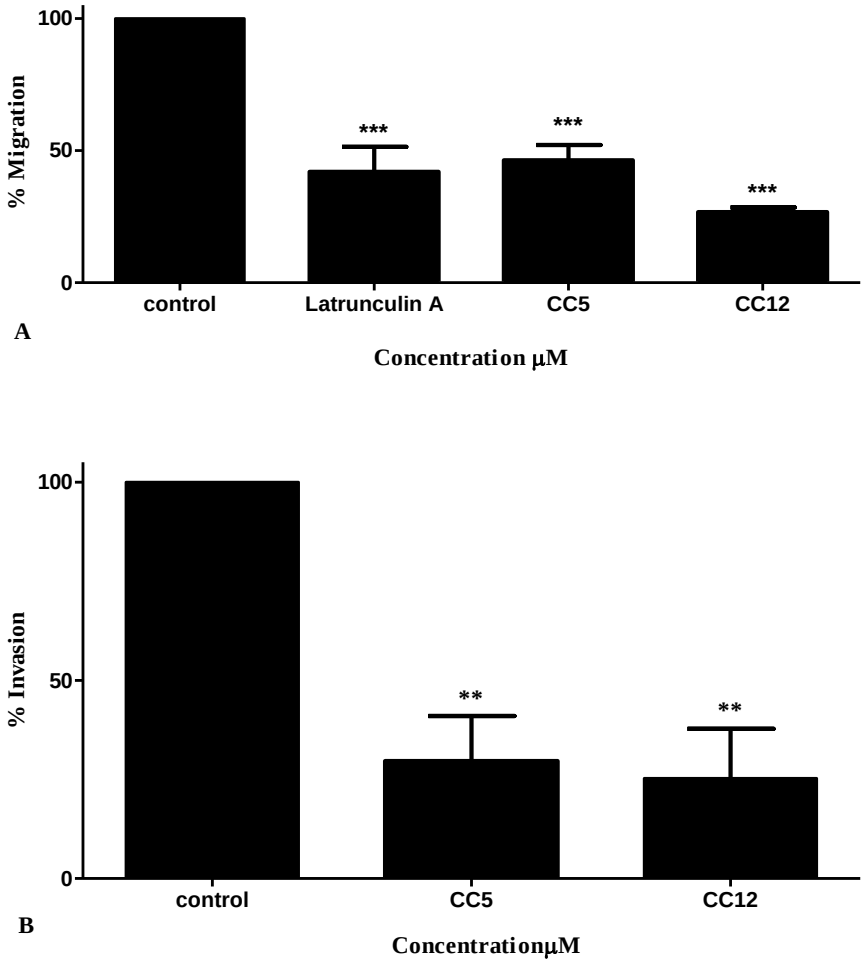

Figure 4. 20: Effect of CC5 and CC12 on the migration (A) and invasion (B) of PANC-1 cells using a InnoCyte^{TM} Cell Migration and Invasion Assay, 24-well plate. Cells were trypsinised and adjusted to $1x10^6$ cells/ml in serum free DMEM medium with CC5 at 11.9µM and CC12 at 34.5µM. Then the cells were incubated for 24h at 37ºC in an atmosphere containing 5% CO_2, then fluorescence readings were taken at 485-538nm. The data were analysed by Dunnett post-test. ** and *** indicates significant differences ($p < 0.01$, $p < 0.001$) compared with the control.

Metastases are the cause of 90% of human cancer deaths since the ability of a cancer cell to undergo migration and invasion allows tumour cells to escape from the primary tumour mass and spread to other parts of the body (Velez *et al.*, 2012). Adhesion of cancer cells is mediated by the interaction of the ECM with cell surface molecules. Deer *et al.* (2010) reported that PANC-1 cancer cells have the affinity to bind to fibronectin and collagen IV, that are molecules found in connective tissues and basement membranes. Integrins act as adhesion receptors and play important roles in cell adhesion and activate many intracellular signalling pathways, that regulate diverse processes including adhesion, migration and tumour invasion (Thomas *et al.*, 2006; Hynes, 2002). Integrins mediate cell to cell and cell to ECM interactions (Schaffner *et al.*, 2013; Niu and Li, 2017). The results obtained from this work suggest that CC5 is specific for binding to the integrin family of adhesion receptors (collagen IV), whereas CC12 is not specific for certain integrins and ECM.

The specific integrins mediating PANC-1 cells interactions with type IV collagen and fibronectin, have not been determined in the current work because of the limitation of time. On searching the literature, Grzesiak and Bouvet (2008) reported that β1 integrin-mediated cell adhesion to fibronectin and type IV collagen. However, cancer cells undergo changes in integrin expression all the time during tumour migration and growth (Maschler *et al.*, 2005). Therefore, future work could be focussed on the study of the integrin expression of PANC-1 cancer cells.

In the current work, both sesquiterpene CC5 and CC12 were found to have inhibitory effect on migration and invasion.

On searching the literature, there are numerous reports about the role of matrix metalloproteinases (MMPs) in the progression of pancreatic cancer. MMPs, are responsible for remodelling the ECM and such processes are necessary for a vast range of physiological events, such as wound repair, organismal growth and development. However, the increased expression of MMPs leads to degradation of ECM which correlates to increased cancer cell spread and an increase in tumour size as the cancer cells require integrins for adhesion and MMPs for proteolysis (Cathcart *et al.*, 2015; Said *et al.*, 2014). MMPs are known as significant enhancers of cancer cell migration and invasion (Haage and Schneider, 2014; Bloomston *et al.*, 2002). It has been reported that in pancreatic cancer, MMP-2 and MMP-9 show high levels of

expression, particularly MMP-2 and they play an important role in the pathogenesis of pancreatic cancer (Bloomston *et al.*, 2002). It has been reported that, in many human solid tumours, MMP-2 and MMP-9 are markedly overexpressed during the invasive and metastatic phases and they facilitate invasion and migration by causing degradation of collagen and the fibronectin matrix (Tabata *et al.*, 2015; Ribatti *et al.*, 2004). These enzymes were found to regulate various physiological processes and signalling events, and therefore they represent key players in the molecular communication between tumour and stroma (Kessenbrock *et al.*, 2010). Kenny and Lengyel (2009) demonstrated that the mechanism by which MMP-2 facilitates early adhesion and invasion involves cleavage of multiple ECMs into smaller fragments that serve as better attachment sites.

It has been reported that natural products play a significant role in cancer treatment, since the compounds from natural resources have provided many lead structures which act as templates for producing novel drugs with enhanced anticancer potential (Yue *et al.*, 2015). The current work examined the effect of sesquiterpene lactones CC5 and CC12 isolated from *C. cyrenaica* against PANC-1 cancer cells, and both have showed marked inhibitory effect on cell viability and metastasis. There have been numerous studies reporting that sesquiterpene lactones have exhibited anticancer effects via prevention of metastasis (Jain *et al.*, 2016). Some of these include artemisinin isolated from *Artemisia annua* (Crespo-Ortiz and Wei, 2011) and alantolactone separated from *Inula helenium* (Compositae) that affected HeLa and PANC-1 cells (Rasul *et al.*, 2013). Another study reported that the dried roots of *Saussurea lappa* (Compositae), called costus roots, are used in the traditional system of medicine for cancer treatment (Robinson *et al.*, 2008).

Singh *et al.* (2017) and Pandey *et al.* (2007) inferred that sesquiterpene lactones were the major phytoconstituents of *Saussurea lappa*. Sarangi (2014) reported that sesquiterpenes and costunolide dehydrocostuslactone, isolated from *S.* lappa inhibited the growth and spread of breast cancer. In support of this, Tabata *et al.* (2015) reported that sesquiterpene lactones (dehydrocostus lactone and costunolide) isolated from *S. lappa* inhibited migration and invasion in neuroblastoma cells. This study also revealed that dehydrocostus lactone and costunolide demonstrated marked downregulation of the expression of MMP-2 in the cancer cells after 48h of application. The results indicate that the downregulation of MMP-2 expression by

these compounds may be related to the inhibition of the migration and invasion characteristics of the cells. Kim *et al.* (2014) investigated the inhibitory effect of the dried root of *S. lappa* on MMP-9 expression in breast cancer cells and the results showed that the plant extract produced a potent inhibition of MMP-9 expression. Parthenolide (PTL), a sesquiterpene lactone isolated from *Tanacetum parthenium*, commonly known as feverfew, has been investigated for the treatment of several cancers, including pancreatic cancer (Karmakar *et al.*, 2015). Another study, reported that PTL produced apoptosis of CRC (human colorectal cancer) and showed marked inhibition of migration and invasion-related matrix metalloproteinases expression such as MMP-2 and MMP-9 (Liu *et al.*, 2017).

It is clear that the current study has opened up a new area of research particularly for CC5 and CC12, which could provide new targets for possible therapeutic applications for the treatment of cancer as CC5 and the novel compound CC12 have showed marked inhibitory effects on adhesion, migration and invasion of PANC-1 cells. However, the mechanism of action is still unknown. The current work suggests that further work could focus on the study of the effect of CC5 on integrins expressed by PANC-1 and the effect on the process of metastasis of PANC-1 cells and effect of CC12 on MMP-2 overexpression in PANC-1 cancer cells.

CHAPTER V
5. CONCLUSIONS AND FUTURE WORK

5.1 Summary of key findings

The present work aimed to carry out a phytochemical investigation on the Libyan plants, *C. cyrenaica and C. rohlfsianum.* Soxhlet extraction of the plants materials; flower heads, root, leaf and stem of *C. cyrenaica* and tuber of *C. rohlfsianum* were carried out using solvents of increasing polarity. The fractionation of the resulting extracts and the subsequent purification using different chromatographic techniques led to the isolation of various types of compounds such as triterpene, flavonoid, sesquiterpene lactones and saponin. These types of natural components particularly sesquiterpene lactones in *C. cyrenaica* and saponin in *C. rohlfsianum* were expected to be found in these plants as a result of a literature search for other *Cynara* and *Cyclamen* species.

A total 13 compounds were separated from *C. cyrenaica*, from different plant parts, two of them were identified as novel compounds of sesquiterpene lactones type CC12 and CC13 and they were the most abundant compounds in the plant, and their given names were 3β-hydroxy-8α-[(S)-4-hydroxy-3-methylbutanyloxy]-guaian-4(15), 10(14), 11(13)-trien-1α, 5α, 7α, 6βH-12, 6-olide and 11,13 epoxy-guaian-4(15), 10(14)-dien-1α, 5α, 7α, 6βH-12, 6-olide -3-yl acetate, respectively. In addition, some known compounds including triterpenes such as taraxasterol (CC1) and pseudotaraxasterol (CC4), sesquiterpene lactones such as ll, 13-epoxysolstitialin (CC5), flavonoids - apigenin (CC3), luteolin-7-*O*-β-D-glucopyranoside (CC7) and luteolin (CC9), as well as catechin7-*O*-gallate (CC10) which was isolated for the first time from *Cynara*. Caffeoylquinic acids such as 1, 3 -dicaffeoylquinic acid (CC8) and a sterol daucosterol (CC2), a simple phenolic compound - ferulic acid (CC6) and the simple compound 1-monoacetyl glycerol (CC11) were separated from *C. cyrenaica*. Fractionation of *C. rohlfsianum* tuber methanolic extract (CYMT) led to the isolation of triterpenoid saponin (CY1).

In the current work some of the isolated compounds provided some promising results regarding *in vitro* antidiabetic activity and cytotoxicity followed by anti-metastasis activity. The *in vitro* antidiabetic screening of the plants showed that CC10 and CYMT along with the pure compound CY1 isolated from it have showed potent antidiabetic activity on α-glucosidase and produced dose dependent inhibition. These findings suggest that the antidiabetic activity of *Cynara* species extracts could be attributed to

the presence of CC10, as numerous studies reported the effect of catechin gallate as a natural α-glucosidase inhibitor. In addition, the antidiabetic potential of CYMT and CY1 in the current work provides scientific support for the traditional use of *C. rohlfsianum* as antidiabetic. For α-amylase none of the extracts or separated compounds from both plants were considered to be active on α-amylase. For PTP1B, only CC9 showed inhibition activity in a dose-dependent manner.

The extracts along with the screened compounds showed varying degrees of cytotoxicity on the examined cell lines. Among the compounds, CC1 showed selective inhibition against HeLa cells. CC13 the novel compound showed cytotoxic effects on PANC-1 cells at the highest concentration (82.2 µM) and the small quantity of this compound prevented further studies from being carried out. CC5, CC9 and the novel compound CC12 were active against all the examined cancer cells, however, CC5 and CC12 were potent against PANC-1. In addition, CYMT and the pure compound isolated from it CY1 also showed potent cytotoxic effects against all the examined cancer cells, hence the effectiveness of the crude extract CYMT against all cancer cells was suggested to be mainly attributable to presence of CY1. However, both were very toxic to PNT2 cells. Both sesquiterpene CC5 and CC12 were found to have inhibitory effects on migration and invasion of potential metastastatic PANC-1 cells, however, the mechanism of their action is still unknown.

Overall, this work revealed new *C. cyrenaica* constituents which possess biological activity and confirmed the presence of some interesting compounds which could be employed as lead compounds for new drug discovery. In addition, this work demonstrated the compound that is potentially responsible for antidiabetic effect of *C. rohlfsianum* and the current work revealed the powerful of luteolin (CC9) as an antidiabetic and cytotoxic agent against all the examined cancer cells and could also be considered as candidates for chemotherapeutic agents.

5.2 Recommendations for future work

- This project proved that there is still a lot more to be discovered about the plants, their constituents and their use. Some of the crude extracts possessed strong biological activity and should be further fractionated and purified such as CEL has showed strong cytotoxic effect against PANC-1 with IC_{50} value of 0.004 ± 1.02 µg/ml.

- CYHT and CYET were not fractionated due to limitations in time although these crude extracts were not active against the examined cells, it is recommended that these should be fractionated and studied against other cancer cell lines.

- For the isolated pure compounds CC10 and CY1, further investigations are needed to study structure-activity-relationship in relation to anti-diabetic activity in order to determine the effect of changes in functional groups on their biological activity. It is recommended to investigate the effects of CC10, CYMT and CY1 *in vivo.*

- It is recommended that further investigation is needed to study structure-activity-relationship and correlation with cytotoxicity of CC5 and CC12.

- Future work - could be focussed on the study of the integrin expression of PANC-1 cancer cells and to determine the integrins used by the cells to adhere to different ECM proteins. In addition, further work should examine the ability of CC5 on integrin inhibition and CC12 on MMPs inhibition.

REFERENCES

Akihisa, T., Yasukawa, K., Oinuma, H., Kasahara, Y., Yamanouchi, S., Takido, M., Kumaki, K. and Tamura, T. (1996) 'Triterpene alcohols from the flowers of compositae and their anti-inflammatory effects', *Phytochemistry,* 43(6), pp. 1255-1260.

Alghazeer, R., El-Saltani, H., Saleh, N. A., Al-Najjar, A., Naili, M. B., Hebail, F. and El-Deeb, H. (2012) 'Antioxidant and antimicrobial activities of *Cynara scolymus* L. rhizomes', *Modern Applied Science,* 6(7), pp. 54-63.

Alonso-Castro, A. J., Villarreal, M. L., Salazar-Olivo, L. A., Gomez-Sanchez, M., Dominguez, F. and Garcia-Carranca, A. (2011) 'Mexican medicinal plants used for cancer treatment: pharmacological, phytochemical and ethnobotanical studies', *Journal of ethnopharmacology,* 133(3), pp. 945-972.

Altunkeyik, H., Gulcemal, D., Masullo, M., Alankus-Caliskan, O., Piacente, S. and Karayildirim, T. (2012) 'Triterpene saponins from *Cyclamen hederifolium*', *Phytochemistry,* 73(1), pp. 127-133.

Arulselvan, P., Ghofar, H. a. A., Karthivashan, G., Halim, M. F. A., Ghafar, M. S. A. and Fakurazi, S. (2014) 'Antidiabetic therapeutics from natural source: A systematic review', *Biomedicine & Preventive Nutrition,* 4(4), pp. 607-617.

Belmokhtar, C. A., Hillion, J. and Segal-Bendirdjian, E. (2001) 'Staurosporine induces apoptosis through both caspase-dependent and caspase-independent mechanisms', *Oncogene,* 20(26), pp. 3354-3362.

Ben Salem, M., Affes, H., Athmouni, K., Ksouda, K., Dhouibi, R., Sahnoun, Z., Hammami, S. and Zeghal, K. M. (2017) 'Chemicals compositions, antioxidant and anti-inflammatory activity of *Cynara scolymus* leaves extracts, and analysis of major bioactive polyphenols by HPLC', *Evidence-Based Complementary and Alternative Medicine,* 2017(4), pp.1-14

Bloomston, M., Zervos, E. E. and Rosemurgy, A. S., 2nd (2002) 'Matrix metalloproteinases and their role in pancreatic cancer: a review of preclinical studies and clinical trials', *Ann Surg Oncol,* 9(7), pp. 668-674.

Bloor, S. J. and Qi, L. (1994) 'Cytotoxic saponins from new zealand *Myrsine* species', *Journal of natural products,* 57(10), pp. 1354-1360.

Cai, X., Lu, W., Ye, T., Lu, M., Wang, J., Huo, J., Qian, S., Wang, X. and Cao, P. (2012) 'The molecular mechanism of luteolin-induced apoptosis is potentially related to inhibition of angiogenesis in human pancreatic carcinoma cells', *Oncology reports,* 28(4), pp. 1353-1361.

Calis, T., Satana, M. E., Yuruker, A., Kelican, P., Demirdamar, R., Alacam, R., Tanker, N., Ruegger, H. and Sticher, O. (1997) 'Triterpene saponins from *Cyclamen mirabile* and their biological activities', *J Nat Prod,* 60(3), pp. 315-318.

Cathcart, J., Pulkoski-Gross, A. and Cao, J. (2015) 'Targeting matrix metalloproteinases in cancer: Bringing new life to old ideas', *Genes & Diseases,* 2(1), pp. 26-34.

Chadwick, M., Trewin, H., Gawthrop, F. and Wagstaff, C. (2013) 'Sesquiterpenoids lactones: benefits to plants and people', *International journal of molecular sciences,* 14(6), pp. 12780-12805.

Chen, S.-L., Yu, H., Luo, H.-M., Wu, Q., Li, C.-F. and Steinmetz, A. (2016) 'Conservation and sustainable use of medicinal plants: problems, progress, and prospects', *Chinese medicine,* 11(1), pp. 1-10.

Chhabra, B., Gupta, S., Jain, M. and Kalsi, P. (1998) 'Sesquiterpene lactones from Saussurea lappa', *Phytochemistry,* 49(3), pp. 801-804.

Chiruvella, K. K., Mohammed, A., Dampuri, G., Ghanta, R. G. and Raghavan, S. C. (2007) 'Phytochemical and antimicrobial studies of methyl angolensate and luteolin-7-*O*-glucoside isolated from callus cultures of *Soymida febrifuga*', *International journal of biomedical science: IJBS,* 3(4), pp. 269-278.

Christaki, E., Bonos, E. and Florou-Paneri, P. (2012) 'Nutritional and functional properties of *Cynara* crops (Globe Artichoke and Cardoon) and their potential application: a review', *International Journal of Applied Science and Technology,* 2(2), pp.64-70

Ciancolini, A., Alignan, M., Pagnotta, M., Miquel, J., Vilarem, G. and Crinò, P. (2013) *Morphological characterization, biomass and pharmaceutical compounds in Italian globe artichoke genotypes,*2013(49), pp.326-333

Coll, J. C. and Bowden, B. F. (1986) 'The application of vacuum liquid chromatography to the separation of terpene mixtures', *Journal of Natural Products,* 49(5), pp. 934-936.

Cragg, G. M. and Newman, D. J. (2005) 'Plants as a source of anti-cancer agents', *Journal of ethnopharmacology,* 100(1-2), pp. 72-79.

Crespo-Ortiz, M. P. and Wei, M. Q. (2011) 'Antitumor activity of artemisinin and its derivatives: from a well-known antimalarial agent to a potential anticancer drug', *BioMed Research International,* (2012), PP.1-18

Danino, O., Gottlieb, H. E., Grossman, S. and Bergman, M. (2009) 'Antioxidant activity of 1, 3-dicaffeoylquinic acid isolated from Inula viscosa', *Food research international,* 42(9), pp. 1273-1280.

Davis, A. L., Cai, Y., Davies, A. P. and Lewis, J. (1996) '1H and 13C NMR assignments of some green tea polyphenols', *Magnetic resonance in Chemistry,* 34(11), pp. 887-890.

De Assis Carneiro, A., De Barros, Y. Y., De Freitas, M. M., Simeoni, L. A., Magalhaes, P. O., Silveira, D. and Fonseca-Bazzo, Y. M. (2017) 'Identification and quantification of caffeoylquinic acid derivatives in *Cynara scolymus* L. tablets and capsules', *African Journal of Pharmacy and Pharmacology,* 11(6), pp. 94-102.

De Falco, B., Incerti, G., Amato, M. and Lanzotti, V. (2015) 'Artichoke: botanical, agronomical, phytochemical, and pharmacological overview', *Phytochemistry reviews,* 14(6), pp. 993-1018.

Deer, E. L., Gonzalez-Hernandez, J., Coursen, J. D., Shea, J. E., Ngatia, J., Scaife, C. L., Firpo, M. A. and Mulvihill, S. J. (2010) 'Phenotype and genotype of pancreatic cancer cell lines', *Pancreas,* 39(4), pp. 425-435.

Dey, S., Sarkar, M. and Giri, B. (2016) 'Anti-inflammatory and anti-tumor activities of parthenolide: an update', *J Chem Biol Ther,* 2(1), pp. 1-6.

Ding, Y., Nguyen, H. T., Kim, S. I., Kim, H. W. and Kim, Y. H. (2009) 'The regulation of inflammatory cytokine secretion in macrophage cell line by the chemical constituents of Rhus sylvestris', *Bioorganic & medicinal chemistry letters,* 19(13), pp. 3607-3610.

El-Darier, S. and El-Mogaspi, F. (2009) 'Ethnobotany and relative importance of some endemic plant species at El-Jabal El-Akhdar Region (Libya)', *World Journal of Agricultural Sciences,* 5(3), pp. 353-360.

El-Mokasabi, F. (2014) 'Floristic composition and traditional uses of plant species at Wadi Alkuf, Al-Jabal Al-Akhder, Libya', *American-Eurasian J Agric Environ Sci,* 14(8), pp. 685-697.

El Hosry, L., Di Giorgio, C., Birer, C., Habib, J., Tueni, M., Bun, S. S., Herbette, G., De Meo, M., Ollivier, E. and Elias, R. (2014) 'In vitro cytotoxic and anticlastogenic activities of saxifragifolin B and cyclamin isolated from *Cyclamen persicum* and *Cyclamen libanoticum*', *Pharm Biol,* 52(9), pp. 1134-40.

ELabbar, F. A., Habel, A. M., Bozkeha, N. M. A and Awina, T. M. (2014) 'Isolation and identification of some compounds from cyclamen rohlfsianum (primulaceae) from Libya', *Sci. Revs. Chem. Commun,* 4(1), pp. 1-10.

Elberry, A. A., Harraz, F. M., Ghareib, S. A., Gabr, S. A., Nagy, A. A. and Abdel-Sattar, E. (2015) 'Methanolic extract of Marrubium vulgare ameliorates hyperglycemia and dyslipidemia in streptozotocin-induced diabetic rats', *International Journal of Diabetes Mellitus,* 3(1), pp. 37-44.

Elsayed, S., Nazif, N., Hassan, R., Hassanein, H., Elkholy, Y., Gomaa, N. and Shahat, A. (2012) 'Chemical and biological constituents from the leaf extracts of the wild artichoke (*Cynara cornigera*)', *Int J Pharm Pharm Sci,* 4(5), pp. 396-400.

Elsebai, M. F., Mocan, A. and Atanasov, A. G. (2016) 'Cynaropicrin: A comprehensive research review and therapeutic potential as an anti-hepatitis C virus agent', *Frontiers in pharmacology,* 7(472), pp. 1-15.

Erikstein, B. S., Hagland, H. R., Nikolaisen, J., Kulawiec, M., Singh, K. K., Gjertsen, B. T. and Tronstad, K. J. (2010) 'Cellular stress induced by resazurin leads to autophagy and cell death via production of reactive oxygen species and mitochondrial impairment', *J Cell Biochem,* 111(3), pp. 574-84.

Fantini, N., Colombo, G., Giori, A., Riva, A., Morazzoni, P., Bombardelli, E. and Carai, M. A. (2011) 'Evidence of glycemia-lowering effect by a *Cynara*

scolymus L. extract in normal and obese rats', *Phytother Res,* 25(3), pp. 463-466.

Farag, M. A., El-Ahmady, S. H., Elian, F. S. and Wessjohann, L. A. (2013) 'Metabolomics driven analysis of artichoke leaf and its commercial products via UHPLC–q-TOF-MS and chemometrics', *Phytochemistry,* 95, pp. 177-187.

Farid, M. M., Hussein, S. R., Ibrahim, L. F., El Desouky, M. A., Elsayed, A. M., El Oqlah, A. A. and Saker, M. M. (2015) 'Cytotoxic activity and phytochemical analysis of *Arum palaestinum* Boiss', *Asian Pacific Journal of Tropical Biomedicine,* 5(11), pp. 944-947.

Fratianni, F., Tucci, M., De Palma, M., Pepe, R. and Nazzaro, F. (2007) 'Polyphenolic composition in different parts of some cultivars of globe artichoke (*Cynara cardunculus* L. var. *scolymus* (L.) Fiori)', *Food chemistry,* 104(3), pp. 1282-1286.

Fritsche, J., Beindorff, C. M., Dachtler, M., Zhang, H. and Lammers, J. G. (2002) 'Isolation, characterization and determination of minor artichoke (*Cynara scolymus* L.) leaf extract compounds', *European Food Research and Technology,* 215(2), pp. 149-157.

Gao, J., Xu, P., Wang, Y., Wang, Y. and Hochstetter, D. (2013) 'Combined effects of green tea extracts, green tea polyphenols or epigallocatechin gallate with acarbose on inhibition against alpha-amylase and alpha-glucosidase in vitro', *Molecules,* 18(9), pp. 11614-23.

Garbetta, A., Capotorto, I., Cardinali, A., D'antuono, I., Linsalata, V., Pizzi, F. and Minervini, F. (2014) 'Antioxidant activity induced by main polyphenols present in edible artichoke heads: influence of in vitro gastro-intestinal digestion', *Journal of Functional Foods,* 10, pp. 456-464.

Gobert, C. P. and Duncan, A. (2008) 'Use of natural health products by adults with Type 2 diabetes', *Canadian Journal of Diabetes,* 32(4), pp. 260-272.

Grzesiak, J. J. and Bouvet, M. (2008) 'Divalent cations modulate the integrin-mediated malignant phenotype in pancreatic cancer cells', *Cancer Sci,* 99(8), pp. 1553-1563.

Haage, A. and Schneider, I. C. (2014) 'Cellular contractility and extracellular matrix stiffness regulate matrix metalloproteinase activity in pancreatic cancer cells', *Faseb j,* 28(8), pp. 3589-99.

Hădărugă, N., Hădărugă, D., Tatu, C., Gruia, A., Costescu, C. and Lupea, A. (2009) 'Multivariate analysis (PCA) in Compositae biocompounds class', *Journal of Agroalimentary Processes and Technologies,* 15(2), pp. 201-210.

Hand, R. and Hadjikyriakou, G. (2009) '*Cynara makrisii* (Asteraceae, Cardueae), a new artichoke species in Cyprus', *Willdenowia,* 39(1), pp. 77-81.

Hatzakis, E., Agiomyrgianaki, A., Kostidis, S. and Dais, P. (2011) 'High-resolution NMR spectroscopy: an alternative fast tool for qualitative and quantitative analysis of diacylglycerol (DAG) oil', *Journal of the American Oil Chemists' Society,* 88(11), pp. 1695-1708.

Hegazy, M.-E. F., Ibrahim, A. Y., Mohamed, T. A., Shahat, A. A., El Halawany, A. M., Abdel-Azim, N. S., Alsaid, M. S. and Paré, P. W. (2016) 'Sesquiterpene lactones from *Cynara cornigera*: acetyl cholinesterase inhibition and in silico ligand docking', *Planta medica,* 82(01/02), pp. 138-146.

Huang, J., Ogihara, Y., Zhang, H., Shimizu, N. and Takeda, T. (2000) 'Triterpenoid saponins from Ardisia mamillata', *Phytochemistry,* 54(8), pp. 817-822.

Hynes, R. O. (2002) 'Integrins: bidirectional, allosteric signaling machines', *Cell,* 110(6), pp. 673-87.

Ishizaka, H., Yamada, H. and Sasaki, K. (2002) 'Volatile compounds in the flowers of *Cyclamen persicum*, C. purpurascens and their hybrids', *Scientia Horticulturae,* 94(1), pp. 125-135.

Jacociunas, L. V., Dihl, R. R., Lehmann, M., Ferraz, A. D. B. F., Richter, M. F., Silva, J. D. and Andrade, H. H. R. D. (2014) 'Effects of artichoke (*Cynara scolymus*) leaf and bloom head extracts on chemically induced DNA lesions in Drosophila melanogaster', *Genetics and molecular biology,* 37(1), pp. 93-104.

Jain, S., Dwivedi, J., Jain, P. K., Satpathy, S. and Patra, A. (2016) 'Medicinal plants for treatment of cancer: A brief review', *Pharmacognosy Journal,* 8(2), pp.87-102

Jia, Z., Koike, K., Ohmoto, T. and Ni, M. (1994) 'Triterpenoid saponins from *Ardisia crenata*', *Phytochemistry*, 37(5), pp. 1389-1396.

Jiang, C. S., Liang, L. F. and Guo, Y. W. (2012) 'Natural products possessing protein tyrosine phosphatase 1B (PTP1B) inhibitory activity found in the last decades', *Acta Pharmacol Sin*, 33(10), pp. 1217-45.

Jones, L. J. and Singer, V. L. (2001) 'Fluorescence microplate-based assay for tumor necrosis factor activity using SYTOX Green stain', *Analytical biochemistry*, 293(1), pp. 8-15.

Karmakar, A., Xu, Y., Mustafa, T., Kannarpady, G., Bratton, S. M., Radominska-Pandya, A., Crooks, P. A. and Biris, A. S. (2015) 'Nanodelivery of Parthenolide Using Functionalized Nanographene Enhances its Anticancer Activity', *RSC Adv*, 5(4), pp. 2411-2420.

Kenny, H. A. and Lengyel, E. (2009) 'MMP-2 functions as an early response protein in ovarian cancer metastasis', *Cell Cycle*, 8(5), pp. 683-688.

Kessenbrock, K., Plaks, V. and Werb, Z. (2010) 'Matrix metalloproteinases: regulators of the tumor microenvironment', *Cell*, 141(1), pp. 52-67.

Kim, D. H., Lee, S., Chung, Y. W., Kim, B. M., Kim, H., Kim, K. and Yang, K. M. (2016) 'Antiobesity and Antidiabetes Effects of a *Cudrania tricuspidata* Hydrophilic Extract Presenting PTP1B Inhibitory Potential', *Biomed Res Int*, 2016, pp. 1-12.

Kim, H. R., Kim, J. M., Kim, M. S., Hwang, J. K., Park, Y. J., Yang, S. H., Kim, H. J., Ryu, D. G., Lee, D. S., Oh, H., Kim, Y. C., Rhee, Y. J., Moon, B. S., Yun, J. M., Kwon, K. B. and Lee, Y. R. (2014) 'Saussurea lappa extract suppresses TPA-induced cell invasion via inhibition of NF-kappaB-dependent MMP-9 expression in MCF-7 breast cancer cells', *BMC Complement Altern Med*, 14(170), pp. 1-9.

Kremmer, T. and Boross, L. (1979) *Gel chromatography: theory, methodology, applications.* John Wiley & Sons, p.299

Kumari, M. S., Lakshmi, K. N., Prasanna, T., Swapna, K., Jyothi, A. S. and Prasanthi, T. (2016) 'Natural herbs vs allopathic drugs: To treat diabetes',

INDO AMERICAN JOURNAL OF PHARMACEUTICAL SCIENCES, 3(5), pp. 415-422.

Kurkin, V. A. (2015) 'Saffloroside, a new flavonoid from flowers of Carthamus tinctorius L', *Journal of Pharmacognosy and Phytochemistry*, 4(1).

Lahlou, M. (2013) 'The success of natural products in drug discovery', *Pharmacol Pharm*, 4(3A), pp. 17-31.

Lattanzio, V., Kroon, P. A., Linsalata, V. and Cardinali, A. (2009) 'Globe artichoke: a functional food and source of nutraceutical ingredients', *Journal of functional foods*, 1(2), pp. 131-144.

Liu, S., Yu, Z., Zhu, H., Zhang, W. and Chen, Y. (2016) 'In vitro alpha-glucosidase inhibitory activity of isolated fractions from water extract of Qingzhuan dark tea', *BMC Complement Altern Med*, 16(1), pp. 1-8.

Liu, Y. C., Kim, S. L., Park, Y. R., Lee, S. T. and Kim, S. W. (2017) 'Parthenolide promotes apoptotic cell death and inhibits the migration and invasion of SW620 cells', *Intest Res*, 15(2), pp. 174-181.

Lombardo, S., Pandino, G., Mauromicale, G., Knödler, M., Carle, R. and Schieber, A. (2010) 'Influence of genotype, harvest time and plant part on polyphenolic composition of globe artichoke [*Cynara cardunculus* L. var. *scolymus* (L.) Fiori]', *Food Chemistry*, 119(3), pp. 1175-1181.

Ma, D., Tremblay, P., Mahngar, K., Akbari-Asl, P., Pandey, S., Collins, J. and Hudlicky, T. (2011) 'Induction of apoptosis and autophagy in human pancreatic cancer cells by a novel synthetic C-1 analogue of 7-deoxypancratistatin', *American Journal of Biomedical Sciences*, 3(4), pp.278-291.

Mahato, S. B. and Kundu, A. P. (1994) '13C NMR spectra of pentacyclic triterpenoids—a compilation and some salient features', *Phytochemistry*, 37(6), pp. 1517-1575.

Maldonado, E. M., Svensson, D., Oredsson, S. M. and Sterner, O. (2014) 'Cytotoxic Sesquiterpene Lactones from *Kauna lasiophthalma Griseb*', *Sci Pharm*, 82(1), pp. 147-60.

Marco, J. A., Sanz, J. F., Sancenon, F., Susanna, A., Rustaiyan, A. and Saberi, M. (1992) 'Sesquiterpene lactones and lignans from *Centaurea* species', *Phytochemistry,* 31(10), pp. 3527-3530.

Maschler, S., Wirl, G., Spring, H., Bredow, D. V., Sordat, I., Beug, H. and Reichmann, E. (2005) 'Tumor cell invasiveness correlates with changes in integrin expression and localization', *Oncogene,* 24(12), pp. 2032-2041.

Mazouz, W. and Djeddi, S. (2013) 'A Biological Overview On The Genus *Cyclamen*', *European Journal of Scientific Research,* 1(110), pp. 7-22.

Mcchesney, J. D., Venkataraman, S. K. and Henri, J. T. (2007) 'Plant natural products: back to the future or into extinction?', *Phytochemistry,* 68(14), pp. 2015-2022.

Megalla, S. E. (1983) 'Rapid, economical qualitative method for separation of aflatoxins B-1, B-2 & G-1, G-2 by dry column chromatography', *Mycopathologia,* 84(1), pp. 45-47.

Metin, H., Aydin, C., Ozay, C. and Mammadov, R. (2013) 'Antioxidant activity of the various extracts of *Cyclamen graecum* link tubers and leaves from Turkey', *Journal of the Chemical Society of Pakistan,* 35(5), pp. 1332-1336.

Mohammed, A. E.-S. I. (2015) 'Phytoconstituents and the study of antioxidant, antimalarial and antimicrobial activities of *Rhus tripartita* growing in Egypt', *Journal of Pharmacognosy and Phytochemistry,* 4(2), pp.276-281.

Mori, A., Nishino, C., Enoki, N. and Tawata, S. (1988) 'Cytotoxicity of plant flavonoids against HeLa cells', *Phytochemistry,* 27(4), pp. 1017-1020.

Mutalib A.G Nasser, A. (2017) 'Phytochemical Study of *Cynara scolymus* L. (Artichoke) (Asteraceae) Cultivated in Iraq, Detection and Identification of Phenolic Acid Compounds Cynarin and Chlorogenic Acid', *Iraqi Journal of Pharmaceutical Sciences (ISSN: 1683 - 3597 , ESSN : 2521 - 3512),* 21(1), pp. 6-13.

Nakano, H. and Omura, S. (2009) 'Chemical biology of natural indolocarbazole products: 30 years since the discovery of staurosporine', *J Antibiot (Tokyo),* 62(1), pp. 17-26.

Nassar, M. I., Mohamed, T. K., Elshamy, A. I., El-Toumy, S. A., Lateef, A. M. A. and Farrag, A. R. H. (2013) 'Chemical constituents and anti-ulcerogenic potential of the scales of *Cynara scolymus* (artichoke) heads', *Journal of the Science of Food and Agriculture,* 93(10), pp. 2494-2501.

Nemudzivhadi, V. and Masoko, P. (2014) 'In Vitro Assessment of Cytotoxicity, Antioxidant, and Anti-Inflammatory Activities of *Ricinus communis* (Euphorbiaceae) Leaf Extracts', *Evid Based Complement Alternat Med,* 2014, pp. 1-8.

Newman, D. J. and Cragg, G. M. (2016) 'Natural products as sources of new drugs from 1981 to 2014', *Journal of natural products,* 79(3), pp. 629-661.

Niu, J. and Li, Z. (2017) 'The roles of integrin alphavbeta6 in cancer', *Cancer Lett,* 403, pp. 128-137.

O'brien, J., Wilson, I., Orton, T. and Pognan, F. (2000) 'Investigation of the Alamar Blue (resazurin) fluorescent dye for the assessment of mammalian cell cytotoxicity', *Eur J Biochem,* 267(17), pp. 5421-5426.

Oliver-Bever, B. (1983) 'Medicinal plants in tropical West Africa. III. Anti-infection therapy with higher plants', *J Ethnopharmacol,* 9(1), pp. 1-83.

Özgen, U., Mavi, A., Terzi, Z., Kazaz, C., Asçi, A., Kaya, Y. and Seçen, H. (2011) 'Relationship between chemical structure and antioxidant activity of luteolin and its glycosides isolated from *T. sipyleus* subsp. *sipyleus* var. *sipyleus*', *Records of Natural Products,* 5(1), pp. 12-21.

Ozkan, G., Kamiloglu, S., Ozdal, T., Boyacioglu, D. and Capanoglu, E. (2016) 'Potential use of Turkish medicinal plants in the treatment of various diseases', *Molecules,* 21(3), pp. 1-32.

Pagnotta, M. A. and Noorani, A. (2014) 'Genetic Diversity Assessment in European *Cynara* Collections', *Genomics of Plant Genetic Resources*: Springer, pp. 559-584.

Pandey, M. M., Rastogi, S. and Rawat, A. K. (2007) 'Saussurea costus: botanical, chemical and pharmacological review of an ayurvedic medicinal plant', *J Ethnopharmacol,* 110(3), pp. 379-390.

Pandino, G., Lombardo, S., Williamson, G. and Mauromicale, G. (2012) 'Polyphenol profile and content in wild and cultivated *Cynara cardunculus* L', *Italian Journal of Agronomy,* 7(3), pp. 254-261.

Patel, D., Kumar, R., Laloo, D. and Hemalatha, S. (2012) 'Natural medicines from plant source used for therapy of diabetes mellitus: An overview of its pharmacological aspects', *Asian Pacific Journal of Tropical Disease,* 2(3), pp. 239-250.

Pedro, A., Barracosa, P., Guiné, R. and Gonçalves, F. 'Effect of drying on the phenolic content and antioxidant activity of thistle flower'. *ICEUBI2013–International Conference on Engineering*.

Pelletier, S. W., Chokshi, H. P. and Desai, H. K. (1986) 'Separation of diterpenoid alkaloid mixtures using vacuum liquid chromatography', *Journal of natural products,* 49(5), pp. 892-900.

Phillipson, J. D. (2001) 'Phytochemistry and medicinal plants', *Phytochemistry,* 56(3), pp. 237-243.

Pinelli, P., Agostini, F., Comino, C., Lanteri, S., Portis, E. and Romani, A. (2007) 'Simultaneous quantification of caffeoyl esters and flavonoids in wild and cultivated cardoon leaves', *Food chemistry,* 105(4), pp. 1695-1701.

Podolak, I., Janeczko, Z., Galanty, A., Michalik, M. and Trojanowska, D. (2007) 'A triterpene saponin from *Lysimachia thyrsiflora* L', *Acta Pol Pharm,* 64(1), pp. 39-43.

Ramos, P. A., Guerra, A. N. R., Guerreiro, O., Freire, C. S., Silva, A. M., Duarte, M. F. and Silvestre, A. J. (2013) 'Lipophilic extracts of *Cynara cardunculus* L. var. *altilis* (DC): a source of valuable bioactive terpenic compounds', *Journal of agricultural and food chemistry,* 61(35), pp. 8420-8429.

Ramos, P. A., Guerra, Â. R., Guerreiro, O., Santos, S. A., Oliveira, H., Freire, C. S., Silvestre, A. J. and Duarte, M. F. (2016) 'Antiproliferative effects of *Cynara cardunculus* L. var. *altilis* (DC) Lipophilic extracts', *International journal of molecular sciences,* 18(1), pp. 1-15.

Ramos, P. A., Santos, S. A., Guerra, Â. R., Guerreiro, O., Freire, C. S., Rocha, S. M., Duarte, M. F. and Silvestre, A. J. (2014) 'Phenolic composition and

antioxidant activity of different morphological parts of *Cynara cardunculus* L. var. altilis (DC)', *Industrial Crops and Products,* 61, pp. 460-471.

Rangboo, V., Noroozi, M., Zavoshy, R., Rezadoost, S. A. and Mohammadpoorasl, A. (2016) 'The effect of artichoke leaf extract on alanine aminotransferase and aspartate aminotransferase in the patients with nonalcoholic steatohepatitis', *International journal of hepatology,* 2016, pp.1-6.

Rasul, A., Khan, M., Ali, M., Li, J. and Li, X. (2013) 'Targeting apoptosis pathways in cancer with alantolactone and isoalantolactone', *ScientificWorldJournal,* 2013, pp. 1-9.

Reis, L., Tavares, M. R., Palma, F. and Marcelo-Curto, M. (1992) 'Sesquiterpene lactones from *Cynara humilis*', *Phytochemistry,* 31(4), pp. 1285-1287.

Ren, C., Han, C., Zhang, J., He, P., Wang, D., Wang, B., Zhao, P. and Zhao, X. (2011) 'Detection of apoptotic circulating tumor cells in advanced pancreatic cancer following 5-fluorouracil chemotherapy', *Cancer biology & therapy,* 12(8), pp. 700-706.

Ribatti, D., Marimpietri, D., Pastorino, F., Brignole, C., Nico, B., Vacca, A. and Ponzoni, M. (2004) 'Angiogenesis in neuroblastoma', *Ann N Y Acad Sci,* 1028, pp. 133-142.

Robinson, A., Kumar, T. V., Sreedhar, E., Naidu, V., Krishna, S. R., Babu, K. S., Srinivas, P. and Rao, J. M. (2008) 'A new sesquiterpene lactone from the roots of *Saussurea lappa*: structure–anticancer activity study', *Bioorganic & medicinal chemistry letters,* 18(14), pp. 4015-4017.

Romani, A., Pinelli, P., Cantini, C., Cimato, A. and Heimler, D. (2006) 'Characterization of Violetto di Toscana, a typical Italian variety of artichoke (*Cynara scolymus* L.)', *Food Chemistry,* 95(2), pp. 221-225.

Roth, B. L., Poot, M., Yue, S. T. and Millard, P. J. (1997) 'Bacterial viability and antibiotic susceptibility testing with SYTOX green nucleic acid stain', *Applied and environmental microbiology,* 63(6), pp. 2421-2431.

Safamansouri, H., Nikan, M., Amin, G., Sarkhail, P., Gohari, A. R., Kurepaz-Mahmoodabadi, M. and Saeidnia, S. (2014) 'alpha-Amylase inhibitory

activity of some traditionally used medicinal species of Labiatae', *J Diabetes Metab Disord,* 13(1), pp. 1-5.

Said, A. H., Raufman, J. P. and Xie, G. (2014) 'The role of matrix metalloproteinases in colorectal cancer', *Cancers (Basel),* 6(1), pp. 366-375.

Sajjadi, S. E., Shokoohinia, Y. and Moayedi, N. S. (2012) 'Isolation and Identification of Ferulic Acid From Aerial Parts of *Kelussia odoratissima Mozaff*', *Jundishapur J Nat Pharm Prod,* 7(4), pp. 159-162.

Salem, M. B., Affes, H., Ksouda, K., Dhouibi, R., Sahnoun, Z., Hammami, S. and Zeghal, K. M. (2015) 'Pharmacological studies of artichoke leaf extract and their health benefits', *Plant foods for human nutrition,* 70(4), pp. 441-453.

Salem, M. B., Kolsi, R. B. A., Dhouibi, R., Ksouda, K., Charfi, S., Yaich, M., Hammami, S., Sahnoun, Z., Zeghal, K. M. and Jamoussi, K. (2017) 'Protective effects of *Cynara scolymus* leaves extract on metabolic disorders and oxidative stress in alloxan-diabetic rats', *BMC complementary and alternative medicine,* 17(1), pp. 1-19.

Sarangi, M. (2014) *Plants with potential anticancer activities - a Review.*

Saúde-Guimarães, D. A., Raslan, D. S. and Oliveira, A. B. (2014) 'In Vitro Antitumor Activity of Sesquiterpene Lactones from *Lychnophora trichocarpha*', *Revista Brasileira de Plantas Medicinais,* 16, pp. 275-282.

Schaffner, F., Ray, A. M. and Dontenwill, M. (2013) 'Integrin alpha5beta1, the Fibronectin Receptor, as a Pertinent Therapeutic Target in Solid Tumors', *Cancers (Basel),* 5(1), pp. 27-47.

Schütz, K., Persike, M., Carle, R. and Schieber, A. (2006) 'Characterization and quantification of anthocyanins in selected artichoke (*Cynara scolymus* L.) cultivars by HPLC–DAD–ESI–MSn', *Analytical and bioanalytical chemistry,* 384(7-8), pp. 1511-1517.

Shakeri, A. and Ahmadian, M. (2014) 'Phytochemical studies of Some Terpene compounds in roots of *Cynara scolymus*', *International Journal of Farming and Allied Science,* 3(10), pp. 1065-1068.

Sheikh, N., Kumar, Y., Misra, A. and Pfoze, L. (2013) 'Phytochemical screening to validate the ethnobotanical importance of root tubers of *Dioscorea* species of Meghalaya, North East India', *Journal of Medicinal Plants,* 1(6), pp.62-69.

Shimoda, H., Ninomiya, K., Nishida, N., Yoshino, T., Morikawa, T., Matsuda, H. and Yoshikawa, M. (2003) 'Anti-hyperlipidemic sesquiterpenes and new sesquiterpene glycosides from the leaves of artichoke (*Cynara scolymus* L.): structure requirement and mode of action', *Bioorganic & Medicinal Chemistry Letters,* 13(2), pp. 223-228.

Singh, R., Chahal, K. and Singla, N. (2017) 'Chemical composition and pharmacological activities of *Saussurea lappa*: A review', *Journal of Pharmacognosy and Phytochemistry,* 6(4), pp. 1298-1308.

Soofiniya, Y. (2011) 'Hypolipidemic and hypoglycemic effects of aerial part of *Cynara scolymus* in streptozotocin-induced diabetic rats', *Journal of Medicinal Plants Research,* 5(13), pp. 2717-2723.

Speroni, E., Cervellati, R., Costa, S., Dall'acqua, S., Guerra, M. C., Panizzolo, C., Utan, A. and Innocenti, G. (2007) 'Analgesic and antiinflammatory activity of *Cyclamen repandum* S. et S', *Phytother Res,* 21(7), pp. 684-689.

Tabata, K., Nishimura, Y., Takeda, T., Kurita, M., Uchiyama, T. and Suzuki, T. (2015) 'Sesquiterpene lactones derived from *Saussurea lappa* induce apoptosis and inhibit invasion and migration in neuroblastoma cells', *J Pharmacol Sci,* 127(4), pp. 397-403.

Tanaka, T., Nonaka, G.-I. and Nishioka, I. (1983) '7-O-galloyl-(+)-catechin and 3-O-galloylprocyanidin B-3 from *Sanguisorba officinalis*', *Phytochemistry,* 22(11), pp. 2575-2578.

Tanjung, M., Mujahidin, D., Juliawaty, L. D., Makmur, L., Achmad, S. A., Hakim, E. H. and Syah, Y. M. (2008) 'Flavonoids from *Macaranga gigantea* (Euphorbiaceae)'. *Proc. Int. Seminar on Chemistry, Jatinangor, Indonesia*, 2008, pp.252-255.

Thomas, G. J., Nystrom, M. L. and Marshall, J. F. (2006) 'Alphavbeta6 integrin in wound healing and cancer of the oral cavity', *J Oral Pathol Med,* 35(1), pp. 1-10.

Toyang, N. J., Wabo, H. K., Ateh, E. N., Davis, H., Tane, P., Sondengam, L. B., Bryant, J. and Verpoorte, R. (2013) 'Cytotoxic sesquiterpene lactones from the leaves of *Vernonia guineensis* Benth.(Asteraceae)', *Journal of ethnopharmacology,* 146(2), pp. 552-556.

Upadhyay, R. K. (2016) 'Antidiabetic potential of plant natural products: A review', *International Journal of Green Pharmacy,* 10(3), pp. 96-113.

Vamanu, E., Vamanu, A., Nita, S. and Colceriu, S. (2011) 'Antioxidant and antimicrobial activities of ethanol extracts of *Cynara scolymus* (*Cynarae folium,* Asteraceae family)', *Tropical Journal of Pharmaceutical Research,* 10(6), pp. 777-783.

Velez, Z., Campinho, M. A., Guerra, Â. R., García, L., Ramos, P., Guerreiro, O., Felício, L., Schmitt, F. and Duarte, M. (2012) 'Biological characterization of *Cynara cardunculus* L. methanolic extracts: antioxidant, anti-proliferative, anti-migratory and anti-angiogenic activities', *Agriculture,* 2(4), pp. 472-492.

Wan, C., Li, S., Liu, L., Chen, C. and Fan, S. (2017) 'Caffeoylquinic Acids from the Aerial Parts of *Chrysanthemum coronarium* L', *Plants,* 6(1), pp. 1-7.

Webby, R. F. and Boase, M. R. (1999) 'Peonidin 3-*O*-neohesperidoside and other flavonoids from *Cyclamen persicum* petals', *Phytochemistry,* 52(5), pp. 939-941.

Winder, O., Friedrich, C., Denis, J., Griengl, H. and Kartnig, T. (1995) *Cyclamin, a new Molluscicide from the tubers of Cyclamen purpurascens Mill. tested against the snail Biomphalaria glabrata (Say),* 31(4), pp229-232.

Xie, H.-G., Chen, H., Cao, B., Zhang, H.-W. and Zou, Z.-M. (2007) 'Cytotoxic germacranolide sesquiterpene from *Inula cappa*', *Chemical and Pharmaceutical Bulletin,* 55(8), pp. 1258-1260.

Yang, A.-M., Liu, X., Lu, R.-H. and Shi, Y.-P. (2006) 'Triterpenoids from *Pyrethrum tatsienense*', *Die Pharmazie-An International Journal of Pharmaceutical Sciences,* 61(1), pp. 70-73.

Yayli, N. and Baltaci, C. (1996) 'The sterols of *Cyclamen coum*', *Turkish Journal of Chemistry,* 20(4), pp. 329-334.

Yayli, N., Baltaci, C., Zengin, A., Kucukislamoglu, M. and Genc, H. (1998) 'A triterpenoid saponin from *Cyclamen coum*', *Phytochemistry*, 48(5), pp. 881-884.

Yıldız, M., Bozcu, H., Tokgun, O., Karagür, E., Akyurt, O. and Akca, H. (2013) *Cyclamen Exerts Cytotoxicity in Solid Tumor Cell Lines: a Step Toward New Anticancer Agents?, Asian Pac J Cancer Prev,* 14 (10), pp. 5911-5913

Yilmazer-Musa, M., Griffith, A. M., Michels, A. J., Schneider, E. and Frei, B. (2012) 'Grape seed and tea extracts and catechin 3-gallates are potent inhibitors of alpha-amylase and alpha-glucosidase activity', *J Agric Food Chem*, 60(36), pp. 8924-8929.

Yoshizawa, S., Fujiki, H., Suguri, H., Suganuma, M., Nakayasu, M., Matsushima, R. and Sugimura, T. (1990) 'Tumor-promoting activity of staurosporine, a protein kinase inhibitor on mouse skin', *Cancer Res*, 50(16), pp. 4974-4978.

Yue, Z., Zhang, W., Lu, Y., Yang, Q., Ding, Q., Xia, J. and Chen, Y. (2015) 'Prediction of cancer cell sensitivity to natural products based on genomic and chemical properties', *PeerJ*, 3, pp. 1-14.

Zhang, D.-M., Wang, Y., Tang, M.-K., Chan, Y.-W., Lam, H.-M., Ye, W.-C. and Fung, K.-P. (2007) 'Saxifragifolin B from Androsace umbellata induced apoptosis on human hepatoma cells', *Biochemical and biophysical research communications*, 362(3), pp. 759-765.

Zheng, Z.-F., Xu, J.-F., Feng, Z.-M. and Zhang, P.-C. (2008) 'Cytotoxic triterpenoid saponins from the roots of *Ardisia crenata*', *Journal of asian natural Products research*, 10(9), pp. 833-839.

Zhu, X., Zhang, H. and Lo, R. (2004) 'Phenolic compounds from the leaf extract of artichoke (*Cynara scolymus* L.) and their antimicrobial activities', *Journal of Agricultural and Food Chemistry*, 52(24), pp. 7272-7278.

http://www.flickr.com/photos/tiggrx/10570158013/

http://es.treknature.com/gallery/photo279766.htm